The University of Strathclyde

Strathclyde institute of Pharmaceutical and Biomedical Sciences

The development of novel combinations therapies for the treatment of triple negative breast cancer

Hannah Gardiner

A thesis submitted in fulfilment of the requirements for the degree of Doctor of Philosophy

August 2023

Declaration

‘This thesis is the result of the author’s original research. It has been composed by the author and has not been previously submitted for examination which has led to the award of a degree.’

Signed:

Date: 22/08/23

Abstract

Introduction: Cancer has one of the highest mortality rates in humans, second only to heart disease. In 2018 there was an estimated 9.6 million deaths due to cancer. Cancer survival rates vary according to malignancy type, however modern medicine has improved cancer survival rates globally. Despite recent advancements, certain hard to treat cancers such as brain, pancreatic and triple negative breast cancer still have a poor prognosis. Therapy resistance is one of the major contributing factors to the failure of cancer therapy, leading to relapse, metastasis, and mortality. Radio- and chemoresistance can occur for a variety of reasons. One of the major contributing factors to therapy resistance is tumour heterogeneity, related to epigenetics, genomic instability, and therapy related mutagenesis. Thus, during treatment, cancer cells continue to evolve and mutate often to therapy resistant phenotypes. Over the course of the disease and its treatment, cancers therefore become more heterogeneous and are composed of pockets of tumour cells which are molecularly distinct from others and possess differential levels of sensitivity to therapies. As a result of this, many current cancer therapies have limited success and more optimal combination chemoradiotherapies are therefore required.

Materials and methods; Triple negative breast cancer cells were cultured in 2D and 3D models to investigate the efficacy of combination therapies designed from either chemotherapy or irradiation and a pre-approved fumaric acids dimethyl fumarate and monomethyl fumarate. Dimethyl fumarate and monomethyl fumarate have been shown to inhibit the NRF2 activation via the DJ-1 stabiliser which induces oxidative stress and promoted cancer cell death, dimethyl fumarate is currently used as a treatment for several autoimmune diseases. Triple negative breast cancer cells resistant to Radiation and Chemotherapy were developed in house by serial culture and used to investigate novel combination therapies to overcome resistance. Clonogenic Assays and Spheroid analysis was used to investigate toxicity and mechanistic studies such as Comet Assay, Cell Cycle analysis, Annexin V, Glutathione Assay and Autophagy Assay were carried out to understand the mechanisms underpinning observed effects. The chick embryo model, a promising method of *in vivo* analysis was also investigated for its potential as a model to be used in the development of novel therapies.

Results and Discussion; Specifically scheduled combination therapies using Chemotherapy and Radiation with monomethyl fumarate in toxicity studies, showed a statistically significantly reduction in cell survival when compared with the control and the individual treatments alone. Mechanistic studies suggest an increase in DNA damage, depletion in glutathione levels and cell cycle arrest between combination therapy, control, and single treatments. These findings in triple negative breast cancer cells were mirrored in the resistant cells, providing a possible combination therapy that can be used to overcome resistance in triple negative breast cancer patients.

Conclusion: Our research focuses on utilising medicines already approved for other conditions and using them in combination with current therapies to improve the efficacy of the treatment and potentially reduce the amount of chemotherapy/radiotherapy required. The results found provide a promising potential treatment option for TNBC patients with recurring cancer. In addition, it was determined that the chick embryo model could be used as an *in vivo* model to investigate novel therapies to treat cancer.

COVID Impact Statement

The laboratory work that was carried out as part of this thesis began in October 2019 to March 2023, and as a result was impacted due to lockdown limitations during the COIVD-19 pandemic.

Between the months of March 2020 to May 2021 there was severely reduced laboratory access with around 2.5-3 days per week because of the University social distancing measure there was a limited number of persons allowed in the laboratory space at the same time.

Unfortunately, there was several experiments that were not completed. It was hoped that some murine *in vivo* experiments would be carried out to investigated potential treatments that were investigated during the project. I was however able to obtain my personal animal handling licence from the home office in December of 2019. Additionally, it was planned for a more extensive analysis of the chick embryo model would be completed using triple negative breast cancer cell lines to investigate potential therapies. Finally, it was hoped that a more detailed analysis of in-house developed resistant cells would be carried out. However, due to time constraints these investigations have been passed onto post doctorate members of the Boyd lab to analyse metabolomics of these developed cells.

Additionally, there was many delays the delivery of in certain essential plastics and reagents in some cases 6 months post covid which was a very limiting factor when carrying out experimental work.

Acknowledgements

I would firstly like to thank my supervisor Dr Marie Boyd, for her help, guidance, and support over the last 4 years. Furthermore, I would like to thank Dr Annette Sorensen who has helped and supported me greatly over the course of my studies. If I had not met Marie and Annette, I would never had considered it a possibility that I could have taken on a PhD, I am incredibly grateful for the help, kindness, and belief that they have both given me over the past 5 years.

I would like to thank every member of the Boyd lab, Samantha, Calum, Yasir, Olena, Rosh, Sara, Manal, and Reem, your help and friendship has been made my time as a PhD student truly special and I am grateful to be able to work with such an incredible team of people.

I would also like to thank my friends and family for their continuous support and encouragement (Creamers, Lindies, Houstons, Jacksons, Friels and Gardiners). I am incredibly fortunate to have an amazing family that has always encouraged me, but I would like to give special thanks to my Aunt Margaret, Vicki, Aunt Lorna, and Erin.

Finally, I would like to thank my Mum, Dad and brother Harry, your tireless and unwavering love is what has driven me to be the person I am today. They have raised me to believe that you can do anything you set your mind to and everything I have achieved is because of them. I would like to thank my boyfriend and best friend Elliott for everything, you have always believed in me and been there for me, I am incredibly lucky to have you.

I was incredibly blessed to have two amazing grandmothers Ruby and Ellen who passed away before the completion of this effort and who I would like to dedicate this work to. The loved us all fiercely and the strength and wisdom they passed on will continue to influence the person I will become. I will always be grateful for having you all, words cannot express how much you all mean to me.

Table of Contents

List of Figures

Chapter 1

Chapter 2

Chapter 3

List of Tables

List of abbreviations

AR – Androgen receptor
BC – Breast cancer
BRCA - BReast CAncer gene
CAM - Chorioallantoic Membrane
CEF – Chick embryo facility
CEM – Cheick embryo model
DMF - Dimethyl Fumarate
DMSO - Dimethyl sulfoxide
DNA – Deoxyribose nucleic acid
DSB – Double strand breaks
DOX - Doxorubicin
DJ-1 - Protein deglycase
EGFR – Endothelial growth factor receptor
EMF - Diroximel Fumarate
ER – Estrogen receptor.
FACS - Fluorescence-activated cell sorting
FDA – Food and drugs administration
Gy – Gray (radiation unit)
HER2 - human epidermal growth factor receptor 2
HIF – Hypoxia inducing factor.
HR – Homologous recombination
IHC - Immunohistochemistry
KRAS - Kirsten rat sarcoma viral oncogene homolog
MMF - Monomethyl Fumarate
MS – Multiple Sclerosis
MTS – Multicellular tumour spheroids
Nrf2 - Nuclear factor erythroid 2–related factor 2
OS – Oxidative stress
PARP - Poly-ADP ribose polymerase
PBS – Phosphate buffered saline.
PR – Progesterone receptor
ROS – Reactive oxygen species
SD – Standard Deviation

SSB – Single strand breaks

TNBC – Triple negative breast cancer

UK – United Kingdom

WHO – World health organisation

μM - Micromolar

Chapter 1

Introduction

1.1 Cancer Incidence

Cancer is the collective term for an extensive group of diseases, characterised by the uncontrollable growth and division of abnormal cells. These cells are not restricted by conventional growth control mechanisms present in non-cancerous cells and these cancerous cells can invade into surrounding tissues and spread to other organs, in the process known as metastasis (Fidler *et al*., 2011). Cancer occurs due to the accumulation of a variety of molecular mutations, each cancer is unique. Therefore, each case of cancer ideally requires a specific treatment regime tailored to the molecular make-up of the cells which make up the tumour (Yan and Liu., 2013).

Cancer is a prolific disease as is demonstrated by the fact that cancer deaths totalled almost 10 million worldwide in 2021 (World Health Organisation, *Cancer*, 2021). Unfortunately, even when a patient survives their initial cancer diagnosis, the treatment can leave the patient with significant disabilities and suffering from multiple morbidities such as secondary cancers, nerve damage, dental problems, lung disease and infertility (Mayo Clinic, Cancer Symptoms, 2021). Early diagnosis, screening and personalised treatment are urgently required to improve survival for complex cancers and reduce treatment related toxicities that can hamper survivors' quality of life. Treatment is dependent on each individual and may include surgery, chemotherapy or molecule therapies and/ or radiotherapy. The patient's individual treatment varies depending on the specific type of cancer and molecular make-up, stage of the disease and recourses available to the patient (Lambin *et al*., 2012). Important treatment decisions can be based on cancer pathology, imaging, blood biomarkers and genomics and proteomics and the general state of health of the patient. All these factors greatly influence the outcome of a patient's cancer diagnosis. The more detailed information gathered, the more likely it is that the make-up of a patient's tumour is understood, and specific aspects of their tumour targeted.

In recent years personalised medicine has been at the forefront of research and development. There are however several challenges emerging such as the cost of personalised therapies and extensiveness of tests required (Hughes *et al.,* 2018). There has also been an increase in patients experiencing acquired resistance to personalised therapies such as those targeting specific molecular pathologies such as the KRAS G12C mutation (Blaquier *et al*., 2021). This mutation activates an

alternative RAS dependant pathway and ultimately the patient develops resistance to this therapy (Indini *et al.,* 2021). An ideal treatment would be one which covers multiple molecular pathologies as this opens a larger cancer market.

1.2 Tumour Heterogeneity

Cancer remains one of the highest causes of death worldwide and one reason that cancer is so difficult to treat is inter and intra-tumour heterogeneity (different cellular mutations within the same tumour) (Ramón e*t al.,* 2020). Tumour heterogeneity results in the need to target multiple regions with different molecular and cellular characteristics within the tumour. Different cells within a tumour and between tumours contain varying mutations, there is therefore a need to gain a greater understanding of the entire tumour molecular makeup when deciding treatment options (Fisher *et al*., 2013) and this is particularly true in relation to the application of personalised cancer therapy. The identification of multiple biomarkers which identify molecular targets and enable design of personalised combination anti-cancer therapies could revolutionise cancer treatment.

Additionally, the confirmation that biopsies are cancerous is also dependent on the clinician's visual interpretation of the sample which can be inconsistent due to subjectivity and opinion (Hopkinsmedicine.org, 2019). The diagnostic capabilities of tumour biopsies and immunohistochemistry (IHC) have been scrutinised in recent years since a single biopsy does not consider the heterogeneity of a tumour (Sala *et al*., 2017). Tumours are heterogenous and as cancer grows the heterogeneity of the tumour becomes greater as the tumour cells acquire subsequent mutations and evolve. This exacerbates drug resistance leading to treatment failure and multiple sampling of a tumour has not been widely adopted due to the risks of multiple invasive procedures (Lee *et al*., 2017; Dagogo-Jack and Shaw., 2017).

It has been demonstrated that the genetic heterogeneity of a tumour is reflected by the level of histopathologic diversity i.e., the degree of proliferation and inflammation (Hanahan and Weinburg., 2012). There is therefore a growing need to identify malignant sub clonal cells and their drivers, as therapies have traditionally focused on the dominant clonal mutations (Truke *et al*., 2010). This transformational understanding of tumour genetic classification has revolutionised cancer treatment to

have a more personalised medical approach, by understanding each individual patient's tumour heterogeneity (Curtis *et al*., 2012).

There are treatments that are efficacious regardless of tumour heterogeneity such as radiotherapy (Moding *et al.,* 2013). Combination therapy has also been a strategy used to overcome tumour heterogeneity, such as surgery before or after chemotherapy or radiotherapy before chemotherapy etc. (Malhotra *et al*., 2003). Additionally, chemotherapy in combination with immunotherapy treatments have shown promising clinical results (Schmid *et al.,* 2018). One example is the use of Atezolizumab and Nab-Paclitaxel to treat triple negative breast cancer (TNBC) in a phase III trial, involving patients with metastatic TNBC an improvement in progression free survival was observed (Schmid *et al.,* 2018).

Clinical application of combination therapies is an area of research that has been greatly developed in the last 60 years since its initial proposal in 1965 for the treatment of leukaemia (Frei *et al*., 1965). Combination therapies have been investigated in research for many reasons, including the added benefit of have the potential to create synergistic effects. Meaning therapies given in a designed combination exhibit more effective outcomes than if each individual therapy was given alone. They have the capacity to treat different heterogeneous populations within a tumour, as different therapies within a combination schedule may be specific to different cellular or molecular targets (Bukowska *et al.,* 2015). There have however been challenges when developing combination therapies, the pharmacokinetics and synergistic capacity of therapies administered together is not always predictable and often doses of therapies must be altered to avoid toxicity in patients (Chou *et al.,* 2010). There is also the potential for patients to develop multi-drug resistance following combination therapy which can result in a patient with very limited treatment options should they experience tumour reoccurrence (Liu *et al*., 2022).

1.3 Breast Cancer

Breast cancer (BC) is a leading cause of mortality with 50,000 women and 350 men diagnosed annually in the UK (Cancer Research UK, 2020). Prognosis for women expressing the human epidermal growth factor receptor 2 (HER2), and/or oestrogen receptor (ER) has improved, as biological therapies such as Herceptin and aromatase inhibitors target these receptors. However, in 10-20% of BCs, known as triple negative breast cancer (TNBC), these receptors are absent limiting therapeutic options (Bianchini *et al*., 2016) (Figure 1.1).

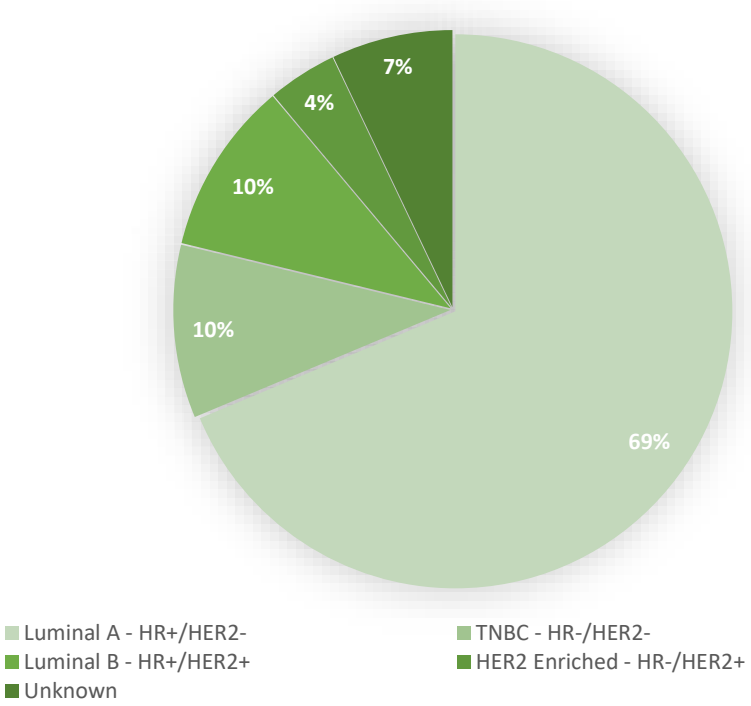

Figure 1. 1 The incidents of breast cancer and their subtypes.

These statistics were taken from the National Cancer Institute (Female breast cancer subtypes - cancer stat facts (11/4/23) *SEER* 22 2015–2019.) The statistics represent the breast cancer subtypes diagnosed between 2015 and 2019. Luminal A accounts for 69%, Luminal B 10%, TNBC 10%, HER2 Enriched 4% and unknown 7%.

TNBC occurs at an earlier age and has a high mortality and recurrence rate; only 77% of patients survive five years in comparison to 93% in other BC subtypes (Zhang and Zhang, 2018; Deo *et al.,* 2017; and Andreopoulou *et al.,* 2015). Since the hormonal receptor and HER-2 antagonists typically used for other BCs are ineffective in TNBC,

the main treatments are surgery and combination chemotherapy with or without radiotherapy (Canny *et al*., 2011). These treatments have limited efficacy and induce significant toxicities.

Genetically TNBC is a highly heterogeneous group of malignancies with variation between patients and within the same tumor resulting in therapy resistant cell sub-populations. TNBCs can be subdivided into 6 different subtypes by gene expression studies (Table 1.1) (Yin *et al.,* 2020). These include the basal subtype, BL1 and BL2 (p53 and BRAC1 mutated tumours), a subtype with an AR/apocrine signature, immunomodulatory, mesenchymal-like and mesenchymal stem cell-like (McKenna *et al.,* 2003; Potiron *et al.,* 2013).

<table>
<tr><td colspan="5">Molecular classification
A better prognosis Poor Prognosis Worst Prognosis</td></tr>
<tr><td>Luminal A</td><td>Luminal B</td><td>Her -2</td><td>Basal</td><td>Claudin</td></tr>
<tr><td>Her – 2 – ve</td><td>Her -2 +ve</td><td>Her -2 +ve</td><td>Her -2 -Ve</td><td>a/w addition molecules</td></tr>
<tr><td colspan="2" rowspan="2">ER +
PR +
Associated with BRAC2 mutation</td><td>ER-ve</td><td>ER -</td><td rowspan="3"></td></tr>
<tr><td>PR-ve</td><td>PR -</td></tr>
<tr><td colspan="2"></td><td></td><td>TNBC – a/w BRCA 1 gene mut,</td></tr>
</table>

Table 1. 1 Molecular classification of breast cancers.

Taken and adapted from Yin *et al.*, 2020 using Open Access Creative Commons Attribution License 3.0 (CC BY 3.0).

Currently options for TNBC patients are surgery and conventional chemotherapy if the disease has begun to metastasis. Patients receive common chemotherapeutics such as platinates, anthracyclines and taxol's which are the only systemic therapy options for TNBC patients (Nedeljković & Damjanović, 2019). These therapies are however relatively ineffective as many TNBC are resistant to chemotherapy and

chemotherapy is also associated with several toxicities. There have however been 2 new immunotherapy drugs approved in 2023 for the treatment of TNBC in combination with chemotherapy drugs; Olaparib (PARP inhibitor) and Pembrozolumab (PDL-1 inhibitor) (Breast Cancer Now, Pembrolizumab (Keytruda) | Breast Cancer now, 2023). Additional clinical trials are still underway investigating the use of immunotherapy drugs and chemotherapy, such as the Phase 2 trial (Begonia NCT03742102), investigating the potential of durvalumab in combination with the chemotherapeutic paclitaxel (Clinical trials.gov, 2023).

1.4 BRCA

The BReast CAncer genes (*BRCA*s) - are tumour suppressor genes that are involved in DNA damage and repair, there are two types of *BRCA* genes: *BRCA*1 and *BRCA*2. Mutations of genes *BRCA*1 and *BRCA*2 increase the risk of developing breast cancer and or ovarian cancer (Peng *et al*., 2016). People who have a genetic mutation in one of these genes have an increased risk of developing breast cancer. It is estimated that 55-65% of women with *BRCA*1 will be diagnosed with BC before the age of 70 and 45% of woman carrying the *BRCA*2 gene will be diagnosed with BC (*BRCA*: The breast cancer gene - *BRCA* mutations & risks, 2023). Those with the *BRCA*1 gene mutation are more likely to have triple-negative breast cancer (TNBC), which is a fast-growing and aggressive form of breast cancer. Current data suggests that breast cancer patients with *BRCA*1^{mut} are more likely to have a higher nuclear grade and larger tumour mass, the higher the nuclear grade the more abnormal and aggressive the tumour (Musolino *et al*., 2007; Byrski *et al*., 2008; Kirk, 2010). *BRCA1* mutations are highly likely to results in breast tumours with ER (oestrogen receptor)-negative/PR (progesterone receptor)-negative characteristics while *BRCA*2 mutations usually produce breast tumours with characteristics that are like breast cancer tumours of patients with unmutated *BRCA* genes (Noguchi *et al*., 1999). It was discovered by Comen *et al.,* (2011), that TNBC patients possess not only *BRCA1* mutations but a significant number of TNBC patients also have *BRCA2* mutations. This relationship between *BRCA* gene mutations and TNBC requires further investigation to clarify any mechanisms of interaction as this has not yet been elucidated.

Chen *et al.,* (2018), carried out a meta-analysis of TNBC patients to determine the relationship between TNBC and *BRCA* mutations. It was reported that TNBC was

more common among the breast cancer patients with *BRCA*1^{Mut} than those of patients with *BRCA*2^{Mut} or non-carriers. Surprisingly it was also found that TNBC patients with a *BRCA* mutation had a significantly lower chance of cancer relapse (Gonzalez-Angulo *et al*., 2011). As previously mentioned, the mechanisms that link *BRCA* and ER negative tumours has been of great interest in many investigations. For example, it was reported that the lack of ER expression found in *BRCA*1^{mut} tumours is a result of the absence of *BRCA*1 mediated transcriptional activation of the oestrogen receptor (Hosey *et al.,* 2007). However, the specific mechanisms of action underlying the transcription of *BRCA* is still unknown, therefore additional investigation are required to determine the relationship between *BRCA*1 and ER as well as potential effects on the PR and the human epidermal growth factor receptor (HER2), a protein that is known to promote the growth of cancerous cells (Mayo Clinic, 2022).

1.5 Emerging therapies for TNBC

Due to TNBC heterogeneity it is unlikely that single therapies will eradicate all tumour cells, resulting in tumour recurrence. However, several novel targets are currently undergoing clinical assessment. For example, therapies that target PI3K-mTOR, are in early clinical interrogation (NCT02208375, NCT02423603, NCT01964924). The most recently approved treatment for TNBC approved in Scotland is PARP inhibitors which inhibit the enzyme poly ADP ribose polymerase (PARP) (McCann and Hurvitz, 2018). The role of PARP is to identify single strand DNA breaks and engage DNA repair complexes, ultimately preventing the damaged cell from dying. The logic behind developing an inhibitor of these pathways, is that single strand breaks would be prevented from repairing and accumulate, resulting in double strand breaks and ultimately lead to cancer cell death. In cells positive for *BRCA*1 and 2 such as TNBC cells, homologous recombination is deficient (HRD) these cells are the ideal candidates for PARP inhibitors (PARPi) and as such have been investigated markedly in recent years (Rose, *et al.* 2020). This method of targeting a genetic mutation that is present in cancer cells only, is known as synthetic lethality and is a well-known target of drug development to target cancer cells (Synthetic lethality: Accelerating precision cancer treatments, 2023). Cancers with a deficiency in homologous recombination repair such as *BRCA*1 and 2 positive tumours are unable to repair DNA double strand breaks through this pathway (Stewart *et al.,* 2022).

As a substantial proportion of TNBC patients have *BRCA* mutations, it is currently of great interest to investigate the effectiveness of poly adenosine diphosphate-ribose polymerase inhibitors (PARPi's) in combination with both chemotherapy and radiotherapy for TNBC *BRCA* mutated cell lines. At present there is a Phase 2 trial running in Massachusetts USA which is in the recruiting phase. This clinical trial is investigating the combination of PARPi's and Radiotherapy (NCT04837209). This combination has been chosen as radiation induced SSB and these can be converted into DSB in HR deficient cells, therefore by combining this radiotherapy with a PARPi, the DNA repair complexes will fail to be initiated and the cell will die. This trial/will/be particularly important as there is currently no approved combination therapy involving PARPis and radiotherapy in Scotland.

As described, PARPi's have a therapeutic role in *BRCA*1/2 mutant tumours deficient in homologous recombination (HR) (Kimbung *et al.,* 2012) and TNBC patients often have *BRCA* mutations. However, even individuals not carrying mutations, behave similarly to *BRCA1*-deficient tumours, with similar gene expression profiles (Murai *et al*., 2014). Many hypothesise that the PARPi Olaparib could synergise with PARPi's in TNBC patients with no *BRCA*1/2 function loss, as it was demonstrated that an AKT inhibitor utilised in *BRCA*+ TNBC cell lines, caused HR functional changes. This HR abrogation sensitised cells to PARPi's by downregulating *BRCA*1 favouring the action of Olaparib (PARPi) with subsequent reduction in cell survival (Murai *et al*., 2014). Studies also demonstrated efficacy with the combination of PARPis and PI3K inhibitors in *BRCA*1-deficient cells, provide a rationale for further research in TNBC (Bhamidipati *et al.,* 2023).

The androgen receptor (AR) is expressed on a subtype of TNBCs and has thus been investigate as a potential target to treat TNBC patients (McGhan *et al.,* 2014). The AR is a steroid nuclear receptor that is essential for normal breast development, the receptor binds to testosterone and dihydrotestosterone (DHT) in the cytoplasm, and it translocate to the nucleus to regulate gene expression (Tozbikian *et al.,* 2019). Around 25-35% of TNBCs express the AR receptor and the AR receptor has been recently investigated for its use as a targetable receptor in TNBC (McNamara et *al.,* 2013). However, there is still much to be understood about AR signalling, for example it was found in a study by Thakkar *et al (*2016), that in TNBC the anti-proliferative effect exhibited by AR antagonists may be the result of off-target effects, therefore

meriting the need for deeper genetic investigations. There has been progress in AR antagonists as the AR antagonists bicalutamide and enzalutamide have been investigated and a recent Phase II trial carried out by Traina *et al*., (2018) (NCT01889238) demonstrated their clinical activity in TNBC patents. Although this study reports encouraging results, there is a need for a more extensive investigation in the AR and its use as a targetable receptor to treat TNBC clinically.

Due to the challenging intracellular mechanisms involved in breast cancer as mentioned above, the importance of selecting the most suitable cell line is of the utmost importance when carrying out *in vitro* investigations. Each method of assessment of cell death in breast cancer cell lines has advantages and disadvantages, each method must assess various cellular functions to quantify the cytotoxicity of each of these agents. An ideal investigation into any breast cancer therapy must consider not only the correct cell line but the optimum methods of investigation.

1.6 Current therapies

TNBC is among the leading cause of death among working age women and surgical removal is one of the most common treatment options for patient (Baranova *et al.,* 2022). Surgery aims to remove the localized tumour area and any areas of metastasis where possible. For TNBC patients a mastectomy is performed in approximately 67% of patients and organ-preserving surgery in approximately 33% of patents, respectively (Fayaz *et al*., 2019). In most cases surgery is followed by adjuvant therapy, in a study conducted by Zumsteg *et al*., (2013), it was found that 81% of patents went on to receive chemotherapy with a 5- year locoregional recurrence of (4.7%).

1.6.1 The effect of Radiotherapy on cells.

Radiobiology is the study of the action of ionizing radiation on living things (Hall and Giaccia, 2012, p. 3). There are 2 types of ionizing radiation that occur due to the biological material absorbing radiation energy. These are **excitation** and **ionization**. Excitation is the movement of an electron to a higher energy level within an atom or a molecule. Ionization is the ejection of one or more electrons from the energy levels of a molecule or atom, this type of radiation is referred to as **Ionizing Radiation** (Hall and Giaccia, 2012, p 3)**.**

Energy, for example, in the form of X-rays, can be absorbed by living material. Once absorbed this energy is not always distributed evenly. Large individual packets of energy are used to quantify the energy given in a beam of X-rays. This means that packets of energy are energetic enough to cause damage at a cellular level, breaking chemical bonds and causing chains of events that can eventually lead to change at a biological level. The difference between ionizing and non-ionizing radiation is the size of these packets of energy given out and not the total energy involved (Hall and Giaccia, 2012, p. 7-8).

There are many types of radiation that occur naturally, and some are used in scientific experiments and clinical practice. These different types of radiation have different uses and provide huge potential in healthcare for diagnostics and radiotherapy.
Electrons are small, negatively charged particles that can be accelerated using a linear accelerator or other such electrical devices and are used for cancer therapy. However, they are not commonly used to treat large internally located solid tumors due their ability to only penetrate a few centimeters through skin, therefore they are primarily used to treat superficial tumors (External beam radiation therapy for cancer, 2023). Proton beam therapy is becoming more popular in the world of cancer research due to the method in which they distribute energy. α-particles are nuclei of helium atoms and consist of two protons and two neutrons in close reassociation. Much like that of protons α-particles are positively charged, targeted alpha-particle therapy is of great interest in current literature as alpha particles can induce damage to tumours while causing minimal toxicity to the surrounding tissue, much like those used to accelerate protons (Tafreshi *et al.,* 2019; L'Annunziata., 2008). Neutrons are neutral particles and do not carry a positive or negative charge, they are a similar size to that of protons, these particles are not electrically charged and as such they cannot be accelerated (Meyers, 2004). Heavy charged particles consist of nuclei of positively charged elements (e.g., carbon, argon, neon, and iron) because of planetary electrons that have been removed from their orbit. These types of particles can be used for radiation therapy; however, they must be accelerated to extremely high energies and as a result there are only a small number of specialised facilities globally (Hall and Giaccia, 2012, p. 11).

Most radiotherapy is delivered using X-ray photons; these are delivered via a LINAC and can be localised using IMRT, thus, minimising dose to normal organs. However,

when patients receive radiotherapy, normal tissue is irradiated in the surrounding site of the tumour. This can lead to a to unwanted morbidity for example, when patients receive radiation therapy for breast cancer of the left breast, they have a 30% greater risk of developing cardiovascular disease and a 38% greater risk of cardiovascular related death than non-irradiated women (Wenski *et al., 2020)*. Therefore, there is still a clinical need to find ways to limit the off-target effects for patients, for example by combination therapies that allow the use of even lower radiation doses.

The main aim of radiation therapy is to induce damage to the DNA. When radiation interacts with biological tissue the damage can be direct or indirectly ionizing. If the particles have enough energy, they can disrupt the atomic structure of the absorber they pass through directly and can cause chemical or biological changes (Desouky, and Zhou., 2015). High linear energy transfer (LET- energy that is transferred form an ionizing particle to living material), involves the direct interaction with important targets of the cell, the atoms of this target may be ionized or excited causing damage themselves, more often double strand breaks in DNA which are the therapeutic goal of radiotherapy. As for cancer cells, DSBs are more difficult to repair and thus lead to cancer cell death. Indirect action may also occur, this involves the radiation interacting with molecules other than the target (particularly water) to produce free radicals that are then able to damage the target. Low LET is more likely to cause single strand breaks that are more easily repaired by cancer cells and as such the goal of radiotherapy is to drive the damage to double strand breaks as described in Figure 1.2.

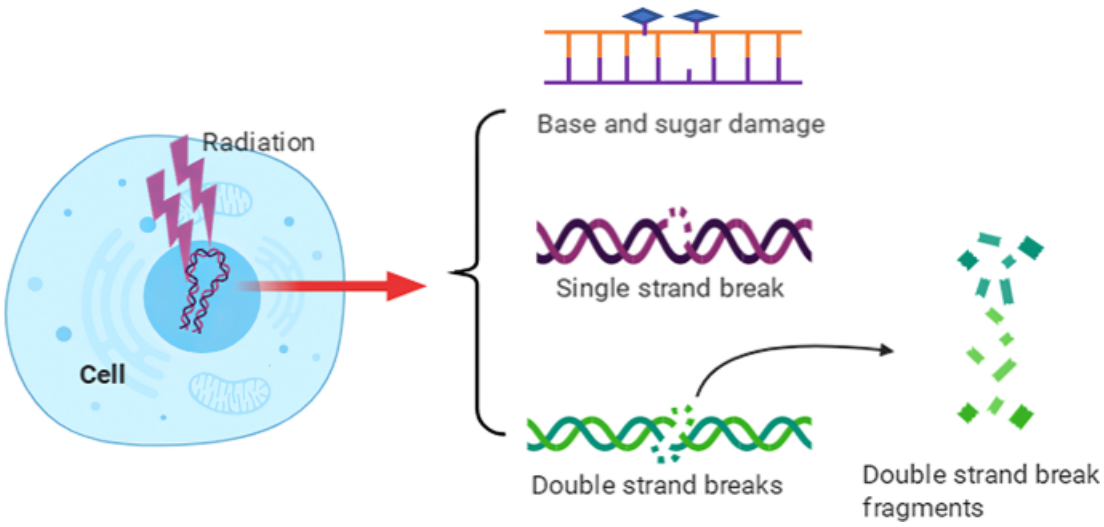

Figure 1. 2 DNA damage induced by ionizing radiation.

The major types of DNA damage induced by IR include base and sugar damage, single-strand breaks, double-strand breaks, clustered DNA damage, and covalent intrastrand or interstrand crosslinking. Taken and adapted with permission from from Husng *et al.,*2020 using Open Access Creative Commons Attribution License 3.0 (CC BY 3.0).

SSB (single strand breaks) are of little consequence to the cell as they are mostly readily repaired by the cell. If the repair is incorrect (mis-repair) however, then a mutation can occur. If the 2 strands of DNA are broken at different points, then these are also easily repaired. However, if both strands of DNA are broken at the same point within the DNA, then this can lead to conversion of SSBs to DSBs (double strand break), which leads to the cleavage of chromatin into two pieces. These are crucial lesions caused in chromosomes by radiation and can lead to cell death, mutation, or carcinogenesis. DSB can be caused by both direct ionization and free radicals (Mladenov *et al.,* 2013). Part of the goal of combination therapy is to utilize various aspects of individual therapies and combine them to give optimal cancer cell death. In recent years radiotherapy has been investigated as part of a combination regime with immunotherapy. In a recent study carried out by Zhang *et al.,* (2022) it was reported that radiotherapy can be used to trigger an antitumor response and that through combination with immunotherapy agents, it can be used as a systemic cancer treatment for a variety of cancers. As mentioned, radiotherapy can induce single strand and double strand breaks in the target cancer cells DNA. However, cancer cells can develop adaptive repair mechanisms to repair such damage and often

aberrantly which leads to the continued survival of daughter cancers cells with even more heavily mutated DNA which often have more resistant phenotypes (Borrego-Soto *et al*., 2015).

Thus, many strategies in combination therapy involve targeting of the cell's DNA damage response pathways such as the use of PARP inhibitors as previously mentioned (Cho *et al*., 2022). Inhibiting the cancer cells from DNA repair, inducing catastrophic cell cycle arrest, and inducing apoptosis. Other strategies have involved the targeting of other various mechanisms cancer cells use to survive therapeutic challenge, such as the upregulation of antioxidants to neutralize reactive oxygen species (ROS) generated by radiotherapy or chemotherapy (Gupta *et al*., 2020). For example, the chemotherapeutic agent imexon, has been shown to alter the activity of the antioxidant glutathione, resulting in cell death, this drug is used to treat several advanced cancers including breast, lung, and prostate (Moulder *et al.,* 2010 and Sheveleva *et al*., 2012).

1.6.2 Mechanism of action of Doxorubicin

As mentioned above, chemotherapy is the main form of treatment available for TNBC. Doxorubicin (DOX) is one of the most common drugs given as part of this regimen to patients with TNBC. DOX is one of the most widely used chemotherapeutic agents and has been in use since the1960s. It is part of the anthracycline family of chemotherapeutic agents and is derived from *Streptomyces peucetius* bacterium. DOX intercalates in the DNA and alters topoimerase II mediated DNA repair, which can ultimately lead to cell apoptosis (Taymaz-Nikerel *et al.,* 2018). DOX can also generate ROS which are free radicals that can induce single strand (SS) and double strand (DS) breaks. When accumulated these breaks lead to the activation of caspase 3 and through the apoptotic pathway result in cell death (Gewirtz *et al.,* 1999). DOX is given to patients intravenously and has been coined "the red death" or "the red devil" due to its red pigmentation. Unfortunately, the are many adverse side effects associated with DOX such as nausea, fatigue, alopecia, and vomiting (Cancer Research UK, 2021). Patients on long term treatment also may suffer from cardiotoxicity which occurs in 11% of patients (Saadettin *et al.,* 2005), which can limit treatment options for patients who have recurring cancer (Oikonomou *et al*., 2019). Similarly to patients who undergo radiotherapy (as discussed above Section 1.7.1) cardiotoxicity can also be experienced by patients who undergo DOX chemotherapy.

The method in which DOX induces cardiotoxicity involves an increase in oxidative stress, induction of cardiac specific genes and the induction of cardiac myocytes (Luu *et al*., 2018). Congestive heart failure can also occur in patients depending on age, treatment time and underlying heath conditions. If patients develop congestive heart failure, the 1-year survival rate is only 50% (Johnson-Arbor, Dubey 2020).

Therefore, by reducing the doses of DOX and radiotherapy this may lead to lesser complications, and a combination therapy composed of appropriate agents may enable this.

1.6.3 Therapy resistance in TNBC

The success of the standard treatment of care described above is limited as it is well documented that TNBC patients initially respond very well to chemotherapy however eventually develop therapy resistance and tumour metastasis (Isakoff, 2010). One of the main issues in TNBC is the acquired resistance to treatment, thus any development of novel therapies needs to fill that clinical space of overcoming therapy resistance. To date there have been a small number of targeted drugs approved for the treatment of TNBC, including PARP1 inhibitors (Talazoparib and Olaparib), programmed cell death-1 ligand (pembrolizumab, atezolizumab) and antibody conjugate drug (sacituzumab-govitecan) (Lee *et al.,* 2021). However, these therapies do not fully meet the clinical need (Xupeng *et al.,* 2021). Therapy resistance remains the main issues faced with TNBC patients as detailed in Figure 1.3.

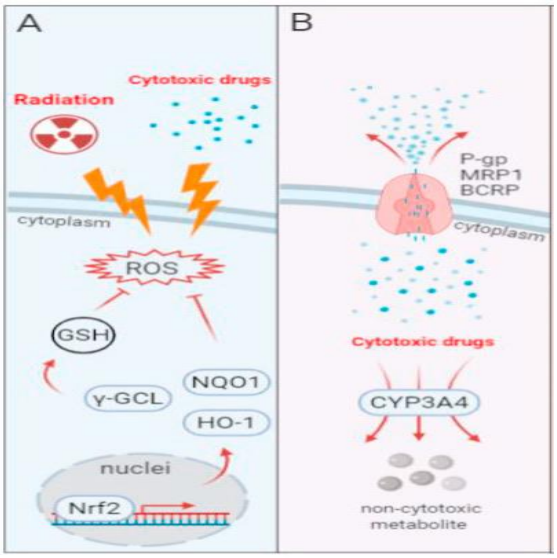

Figure 1. 3 Mechanisms underlying TNBC therapeutic resistance.

(A) Stronger antioxidant ability is mainly mediated by the over-activation of Nrf2 that promotes the protein expression of antioxidant genes, including NQO1, HO-1, and γ-GCL, and increases the intracellular level of GSH to reduce radiation- or drug-induced intracellular ROS accumulation. (B) The higher expressions of P-gp, MRP1, and BCRP mediate drug efflux and reduce intracellular drug accumulation, while phase I xenobiotic-metabolizing enzymes, such as CYP3A4, mediate intracellular detoxification of cytotoxic drugs. acid-binding Ig-like lectin 10. Taken and adapted with permission from Cancer letters Copyright Clearance Centre's Rights Link® service (Bai *et al*., 2021).

It has been demonstrated by previous studies such as one undertaken by Sarmiento-Salinas *et al.,* (2019), that TNBC cells contain higher intracellular GSH level than other types of breast cancer. As a result, the NRF2 pathway is often activated to prevent damage caused by ROS as seen in Figure 1.3A and in therapy resistant cells this antioxidant mechanism is enriched, supporting the targeting of this GSH pathway as a strategy that may solve this clinical need. Another well documented mechanism of therapy resistance is drug efflux and metabolism mediated chemoresistance as seen in Figure 1.3B. Although some clinical success has been seen when using drug efflux inhibitor in ovarian cancer, these drugs have not been clinically evaluated in TNBC patients (Johnatty *et al.,* 2013)

Therefore, to undertake meaningful experiments, we must therefore test any novel schemes in a range of cell lines with varying levels of resistance to existing therapies. To model this phenomenon within this project we developed therapy resistance cell lines. We have initiated the production of MB-MDA-231 cells serially incubated with DOX and or radiation therapy with surviving colonies serially exposed and collected. This process was repeated for several months to generate a large bank of doxorubicin and radiation resistant cells similarly to the process carried out by McDermott *et al.,* (2014).

1.7 New approaches to the treatment of TNBC

1.7.1 Glutathione

Due to the lack of targetable receptors in TNBC, advances in treatments have been relatively stagnant for many years, suggesting the need for a different therapeutic approach such as targeting cellular metabolites. In a study carried out by Beatty *et al*., (2017), it was discovered that TNBC cells are reliant on glutathione biosynthesis. Glutathione (GSH) is a thiol and the most abundant non-protein molecule found in cells, it acts as a free radical scavenger and protects cells from reactive oxygen species (ROS) damage (Kennedy *et al.,* 2019). Glutathione binds to potential toxins via its reactive sulfhydryl moiety (Balendiran *et al*., 2004; Sies, 1999). In healthy cells, GSH is essential for detoxification, however, in cancer cells it is associated with poor prognosis and development of therapy resistance (Kennedy *et al*., 2020). These findings that TNBC is sensitive to glutathione levels were also consistent with other publications which reported that agents that limit the availability of glutathione precursors enhance both glutathione depletion and TNBC cell killing by γ–glutamyl cysteine ligase inhibitors *in vitro* (Gross *et al.,* 2014; Lien *et al*., 2016 and Timmerman *et al.,* 2013). In a study carried out by Miran *et al.,* (2018), it was found that by altering the intracellular levels of glutathione in TNBC the activation of apoptotic pathways was promoted. Ultimately, the literature surrounding this area of research suggests that in TNBC, high levels of glutathione are associated with poor patient prognosis as it supresses the reactive oxygen species induced by both radiation and chemotherapy drugs, inhibiting apoptotic pathways and promotes cancer cell survival (Beatty *et al*., 2018).

ROS are a group of molecules known as free radicals, they contain oxygen, and an accumulation of these particles can lead to intracellular DNA damage which often results in cell death (Nakamura *et al.,*2021). A known target of ROS are mitochondria, owing to their potential to initiate apoptosis via caspase induced mechanism of action. In cancer cells ROS play a key role in therapy resistance. The Nuclear factor E2-related factor 2 (NRF2) protein protects cells again damage via ROS and is known to be upregulated in cancer cells and is associated with poor prognosis (Jeddi *et al.,*2017). Therefore, the potential of targeting the glutathione biosynthetic pathway as a therapeutic strategy in TNBC should be further investigated.

Given the mechanism of action of these therapies discussed, it was hypothesised that doxorubicin administered in combination with a glutathione inhibiting agent may produce a synergistic combination therapy. By inhibiting the synthesis of the antioxidant glutathione, this would allow ROS generated by DOX or radiation therapy to induce SSB and DSB, which when accumulated would activate the caspase 3 pathway resulting in cell death via apoptosis.

1.7.2 Fumaric Acids

Dimethyl fumarate (DMF) is currently used as a treatment for multiple sclerosis (Mills *et al.,* 2018). However, in recent years DMF has been investigated as a treatment for cancer as a NRF2 axis inhibitor and a Phase I investigation into its use in glioblastoma in combination with temozolomide and radiation begun in 2020 (Shafer *et al.,* 2020). Promisingly, it has been reported that DMF has no significant toxic effects on non-tumorigenic cells (Fig 1.4) (Saidu *et al*., 2018).

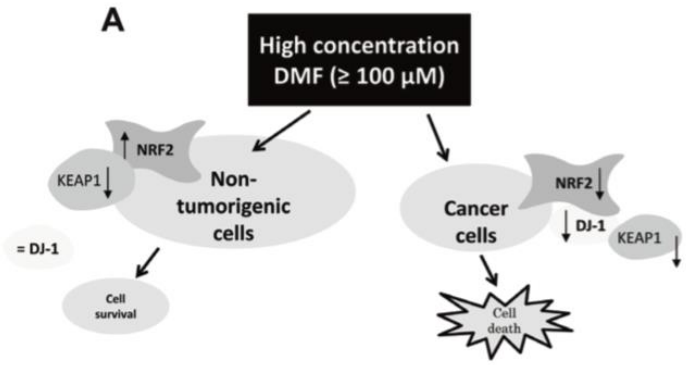

Figure 1. 4 Proposed mechanism of DMF-induced cell death in malignant and non-tumorigenic cells.

Taken and adapted with permission from Saidu *et al* 2018 using Open Access Creative Commons Attribution License 3.0 (CC BY 3.0).

This study carried out by Saidu *et al.,* (2018), showed that the NRF2 pathway enhances cancer cell proliferation and promotes chemoresistance in several cancers and as previously described, acts as an antioxidant to the ROS that is upregulated following treatments such as radiotherapy and DOX treatment. This enriched activation of NRF2 has also been documented in TNBC cells (Syu *et al.,* 2016) and is shown to result in therapy resistant TNBC cells. In non-cancerous cells, DMF has also been reported to enhance NRF2 activity. In studies carried out by Saidu *et al*., (2018), the authors reported that the concentration of DMF was critical in inducing cancer cell death, at concentrations of <25μM DMF induced a protective NRF2 antioxidant pathway. However, at concentration >25μmol, DMF was found to induce oxidative stress and cause the death of cancer cells in several different cell lines such as OVCAR3 (human ovarian cancer cell lines) (Figure 1.5).

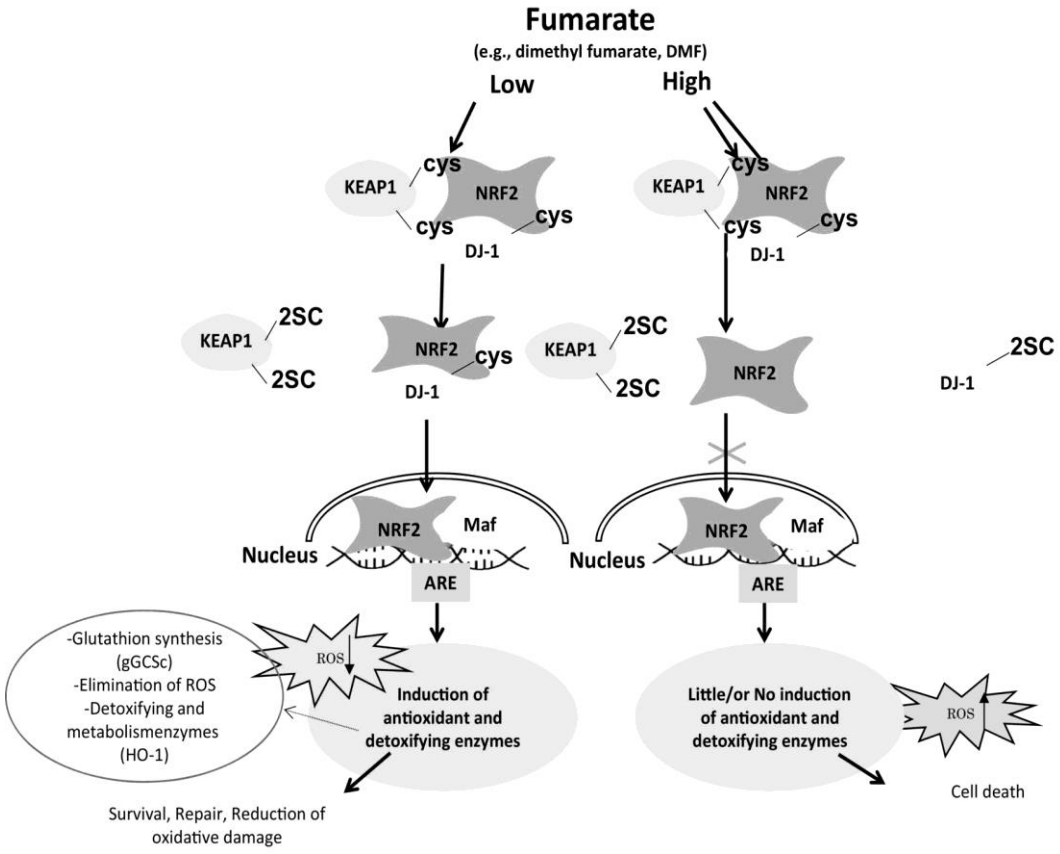

Figure 1. 5 Proposed mechanism of DMF-induced cancer cell death.

Low concentrations of DMF can induce the NRF2 antioxidant pathway, allowing NRF2 nuclear translocation and binding to the antioxidant response elements leading to the transcription of antioxidant and detoxifying enzymes, thereby promoting cell survival. High concentrations of DMF, however, induce disruption of the NRF2 stabilizer DJ-1, which in turn impairs NRF2 induction and transcriptional activities in response to DMF, ultimately inducing ROS generation, GSH depletion, hence facilitates cancer cell death.

This induced cell death was found to be in direct relation to downregulation of the NRF2 gene. The authors investigated this relationship using human ovarian cancer OVCAR3 cells and determined that DMF alters the expression of an NRF2 protein stabilizer called DJ-1 (which is found to mediate the activation of NRF2) antioxidant defences and cell death in the ovarian cancer cell line (Figure 1.5). It is known that in cancer cells a higher base level of NRF2 is present (Saidu *et al.,* 2018). By administering a high concentration of DMF, this inhibits NRF2 translocation to the nucleus via the NRF2/DJ-1 pathway (Figure 1.5) and in turn inhibits the production of antioxidants, such as GSH. In cancer cells DMF is also able to able to inhibit γ-GCS which is the first enzyme in the biosynthesis of GSH. This results in a reduction in GSH production intracellularly. This is carried out via a Michaels Reaction which induced oxidative stress through the depletion of intracellular GSH (Okazaki *et al.,* 2020).

This reflects the findings of previous studies that suggest that tumour resistance to chemotherapies are possibly dependant on the upregulation of glutathione and the overexpression of NRF2 (Jaramillo *et al.,* 2013). Taken together these results imply that the mechanisms of action of DMF are dose dependant for the induction of cancer cell death. These studies highlight the need to evaluate DMF at various concentrations as the balance between protective and cell death induction is critical for the success of this therapy to bind to glutathione and prevent the free radical scavenger from neutralising ROS, in turn sensitising the cells to ROS damage.

There has however been concerns expressed about the utility of DMF as a cancer therapy. The mechanism of action of DMF as described by Brennan *et al.,* (2015), suggested that although DMF was shown to produce an acute concentration-dependent depletion of GSH initially, 24 hours after treatment the GSH level rose exponentially to above the initial base line recorded prior to any treatment. These findings support the idea that there is a much deeper investigation into the role of DMF in cancer treatment that is needed to better understand its potential. As previously described, GSH is a key target to mediate cellular response to ROS. By inhibiting the intracellular GSH via DMF administration. I hypothesises that by inhibiting GSH synthesis and preventing the neutralisation of ROS, generated via chemotherapy or radiotherapy, this will result in an increase in cell death as the protective mechanism that is preventing damage via ROS will be inhibited in cell exposed to DMF.

1.7.3 Monomethyl Fumarate

Monomethyl fumarate (MMF) is the direct metabolite of DMF and in the body, DMF is rapidly hydrolysed by esterase's and is subsequently converted to its only active metabolite, as is shown in Figure 1.6 (Lategan, T.W. *et al.* 2021).

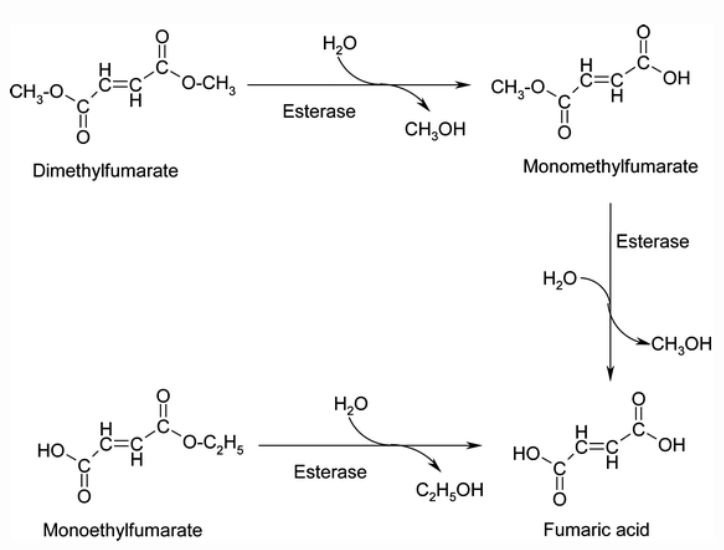

Figure 1. 6 Structures of fumaric acid esters and possible ways of hydrolysis in vivo. Taken with permission from Archives of Dermatological research Copyright Clearance Centre's Rights Link® service. (Rostami-Yazdi, Clement and Mrowietz, 2010).

The mechanisms of action of MMF intracellularly are not fully understood, although recent investigations suggest that MMF has a different mechanism of action than DMF (Brennan *et al.,* 2015). At present, the understanding is that both DMF and MMF act in the same manner, inhibiting intracellular synthesis of glutathione and as a result, the cell fails to neutralise ROS which have been generate and the cell is left unable to protect itself from DNA damage induced by these ROS (Okazaki *et al.,*2020).

1.7.4 Diroximel Fumarate (EMF)

Diroximel Fumarate (EMF) was approved in 2019 (in the US) for the treatment of Multiple Sclerosis (MS) and is less likely to cause gastrointestinal problems than DMF (Palte *et al*., 2019). Again, the mechanism of action of this drug is yet to be fully understood although it is thought to have the same mechanism of action as DMF. MMF is the active metabolite of EMF, and upon administration binds to the antioxidant GSH, ultimately leading to an accumulation of ROS and the damage induced by them such as, DBS (as previously discussed) (Okazaki *et al.,*2020). Due to the lack of a methanol leaving group in the chemical structure of EMF, and the substitution 2-hydroxyethyl succinimide, this results in reduced gastrointestinal problems with this drug (Diroximel fumarate - Drug Bank, 2020). This drug will also be investigated alongside MMF and DMF to determine of it has any potential to enhance cancer cell kill when administered in combination with chemotherapy or radiation.

1.8 Drug Repurposing

There are many positive attributes to repurposing already licensed drugs to treat a variety of diseases, one such aspect is the financial attractiveness of developing pre-approved drugs. Once a clinically utilised drug patent has expired, the market value of the compound decreases dramatically, making it more financially accessible for research and development opportunities (Vondeling *et al.,* 2018). Additionally, there is an accelerated process when putting a therapy forward for clinical evaluation if this therapy has already gone through all phases of a clinical trial for licencing. For example, there is no need to perform a Phase 1 trial as the results are already known (Drug repurposing: Advantages and key approaches 2023). Additionally, the off-target effects and metabolic processes of the drug are already known and have been accepted previously. There is also the added aspect of accelerated time that it takes to progress these repurposed drugs through clinical approval. On average it takes

three to four years to reach clinical trial stage of development with the reduced cost from 12 million USD to 1.6 million USD (Ashburn *et al*., 2004; Ismail *et al.,*2018).

One known example of repurposing a drug across different therapeutic areas of research is Clarithromycin, an antibiotic used to treat bacterial infections (Clarithromycin: Uses, dosage & side effects 2023). This drug is currently being investigated for the treatment of cancers including multiple myeloid leukaemia, chronic myeloid leukaemia and lung cancer and colorectal cancer (Van Nuffel *et al.,* 2015 and Petroni *et al.,* 2020).

Much like clarithromycin, DMF would be a useful drug to repurpose for the treatment of TNBC. This drug has been long since approved (2014) making the drug cheap to purchase for research and development, as well as the non-toxic effects that DMF exhibits on non-cancerous cells being well documented through previous clinical trials (Tecfidera, inn-dimethyl fumarate - European medicines agency 2023). From a pharmaceutical investment point of view, repurposing a drug such as DMF to treat a cancer that is in desperate need more effective treatments such as TNBC, is cheaper and faster mode of action to get a therapy to clinical trial.

1.9 Spheroid tumour model

The initial stages of *in vitro* work when investigating a novel cancer treatment is 2D cell culture assays, however there are several issues when relating 2D cell cultures to patient tumours. Cell morphology, behaviour and heterogeneity are among the main differences observed between 2D and 3D cancer models (Theodossiou *et al*., 2019). It has also been shown by Hirschhaeuser *et al*., (2010), that in 3D cell models, there are significant differences in which genes are expressed and what signaling pathways are activated compared to 2D cell culture models. Therefore, 3D models such as multicellular tumor spheroids (MTS), are widely accepted as the next step following on from 2D viability assays such as clonogenic assay as they provide a much more accurate representation of how cancer cells within a tumor would behave when exposed to novel treatments (Haycock, 2011; Mehta *et al*., 2012) (Figure 1.7).

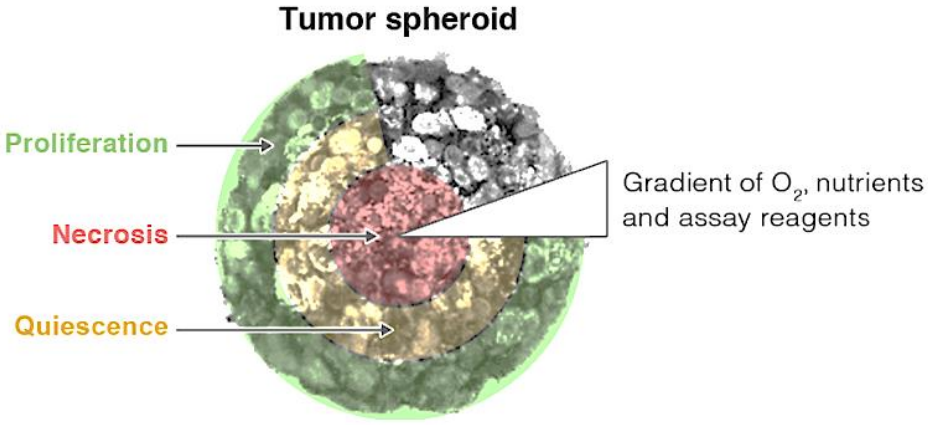

Figure 1. 7 Image of a spheroid tumour model. Detailing cells in different states, proliferating, quiescent and hypoxic as concentration gradient of oxygen decreases moving into the centre of the spheroid. Take from (Introduction to 3D Cell Culture, 2021).

The size of the spheroids matters a great deal when investigating novel treatments using this model. As the spheroids begin to grow, they consist of proliferating cells which then develop a concentration gradient for essential nutrients that the 3D structure needs to continue to grow (oxygen and disposal of waste). This causes an inner necrotic core in the spheroid as the cells at the center of this 3D model are farthest away from nutrients and oxygen (Figure 1.7). This usually begins to occur when the spheroid grows to around 350 µm. The MTS continue to grow, now consisting of an outer proliferating layer of cells a middle quiescent layer (non-dividing cells) and an inner necrotic core that is more representative of a patient tumour which consists of an active proliferating outer layer and a hypoxic centre deprived of oxygen and nutrients (Mehta *et al*., 2012). Critically a quiescent middle layer where cells are viable but not dividing is also like an *in vivo* tumor. It is critical to consider this cell population when considering any new therapies as non-dividing, but viable cells are less likely to be affected by cycle specific therapies such as chemotherapy and radiotherapy. Monolayers are all proliferating cells and contain no quiescent and hypoxic cells, this is critical when investigating cancer as many treatments fail due to not being able to kill hypoxic cells or which are cycle specific (Graham and Unger, 2018).

1.10 Chick Embryo Model

The Chorioallantoic Membrane (CAM), also known as the chorioallantois, is a highly vascularized membrane found in the eggs of certain amniotes like birds and reptiles (Garcia *et al.,* 2021). It is formed by the fusion of the mesodermal layers of two extra-embryonic membranes – the chorion and the allantois and it is the avian homologue of the mammalian placenta. It is the outermost extra-embryonic membrane which lines the non-vascular eggshell membrane. Given the characteristics of this membrane, researchers have been investigating the use of the CAM for development of a variety of *in vivo* models which have the potential to reduce and replace procedures in rodents (Swadi *et al*., 2019). The CAM model involves undertaking procedures in chick embryos where the CAM develops as this is a lower sentience model than rodent models which reduces suffering and is a much cheaper alternative to rodent models with a potentially higher throughput.

Due to the award of an NC3Rs grant we received funding to translate this model for use as an alternative cancer model to mouse xenographs and to set up a chick embryo model (CEM) facility with replicable methodology at the University of Strathclyde. The aim of our project is to train and equip researchers primarily at the University of Strathclyde to be competent with the model and its methodologies including the correct storage and handling of the chick embryos. We have transferred methods developed in the University of Liverpool, with the aim to develop CAM tumour models and use them to analyse cancer cells, the efficacy of combination therapies and drug gene delivery systems. Part of this project was therefore to develop a methodology to grow TNBC cells in the CAM model to allow for investigations that involve the use of novel single or combination therapies and to validate the model by comparison to our existing mouse xenograft data.

1.11 Aim

The aims of this project were to;

- Investigate the use of novel combination therapies using repurposed drugs (DMF, MMF and EMF) for the treatment of TNBC in combination with DOX or radiotherapy. This was carried out using 2D and 3D cell culture models, as well as a variety of mechanistic investigations to determine if any critical intracellular pathways were altered by combination therapies.

- To determine if a combination of DOX or radiation with repurposed drugs have the potential for greater toxicity than the current gold standard for TNBC patients, the aims focused on the synergistic effects of these two therapies in combination with non-toxic fumaric acids. This was determined using clonogenic survival assay and spheroid models to identify any synergism found when administering scheduled combination therapies.
- To determine whether administering the combination therapies in a scheduled manner has any impact on the survival of TNBC cells using methods previously mentioned.
- To develop TNBC resistant cell lines and determine if the developed combination therapy can reduce the survival of these cells, potentially highlighting a therapy that could be used to treat patients with recurring TNBC. Again, this investigation will be carried out using 2D and 3D methods as previously described.
- To develop the CEM for its use as an *in vivo* model that can be used for cancer research investigations to test novel therapies with the focus on reducing *in vivo* murine models that are currently used for preclinical investigations.

It was hypothesised that the combination of DOX + DMF/MMF or the combination radiation + DMF/MMF will lead to a more enhanced cell kill of TNBC cells, than the single therapies DOX or RAD alone. Given their mechanism of action of DMF/MMF, inhibiting the synthesis of antioxidants such as GSH, it was hypothesised that this will allow for DOX or radiotherapy to generate ROS that will induce SSB and DSB, which when accumulated activate the caspase 3 pathways and ultimately result in cell death via apoptosis.

Additionally, it was hypothesised that following the generation of DOX or radiation resistant cells, the designed combinations will have the desired effect of re-sensitising the resistant cells to death via DOX or radiotherapy by inhibiting the above-described synthesis of cellular protective antioxidants. Further hypothesises were that these novel combinations will achieve a more effective, less toxic induction of cancer cell death in TNBC cell lines regardless of the cell's mutational status.

1.11.1 Project Impact.

Most importantly, the project has the potential to impact the survival and quality of life of patients with triple negative breast cancer and their families. The project is anticipated to lead to a novel therapy in an area of real clinical need which is more efficacious and less toxic than the current gold standard. As the proposed combination utilises drugs which are already in the clinic and we are repurposing already approved treatments, this offers a more rapid and less expensive route to clinical adaptation thus hastening future impact.

This study will also add scientific knowledge and benefit researchers in the field and will lead to research publication and esteem for the Group, Department and University. The project also has the potential to engage company partners in the latter stages and the combination may be novel and commercially attractive thus offering income generating opportunities and novel intellectual property.

Chapter 2

Treatment of TNBC cells in 2D culture using Doxorubicin and Radiation in combination with Fumaric Acids

2.1.1 Introduction

The standard of care for triple negative breast cancer (TNBC) patients remains surgery and cytotoxic systemic chemotherapy, with DOX being one of the most used chemotherapeutic drugs (Arora *et al.,* 2021). DOX is an anthracycline and as well as blocking the enzyme topoisomerase II, which is responsible for the repair of DNA strand breaks, it is also able to initiate a cascade of events that induce ROS and mediate changes of intracellular calcium (Nitiss and Nitiss 2014). DOX is an inhibitor of Topoisomerase ii, meaning that ultimately cell proliferation is inhibited, and DNA damage is induced which results in cell cycle arrest and potentially cell death. There are however side effects associated with DOX, including nausea, vomiting, alopecia, and cardiotoxicity (Nedeljković and Damjanović, 2019). The reason for the previously described lack of targetable receptors on the surface of TNBC cell are preventing the development of less toxic therapies for TNBC patients. Unlike ER+ breast cancer cells or HER+ breast cancer cells, there are not yet identified receptors to pharmacologically target TNBC (Bianchini *et al*., 2016). With the focus on improving this treatment, development has been on targeting the molecular pathology of the TNBC cell as described in chapter 1 and identify potential bio markers that would act as prognostic indicators such as HIF-1α, RNUX or NRF2 (Jögi *et al* 2019, Fu *et al.,* 2022 and Almeida *et al.,* 2020).

Another important factor to consider when treating TNBC is the age of the patients, generally the average age of a person with TNBC was found to be 46.26 ± 12.22 years, while the average age of patients with other types of breast cancer being 52.90 ± 9.78 years (Sajid *et al*., 2014). TNBC patients can first develop the disease at a much younger age than other breast cancer patients, meaning that their lifestyles and quality of life differs from other older cancer patients. Furthermore, the current treatments have many off target effects and can leave the patient with severe morbidities and unable to care for dependants, leading to increased living costs (Huang *et al.,* 2022). It is therefore of great urgency to find treatments for TNBC patients that are more effective, but also less toxic, as this will increase the quality of life of TNBC patients.

2.1.2 Radiotherapy

Although there are still clinical issues in treating TNBC, it is understood that the use of radiotherapy post-surgery is beneficial to the survival of patients (He *et al.,* 2018). However, much like the pharmacological targeting of TNBC, there are still challenges to overcome when using radiotherapy to treat TNBC (Azoury *et al*., 2022). A meta-analysis carried out by Kyndi *et al.,* (2008) indicated that the recurrence of TNBC after radiotherapy was higher than that of other types of breast cancer (BC), and it was found that the TNBC cell lines were more likely to develop radio-resistance than other Luminal BC cells (Hou *et al.,* 2016). As previously mentioned, there are off target effects associated with breast radiotherapy, particularly cardiotoxicity when the left breast undergoes radiotherapy (Vadivelu *et al*., 2013). There is therefore a clinical need to reassess radiotherapy as a treatment for TNBC, to reduce toxicity to normal tissue and to overcome resistance patients ultimately develop or to mediate the dose of radiation patients receive to reduce off target effects.

2.1.3 Glutathione

GSH is an intracellular antioxidant, tripeptide formed of three amino acids; Glutamic acid, Cysteine and Glycine, and is synthesised in the cytosol and actively pumped into the mitochondria of cells. GSH is an antioxidant which neutralises reactive oxygen species by donating a H^+ and is also involved in the detoxification of chemicals and pollutants (Lu, 2013). GSH plays a key role in the detoxification of endogenous compounds and xenobiotic compounds as it facilitates the excretion of mercury from cells and neutralizes oxidative chemicals (Pizzorno *et al*., 2014). GSH exists in 2 forms intracellularly (Figure 2.1) reduced (GSH) and oxidized (GSSG). The balance of these two compounds is essential to maintaining healthy homeostasis

intracellularly, giving GSH both protective and pathogenic roles. When the ratio of these two compounds drops to 1 in 10, the cells become sensitive to oxidative stress.

Figure 2. 1 The two states in which glutathione exists.

Taken and adapted with permission from Saidu *et al* 2018 using Open Access Creative Commons Attribution License 3.0 (CC BY 3.0).

There are several diseases associated with depletion of GSH including Alzheimer's, Parkinson's, COPD, HIV, Hypertension, Liver disease and Cystic Fibrosis (Ballatori *et al*., 2009). GSH levels can be maintained through diet, and although diet can alter glutathione in the body, pharmacological agents such as Fumaric Acids can be used to inhibit the up-regulation of GSH levels in cells (Pizzorno., 2013).

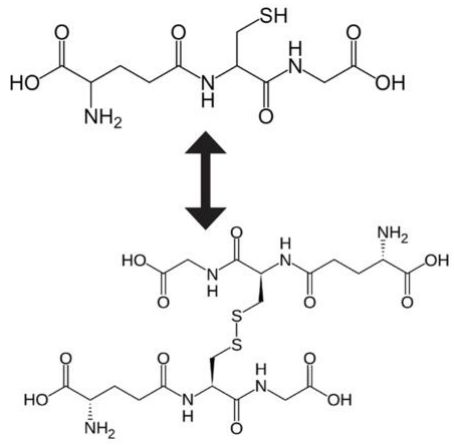

In recent years, the investigation of GSH and its role in cancer has been generating interest in the research community (Figure 2.2). For example, it has been shown that cisplatin resistance was associated with GSH detoxification (Godwin *et al.,* 1992 and Pathania *et al.,* 2018). Decreasing the level of intracellular GSH, as demonstrated by Xu *et al*., (2019) showed that not only was the efficacy of cisplatin increased but the cisplatin resistance was reversed.

Given this mode of action of glutathione, we hypothesised that by reducing the intracellular levels of Glutathione, TNBC cells will be sensitised to damage via agents which induce the production of ROS such as Doxorubicin and Radiotherapy. By reducing the intracellular levels of glutathione through the pharmacological properties of fumaric acids, we hypothesise that the TNBC cells will have a reduced ability to neutralise any reactive oxygen species that would have resulted in DNA damage and that this will ultimately lead to cell death.

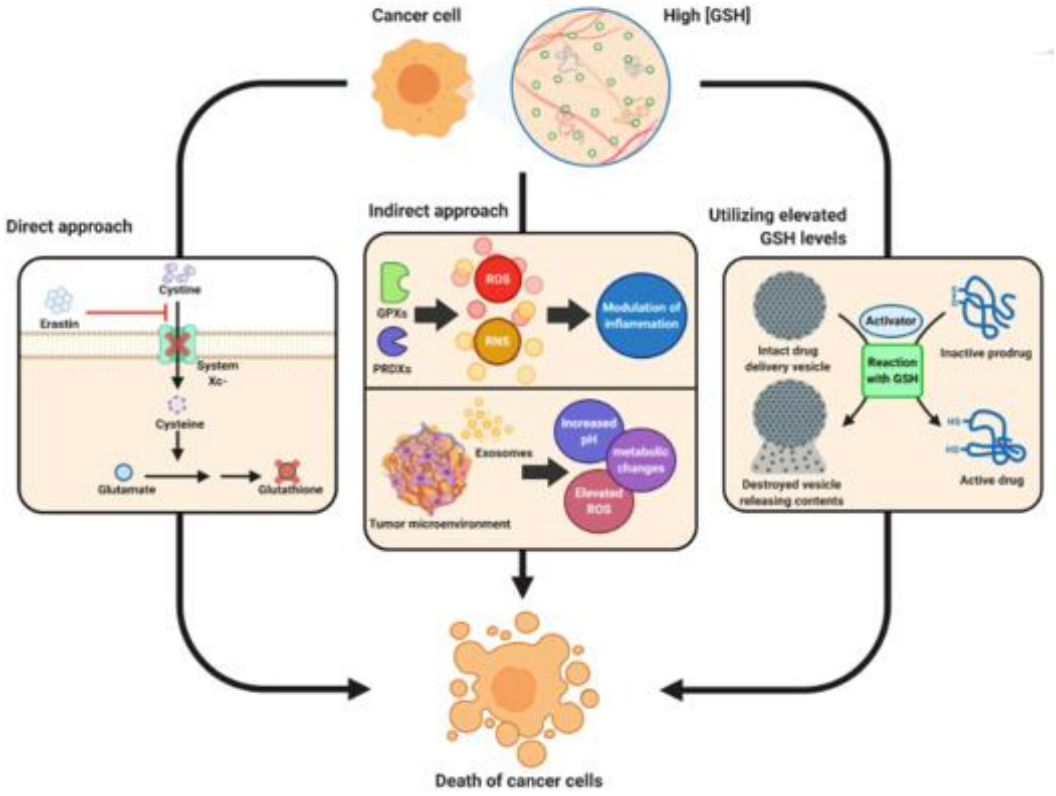

Figure 2. 2 The direct and indirect effects of targeting Glutathione.
How utilising the levels of intracellular glutathione can lead to cell death in cancer cells. taken from Taken and adapted with permission from Kennedy et al., (2020). using Open Access Creative Commons Attribution License 3.0 (CC BY 3.0).

2.2.1 Aims

The aims of this chapter are:

- To determine the cytotoxicity of fumaric acids alone on MDA-MB-231 human TNBC cells via clonogenic assay
- To determine the cytotoxicity of fumaric acids in combination in MDA-MB-231 cells with Doxorubicin and Radiation via clonogenic assay
- To investigate mechanistic underpinning of any observed effects in these cells after treatment with combination therapies.

2. 3 Materials and Methods

2.3.1 Cell Lines

The MB-MDA-231 Triple Negative Breast Cancer cell line derived from the breast tissue of a 51-year-old female (MDA-MB-231 | ATCC, 2021). Cells were maintained in Dulbecco's Modified Eagle Medium (DMEM) supplemented with penicillin/streptomycin (100U/ml), fungizone (2 μM/ml), L-glutamine (200 mM) and 10% (v/v) foetal calf serum (all supplied by Fisher Scientific UK). Media was checked for sterility before use by placing in an incubator set at 37 ^{o}C with 5% CO_2, for 5 days.

2.3.2 Maintaining cells.

Once MDA-MB-231 cells reached 70% confluence, complete media was removed from the T75 cm^2 flasks (Fisher Scientific UK) and washed with 4 mL PBS. 3 mL of 0.05% trypsin (Fisher Scientific UK) was then added to the flasks and then cells were incubated until the cells detached (approximately 10 minutes). 10 mL of fresh complete media was then added to the flask to neutralise the trypsin. A single cell suspension was achieved by gentle passage of the cells through a sterile 25 mm needle (BD Microlance). Three new T75 cm^2 flasks containing 20 mL of complete DMEM media were then seeded with various volumes of the cell suspension (1 mL, 3 mL, and 5 mL) to maintain stock levels of viable cells of varying confluence. Cells were routinely tested for the presence of mycoplasma via a PCR test (Minerva Biolabs GmbH, 56-1010 and 11-1050).

2.3.3 Freezing of Cells

In line with the recommended maintenance of the MD-MBA-231 cell line, cells were cryopreserved in order to preserve healthy cells at low passage number to use in future experiments. After detaching the cells using 0.05% trypsin, the cell suspension was spun down at 1000 RPM for 5 minutes and the media removed. The pellet was resuspended in 5mL complete DMEM media and the cells counted by using a haemocytometer (Jencons, UK) and then $1x10^6$ cells were aliquoted into 1 mL cryovial tubes (StarLab UK) containing cell freezing medium (10% FBS (Fisher Scientific UK), 10% DMSO (Sigma Aldrich, UK), 80% cell suspension in complete media) before freezing at -80 ^{o}C for 2 weeks and subsequently removal to liquid nitrogen for long term storage.

2.3.4 Thawing Frozen Cells

The cryovials containing 1 mL of frozen cells were removed from the -80 ^{o}C freezer and defrosted at room temperature. The tubes were spun at 1000 RPM for 5 minutes and the freezing buffer was removed before resuspending the pellet in 1 mL complete media. The cells were transferred into a T25 cm^2 flask (Fisher Scientific UK) with 5 mL complete DMEM media. This flask was then incubated for 3 to 5 days to allow cells to grow to around 70% confluence before transfer of the cells into a T75 cm^2 flask (Fisher Scientific UK) containing 15 mL complete media.

2.3.5 Cell Doubling Time

A population doubling time (PDT) assay was used determine the time needed for the MD-MBA-231 cells to double in number. This assay was undertaken to establish the time that the cell lines would be incubated with drugs (48 hr doubling time). This protocol was carried out in triplicate, cells were plated out in 7 different T25 cm^2 flasks with 5 mL of complete media added to each flask. At 24-hr intervals, one T25 cm^2 flask was taken, and media was poured off, and the cells were washed with PBS and 2 mL of 0.05% trypsin solution was added. The flask was then incubated until the cells had detached (approximately 10 minutes). A haemocytometer was then used to count the number of viable cells. This process was repeated for 7 days. The cell doubling time was determined using the following equation:

$$\text{Doubling time} = (t2 - t1) \times [\log 2 / \log (q2) - \log (q1)] \qquad \text{(Equation 1)}$$

Where: q1 and q2 are the number of cells measured at initial time t1 and final time t2, respectively.

This assay was carried out in triplicate and the results were analysed in GraphPad prism (version 9.2.1).

2.3.6 Drug preparations

DMF, MMF and EMF stock solutions (Sigma Aldrich UK) were prepared by diluting; 0.25 g of EMF (255.22 g/mol), 140 mg of DMF (MW 144.127 g/mol) and 6.5 mg of MMF (MW= 130.10 g/mol) in 10 mL DMSO. All solutions where then filtered using a 0.2 mm sterile filter (Sigma Aldrich UK). A 500 µM working solution was prepared by

diluting 50 µL DMF in 9.95 mL PBS, 500 µL EMF in 9.5 mL and 1000 µL MMF in 9 mL PBS, all stored at 4 ˚C in the fridge.

Single therapies were treated at doses of; DOX 0.02 µM, MMF 2 µM, DMF 100 µM and X-irradiation 2 Gy. Combinations were also investigated and carried out using 3 combination schedules as detailed below. Again, using the drug concentrations stated (DOX 0.02 µM, MMF 2 µM, DMF 100 µM and X-irradiation 2 Gy).

SCHEDULING	DRUG COMBINATION	ORDER OF ADMINISTRATION
SCHEDULE 1	DOX/ RAD+ Fumaric Acid	Simultaneous
SCHEDULE 2	DOX/ RAD + Fumaric Acid	Dox /Rad1st, Fumaric acid 24hr after
SCHEDULE 3	DOX/ RAD + Fumaric Acid	Fumaric Acid 1st, Dox/ Rad 24 hr after

Table 2.1 This table shows the drug combinations and order of administration (scheduling)

2.3.7 Clonogenic Assay

Clonogenic assays were carried out on MDA-MB-231 cells to calculate the clonogenic capacity of these cells, representing cell survival after exposure to treatments of both drugs and radiation therapies. Cells were then treated with the relevant single agents; Doxorubicin 0.02 µM, X-radiation 2 Gy, 100 µM DMF and MMF 2 µM. The three combination treatment schedules were assessed to investigate their clonogenic potential post treatment between, MMF (2 µM) + DOX (0.02 µM) or X-radiation (2 Gy). As previously described schedule (SCH) 1 (DOX/Rad + MMF/DMF) was administered simultaneously. Schedule (SCH) 2 DOX/Rad was administered 24 hrs before MMF/DMF. Schedule (SCH) 3 MMF/DMF was administered 24 hrs before DOX/Rad.

MDA-MB-231 cells were counted and 2x10^5 cells were added to a T25 cm^2 flask with 5 mL complete media and then incubated at 37 ^{o}C in a 5% CO_2 environment for 48 hrs as this is the cells doubling time. Cells were then treated with the desired drug or exposure to irradiation and incubated for a further doubling time of 48 hrs. The complete media containing the drug was then removed and cells were washed with PBS and detached using 2 mL of 0.05% trypsin. The cell suspension was then

neutralized using 3 mL of complete DMEM media and disaggregated to a single cell suspension by passage through a 21-gauge needle. Cells were then counted using a hemocytometer. 700 MDA-MB-231 cells were then seeded into 60 mm petri dishes (Fisher Scientific UK) with 5 mL of DMEM media, in triplicate. Dishes were then incubated for 14 to 21 days until colonies of more than 50 cells were visible. After the desired time, the DMEM media was removed, and colonies were washed with PBS and fixed using 100% methanol (Fisher Scientific, UK) for 10 minutes. Fixed colonies were then stained with 10% Giemsa solution (VWR, Germany) for 1 hr and then washed with water. Visible cell colonies were then counted by eye. Survival fraction was calculated as below, and data reported was an average of three independent experiments each performed in triplicate.

$$\text{Survival Fraction} = \frac{\text{(Number of colonies / number of colonies seeded)}}{\text{(Number of control colonies / number of colonies seeded)}}$$

2.3.8 Glutathione Assay

MDA-MB-231 cells were plated in T25 cm^2 flasks at 150,000 cells per flask and incubated at 37 ^oC with 5% CO_2 for 48 hrs in complete media. Cells were then treated with the relevant single agents; Doxorubicin 0.02 μM, X-radiation 2 Gy and MMF 2 μM. The three combination treatment schedules were assessed to investigate their potential to alter the intracellular level of glutathione post treatment between MMF (2 μM) + DOX (0.02 μM) or X-radiation (2 Gy). As previously described SCH1 (DOX/Rad + MMF) was administered simultaneously. SCH2 (DOX/Rad) was administered 24 hrs before MMF. SCH3 MMF was administered 24 hrs before DOX/Rad.

Cells were trypsinised and the cell suspension was centrifuged at 1000 RPM for 5 minutes, pellets were washed with PBS and treated as described in Glutathione Assay Kit CS0260-1KT, Sigma-Aldrich.

2.3.9 Cell Cycle analysis

Cell cycle analysis of MDA-MB-231 cells post treatment was carried out to determine the distribution of cells throughout the phases of the cells cycle, (Darzynkiewicz *et al*., 2017).

MDA-MB-231 cells were seeded in T25 cm^2 flasks at 150,000 cells per flask and incubated at 37 ^oC with 5% CO_2 for 48 hrs in complete media. Cells were then treated with the relevant single agents; Doxorubicin (0.02 μM, X-radiation 2 Gy and MMF 2 μM). The three combination treatment schedules use analyses of the cytotoxic interaction between MMF (2 μM) + DOX (0.02 μM) or X-radiation (2 Gy) and were assessed for their potential to alter the percentage of cells in each phase of the cell cycle. As previously described SCH 1 DOX/Rad + MMF was administered simultaneously. SCH 2 DOX/Rad was administered 24 hrs before MMF. SCH 3 MMF was administered 24 hrs before DOX/Rad.

Following exposure to or incubation with the respective treatments, complete media was removed, and cells were incubated with drug free complete DMEM until relevant analysis time was reached; 0 hrs post treatment removal, 24 hrs post treatment removal and 48 hrs post treatment removal. Cells were then washed with PBS and 0.05% trypsin was used to detach the cells from the flask. The cell suspension was then pelleted by centrifugation at 1000 RPM for 5 minutes and the supernatant was removed. The resulting cell pellet was fixed using 70% ice cold ethanol. These pellets were stored at -20 ^oC until time of use. Following this the pellets were washed with PBS and centrifuged at 1000 RPM for 5 minutes before removal of the supernatant.

Fixed pellets were incubated with 50 μg/mL ribonuclease A (Sigma-Aldrich, UK) to degrade and prevent unwanted RNA staining. Propidium Iodide 10 μg/mL (Sigma-Aldrich, UK) was added to the cell pellet to stain DNA content. After staining, the samples were refrigerated at 4 ^oC for 1 hr, in the dark.

For determination of cell cycle distribution, samples were analysed using an Attune™ NxT Flow Cytometer (Thermo Fisher Scientific, USA). The number of events per sample was measured at 10,000, and analysis of flow cytometry data was carried out using Attune NxT. All data was reported as an average of three independent experiments.

2.3.10 Apoptosis Detection

The quantification of apoptosis in MDA-MB-231 cells following relevant treatment was carried out using an anti-annexin V FITC conjugate antibody stain staining buffer (0.1

M Hepes/NaOH pH 7.4), 1.4 M NaCl, 25 mM $CaCL_2$, BD Bioscience) and propidium iodide (BD Bioscience). Each combination of these stains is reflective of a different stage the of apoptotic death pathways (viable, early apoptotic, late apoptotic and necrotic) The percentage of apoptosed cells were measured at 0 hours, 24 hrs and 48 hrs post treatment to allow investigation of cell death dynamics over time.

MDA-MB-231 cells were plated in T25 cm^2 flasks at 150,000 cells per flask and incubated at 37 ^oC with 5% CO_2 for 48 hrs in complete media. Cells were then treated with the relevant single agents; Doxorubicin (0.02 μM, X-radiation 2 Gy and MMF 2 μM). The three combination treatment schedules utilised analyses of the cytotoxic interaction between MMF (2 μM) + DOX (0.02 μM) or X-radiation (2 Gy) and were assessed for their potential to induce apoptosis. As previously described SCH 1 DOX/Rad + MMF was administered simultaneously. SCH 2 DOX/Rad was administered 24hrs before MMF. SCH 3 MMF was administered 24 hrs before DOX/Rad.

Following exposure to or incubation with the respective treatments, complete media was removed, and cells were incubated with drug free complete DMEM until relevant analysis time was reached; 0 hrs post treatment removal, 24 hrs post treatment removal and 48 hrs post treatment removal. Cells were then washed with PBS and 0.05% trypsin was used to detach the cells from the flask. The cell suspension was then pelleted by centrifuged at 1000 RPM for 5 minutes. The supernatant was removed, and the pellet washed with 1mL of PBS. Cells were then re-pelleted at the same centrifuge settings and resuspended at a concentration of $1x10^6$ cells/mL in Annexin V staining buffer (0.1M Hepes/NaOH pH 7.4, 1.4 M NaCl, 25 mM $CaCL_2$). 100 µL of each sample was then placed in an eppendorf tube for 15 minutes at room temperature, after which 5 µL of propidium iodide was added (BD Bioscience, UK).

The flow cytometry analysis was carried out using AttuneTM NxT Flow Cytometer (Thermo Fisher Scientific, USA) to measure 10,000 events per sample, where the percentage of apoptotic cells was representing the total sum of the cells in the early apoptotic phase and cells in the late apoptosis. All data were performed independently in triplicate for each data point and presented as (mean ± SD) of apoptotic cells.

2.3.11 Autophagy Detection

In order to investigate the mode of cell death following treatment, MDA-MB-231 cells were plated in a 96 well flat bottom plate at a density of 500 cells per well seeded at a volume of 100 µL cells per well and incubated at 37 ^{o}C with 5% CO_2 for 24 hrs. Cells were then treated with the relevant single agents; Doxorubicin (0.02 µM, X-radiation 2 Gy and MMF 2 µM). The three combination treatment schedules utilised analyses of the interaction between MMF (2 µM) + DOX (0.02 µM) or X-radiation (2 Gy) and were assessed for their potential to induce DNA fragmentation and inhibit DNA damage repair. As previously described SCH1 DOX/Rad + MMF was administered simultaneously. SCH2 DOX/Rad was administered 24hrs before MMF. SCH 3 MMF was administered 24 hrs before DOX/Rad.

Following exposure to or incubation with the respective treatments, complete media was removed, and cells were incubated with drug free complete DMEM until relevant analysis time was reached; 0 hours post treatment removal, 24 hours post treatment removal and 48 hours post treatment removal. Cells were then washed with PBS and trypsin 0.05% was used to detach the cells from the flask.

Following incubation of the cells with the relevant drug or radiation, the treatments were removed and 100 µL of complete media was added until the desired time post treatment was reached. After, the complete media was removed and 100 µL of assay buffer (Abcam UK ab139484) was used. Following this, 100 µL of the dual colour detection solution was added (Abcam UK, ab139484). Cells were then incubated at 37 $^{\circ}$C with 5% CO_2 for 30 minutes in the dark. At this point the fluorescence of the samples was measured using a microplate reader at set to FITC filter (Excitation ~480 nm, Emission ~530), and the Hoechst 33342 Nuclear Stain was read with a DAPI filter set (Excitation ~405, Emission ~480).

Data analysis was carried out as detailed in; Autophagy Assay Kit (ab139484), Abcam, UK. An increase or decrease in green detection reagent was relative to the FITC reading, an increase in green detection reagent is reflective of the accumulation of autophagic vessels in the cell.

2.3.12 Single cell gel electrophoresis (Comet assay)

Following treatment as described in section 2.3.12, cells were either assayed by single cell electrophoresis immediately, or incubated in fresh complete medium for a further 24 hrs or 48 hrs to allow for possible repair of DNA damage before carrying out the assay.

Following the relative incubation time, Comet SCGE assay kit, ADI-900-166, ENZO, UK was used to carry out SCGE. Complete medium was removed from the cells before addition of 2 mL trypsin 0.05% and after passage through a 23-gauge 25 mm needle (BD Microlance UK) to create a single cell suspension, the cells were counted using a haemocytometer (Jenson UK). Cells were suspended at a density of $5x10^5$ cells/mL and combined with low melting point agarose (1%) (included in ENZO ADI-900-166 kit) at a ratio of 1 in 10 (10 μL cell suspension; 90 μL gel). 75 μL of the cell/agarose mixture was then pipetted onto an ENZO comet slide until set (included in ENZO ADI-900-166 UK). The slides were then covered in lysis solution (included in ENZO ADI-900-166 UK) (25 M NaOH, 100 mM EDTA pH10, 10 mM tris base, 1% sodium lauryl sarcosinate, 1% Triton X-100) then stored at 4 ºC for 2 hours. The slides were then immersed in an alkaline solution (included in ENZO ADI-900-166 UK) (300 mM NaOH, 1 mM EDTA) for 1 hour. Cells were then washed with TBE buffer and placed in a gel tank (filled with TBE buffer, Sigma Aldrich UK) and ran at 45V for 10 minutes. Cells were then stained with 1X SYBR green dilution (included in ENZO ADI-900-166 UK) and left at room temperature in the dark until dry. Following this, slides were imaged using fluorescence microscopy (435-500nm) using an EVOS FL auto system (Life Technologies, UK). Comets were imaged and analysed as described by Geller *et al.,* 1999.
Images of the resulting comets derived from the MDA-MB-231 cells were analysed using ImageJ with plug in OpenComet v1.3. The mean number of comets analysed in each treatment group was 100.

2.3.13 Statistical Analysis

Statistical analysis was carried out using GraphPad Prism Version 9.2.1. Unless otherwise stated, the results were obtained from three independent experiments and expressed as the mean value ± standard deviation (SD). To determine which test was suitable for the specific dataset, a Shapiro-Wilk normality test was carried out. Where

this test revealed normality, a one-way ANOVA followed by Bonferroni's multiple comparison test was carried out. If Shapiro-Wilk normality test revealed data set was not normal, Kruskal-Wallis with Dunn's post hoc multiple comparison testing was carried out to assess the degree of significance. A one-way ANOVA and Kruskal-Wallis are used to determine the significance within the dataset for wither parametric or non-parametric date respectively. Bonferroni and Dunn's post hoc testing carry our pairwise comparisons to determine the significance between each of the samples, treated and untreated for example. Kruskal-Wallis utilised the median of data sets to determine significance, one-way ANOVA compares the mean number of data sets to determine significance.

2. 4 Treatment of MDA-MB-231 TNBC cells using Doxorubicin, Radiotherapy, Dimethyl Fumarate and Monomethyl Fumarate as single therapies.

We first looked at the effects on clonogenic survival of MDA-MB-231 cells incubated with DOX, DMF, MMF and EMF or exposure to X-irradiation as single agents. A clonogenic assay was used as this examines the long-term effect of treatments on cells and measures the ultimate survival of cells or clonogenic capacity. This is important because many cancer treatments do not induce cell death immediately or within 1 cell division but damage the cell so that it is no longer viable and will only replicate once or twice before cell death. This is especially important when looking at the effects of radiation on cell death as the prolonged assays allows time for mitotic catastrophe to occur in which cells are damaged by radiation but are not killed instantly, they are able to carry out several cell cycles before eventually dying.

As there are no current reports on the effect of fumaric acids on MDA-MB-231 cells, the toxicity of these drugs on TNBC cells required investigation. In this initial experiment, each of the fumaric acids DMF, MMF and EMF and their effects on MD-MBA-231 cells were investigated. DMF was selected due to its mechanism of action as it inhibits the synthesis of GSH preventing the neutralisation of ROS via antioxidant production. Inhibiting GSH had already been shown to be beneficial in TNBC as it binds to GSH and allows for higher levels of damage to be induced by ROS leading to a cell death cascade (Kwon *et al.,* 2019). MMF was selected for investigation as it is the metabolite of DMF, however literature now suggests that it has a different mechanism of action that is still unclear therefore, analysis of its activity with MDA-MB-231 cells could provide more clarity (Brennan *et al.,* 2015). The activity of EMF on MDA-MB-231 cells was also investigated as this drug acts using the mechanistic pathway as DMF, however patients receiving EMF for multiple sclerosis (MS) treatments reported that EMF was preferable due to reduced gastrointestinal issues (Diroximel fumarate - DrugBank, 2020).

All drugs were diluted to the above working stocks Section 2.3.6 and then MDA-MB-231 cells incubated with the respective drug for clonogenic analysis as described in the methods above.

2.4.1 Cytotoxicity of Doxorubicin on MDA-MB-231 cells

Figure 2.3 shows the response of MDA-MB-231 following exposure to increasing concentrations of DOX as assessed by clonogenic assay,

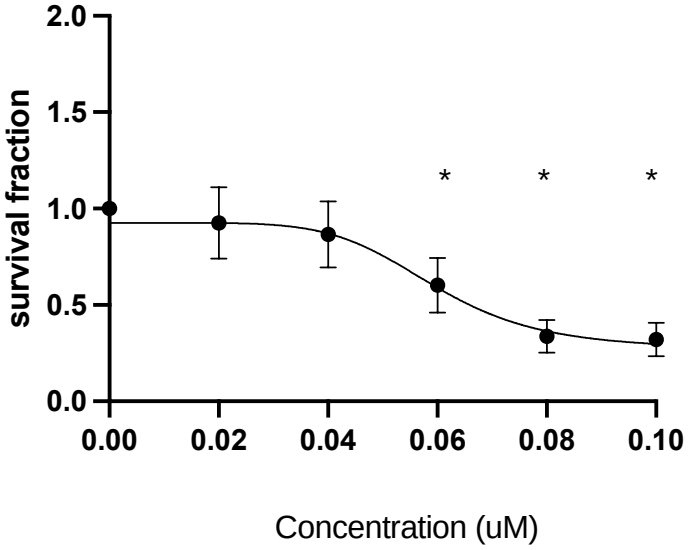

Figure 2. 3 The impact of increasing doses of Doxorubicin (μM) on the clonogenic capacity of MDA-MB-23 cells.
Data shown is an average of at least three independent experiments carried out in triplicate, +/- standard deviation. A 1-way ANOVA with Bonferroni post testing was performed using GraphPad Prism 9.2.1 software, with p-values of <0.0001 = *reported as significant difference of the treated group compared to the untreated control (Applicable to figures 2.3-2.7).

From Figure 2.3, it can be observed that DOX reduced the survival fraction of MDA-MB-231 cells in a dose dependant manner, as the concentration of DOX increased the survival of the cells decreased. There was a statistically significant decrease in the survival fraction of cells when treated with 0.06 μM, 0.08 μM and 0.1 μM of DOX, when compared with the untreated control (all, $p < 0.0001$). The R^2 value of the graph was 0.831 which indicates a good correlation between the data and line fit model used. Using GraphPad prism 10, the line of best fit of data in Figure 2.3 demonstrated an IC_{50} of 0.05950 μm.

2.4.2 Cytotoxicity of Radiotherapy on MDA-MB-231 cells

To assess the radiosensitivity of MDA-MB-231 cells, a clonogenic assay was undertaken and this is demonstrated in Figure 2.4

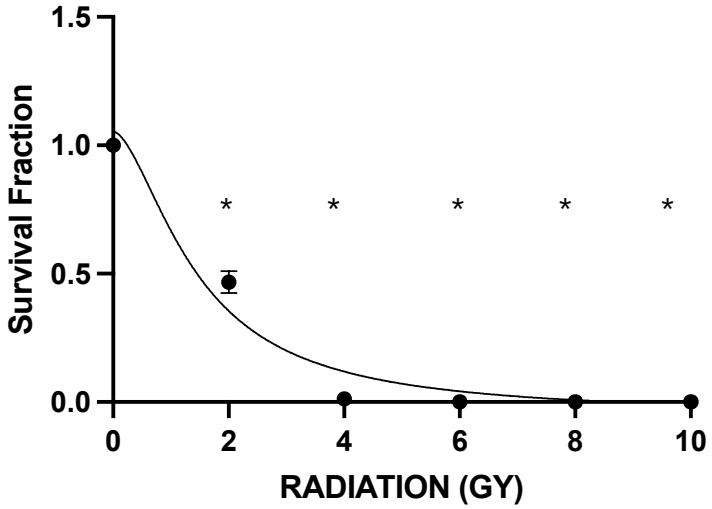

Figure 2. 4 The impact of increasing doses of radiation (Gy) on the clonogenic capacity of MDA-MB-231 cells.

From Figure 2.4 it can be observed that radiation reduced the survival fraction of MDA-MB-231 cells in a dose dependant manner. All doses of administered radiation produced a statistically significant reduction in the survival fraction of MDA-MB-231 cells, when compared with the untreated control cells (all $P<0.0001$). The R^2 value of the graph was 0.9476 which indicates a good correlation between the data and line fit model used.

2.4.3 Cytotoxicity of Dimethyl Fumarate on MDA-MB-231 cell

To determine the cytotoxic capacity of DMF on MDA-MB-231 cells, a clonogenic assay was carried out as seen in Figure 2.5.

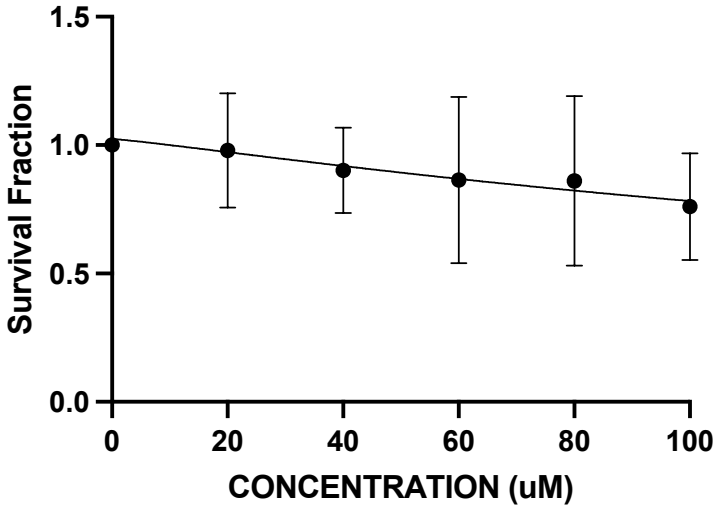

Figure 2. 5 The impact of increasing doses of dimethyl fumarate on the clonogenic capacity of MDA-MB-23 cells.

From Figure 2.5 it can be observed that at all administered concentrations of DMF, the survival fraction of cells was not statistically significantly lower than the control. The survival fraction gradually decreased in a dose dependent manner, with the lowest survival fraction of 0.7609 SD+/- 0.32 (P>0.9999), observed after incubation of cells with 100 µM of DMF. Using GraphPad prism 9.2.1, the line of best fit of data in Figure 2.5 gave an IC_{50} of 603.1 µM.

2.4.4 Cytotoxicity of Monomethyl Fumarate on MDA-MB-231 cells

To assess the cytotoxicity of MMF on MDA-MB-231 cells, a clonogenic assay was carried out as detailed in Figure 2.6.

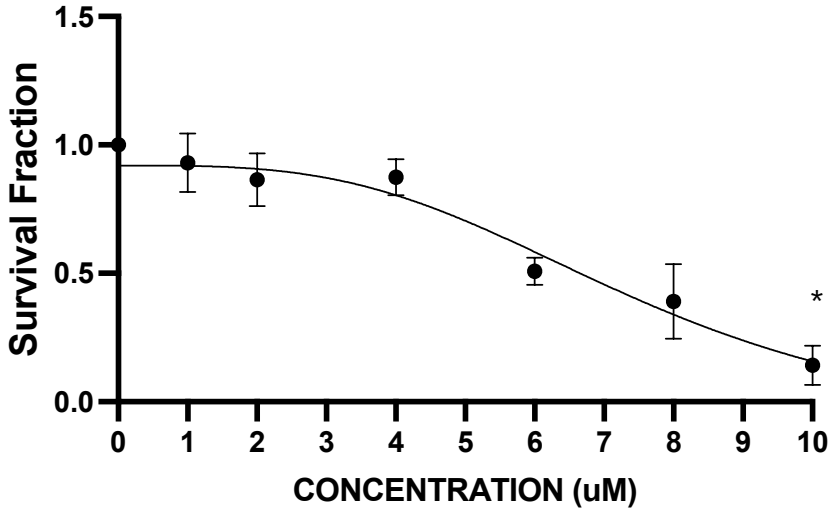

Figure 2. 6 The impact of increasing doses of monomethyl fumarate on the clonogenic capacity of MDA-MB-231 cells.

Figure 2.6 demonstrated that MMF reduced the clonogenic survival of MDA-MB-231 cells in a dose dependant manner. The highest concentration of 10 μM MMF reported a survival fraction of 0.14 (+/- 0.076). This was the only concentration of MMF investigated that produced a statistically significant decrease in the survival fraction of the cells when comparing the data with the untreated control ($P<0.0076$). Using GraphPad prism 9.2.1 the line of best fit of data in Figure 2.6 gave an IC_{50} of 6.631 μM and an R^2 value of 0.7956 which indicates a good correlation between the data and line of fit model used.

2.4.5 Cytotoxicity of Diroxomel Fumarate (EMF) on MDA-MB-231 cells

The cytotoxicity of EMF on MDA-MB-231 cells was investigated using a clonogenic assay as detailed in figure 2.7.

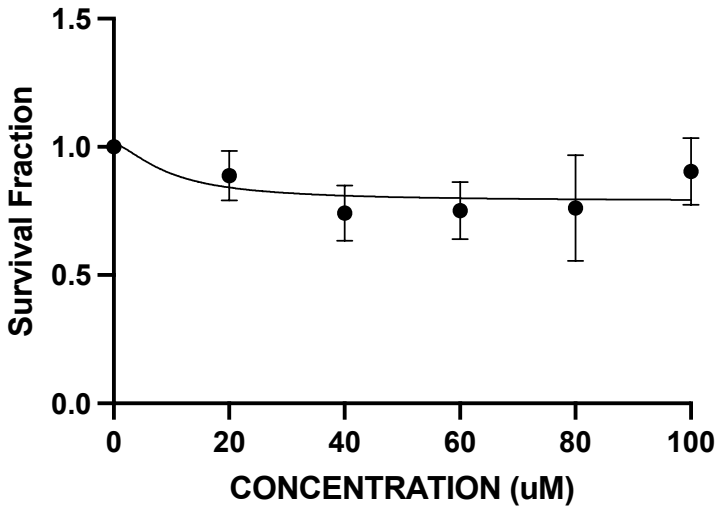

Figure 2. 7 The impact of increasing doses of Diroxomel Fumarate (EMF) on the clonogenic capacity of MDA-MB-231 cells.

Results from Figure 2.7 reported that there was no statistically significant reduction in the survival of MDA-MB-231 cells after treatment with any concentration of EMF. The data reported that at 40 μM of EMF the survival fraction of MDA-MB-231 cells decreases to 0.74 SD+/- 0.1 (P>0.38), the lowest survival fraction observed, however this was not a significant reduction compared to the control. The IC_{50} was 7.308e+019 μM and indeed no administered concentration of EMF reduced clonogenic survival to 50%.

2.4.6 Cytotoxic Effects of combination therapy using Doxorubicin and Dimethyl Fumarate or Monomethyl Fumarate on MDA-MB-231 cells.

The next stage of the project was to use the results obtained from Figures 2.3-2.7 to design combination therapies. This involved the combination of these fumaric acids with the cytotoxic agent DOX and Radiation. The fumaric acids were given in combination with DOX the standard chemotherapy agent used to treat TNBC, as well as radiation at the standard clinical dose of 2 Gy. It was hypothesised that neutralising the antioxidant glutathione and treating the cells with cytotoxic agents following this, would kill a significantly higher percentage of cells relative to controls or either treatment alone. Results from the clonogenic assays detailed above in Figures 2.3-2.7 allows for the calculation of IC_{20}. When investigating combination therapies, it is essential to use treatment concentrations that are minimally cytotoxic to enable the additional benefit of any combinations to be measurable, hence the use of doses and concentrations of agents that induce on 20% survival. For example, if using IC_{50s} to investigate combination therapies using two treatments, one treatment will theoretically kill 50% of cells and the other kill 50% of cells, therefore leaving no remaining cell colonies to measure any synergistic interactions that result in greater than additive cell kills. Therefore, IC_{20} values were used to investigate these combinations, combination index analysis was carried out and this led to the determination on whether the combinations were synergistic, antagonistic, or additive.

Although the results at this stage are preliminary, the most effective fumarate drug at inhibiting MDA-MB-231 cell survival was MMF (Figure 2.6). MMF also gave the lowest IC_{50} value of 6.631 µM. DMF appears to show some cell survival inhibition at higher concentrations, however the IC_{50} was very high at 603.1 µM and no statistically significant reduction in clonogenic survival was observed for any administered concentration (Figure 2.5). The least effective fumarate was EMF, as the clonogenic survival inhibition was not significantly different to the untreated cells even at the highest concentrations tested. The IC_{50} value was the highest of all fumaric acids tested (Figure 2.7). Given the ineffectiveness of EMF at inducing clonogenic cell death in a long term clonogenic assay it was decided that it would not be investigated further.

2.4.7 Scheduling of Treatment administration

Scheduling is incredibly important when designing combination therapies. The order in which drugs are administered is crucial to the outcome of a treatment, particularly in this project which utilises the fumaric acids in combination with doxorubicin and radiation. This is due to the mechanism of action of the fumaric acids being used, DMF and MMF, bind to intracellular glutathione and prevent it from neutralising ROS, as a result, the ROS generated because of radiation or doxorubicin is not neutralised and can induce SSB and DSB resulting in the activation of Caspase 3 pathway and ultimately cell death. Given this mechanistic information, the following combinations were designed in schedules as detailed in section 2.3.6.

It was hypothesised that SCH 3 would induce the greatest reduction in clonogenic capacity due to the mechanism of action of the drugs. Given that Fumaric acids are shown in the literature to inhibit intracellular antioxidant production which then allows for the damage induced by ROS to be uncontrolled it was hypothesised that by inhibiting glutathione synthesis before inducing the ROS and ultimately the DNA damage caused by DOX or radiation, it would be more likely to be catastrophic for the cell. Additionally, it was assumed that SCH 2 administration would induce a reduction in clonogenic capacity however not as effectively as SCH3 as SCH1. SCH1 administration was simultaneous and as such ROS will damage intracellular mechanisms simultaneously as DMF and MMF are inhibiting the generation of new antioxidants. Therefore, the cell will be able to use already existing antioxidants to prevent ROS damage.

It was hypothesised that SCH2 would be the least effective combination therapy at reducing cell survival as this schedule involves administering DMF or MMF after administration of DOX or radiation. This would be insufficient as antioxidants and cell protective mechanisms would already have mitigated damage by ROS and prevented the induction DSB and SSB by chemotherapeutic and radiation administration. However, as it is known ROS are generated in bursts (Zorov *et al.,* 2014) this SCH2 combination would theoretically prevent any cellular protective mechanisms that would be generated in response to these bursts, 24 hrs following DOX or radiation administration. This scheduling would therefore allow us to investigate if inhibiting the initial generation of antioxidants is sufficient to induce cell death or if burst of ROS are equally as critical at inducing cell death.

Figure 2.8 details the response of MDA-MB-231 cells to incubation with DOX, DMF and three scheduled combinations of these therapies. SCH1 one being simulations administration of both drugs, SCH 2 DOX administered 24 hours prior to DMF administrations and SCH 3 DMF administered 24 hours before DOX administration. Doxorubicin was administered at 0.02 μM, MMF 2 μM and DMF at 100 μM, as these concentrations were the calculated IC_{20s}.

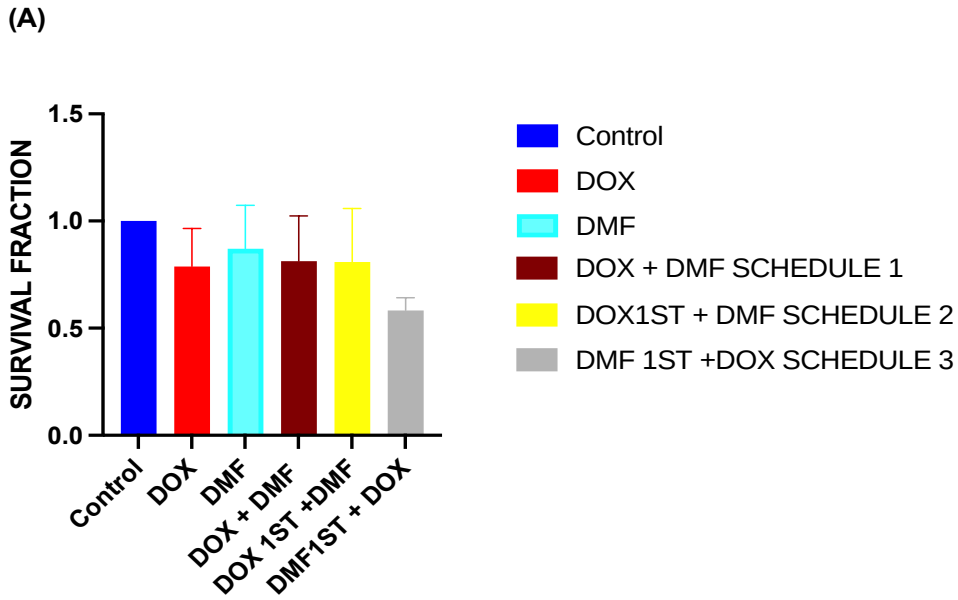

Figure 2. 8 This is a comparison between the survival fraction of DOX, DMF and the combination of three schedules of administration on MDA-MB-231 cells.

Data shown is the average of three independent experiments carried out in triplicate, +/- SD. (B) 1-way ANOVA with Bonferroni post-test was performed using GraphPad Prism 9.2.1 software (applicable to graphs 2.8-2.11).

It can be observed from in Figure 2.8, that MDA-MB-231 cells treated with DMF and DOX alone resulted in minimal cytotoxic effect as Incubation of cells with DOX at 0.02 μM, resulted in the clonogenic survival of 0.83 SD+/- 0.27 which was not significantly less than those cells which were untreated or any other treatment group (P<0.999). DMF administered at a concentration of 100 μM relative to the untreated control, induced a cell kill of 0.87 SD+/- 0.20 that produced a non-significant reduction in survival fraction when compared to the untreated control group or any other treatment

group ($P<0.999$). Treatment of cells with SCH 1 (Simultaneous administration), SCH 2 (DOX administered before DMF) and SCH 3 (DOX administered after DMF) using the same concentrations of drug also failed to induce a statistically significant reduction in survival fraction of MDA-MB-231 cells when compared to the control or any other treatment group. This data suggests that no scheduled combination of DOX + DMF is more effective at reducing the survival fraction of MDA-MB-231 cells than the single therapies alone.

Due to the mechanism of action of DMF, inhibiting the synthesis of antioxidants, it was hypothesised that cells would be unable to prevent damage induced by ROS via DOX treatment. However, this hypothesis has not been supported by the results in Figure 2.8. It may be that the active metabolite of DMF, MMF, will be a more suitable candidate to investigate the potential of fumaric acids as a potential candidate for combination therapies on 2D MDA-MB-231 cells.

Figure 2.9 details the treatment of MDA-MB-231 cells with the same concentration of DOX 0.02 μM as in Figure 2.8, and 2 μM MMF. These were administered alone and in three schedules previously detailed.

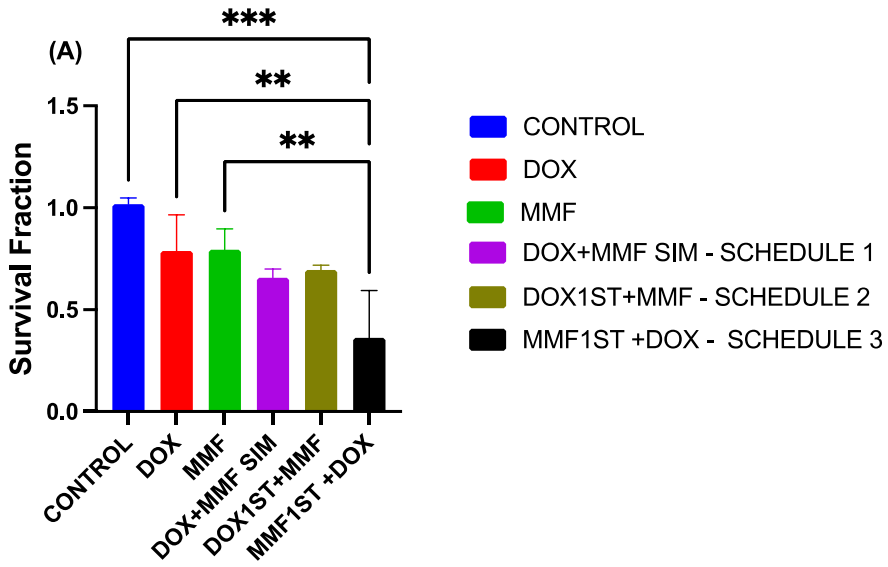

(B)

Bonferroni's multiple comparisons test	Summary	Adjusted P Value
CONTROL vs. SCH3	***	0.0003
DOX vs. SCH3	**	0.0062
MMF vs. SCH3	**	0.0088

Figure 2. 9 This is a comparison between the survival fraction of DOX, MMF and the combination of three schedules of administration on MDA-MB-231 cells.

As we can see from Figure 2.9, when MDA-MB-231 cells were incubated with DOX alone and MMF alone, these drugs as single agents did not induce a statistically significant reduction in survival fraction of cells compared with the control or any other treatment group (P>0.9999, Figure 2.9B). SCH1 (Simultaneous administration) or SCH2 (DOX administered before MMF) did not induce any statistically significant reduction in survival fraction compared with any other treatment group. SCH3 (DOX administered after MMF) however induced a statistically significant reduction in survival fraction when compared to the untreated control (P=0.0003, Figure 2.9B), DOX alone (p=0.0062, Figure 2.9B) and MMF alone (p=0.0088, Figure 2.9B). This was the only statistically significant reduction in survival fraction observed when comparing SCH3 to any other group. These results suggests that scheduled combinations of DOX + MMF can statistically significantly reduce the survival of MDA-MB-231 cells when compared to untreated control cells and individual therapies alone when administered in SCH3 regime. This therefore suggests that combination of SCH3 DOX + MMF could be a more effective treatment than the gold standard DOX alone for TNBC patients.

Figure 2.9 supports the hypothesis that SCH3 is the most effective method of administration of DOX and MMF. This may be due to the mechanism of action in which MMF inhibits the synthesis of intracellular GSH, as a result, ROS generated by DOX treatment can induce SSB and DSB ultimately causing the activation of Caspase 3 resulting in cell death (Kennedy *et al.,* 2020). This combination will also be investigated in Chapter 3, using 3D spheroid model and Chapter 4, using 2D and 3D models to investigate DOX resistance of MDA-MB-231 cells.

To determine if lowering the radiation dose influenced combination efficacy the combination experiment was carried out using 0.5 and 1 Gy and 2 Gy of radiation (data not shown, see appendix 1). There was no additional benefit of reducing the dose of radiation in combination with MMF at any scheduled combination. Therefore, the effects of radiation were investigated at a dose of 2 Gy going forward, as the clinical dose used is approximately 2.7 Gy (Lilley and Murray, 2023).

Figure 2.10 investigated the scheduled combination on MDA-MB-231 cells, of DMF at 100 μM and irradiation at 2 Gy as the clinical dose used is approximately 2.7 Gy (Lilley and Murray, 2023). SCH 1 was a simultaneous administration of DMF 100 μM and 2 Gy of radiation. SCH 2 involved the treatment of cells with 2 Gy dose of radiation 24 hours prior to the administration of 100 μM DMF. SCH 3 involved the administration of DMF100 μM 24 hours prior to the cell's exposure to 2Gy radiation.

Figure 2.10 demonstrated that there was a statistically significant reduction in the cell survival fraction of cells when cells were treated with SCH1 (P=0.0039, Figure 2.10B), SCH2 (P=0.0326, Figure 2.10B) and SCH3 (P=0.0066, Figure 2.10B) when compared with the untreated control. There was also a statistically significant decrease in survival fraction of cells exposed to SCH3 (P=0.042, Figure 2.10B) compared to DMF alone. There were however no statistically significant decreases in survival fraction of cell exposed to SCH 1 or 2 compared to DMF alone (Figure 2.10B). Additionally, there were no statistically significant reductions in survival fraction of cells treated with SCH1,2 or 3 compared with RAD alone.

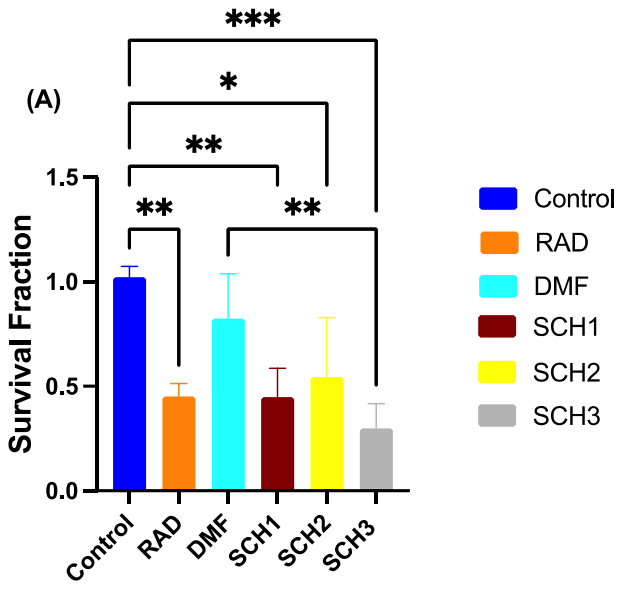

(B)

Bonferroni's multiple comparisons test	Summary	Adjusted P Value
Control vs. RAD	**	0.0040
Control vs. SCH1	**	0.0037
Control vs. SCH2	*	0.0326
Control vs. SCH3	***	0.0003
DMF vs. SCH3	**	0.0042

Figure 2. 10 This is a comparison between the survival fraction of RAD, DMF and the combination of three schedules of administration on MDA-MB-231 cells.

The results from Figure 2.10 support the hypothesis that SCH3 is a more suitable combination administration than SCH2. The results from Figure 2.10 suggest that no combination schedule was more effective at reducing the survival fraction of MDA-MB-231 cells than radiation alone. However, a combination therapy of RAD + DMF will be investigated in Chapter 3 using 3D models and Chapter 4 to determine if this combination therapy is more effective at reducing the survival of radiation resistant MDA-MB-231 cells than radiation alone. This hypothesis is supported by the findings of Bai *et* al., (2021) who reported that resistance in TNBC patients is often linked to an upregulation of antioxidants such as GSH, and that by inhibiting the production of GSH via DMF, this may re-sensitise the cell to death via ROS induced by irradiation.

Figure 2.11 reflects the effects of MDA-MB-231 cells when exposed to RAD 2 Gy and MMF 2 μM in scheduled combination. SCH1 was a simultaneous administration of MMF 2 μM and 2 Gy of radiation. SCH2 involved the treatment of cells with 2 Gy dose

of radiation 24 hours prior to the administration of 2 μM MMF. SCH3 involved the administration of MMF 2 μM 24 hours prior to the cell's exposure to 2 Gy radiation.

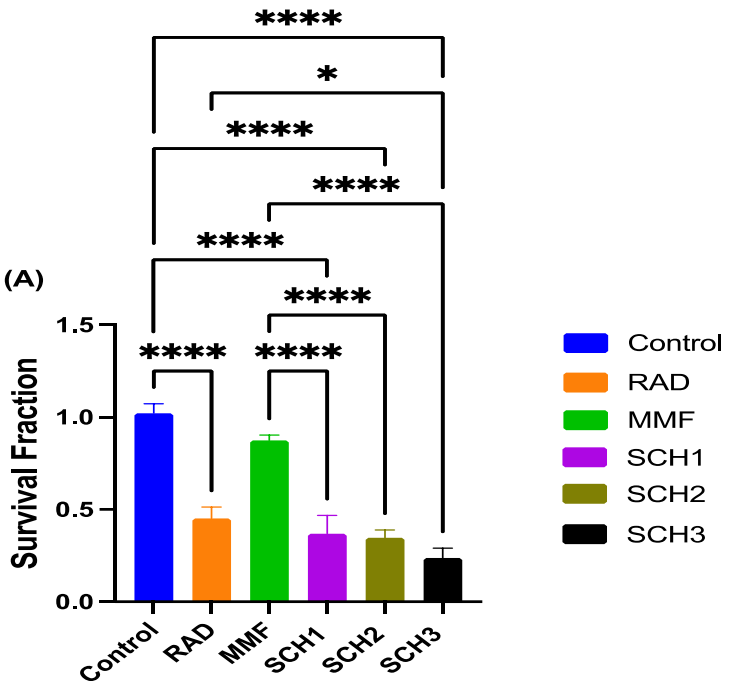

(B)

Bonferroni's multiple comparisons test	Summary	Adjusted P Value
Control vs. RAD	****	<0.0001
Control vs. SCH1	****	<0.0001
Control vs. SCH2	****	<0.0001
Control vs. SCH3	****	<0.0001
RAD vs. MMF	****	<0.0001
RAD vs. SCH3	*	0.0102
MMF vs. SCH1	****	<0.0001
MMF vs. SCH2	****	<0.0001
MMF vs. SCH3	****	<0.0001

Figure 2. 11 This is a comparison between the survival fraction of RAD, MMF and the combination of three schedules of administration on MDA-MB-231 cells.

Figure 2.11 reports a statistically significant decrease in the survival fraction of cells treated with RAD alone, SCH1, SCH 2, and SCH 3 when compared with the control (all, P<0.0001, Figure 2,11B). There was also a statistically significant decrease in the survival fraction of cells treated with RAD alone, SCH1, SCH2 and SCH3 when compared to MMF alone (all, P<0.0001, Figure 2.11B). There was a statistically significant decrease in the survival fraction of cells when treated with SCH3 compared to RAD alone (P=0.0102, Figure 2.11B). This was the only statistically significant

decrease in survival fraction found when comparing any treatment to RAD alone. There were no statistically significant changes in survival fraction when comparing any other the combination therapies to each other (Figure 2.11B).

The data from Figure 2.11 supports the hypothesis that SCH3 is the more appropriate combination schedule of RAD + MMF as it was the only combination therapy that induced a statistically significant decrease in survival fraction compared with both single therapies and the untreated control. This combination will also be investigated in Chapter 3, using 3D spheroid model and Chapter 4, using 2D and 3D models to investigate radiation resistance of MDA-MB-231 cells.

2.4.8 Combination Index analysis of Combination therapy using Doxorubicin and Monomethyl Fumarate on MDA-MB-231 cells.

Combination index analysis is a statistical analysis that investigates the relationship between two or more agents in a system to be defined in terms of their toxicity. There are three types of relationships that can be categorised from this analysis: antagonistic, additive, and synergistic (better than the sum effect of each agent).

The use of combination index analysis is dependent on how well the model fits the data, (also known as the R^2 value). Calcucyn was used to generate these combination index results; this software was developed by Chou *et al* (2005). In this software each agent tested is combined using a dose ratio of Drug X to Drug Y based on the effectiveness of each agent as a single therapy and the effect each combination has on the survival of the sample is proportional to each individual agent tested.

The dose effect of the agents investigated are detailed in Fig 2.12. The analysis of these results is based on the 3 below equations.

Equation 1; fa/fu=(D/Dm) m
Equation 2; D= Dm[fa/fu]1/m
Equation 3; CI= (D)1/(Dx)1+(D)2/(Dx)2+α(D)1(D)2/(Dx)1(Dx)2

For equations 1 and 2; D = dose, Dm = IC50 dose, fa = fraction of cells affected, fu= unaffected fraction of cells and m= coefficient of the sigmoidicity of the dose effect

curve. The logarithmic equation 2 transforms the equation in the form of the equation of a line (y=mx+c), where m= the slope of the line and x= logIC50. For each agent and combination, log(D) against log(fa/fu), z-intercept and slope m were calculated. These were the conditions used to calculate the dose of the combination agents and the doses required to determine the different levels of toxicity according to equation 2. For each concentration of agent and its corresponding toxicity, the combination index was calculated as detailed b equation 3 in which; (D)1 and (D)2 = doses of agents which give rise to x% of cell survival in clonogenics, when used in combination and (DX)1 and (DX)2 = doses of each drug which give rise to x% of cell survival in clonogenics when used as a single agent.

If the combination index results in $\alpha = 0$ then this reflects that the combination of each agent tested is the equivalent to the sum of the first two terms. If the analysis produces a result of $\alpha = 1$ then each agent has an independent mechanism of action, and the combination index is equivalent to the sum of all three terms.
CI >0.9 - Synergistic
CI = 0.9-1.1 – Additive
CI > 1 – Antagonistic

Figure 2.12 is a representation of the data in Fig 2.10 that has been analysed using the Calcucyin software. As MMF was the only fumaric administered in combination with DOX that produced a statistically significant reduction in survival fraction of MDA-MB-231 cells, this was the fumaric acid chosen to be analysed in more detail.
(A)

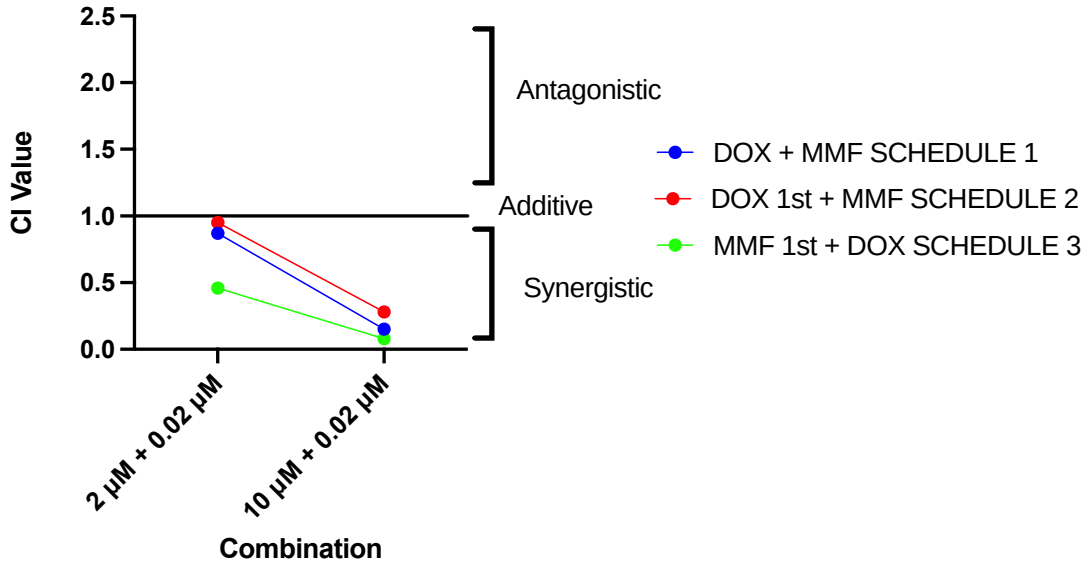

(B)

Drug Concentrations	Schedules		
	SCHEDULE 1	SCHEDULE 2	SCHEDULE 3
MMF 2 µM + DOX 0.02 µM	0.87	0.96	0.47
MMF 10 µM + 0.02 µM	0.15	0.28	0.08

Figure 2. 12 CA (A) Combination Index (CI) after MDA-MB-2312 cells are incubated with DOX and MMF in the 3 treatments Schedules.

Antagonistic <1.1, Additive = 0.9-1.1 and Synergistic > 0.9. Each point represents three independent experiments carried out in triplicate, (B) Values of CI plotted in (A). Data was taken from clonogenic survival assay and analysed suing Calcucyin software as described above.

It can be seen from Figure 2.12, that SCH1 and SCH3 in both concentrations tested produced CI values less than 0.9, therefore these combinations were reported as synergistic (better than the sum of each agent) (Figure 2.12B). SCH2 reported an additive CI value when using 2 μM MMF + 0.02 μM DOX, however a synergistic CI value was reported when using a higher dose of MMF (Figure 2.12B, 4 μM MMF + 0.02 μM DOX). These results support the use of SCH3 as a combination therapy to treat MDA-MB-231 cells. This combination produced synergistic CI values at all concentrations of drug tested.

2.4.9 Cell cycle analysis of MDA-MB-231 cells after combination treatment with Doxorubicin and Monomethyl Fumarate

To better understand the mechanism of action of promising MMF combinations, a range of different assays were carried out, including cell cycle analysis, annexin V, glutathione assay, autophagy assay and comet assay.

The cell cycle can be divided into 2 stages, interphase, and mitosis. Interphase constitutes most of the cell cycle as this is the time frame in which cells prepare to undergo division. Interphase is made up of 3 phases: G1(cells prepare to divide), S (DNA replication) and G2 (cell organises genetic material prior to cell division). Following this the cells enter mitosis (M) in which they undergo complete division to two daughter cells. SubG1 (sG1) is used by many apoptotic detection kits to quantify to amount of fractionated DNA (Ortiz-Ferron, 2020). When cells undergo apoptosis, the DNA within them is broken up into small fragments, these fragments can be identified using a stain such as propidium iodide (PI). Cells which have fragmented DNA may produce a weak PI intensity and produce a peak below the G1 peak, this is known as subG1. Although it is a useful tool to investigate DNA damage using a cell cycle analysis kit, this method is not entirely conclusive. Cells may produce weak PI intensity and appear below the G1 peak; however, this does not always correspond with huge DNA damage as other factors may be influencing this subG1 peak (Plesca *et al*., 2008). Some therapies may cause cell cycle arrest, which means cells become stuck in one phase of the cell cycle unable to continue to process for complete cell division (Li *et al*., 2019).

Therefore, a more specific assay to investigate apoptosis should be used alongside this, such as an Annexin V assay. This kit extracts the fragmented DNA that appears in the subG1 peak as not all these cells are apoptotic, there are several other intracellular factors that may cause a cell to produce peak below G1 after PI stain (chromosome aggregates from mitotic cells for example). As apoptosis can occur at any stage in the cell cycle, some cells may become apoptotic during G2/M phase of the cell cycle and as such would produce a peak above G1, therefore it should not be assumed that all cells in other phases of the cell cycle are healthy (Logue *et al*., 2009). For these reasons both cell cycle analysis and Annexin V were carried out to investigate the effects of potential therapies on MDA-MB-231 cells.

The distribution of MDA-MB-231 cells in each phase of the cell cycle (G1, S, G2/M, sG1) was investigated using Fluorescence-Activated Cell Sorting (FACS) assay. Cells following treatment with either single therapies (DOX, RAD, MMF) or combination therapies (DOX SCH3 and RAD SCH3) were investigated using this assay to determine any disparities found between treatments. Cells were collected after treatment with single agents or combination therapies as described in section 2.3.20. SCH3 MMF was selected as this combination schedule was the only one that produced a statistically significant reduction in MDA-MB-231 cell survival (in clonogenic assay) when compared to the untreated control cells, DOX alone, RAD alone and MMF alone. All concentrations used were the same as those in Figures 2.7-11.

After 48 hrs (cell doubling time) of incubation with respective treatments, the media containing this treatment was removed and cells washed using PBS. Fresh media was added to cells which were then incubated for the following time intervals; 0 hrs (cells harvested immediately after treatment removed), 24 hrs (cells harvested 24 hrs after treatment removed) and 48 hrs (cells harvested 48 hrs after treatment removed). These time frames were selected to allow for accurate determination of cell arrest and repair during the cell cycle (Thu *et al.,* 2018 and Ochs and Kaina, 2000).

MDA-MB-231 cells treated with MMF, DOX and SCH3 (DOX administered after MMF) were analysed immediately after treatment was removed and cell cycle analysis results are detailed in Figure 2.13.

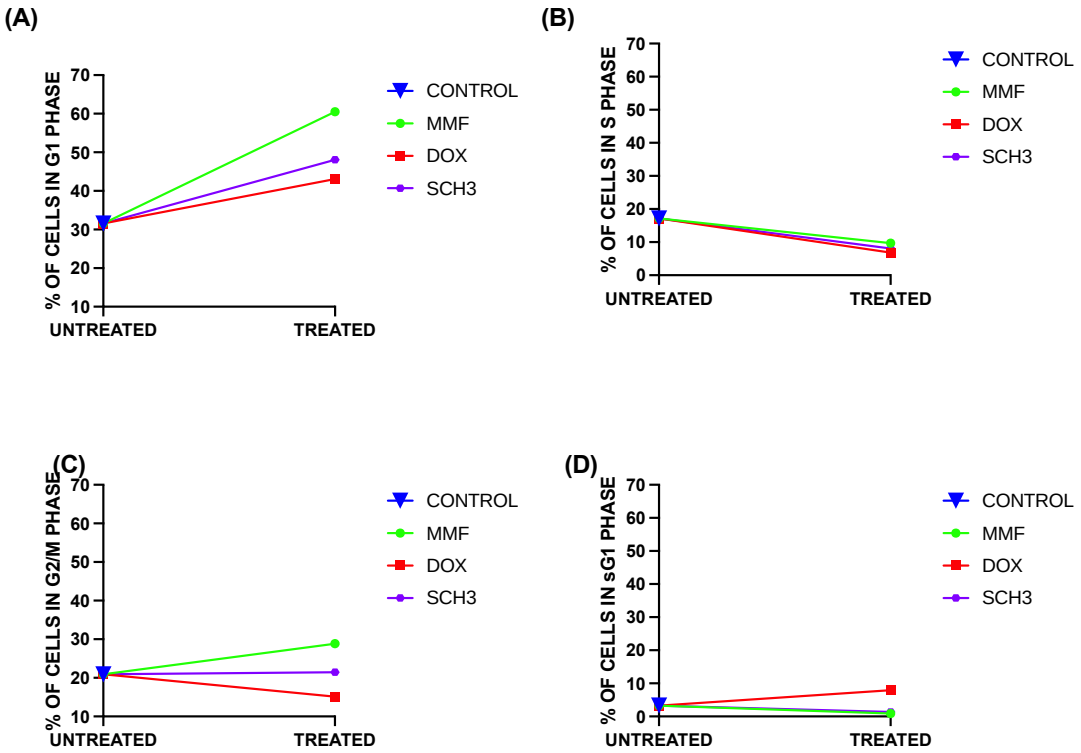

(E)

Bonferroni's multiple comparisons test	G1 - P Value	S – P Value	G2/M – P Value	sG1 – P Value
CONTROL vs. MMF	<0.0001	<0.0001	<0.0001	0.0024
CONTROL vs. DOX	<0.0001	<0.0001	<0.0001	<0.0001
CONTROL vs. SCH3	<0.0001	<0.0001	>0.9999	0.0091
MMF vs. DOX	<0.0001	0.0004	<0.0001	<0.0001
MMF vs. SCH3	<0.0001	0.0135	<0.0001	>0.9999
DOX vs. SCH3	<0.0001	0.0684	<0.0001	<0.0001

Figure 2. 13 Shows the cell cycle distribution of untreated MDA-MB-231 cells and treated MDA-MB-231 cells 0hrs post treatment removal.

With the corresponding agents in the figure legend (MMF 2μM, DOX 0.02μM SCH3 – MMF2μM1st+ DOX 0.02μM 24hours later). The figure above represents the percentage of cells in each phase of the cell cycle, results displayed as an average of 3 independent experiments carried out in triplicate (A) – G1, (B)- S, (C)- G2/M and (D)- sG1. (E) A one-way ANOVA with Bonferroni post-test was utilized to compare the means of the cell cycle phases after treatment cells versus untreated control cells and demonstrated in the above Tables where, *P<0.05, **P<0.01, ***P<0.001 and ****P<0.0001 (Applicable for Figures 2.13-2.15).

The results from Figure 2.13A suggest that there was a statistically significant increase in the percentage of cells in G1 phase of the cell cycle after treatment with DOX alone, MMF alone and SCH3 combination, compared with the untreated control cells and other treatment groups (all P<0.0001, Figure 2.13E). Figure 2.13B showed that there was a statistically significant decrease in the percentage of cells in S phase of the cell cycle when treated with DOX alone, MMF alone and SCH3 compared with the untreated control (all, P<0.0001). There was also a statistically significant decrease in the percentage of cells in S phase of the cell cycle when cells were treated with DOX alone (P=0.0004, Figure 2.32E) and SCH3 (P=0.0135, Figure 2.212E) compared to MMF alone treated cells. Figure 2.13C suggests that there was a statistically significant increase in the percentage of cells in G2/M phase of the cell cycle when cells were treated with MMF alone, compared to the untreated control (P<0.0001, Figure 2.13E). There was a statistically significant decrease in the percentage of cells in G2/M phase of the cell cycle when cells were treated with DOX alone compared with the untreated control cells (P<0.0001, Figure 2.13E). There was also a statistically significant decrease in the percentage of cells in G2/M phase of the cell cycle when treated with DOX alone and SCH3 compared with MMF alone treated cells (both P<0.0001, Figure 2.13E). Figure 2.12D suggests a statically significant increase in the percentage of cells in sG1 phase of the cell cycle when treated with DOX alone, compared with the untreated control cells, MMF alone and SCH3 (all, P<0.0001, Figure 2.13E). There was a statistically significant decrease in the percentage of cells in sG1 phase of the cell cycle when treated with MMF alone (P=0.024, Figure 2.13E) and SCH3 alone (0.0091, Figure 2.13E) compared with the untreated control.

These results suggest that there is a difference in the dispersion of treated cells within the various phases of the cell cycle, treated cells reported a significant increase in cells in G1 phase of the cell cycle and decrease in S phase of the cell cycle when compared with the control.

MDA-MB-231 cells treated with MMF, DOX and SCH3 (DOX administered after MMF) were then analysed 24 hrs after treatment removed and cell cycle analysis results are detailed in Figure 2.14.

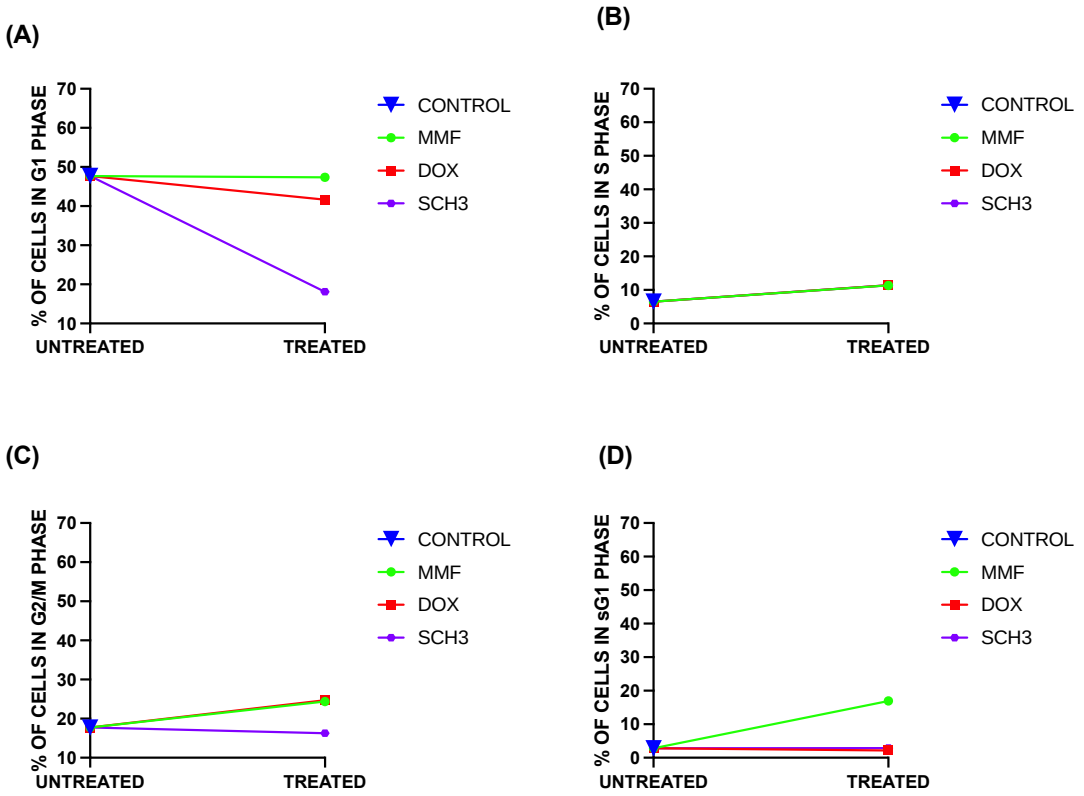

(E)

Bonferroni's multiple comparisons test	G1 - P Value	S – P Value	G2/M – P Value	sG1 – P Value
CONTROL vs. MMF	>0.9999	<0.0001	<0.0001	<0.0001
CONTROL vs. DOX	<0.0001	<0.0001	<0.0001	>0.9999
CONTROL vs. SCH3	<0.0001	<0.0001	0.0600	>0.9999
MMF vs. DOX	<0.0001	>0.9999	>0.9999	<0.0001
MMF vs. SCH3	<0.0001	>0.9999	<0.0001	<0.0001
DOX vs. SCH3	<0.0001	>0.9999	<0.0001	>0.9999

Figure 2. 14 Shows the cell cycle distribution of untreated MDA-MB-231 cells and treated MDA-MB-231 cells with the corresponding agents. 24 hrs post treatment removal.

Figure 2.14A demonstrates that there was a statistically significant decrease in the percentage of cells in G1 phase of the cell cycle following treatment with DOX alone and SCH3 compared with the untreated control cells (both P<0.0001, Figure 2.14E). There was also a statistically significant decrease in the percentage of cells in G1 phase of the cell cycle following treatment with DOX alone and SCH3 compared with MMF alone (both P<0.0001, Figure 2.14E). There was a statistically significant

decrease in the percentage of cells in G1 phase of the cell cycle when treated with SCH3 compared with DOX alone treated cells (P<0.0001, Figure 2.14E). Figure 2.13B reported that there was a statistically significant increase in the percentage of cells in S phase of the cell cycle following treatment with MMF alone, DOX alone and SCH3 compared with the intreated control (all P<0.0001, Figure 2.14E). Figure 2.13C reported that there was a statistically significant increase in the percentage of cells in G2/M phase of the cell cycle when treated with DOX and MMF alone compared with the untreated control (P<0.0001, Figure 2.14E) and SCH3 (P<0.0001, Figure 2.14E). Figure 2.13D reported there was a statistically significant increase in the percentage of cells in sG1 phase of the cell cycle when treated with MMF alone compared with the untreated control, DOX alone and SCH3 (all P<0.0001, Figure 2.14D).

Taken together These results suggest that 24hrs after treatment is removed, SCH3 treated cells have a significantly smaller percentage of cells in G1 phase of the cell cycle when compared to the control and other treatment groups. This may be due to a reduced percent of SCH3 treated cells are able to enter the cell cycle process 24hrs after treatment is removed.

MDA-MB-231 cells treated with MMF, DOX and SCH3 (DOX administered after MMF) were analysed 48 hrs after treatment was removed and cell cycle analysis results are detailed in Figure 2.15.

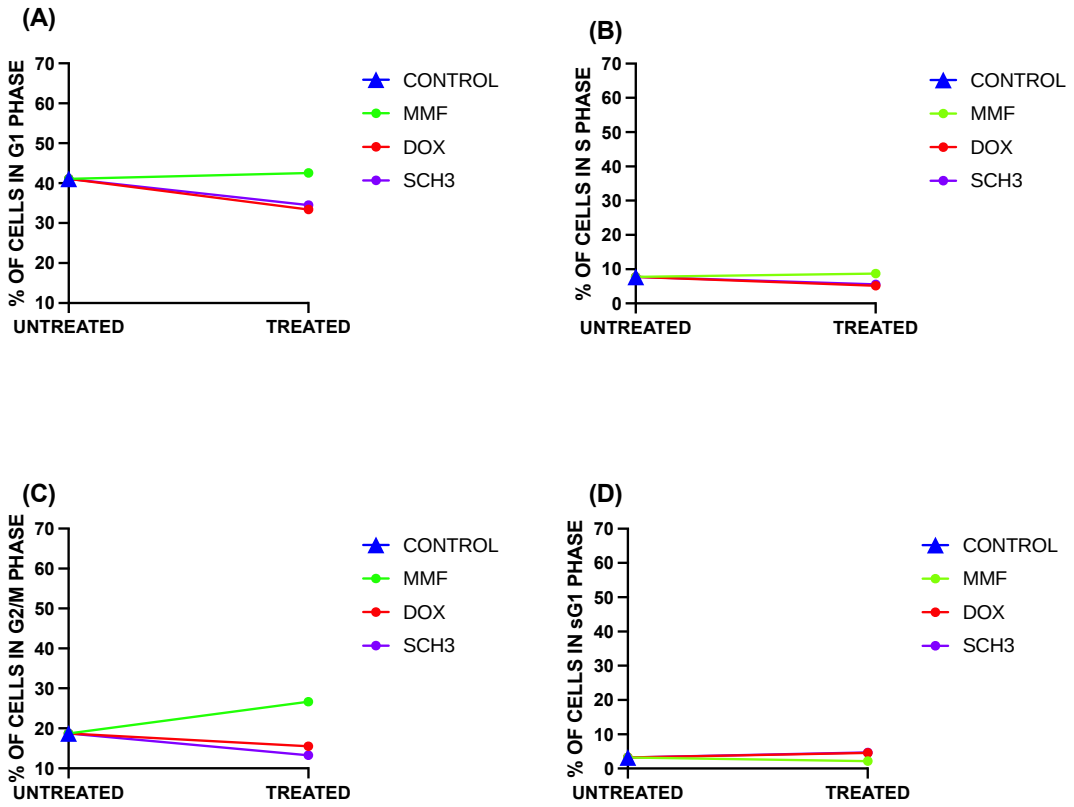

(E)

Bonferroni's multiple comparisons test	G1 - P Value	S – P Value	G2/M – P Value	sG1 – P Value
CONTROL vs. MMF	0.0357	0.3414	<0.0001	0.6774
CONTROL vs. DOX	<0.0001	0.0028	0.0002	0.3143
CONTROL vs. SCH3	<0.0001	0.0083	<0.0001	0.2461
MMF vs. DOX	<0.0001	0.0003	<0.0001	0.0219
MMF vs. SCH3	<0.0001	0.0007	<0.0001	0.0177
DOX vs. SCH3	0.1594	>0.9999	0.0025	>0.9999

Figure 2. 15 Shows the cell cycle distribution of untreated MDA-MB-231 cells and treated MDA-MB-231 cells with the corresponding agents, 48 hrs post treatment removal.

Figure 2.15A suggests that there was a statistically significant increase in the percentage of cells in G1 phase of the cell cycle when treated with MMF alone, compared to the untreated control cells (P=0.0357, Figure 2.14E), DOX alone, and SCH3 (both P<0.0001, Figure 2.15E). There was a statistically significant decrease in the percentage of cells in G1 phase of the cell cycle when treated with DOX alone and SCH3 compared with the untreated control (both P<0.0001, Figure 2.15E). Figure 2.14B reported that there was a statistically significant decrease in the percentage of cells in the S phase of the cell cycle when treated with DOX alone (P=0.0028, Figure

2,14E) and SCH3 (P=0.0083, Figure 2.15E), compared with the untreated control. Additionally, there was a statistically significant decrease in the percentage of cells in S phase of the cell cycle when treated with DOX alone (P=0.0003, Figure 2.15E) and SCH3 (P=0.0007, Figure 2.15E) compared to MMF alone treated cells. Figure 2.4C reported that there was a statistically significant increase in the percentage of cells in G2/M phase of the cell cycle when treated with MMF alone, compared to the untreated control, DOX alone and SCH3 (all P<0.0001, Figure 2.15E). There was also a statistically significant decrease in the percentage of cells in the G2/M phase of the cell cycle when cells were treated with DOX alone (P=0.0002, Figure 2.15E) and SCH3 (P<0.0001, Figure 2.15E), compared with the untreated control cells. There was a statistically significant decrease in the percentage of cells in S phase of the cell cycle when treated with SCH3 compared with DOX alone treated cells (P=0.0025, Figure 2.15E). Figure 2.15E reported that there was a statistically significant decrease in the percentage of cells in sG1 when treated with MMF alone, compared with DOX alone (P=0.0219, Figure 2.15E) and SCH3 (P=0.0177, Figure 2.15E). This was the only statistically significant change in the percentage of cells in sG1 when comparing any treated or untreated group to each other (Figure 2.15E)

These results suggest that after treatment with MMF MDA-MD-231 cells show a similar distribution of cells to that of the control 48 hrs post treatment, suggesting any disruption caused by MMF treatment has been resolved by the cells. SCH3 and DOX treated cells, show a significantly reduced percentage of cells in the G1 and G2/M phase of the cell cycle when compared to the control and MMF treated cells, 48hrs after treatment is removed. This may be due to SCH3, and DOX treated cells being unable to enter the cell cycle and cells within the cell interphase stage of the cell cycle are being inhibited by cell cycle checkpoints and are unable to enter G2/M phase to divide into two complete daughter cells. This may be due to an accumulation of DNA strand breaks; however, this will need to be further assessed using Annexin V apoptotic detection kit.

2.4.10 Apoptosis/Necrosis quantification of MDA-MB-231 cells after combination treatment with Doxorubicin and Monomethyl Fumarate

To investigate the percentage of cells that undergo apoptosis following treatment with MMF, Doxorubicin or combination schedule 3 MMF +DOX, an Annexin V apoptotic

detection assay was caried out (section 2.3.21). These experiments were done in triplicate at 3 different time points to coincide with the time points used to investigate cell cycle analysis in section 2.42.14: 0 hrs post treatment removal, 24 hrs post treatment removal and 48 hours post treatment removal.

An annexin V assay was used as it allows for the quantification of the percentage of cells in a sample that have undergone apoptosis. The stain FITC was used alongside propidium iodide (PI) to allow for differentiation between early, late phase apoptotic cells or necrotic cells. Cells that showed a positive FITC stain and negative PI stain were classified as early apoptotic cells. Cells that tested positive for FITC and PI were classified as late stage apoptotic. Necrotic cells were classified as negative for FITC stain and positive PI. Non-apoptotic (NA) cells were classified as negative for both FITC and PI (Schutte *et al*., 1998).

MDA-MB-231 cells were incubated for 48 hours (cells doubling time) with either DOX 0.02 μM alone, MMF 2 μM alone or the SCH 3 combination of MMF 2 μM 1st + DOX 0.02 μM 24 hours later. After the 48-hr treatment, cells were harvested at different time points. For 0 hr time points cells were immediately following treatment removal, for 24 hour and 48 hr time points, cells were covered in fresh treatment free complete media until time of harvest. These time points allowed for the investigation of apoptosis and MDA-MB-231 cells ability to repair following treatment (Ochs and Kaina, 2000). The kit used to investigate this was from BD Bioscience, Oxford, UK, and methods used to harvest and analyse these cells are detailed in section 2.3.21. Figure 2.16 details the results of an Annexin V assay carried out on MDA-MB-231 cells, 0 hr, 24 hr and 48 hr post treatment removal.

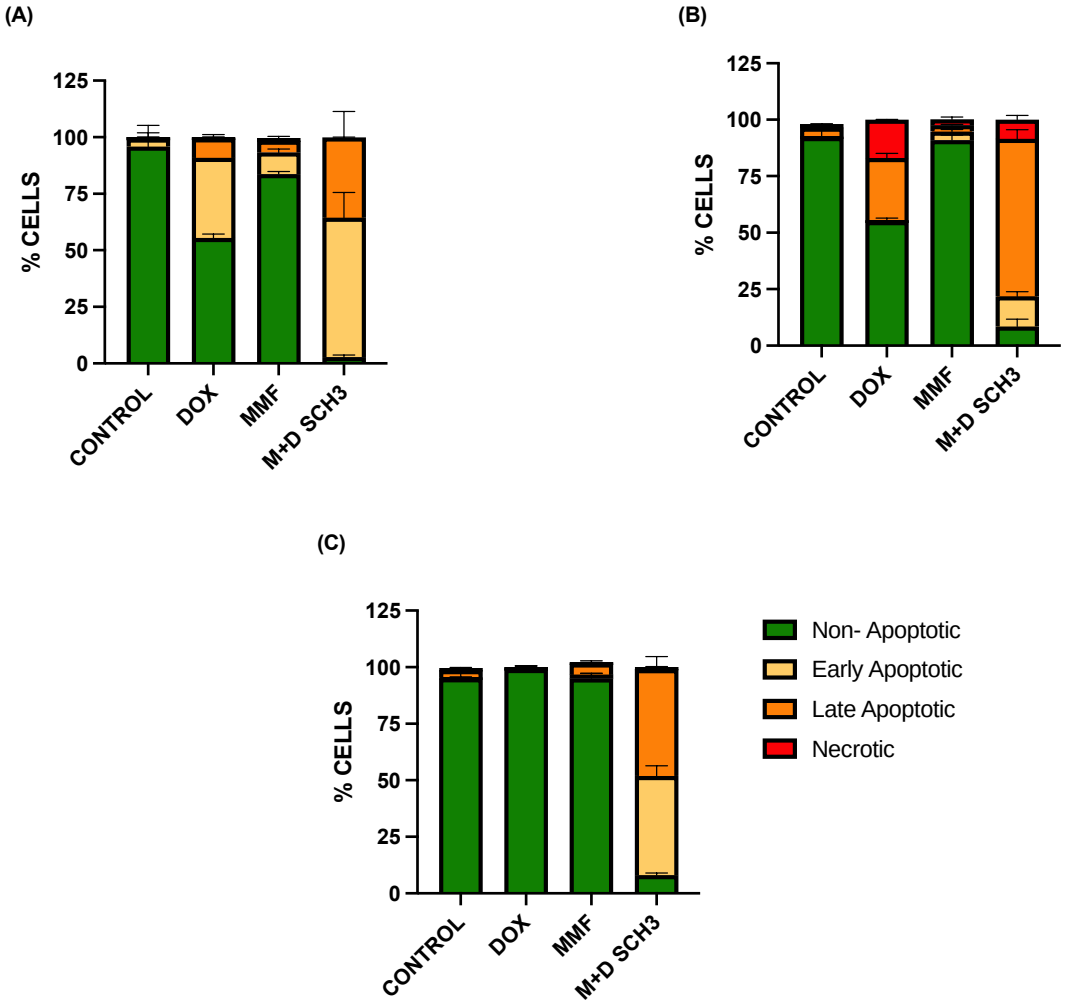

Figure 2. 16 The effect of DOX 0.02 μM, MMF 2 μM and SCH3 M1st 2 μM +D 0.02 μM on the different phases of apoptosis in MDA-MB-231 cells are shown.

Three different time points were used post treatment removal; (A) 0 hr, (B) 24 hr and (C) 48 hr. Data is expressed as mean+/- SD of 3 individual experiments at each time point carried out in triplicate. Statistical Analysis carried out using two-way ANOVA followed by Bonferroni's post-testing, comparing each apoptotic phase separately between all treatments (see appendix 1).

What was of most interest in these Annexin V investigations was the percentage of cells in late phase apoptosis and if the cells were able to repair induced damage or it it was sustained up to 48 hours post treatment.

Figure 2.16A suggests that 0 hrs after treatment was removed there was a statistically significant decrease in the percentage of non-apoptotic (NA) cells following treatment with SCH3, DOX alone and MMF alone compared with the untreated control (control

P=0.0071, DOX P=0.0003, MMF P<0.0001). Furthermore, there was a statistically significant increase in the percentage of cells in early apoptosis following treatment with SCH3 compared with the untreated control (P=0.0241) and following treatment with DOX compared with MMF alone (P=0.0067). There was a statistically significant increase in the percentage of cells in late apoptosis when treated with MMF alone compared to the untreated control P<0.0001). There were no statistically significant changes in the percentage of necrotic cells when comparing any treated or untreated cell groups (Figure 2.16C). Thus, suggesting that D-SCH3 statistically significantly decreases the percentage of non-apoptotic cells 0 hrs post treatment removal compared with the untreated control and all other treated cells.

24 hrs after treatments were removed there was again a statistically significant decrease in the percentage of NA cells following treatment with SCH3 and DOX compared with the untreated control, (DOX P=0.0078 and SCH3 P<0.0001). There was also a statistically significant decrease in the percentage of NA cells after treatment with SCH3 compared with the DOX and MMF (DOX P=0.0027 and MMF P>0.0001, Figure 2.16). Furthermore, as hypothesised, there was a statistically significant increase in the percentage of cells in early apoptosis following treatment with SCH3 compared with the untreated control, DOX alone and MMF alone (control P=0.0467, DOX P=0.0463 and MMF P=0.0311). There was also a statistically significant increase in the percentage of cells in late apoptosis when treated with DOX and SCH3 compared to the untreated control (DOX P=0.0013 and SCH3 P=0.0034) and a statistically significant increase in the percentage of cells in late apoptosis when treated with SCH3 compared with DOX alone and MMF alone (DOX. P=0.0039 and MMF P=0.0073). The only statistically significant increase in the percentage of necrotic cells was when cells were treated with DOX compared to the untreated control and MMF alone (control P<0.0001 and MMF P=0.0073). Thus, suggesting that D-SCH3 statistically significantly decreases the percentage of non-apoptotic cells and increases the percentage of early and late apoptotic cells 24 hrs following treatment removal when comparing D-SCH3 to untreated control cells and all other treated cells.

48 hrs post treatment removal there was a statistically significant decrease in the percentage of NA cells after treatment with SCH3 compared with the untreated control, DOX alone and MMF alone (control P<0.0001, DOX P<0.0001 and MMF P=0.0002). There was again a statistically significant increase in the percentage of

cells in early apoptosis following treatment with SCH3 compared with the untreated control, DOX alone and MMF alone (control P=0.0201, DOX P=0.0203 and MMF P=0.0185) and a statistically significant increase in the percentage of cells in late apoptosis when cells were treated with SCH3 compared with the untreated control, DOX alone and MMF alone (control P=0.0291, DOX P=0.0230 and MMF P=0.0258). There were no statistically significant changes in the percentage of necrotic cells when comparing any treated or untreated group. Thus, suggesting that D-SCH3 statistically significantly decreases the percentage of non-apoptotic cells and increases the percentage of early and late apoptotic cells 48 hrs following treatment removal when comparing D-SCH3 to untreated control cells and all other treated cells.

Overall, the data from Figure 2.16 suggests that MDA-MB-231 cells treated with SCH3 are producing significantly more apoptotic markers than other treated or untreated cells and report an increased percentage of cells in early and late apoptosis, up to 48 hrs post treatment removal. This suggests that cells treated with SCH3 are more likely to enter the apoptotic pathway resulting in cell death, supporting our hypothesis that MMF administered before DOX can enhance cell death by inhibiting cellular protective mechanisms that would neutralise ROS induced by DOX. This is reflective of the findings in our clonogenic analysis of SCH3 doxorubicin combination Section 2.4.7 (Figure 2.9), that reported a statistically significant decrease in the survival fraction of MDA-B-231 cells treated with SCH3 DOX combination, when compared to the untreated control, DOX alone and MMF alone.

2.4.11 Analysis of Glutathione levels in MDA-MB-231 cells after combination treatment with Doxorubicin and Monomethyl Fumarate

As MMF is thought to bind to intracellular GSH this allows for a higher level of ROS to damage cellular DNA beyond repair (Garama *et al.,* 2015, Sullivan *et al.,* 2013). To investigate the effects MMF had on the GSH levels in MDA-MB-231 cells, a GSH assay was carried out, as described in Section 2.3.22. The kit used measures the intracellular glutathione levels and also measures the reduction of; 5,5'-Dithiobis (2-nitrobenzoic acid) (DNTB) to 5-thio- 2-nitrobenzoic acid (TNB) spectrochemically, therefore a relative glutathione level was quantified.

In Figure 2.16, cells were harvested to allow for the GSH levels to be measured; 1 hr after therapy was administered (for combination 1 hr after second therapy administered), 0 hr after the 48-hr treatment were complete, 24 hr after the treatments were removed and 48 hr after the treatment were removed. The results are shown in Figure 2.17.

(A)

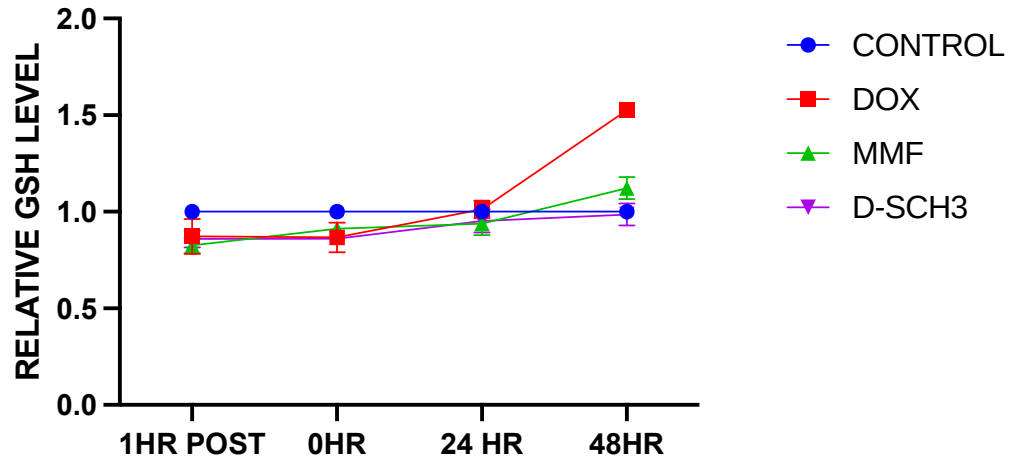

(B)

Bonferroni's multiple comparisons test	P Value 1 HR post	P Value 0HR	P Value 24HR	P Value 48HR
CONTROL vs. DOX	0.1266	0.0211	>0.9999	<0.0001
CONTROL vs. MMF	0.0256	0.0419	0.9340	0.0537
CONTROL vs. SCH3	0.0783	0.0162	>0.9999	>0.9999
DOX vs. MMF	>0.9999	>0.9999	0.5741	<0.0001
DOX vs. SCH3	>0.9999	>0.9999	0.9648	<0.0001
MMF vs. SCH3	>0.9999	0.8919	>0.9999	0.0292

Figure 2. 17 The effect of single therapies of DOX (0.02 μM) and MMF (2 μM), and combination therapy SCH3 MMF (2 μM) 1st + DOX (0.02 μM) 24 hours later, on MDA-MB-231 cells.

(A)Data reported is an average ± standard deviation of three independent experiments carried out in triplicate. (B) A one-way ANOVA with Bonferroni post testing was performed using GraphPad prism 9.2.1 comparing each treated and untreated group to each other, *P<0.05, **P<0.01, ***P<0.001 and ****P<0.0001.

Results from Figure 2.17 indicated that as predicted, there was a statistically significant decrease in the relative GSH levels, 1 hr after treatment was administered, when cells were treated with MMF alone compared to the untreated control (control vs. MMF P=0.0256, Figure 2.17B). Following the 48 hrs incubation, immediately after treatment was removed, the 0 hr analysis of cells suggests that there was a statistically significant decrease in the relative GSH levels when cells were treated with DOX alone, MMF alone and SCH3 (DOX P=0.0211, MMF P=0.0419 and SCH3

P=0.0162, Figure 2.17B). 24 hrs post treatment removal there was no statistically significant changes in the relative GSH levels when comparing any treated or untreated cells. 48 hrs post treatment there was a statistically significant increase in the relative GSH levels of cells treated with DOX alone when compared with the untreated control, MMF alone and SCH3 (control vs DOX P<0.0001, MMF vs. DOX P<0.0001, SCH3 vs. DOX P<0.0001, Figure 2.17B) as expected. Interestingly there was also a statistically significant decrease in the relative GSH levels when cells were treated with SCH3 compared to MMF alone (P=0.0292, Figure 2.17B).

Overall, the results from Figure 2.17 suggest that following treatment with SCH3 and MMF alone, MDA-MB-231 cells show reduced cellular glutathione levels as early as 1 hr post treatment. However, following the administration of DOX in this SCH3 combination the relative GSH levels are reduced and fail to increase at the same rate we observed in the DOX alone and MMF alone treated MDA-MB-231 treated cells. This may be due to MMF inhibiting the synthesis of new GSH and as such the GSH already in the intracellular matrix is used by the cells to mediate damage following initial DOX administration, however as the cell is unable to synthesis more GSH, the level of GSH does not increase following its depletion.

2.4.12 Detection of Autophagic MDA-MB-231 cells after combination treatment with Doxorubicin and Monomethyl Fumarate

We wished to further investigate the mechanism by which MMF in combination induced a significant reduction in clonogenic survival compared to the untreated control and doxorubicin. Thus, as well as investigating the induction of apoptosis we also wished to investigate if MMF induced other modes of cell's death as a paper by Lee *et al.,* (2021) had suggested that DMF is able to induce autophagy in microglial cells. Therefore, to determine of this induction of autophagy was also evident in cancer cells, we undertook an investigation to see if the percentage of cells that undergo autophagy because of treatment using an autophagy assay as described in Section 2.3.23. MDA-MB-231 cells were treated with DOX alone (0.02 μM), MMF alone (2 μM) and the SCH3 combination of MMF1st+DOX. The kit measures autophagic vacuoles and monitors autophagic change in live cells via quantification on a microplate reader. A Green Detection Reagent was used as it detects the dye that fluoresces when incorporated into pre autophagosomes and autophagosomes.

This absorbance was measures at 412 nm. This assay was carried out in triplicate at 3 different time points to co-inside with the Cell Cycle analysis data (Section 2.42.14).

Figure 2.18 details the effect of DOX alone (0.02 μM), MMF alone (2 μM) and the schedule 3 combination of MMF1st (2 μM) + DOX (0.02 μM) on MDA-MB-231 cells to investigate the autophagic properties of MDA-MB-231 cells after treatment.

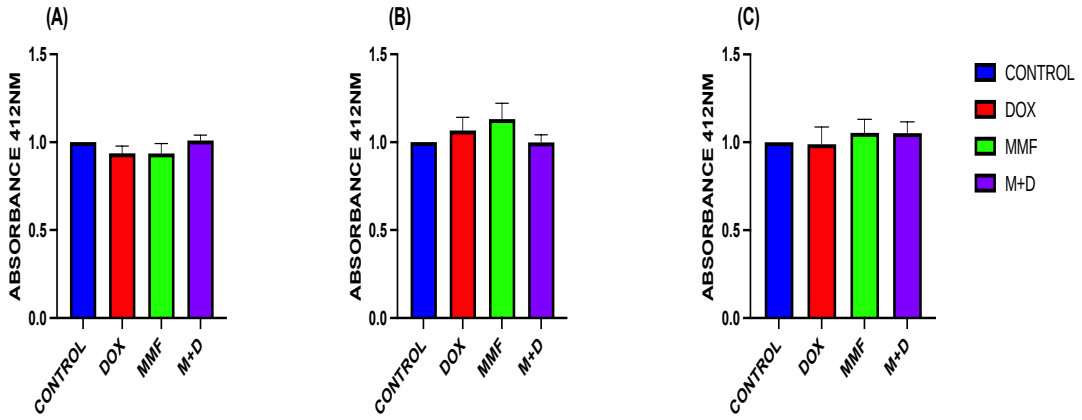

Figure 2. 18 The effect of; DOX alone 0.02μM, MMF alone 2μM or Schedule 3 combination MMF1st 2 μM+ Dox 0.02 μM 24 hours later, on Green Detection Reagent.

Data is expressed relative to the control. Cells were measure on a fluorescent microplate reader at 412 nm. (A) 0 hours after treatment removed. (B) 24 hours after treatment removed. (C) 48 hours after treatment removed. All graphs are displayed as mean and standard deviation of 3 individual experiments carried out in triplicate. One -way ANVOA was carried out with Bonferroni's post-test using GraphPad prism 9.2.1.

As a green detection reagent was used to measure to autophagy in a cell, an increased signal indicates an accumulation of the probe within cells and therefore the presence of autophagic vesicles. Results were all displayed as a ratio of the control. From Fig 2.18(A, B and C) there were no statistically significant changes in the absorbance of cells when comparing treated or untreated cells at any time point post treatment removal. Overall, there was no significant increase in autophagy detected with any of the treatments suggesting that autophagy was not significantly induced or inhibited by any treatment tested over a 48-hr window.

2.4.13 Quantification of DNA damage and repair using single cell gel electrophoresis (Comet Assay), of MDA-MB-231 cells after combination treatment with Doxorubicin and Monomethyl Fumarate

To investigate the effects MMF, DOX and the SCH 3 combination of MMF + DOX have on MDA-MB-231 cells DNA damage and repair dynamics, single cell gel electrophoresis assay was carried out. This is also known as a comet assay and comprises of single cells embedded in low melting point agarose on a glass microscope slide. The cells are lysed in an alkaline solution to partially unwind from DNA break strand points. The slides are then subject to electrophoresis The more DNA damage observed reflects the more migration found on the slides, giving the distinctive comet tail Figure 2.19, Section 2.3.23. A one-way ANOVA was used to statistically analyse the median tail moment data, this statistical test was used as it was found by Wiklund and Agurell, (2003) that “non-parametric statistical strategies turned out to be generally less efficient than ANOVA models”.

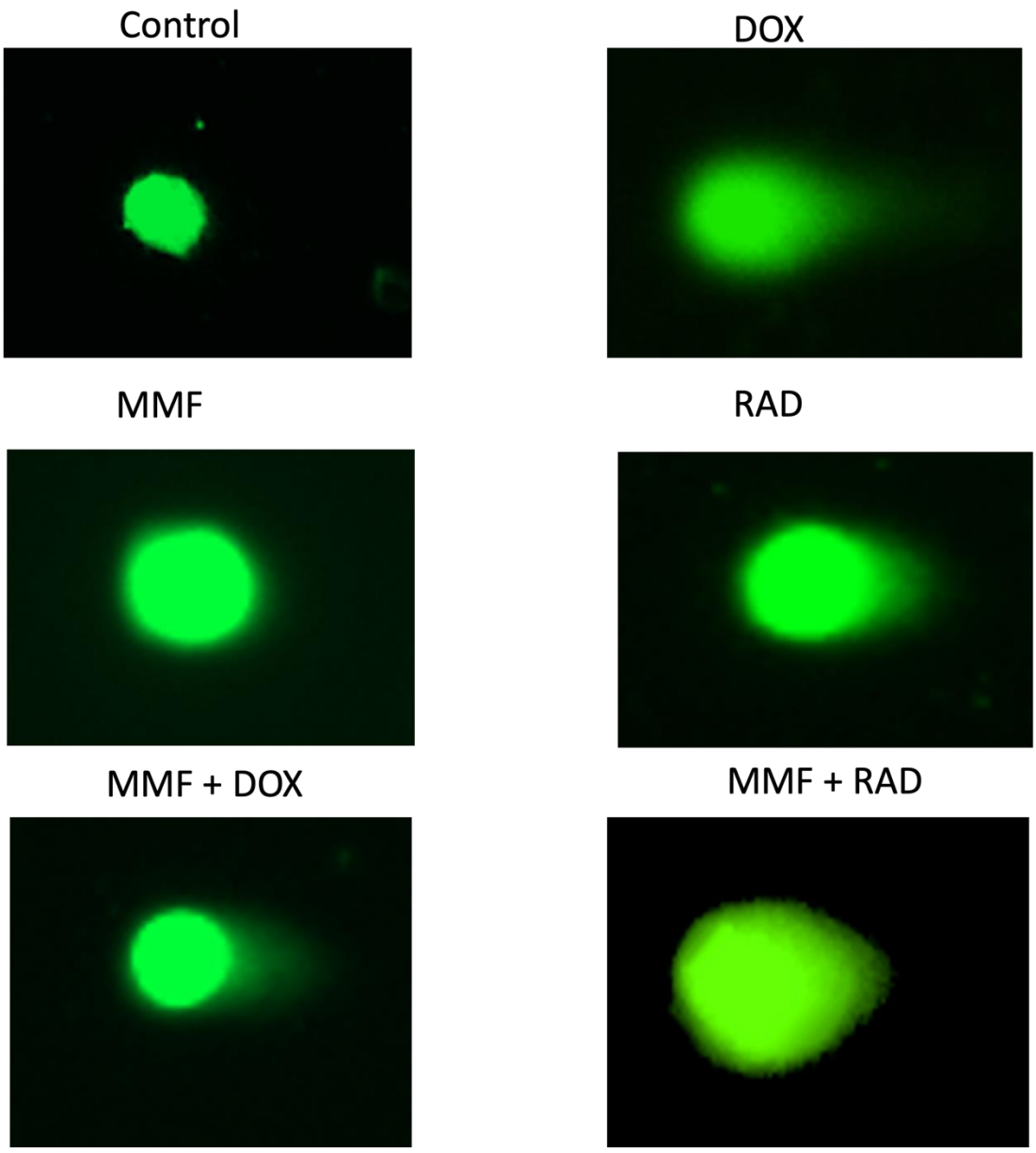

Figure 2. 19 Indicative images of single cells subject to the comet assay.

Images show cells that have been subjected to a Comet Assay. DNA damage visible as it is pulled from the cell towards the anode giving a distinctive tail, panels represent images of untreated and treated cells, relative treatment detail above individual images.

2.4.14 Comparison of DNA fragmentation at 0hr, 24hr and 48hr- Analysis of DNA repair

MDA-MB-231 cells were treated as described in section 2.42.19. As MDA-MB-231 cells were analysed following treatment at 3 different time points the ability of the cellular repair was able to be analysed. Figure 2.20 describes the median tail moment (AU) as a percentage of the control at 0 hrs post treatment, 24 hrs post treatment and 48 hrs post treatment.

As described above, an increase in tail moment indicated an increase in DNA damage caused due to the addition of the treatment regime. Statistical analysis was carried out to determine if there were any statistically significant differences in the median tail moments of each treatment at each time point. The statistical comparisons are detailed in Appendix 2.

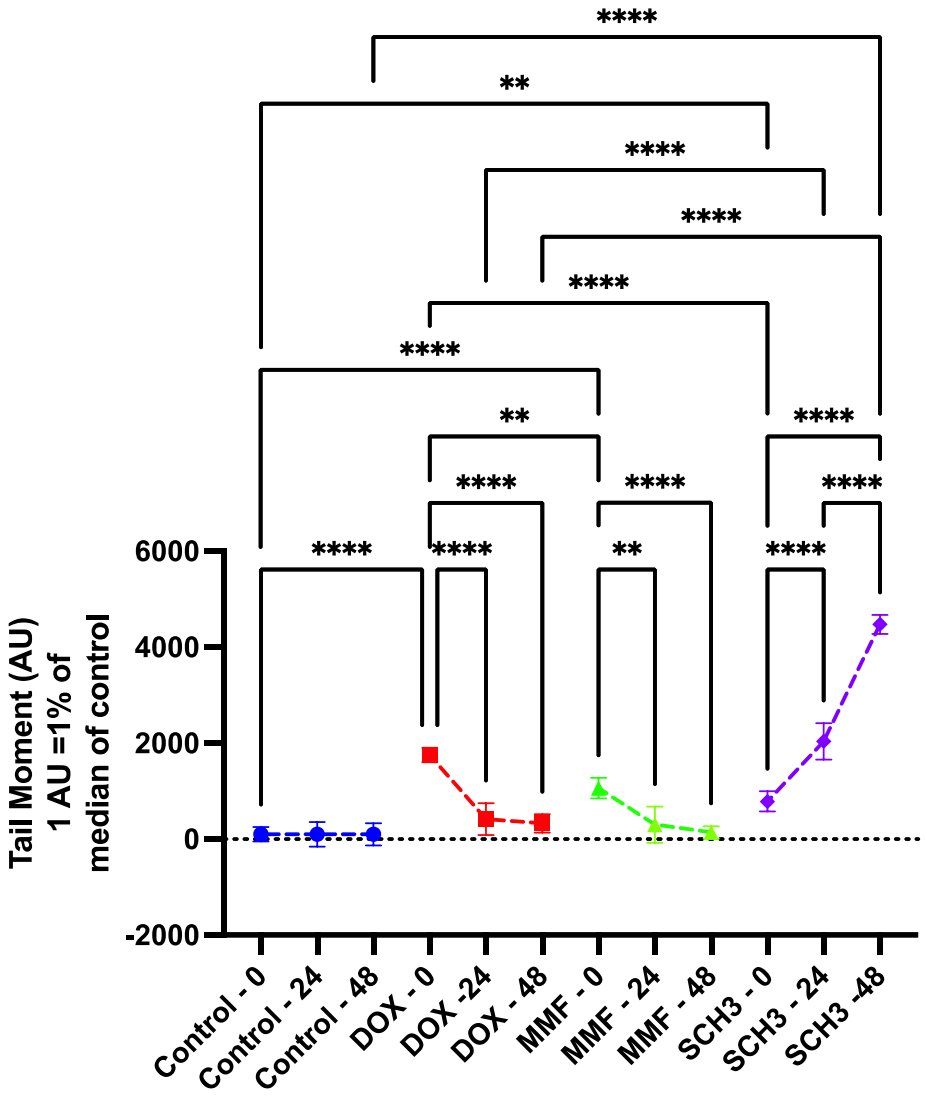

Figure 2. 20 The median DNA damage quantified as Tail Moment (AU) is displayed as a percentage of the control median tail moment.

DOX alone, MMF alone and combination SCH3M+D were the treatments used as described in Figure 18. Results displayed as an average of 3 independent experiments using 70 comets per sample, +/- SD. 3 time points of 0hr post treatment, 24hrs post treatment and 48hrs post treatment are compared for each treatment. Statistical analysis was carried out using a one-way ANOVA with Bonferroni's correction and are detailed in table 3 (see appendix 2).

The results from Figure 2.20 suggest that at 0 hrs post treatment removal there was a statistically significant increase in the median tail moment of all treated cells when compared to the untreated control (DOX and MMF $P<0.0001$, SCH3 $P=0.0079$). Surprisingly, there was also a statistically significant decrease in median tail moment when comparing DOX alone treatment group and SCH3 treatment group 0 hrs post treatment removal ($P<0.0001$). This could however be due to the scheduling of treatment administration. The cells in DOX alone have been exposed to DOX for 48 hrs, whereas the cells in SCH3 have only been exposed to DOX for 24 hrs, therefore there may be a delay in the accumulation of DNA damage. SCH3 was the only treated group of cells to produce statistically significant increased median tail moments 24 hrs and 48 hrs post treatment removal when compared to the untreated control ($P<0.0001$). For both MMF and DOX alone treated cells, there was a statistically significant decrease in the median tail moment when comparing 24 hr and 48 hrs post treatment to 0 hrs post treatment, suggesting that MMF alone and DOX alone treated cells can repair any DNA damage following initial treatment. SCH3 median tail moments at 24 and 48 hrs, however, suggest the opposite, there is a significant increase in median tail moment 24 and 48 hrs when comparing SCH3 to the control and single therapies.

Overall. the results from Figure 2.20 suggest that between 0 hrs and 48 hrs median tail moments decrease in MMF alone and DOX alone treated cells possibly indicating cell repair. However, the median tail moment increases for SCH3 treated cells, suggesting that more DNA damage induced is unable to be repaired and in in fact increasing within the 0 and 48 hr post treatment removal window. Thus, suggesting that the combination therapy D-SCH3 can induce DNA damage to MDA-MB-231 cells which is more difficult for the cells to repair than DNA damage induced by single therapies.

2.4.15. Combination Index analysis of Combination therapy using Radiotherapy and Monomethyl Fumarate on MDA-MB-231 cells.

To determine if the proposed scheduled combinations were acting synergistically, a combination index (CI) was carried out (Figure 2.21). Figure 21 details the CI of MDA-MB-231 cells incubated with either 2 μM MMF or 10 μM MMF and exposed to 2 Gy radiation in the three different schedules.

(A)

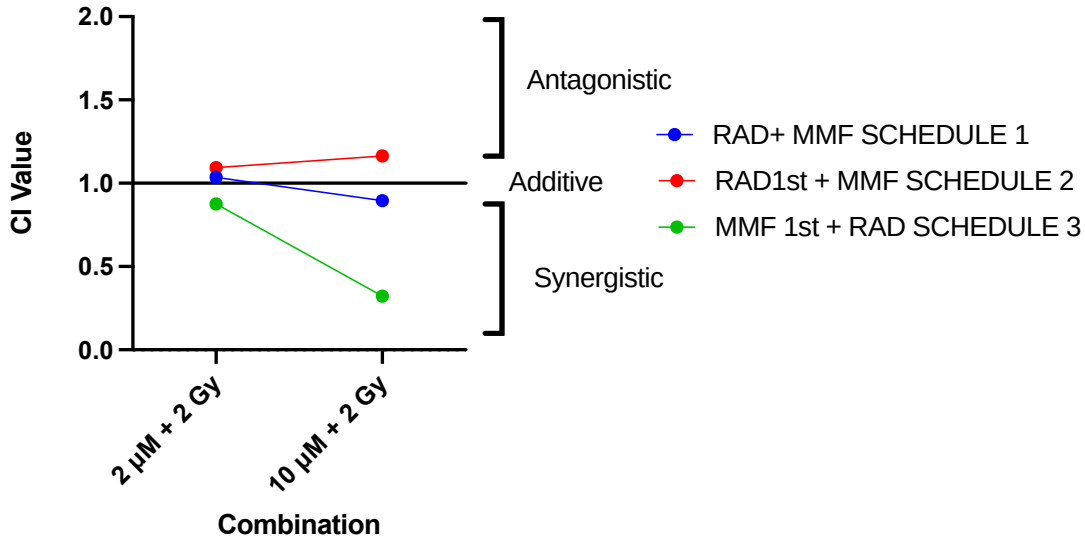

(B)

Drug doses	**Schedules**		
	SCHEDULE 1	SCHEDULE 2	SCHEDULE 3
MMF 2 μM + RAD 2Gy	1.03	1.09	0.9
MMF 10 μM + RAD 2Gy	0.9	1.16	0.32

Figure 2. 21 (A)Combination Index (CI) after MDA-MB-2312 cells are incubated with RAD and MMF in the 3 treatments Schedules.

Antagonistic <1.1, Additive = .9-1.1 and Synergistic > 0.9. Each point represents three independent experiments. (B) Values of CI plotted in (A). Data was taken from clonogenic survival assays and analysed using Calcucyin software as described in section 2.4.8.

Results from Figure 2.21 suggest that SCH1 produced an additive CI value when treated with MMF 2 μM + RAD 2Gy and synergistic CI value when treated with MMF 4 μM + RAD 2Gy (Figure 2.21B). SCH2 induced an additive CI value when treated

with MMF 2 μM + RAD 2Gy and an antagonistic CI when treated with MMF 4 μM + RAD 2Gy (Figure 2.21B). SCH3 was the only combination to produce synergistic CI values for both concentrations of MMF tested (Figure 2.21B). These results suggest that SCH3 is the most appropriate combination to use as it was the only combination to produce a synergistic (better than the sum of each agent) CI value at when using MMF 2 μM + RAD 2Gy.

2.4.16 Cell cycle analysis of MDA-MB-231 cells after combination treatment with Radiotherapy and Monomethyl Fumarate

As described in Section 2.42.14, a cell cycle analysis assay was carried out to investigate the effect each treatment had on the percentage of cells in each phase of the cell cycle. MDA-B-231 Cells in were treated with RAD alone, MMF alone and the SCH3 RAD combination (MMF1st 2 μM + RAD 2 Gy 24 hours after MMF therapy administration) cells were harvested for cell cycle analysis immediately after treatment.

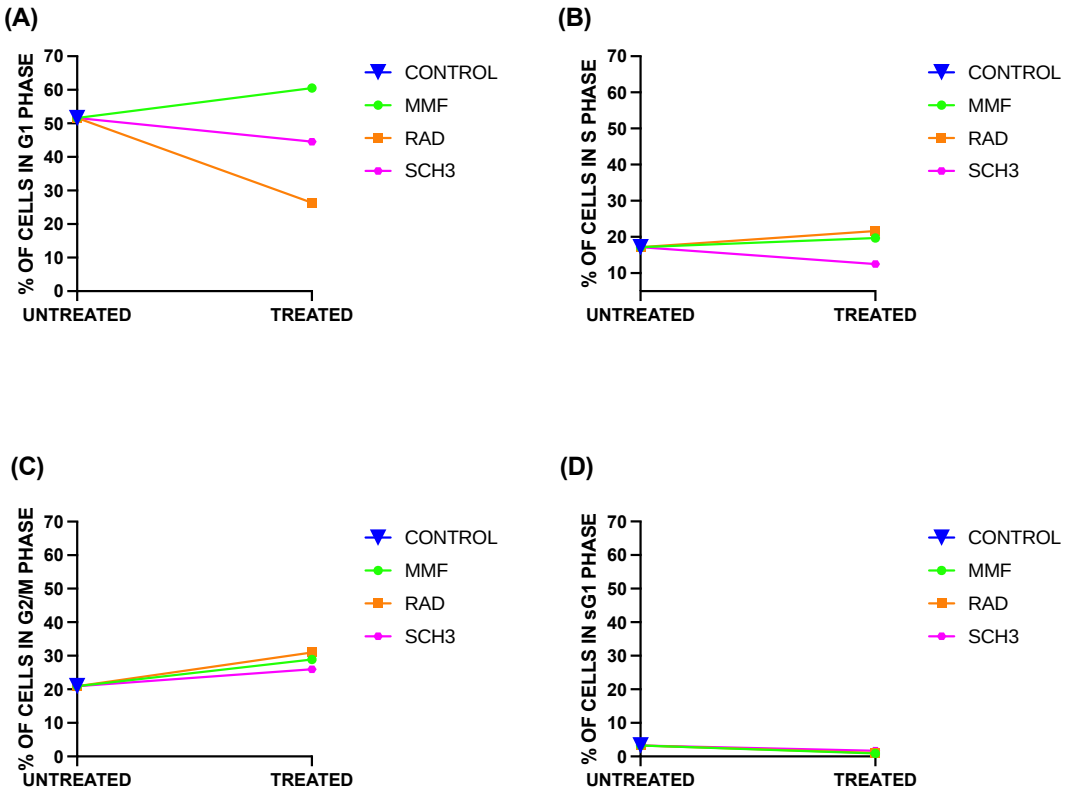

(E)

Bonferroni's multiple comparisons test	G1 - P Value	S – P Value	G2/M – P Value	sG1 – P Value
CONTROL vs. MMF	<0.0001	0.0040	<0.0001	>0.9999
CONTROL vs. RAD	<0.0001	<0.0001	<0.0001	>0.9999
CONTROL vs. SCH3	<0.0001	0.0002	<0.0001	>0.9999
MMF vs. RAD	<0.0001	<0.0001	0.0069	>0.9999
MMF vs. SCH3	<0.0001	<0.0001	0.0008	>0.9999
RAD vs. SCH3	<0.0001	0.7538	<0.0001	>0.9999

Figure 2. 22 Shows the cell cycle distribution of untreated MDA-MB-231 cells and treated MDA-MB-231 cells with the corresponding agents in the figure legend, 0hr post treatment removal.

(MMF 2μM, RAD 2Gy, SCH3 – MMF2μM1st+ RAD 2Gy 24hr later). The figure above represents the percentage of cells in each phase of the cell cycle, results displayed as an average of 3 independent experiments carried out in triplicate (A) – G1, (B)- S, (C)- G2/M and (D)- sG1. (E) A two-way ANOVA test was utilized to compare the means of the cell cycle phases after treatment cells versus untreated control cells and demonstrated in the above Tables where, *P<0.05, **P<0.01, ***P<0.001 and ****P<0.000.1 (applicable to Figures 2.22-2.24).

Figure 2.22A suggests that there was a statistically significant increase in the percentage of cells in G1 phase of the cell cycle when cells were treated with MMF only compared to the untreated control, RAD alone and SCH3, as expected (all P<0.0001, Figure 2.22E). There was also a statistically significant decrease in the percentage of cells in G1 phase of the cell cycle when treated with RAD only and SCH3 when compared with the untreated control MMF alone treated cells, as expected (both P<0.0001, Figure 2.22E). There was a statistically significant increase in the percentage of cell in the S phase of the cell cycle when treated with MMF alone and RAD alone compared with the untreated control and SCH3 (MMF vs. control P=0.0040, RAD vs. control P=<0.0001, MMF vs. SCH3 P=<0.0001, RAD vs. SCH3 P<0.0001, Figure 2.22E). There was a statistically significant increase in the percentage of cells in G2/M compared to the untreated control (P<0.0001, all, Figure 2.22E).

This data suggests the RAD alone, MMF alone and SCH3 change the distribution of cells in the cell cycle compared to the control. MMF, as expected, is causing an accumulation of cells in G1. All treatments appear to cause an accumulation of cells in G2/M, suggesting that cells are being blocked at the G2/M checkpoint. This block in RAD treated cells and SCH3 treated cells in G2/M is supported by the decrease in treated cells distributed in G1, a block in G2/M will prevent cells from fully dividing and as a result the number of cells entering G1 will decrease, as seen 0hrs post treatment removal.

Figure 2.23 details the percentage of cells in each phase of the cell cycle following treatment with MMF alone, RAD alone and SCH3 combination, 24 hours after treatment was removed.

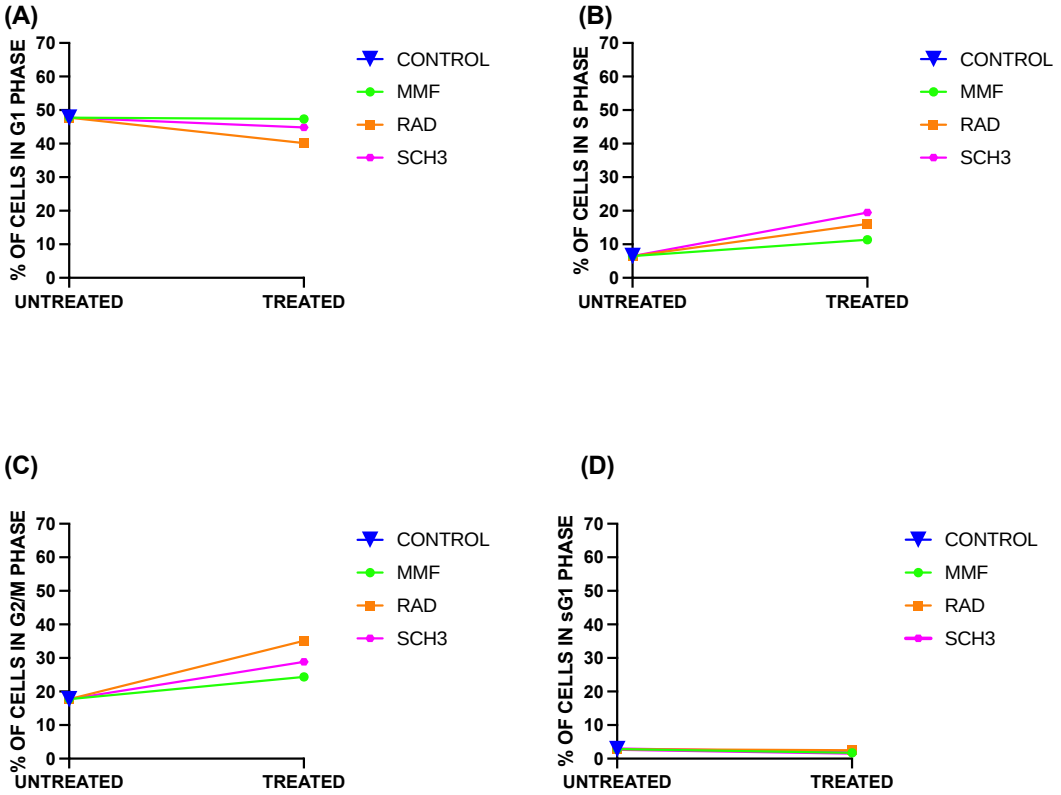

(E)

Bonferroni's multiple comparisons test	G1 - P Value	S – P Value	G2/M – P Value	sG1 – P Value
CONTROL vs. MMF	>0.9999	<0.0001	<0.0001	0.1934
CONTROL vs. RAD	<0.0001	<0.0001	<0.0001	>0.9999
CONTROL vs. SCH3	0.0012	<0.0001	<0.0001	0.1897
MMF vs. RAD	<0.0001	<0.0001	<0.0001	0.6491
MMF vs. SCH3	0.0032	<0.0001	<0.0001	>0.9999
RAD vs. SCH3	<0.0001	0.0005	<0.0001	0.6369

Figure 2. 23 Shows the cell cycle distribution of untreated MDA-MB-231 cells and treated MDA-MB-231 cells with the corresponding agents in the figure legend, 24 hr post treatment removal.

In contrast to immediately after treatment removal, after 24 hours there was a treatment dependent redistribution of cells in the various phases of the cell cycle except for sG1 where there were no differences detected (Figure 2.23 D). In terms of G1 phase, there was a statistically significant decrease in the percentage of cells in this phase of the cell cycle following treatment with RAD alone and SCH3 when compared to the untreated control (RAD vs. control P<0.0001, SCH3 vs. control

P=0.0012, Figure 2.23E). There was also a statistically significant decrease in the percentage of cells in G1 phase of the cell cycle following treatment with RAD and SCH3 compared to MMF alone (RAD vs. MMF P=<0.0001 and SCH3 vs. MMF P=0.0032, Figure 2.23E). There was a statistically significant increase in the percentage of cells in S phase of the cell cycle following all treatments compared with the control (all P<0.0001, Figure 2.23E).There was also a statistically significant decrease in the percentage of cells in S phase of the cell cycle when cells were treated with the RAD alone, MMF alone and the untreated control, compared with SCH3 alone (control vs SCH3 P<0.0001, MMF vs SCH3 P<0.0001 and RAD vs. SCH3 P=0.0005, Figure 2.23E). There was a statistically significant increase in the percentage of cell in G2/M phase of the cell cycle when cells were treated with MMF alone, RAD alone and SCH3 compared with the untreated control (All P<0.0001, Figure 2.23E). There was also a statistically significant increase in the percentage of cells in G2/M phase of the cell cycle when cell was treated with RAD alone compared to MMF alone, SCH3 alone and the untreated control (all, P=0.0001< Figure 2.23E). There were so statistically significant changes in sG1 phase of the cell cycle.

Overall, the data from Figure 2.23 suggest that the SCH3 combination 24 hrs after treatment removal, induces a larger redistribution of cells in the various phases of the cell cycle with an increase in the percent of cells in G2/M and S phase of the cell cycle and a decrease in the percentage of cells In G1 phase of the cell cycle. This may be that the cells previously arrested in G1 have now moved onto S phase, but that there is a reduction in new cells entering the G1 phase as they are arrested in the G2/M phase of the cell cycle because of the radiation as therapy in this combination therapy as seen in Figure 2.22. The cells previously in G1 and S as seen in Figure 2.22 have now accumulated in G2/M phase of the cell cycle as seen above in Figure 2.23. These results are supported by the findings of Hargrave *et al*., (2022), in which the authors reported an increase in G2/M and decrease in G1, 24 hrs following radiation in MDA-MB-231.

Figure 2.24 details the results following MDA-MB-231 cells treated with MMF, RAD and SCH3 (MMF+RAD combo). Cells were harvested 48 hours after treatment removed.

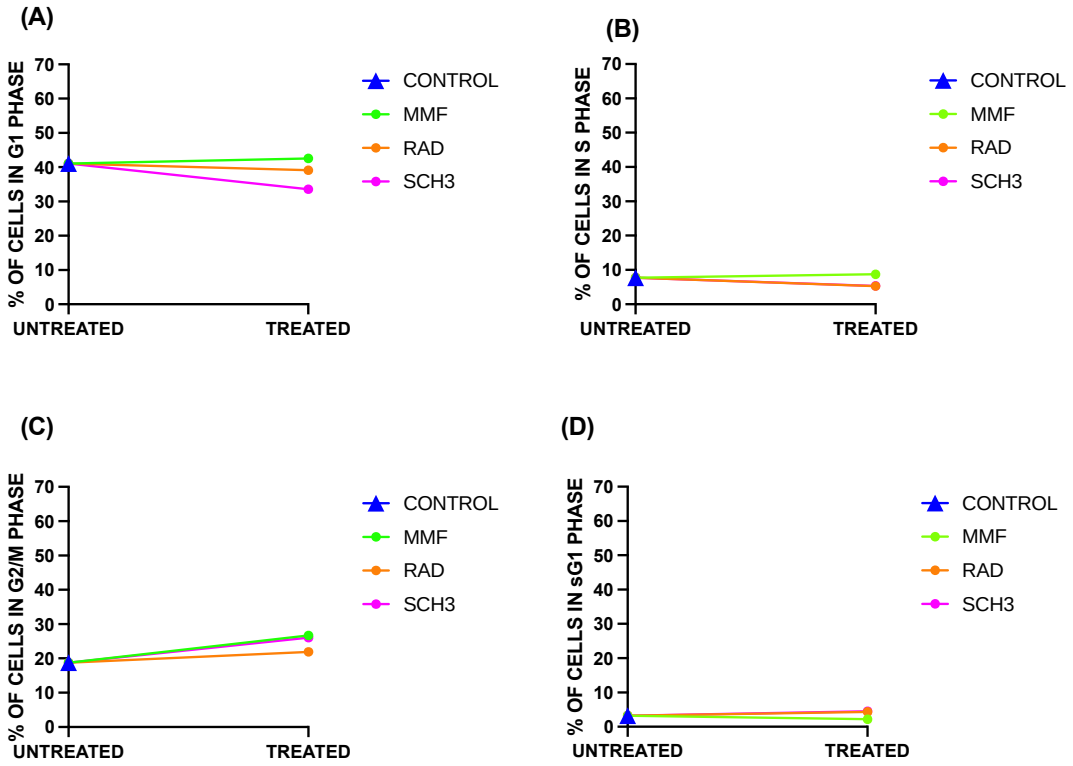

Bonferroni's multiple comparisons test	G1 - P Value	S – P Value	G2/M – P Value	sG1 – P Value
CONTROL vs. MMF	0.0917	0.4318	<0.0001	0.4179
CONTROL vs. RAD	0.0245	0.0055	0.0008	0.3253
CONTROL vs. SCH3	<0.0001	0.0072	<0.0001	0.2193
MMF vs. RAD	0.0006	0.0006	<0.0001	0.0147
MMF vs. SCH3	<0.0001	0.0007	>0.9999	0.0105
RAD vs. SCH3	<0.0001	>0.9999	0.0001	>0.9999

Figure 2. 24 Shows the cell cycle distribution of untreated MDA-MB-231 cells and treated MDA-MB-231 cells with the corresponding agents in the figure legend, 48 hr post treatment removal.

Figure 2.24A suggests that the percentage of cells in each phase of the cell cycle has been redistributed from the 24 hr time point (Figure 2.23) to the 48 hr time point in Figure 2.24 above. There was a statistically significant decrease in the percentage of cells in G1 phase was maintained at 48 hrs, there was a still a statistically significant decrease in the percentage of cells in G1 when treated with RAD alone and SCH3 treated cells compared to the untreated control and MMF alone (control vs. RAD P=0.0245, control vs. SCH3 P<0.0001, MMF vs. RAD 0.0006 and MMF vs. SCH3 P<0.0001, Figure 2.24E). There was a maintained statistically significant increase in

the percentage of cells in S phase following treatment with SCH3 and RAD alone compared with the control and MMF alone (control vs. RAD = 0.0055, control vs. SCH3 P=0.0072, MMF vs. RAD P= 0.0.0006 and MMF vs. SCH3 P=0.0007, Figure 2.24E). There was also a maintained statistically significant increase in the percentage of cells in G2/M phase of the cell cycle when comparing all treated cells to the untreated control (control vs MMF P<0.0001, control vs. RAD P=0.008, control vs. SCH3 P<0.0001, Figure 2.24E). Interestingly there was a statistically significant decrease in the percentage of cells in G2/M following treatment with RAD when compared to SCH3 alone (P<0.0001, Figure 2.24E). This was the opposite of the results in Figure 2.23C, in which SCH3 treated cells had a statistically significantly reduced percentage of cells in G2/M when compared to RAD alone treated cells at the 24 hr time point.

Overall, these results suggest that following treatment with RAD alone and SCH3, the decrease in cells in G1 phase of the cell cycle is maintained for all treated cells 48 hrs after treatment removal, this may be due to the significant increase in the percentage of cells in G2/M reported 24 hrs after treatment removal (Figure 2.23), these cells have now begun apoptotic processes and are prevented from re-entering the cell division process. The statistically significant decrease in the percentage of cells in S may be due to cells in G1 being inhibited by the G1 checkpoint, unable to progress into S phase 48 hrs after treatment removal. The percentage of cells in each phase of the cell cycle after treatment with SCH3 followed a similar pattern to that of RAD, however there was a significant decrease in G1 and increase in G2/M for SCH3 treated cells when compared to RAD alone. MMF treated cells show a similar distribution of cells in each phase of the cell cycle 48 hrs post treatment removal to that of the untreated control, suggesting that these cells have recovered from any disruption caused by MMF treatment. As cells treated with RAD and SCH3 still show significant differences in cell cycle distribution 48 hrs post treatment removal, this would suggest that these cells are still accumulating at checkpoints within the cell cycle and the damage caused by irradiation and the combination has not been fully repaired. These finding are supported by clonogenic data in Figure 2.11 which reported a statistically significant decrease in the survival fraction of cells treated with RAD alone and SCH3 compared to the untreated control. This may be due to an

accumulation of DNA strand breaks; however, this will need to be further assessed using Annexin V apoptotic detection kit.

2.4.17 Apoptosis/Necrosis quantification of MDA-MB-231 cells after combination treatment with Radiotherapy and Monomethyl Fumarate

As previously described in section 2.3.10, an investigation into apoptosis induction in MDA-MB-231 cells was investigated. This section investigated the percentage of cells that undergo apoptosis following treatment both MMF 2 μM and radiation alone (2 Gy) but also as a combination SCH3 MMF 2 μM + RAD 2 Gy. The same Annexin V apoptotic detection assay was caried out as described in section 2.3.10 and section 2.4.10. As detailed in Figure 2.25, these experiments were carried out in triplicate at 3 different time points to coincide with the time points used to investigate cell cycle analysis in section 2.42.24. 0 hrs post treatment removal, 24 hours post treatment removal and 48 hours post treatment removal.

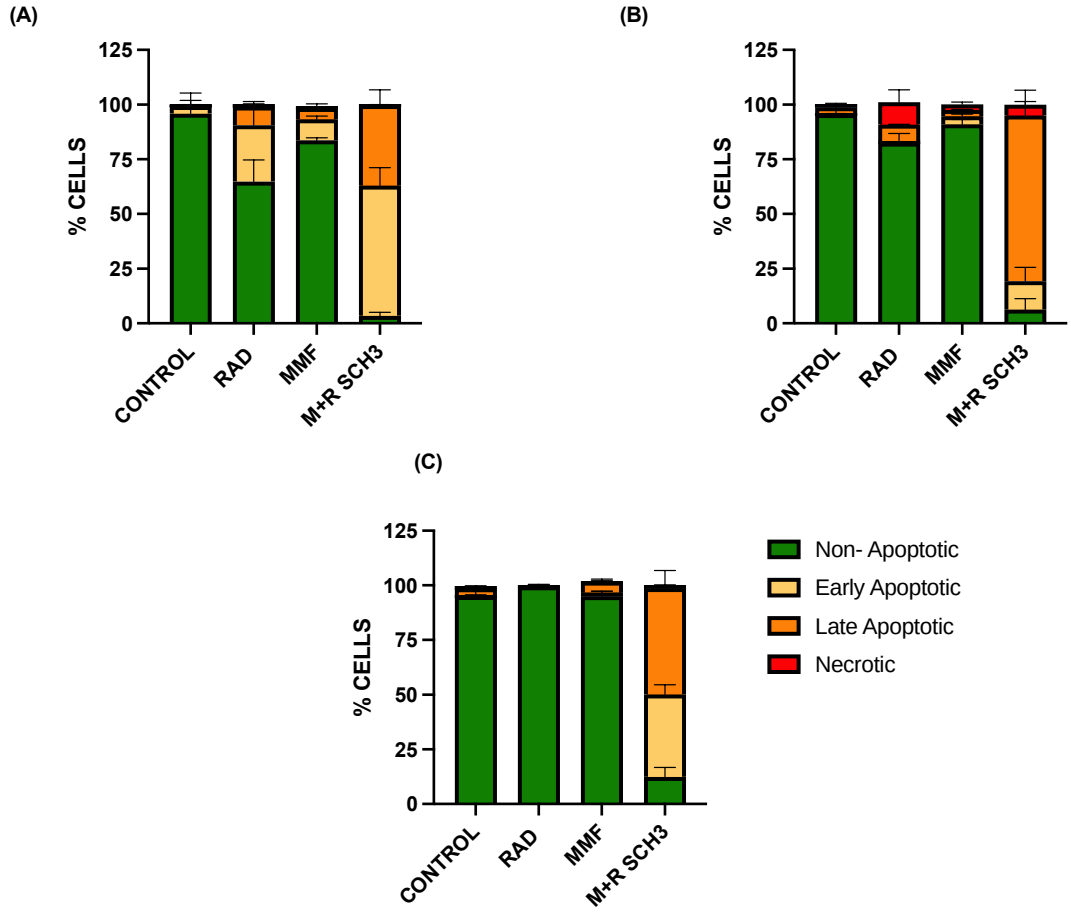

Figure 2. 25 The effect of RAD 2Gy, MMF 2 μM and SCH3 M1st 2 μM +R 2 Gy on the different phases of apoptosis in MDA-MB-231 cells are shown.

Three different time points were used post treatment removal; (A) 0 hr, (B) 24 hr and (C) 48 hr. Data is expressed as mean+/- SD of 3 individual experiments carried out in triplicate, at each time point. Statistical Analysis carried out using two-way ANOVA followed by Bonferroni's post hoc testing, comparing each apoptotic phase separately between all treatments (see Appendix 3).

Results from Figure 2.25A suggest that at 0 hrs post treatment removal, there was a statistically significant decrease in the percentage of non-apoptotic cells following treatment with SCH3 compared with the untreated control and MMF alone (control P=0.0019 and MMF P<0.0001). There was a statistically significant increase in early apoptotic cells following treatment with SCH 3 compared with the untreated control and MMF alone (control P=0.0037 and MMF P=0.0194). There was a statistically significant increase in the percentage of late apoptotic cells when comparing all treated cells with the untreated control (RAD P=0.04222, MMF P<0.0001 and SCH3

P=0.0287). There was a statistically significant increase in the percentage of late apoptotic cells when treated with SCH3 compared to RAD alone and MMF alone (RAD P=0.0454 and MMF P=0.0379). There was no statistically significant change in the percentage of necrotic cells 0 hrs post treatment removal.

Figure 2.24B suggest that the statistically significant decrease in the percentage of non-apoptotic cells following treatment with SCH3 compared to the untreated control, was maintained 24 hrs post treatment removal (P=0.0002). There was a statistically significant decrease in the percentage of non-apoptotic cells when treated with SCH3 compared to the single therapies RAD alone and MMF alone (RAD vs. SCH3 P=0.0002 and MMF vs. SCH3 P=0.0011). There was also a statistically significant increase in the percentage of late apoptotic cells following treatment with SCH3 compared to the untreated control and MMF alone (control P=0.0491, MMF P=0.0493).

Figure 2.24C suggests that 48 hrs post treatment removal SCH3 produced a statistically significant reduction in non-apoptotic cells compared to the untreated control and single therapies RAD alone and MMF alone (control P=0.0006, MMF P=0.0004 and RAD P=0.0032). SCH3 was also the only treated group of cells that produced a statistically significant increase in the percentage of cells in early apoptosis when compared to the untreated control or the single therapies RAD alone and MMF alone RAD (control P=0.0260, MMF P=0.0245, RAD P=.0262).

Therefore, the results from Figure 2.25 suggest that following treatment with SCH3, MDA-MB-231 cells show an increased percentage of cells in early and late apoptosis when compared to the untreated control or single therapies alone up to 48 hrs post treatment removal. This suggests the SCH3 is a more suitable therapy option at inducing apoptosis in TNBC cells than the single therapies alone. Overall, these results are reflective of the finding from clonogenic assessment of SCH3 in Figure 2.11, in with SCH3 reported a statistically significant reduction in the survival fraction of cells when compared to the untreated control, RAD alone and MMF alone.

2.4.18 Analysis of Glutathione levels in MDA-MB-231 cells after combination treatment with Radiotherapy and Monomethyl Fumarate

The results shown in Fig 2.26 were gathered as described in Section 2.3.22. Cells were harvested so GSH levels could be measured; 1 hour after therapy was administered (for combination 1 hr after second therapy administered), 0 hrs after the 48-hr treatment were complete, 24 hrs after the treatments were removed and 48 hrs after the treatment were removed, as previously detailed in Section 2.42.17.

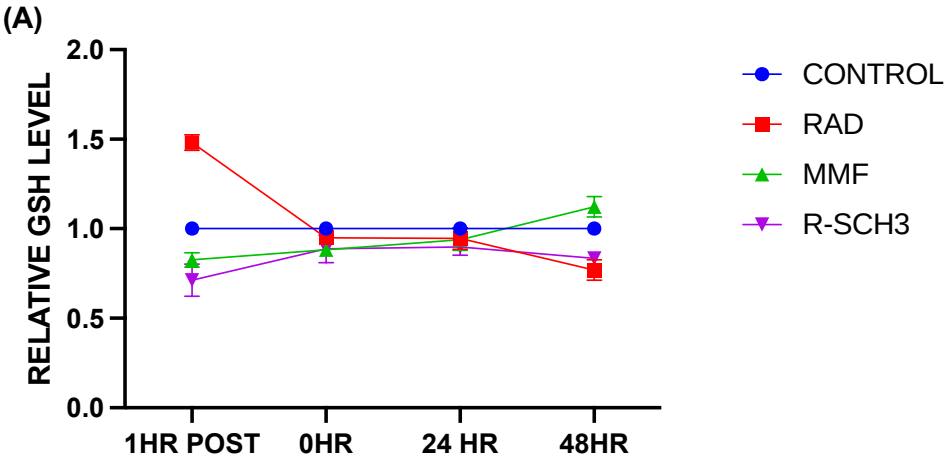

Bonferroni's multiple comparisons test	P Value 1 HR post	P Value 0HR	P Value 24HR	P Value 48HR
CONTROL vs. RAD	0.0032	>0.9999	>0.9999	0.0443
CONTROL vs. MMF	0.3018	0.4183	>0.9999	0.4822
CONTROL vs. SCH3	0.0417	0.4658	0.9785	0.1740
RAD vs. MMF	<0.0001	0.7734	>0.9999	0.0008
RAD vs. SCH3	<0.0001	0.9007	>0.9999	0.9981
MMF vs. SCH3	0.4026	>0.9999	>0.9999	0.0025

Figure 2. 26 The affect single therapies RAD 2Gy and MMF 2 μM, and combination therapy SCH3 MMF 2 μM 1st + RAD 2 Gy 24 hours later.

(A) Data reported is an average of three independent experiments carried out in triplicate. (B)A one-way ANOVA with Bonferroni post testing was performed using GraphPad prism 9.2.1 comparing each treated and untreated group to each other, *P<0.05, **P<0.01, ***P<0.001 and ****P<0.0001.

The results from Figure 2.26 suggests that glutathione levels changed compared to the controls over time with each drug alone and the combination therapy. 1 hr into

treatment administration there was a statistically significant increase in the relative GSH levels when cells were treated with RAD alone compared to the untreated control, MMF alone and SCH3 (control P=0.0032, MMF P<0.0001 and SCH3 P<0.0001, Figure 2.26B). At 0 and 24 hrs post treatment removal there were no statistically significant changes in the relative GSH levels when comparing any treated or untreated cell groups. However, at 48 hrs post treatment removal there were statistically significant decreases in the relative GSH levels when cells were treated with RAD alone compared to the untreated control (RAD vs. control P=0.0448, Figure 2.26B). There was also a statistically significant decrease in the relative GSH levels when cells were treated with SCH3 and RAD alone, compared to MMF alone (RAD vs. MMF P=0.0008 and SCH3 vs. MMF P=0.0025, Figure 2.26B).

Overall, when MDA-MB-231 cells were treated with SCH3 there appears to be an initial decrease in GSH as seen in MMF alone treated cells. This initial level of GSH was maintained to below that of the control GSH level at all time points measured, after the treatment incubation was complete as would be expected with MMFs mode of action as this inhibits the synthesis of GSH. The results of relative GSH levels in SCH3 treated cell are like that of MMF alone treated cells, except for 48 hrs post treatment removal, in which we observe a rebound of MMF relative GSH levels as expected (Lushchak, 2012). The final relative GSH present in SCH3 treated cells was like that of RAD alone, suggesting that there was initially less GSH in SCH3 treated cells and this reduction in GSH was maintained up to 48 hrs post treatment removal. These results are supportive of the findings in Figure 2.25 Annexin V analysis, as it is known that a depletion in glutathione levels is associated with an increase in apoptotic cells due to an increase in ROS (Lu, 2013).

2.4.19 Detection of Autophagic MDA-MB-231 cells after combination treatment with Radiotherapy and Monomethyl Fumarate

As previously described in section 2.42.18 an autophagy assay was used to investigate the percentage of cells that had undergone autophagy because of treatment. However, this section investigated the MDA-MB-231 cells that were treated with MMF 2 μM alone radiation at 2 Gy as well as the schedule 3 combination of MMF 2 μM + Rad 2 Gy, as detailed in Figure 2.27. This assay was carried out in triplicate at 3 different time points to co-inside with the Cell Cycle analysis data (Section 2.42.24).

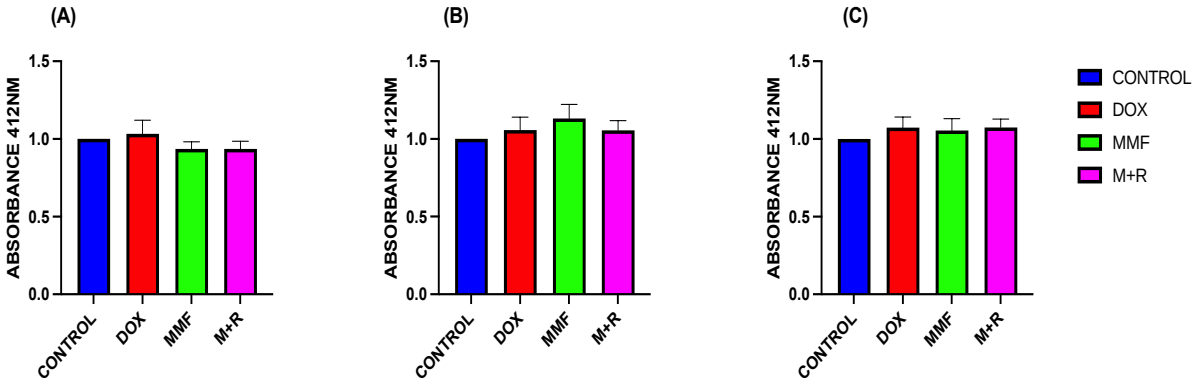

Figure 2. 27 The effect of; RAD alone 2 Gy, MMF alone 2 μM or Schedule 3 combination MMF1st 2 μM+ Rad 2 Gy 24 hours later, on Green Detection Reagent.

Data is expressed relative to the control. Cells were measure on a fluorescent microplate reader at 412 nm. (A) 0 hours after treatment removed. (B) 24 hours after treatment removed. (C) 48 hours after treatment removed. All graphs are displayed as mean and standard deviation of 3 individual experiments carried out in triplicate. One -way ANVOA was carried out with Bonferroni's correction.

From Figure 27 (A), there was no statistically significant difference in the absorbance of treated or untreated cells. Overall, this data suggests that MDA-MB-231 cells are not undergoing autophagy when treated with radiation alone, MMF alone or RAD + MMF SCH3 combination.

2.4.20 Quantification of DMA damage and repair using Comet Assay, of MDA-MB-231 cells after combination treatment with Radiotherapy and Monomethyl Fumarate

A comet assay was used to quantify the DNA damage induced by radiation alone at 2 Gy, MMF alone at 2 μM and the SCH 3 combination of M+R. This assay was previously described in Section 2.42.19. Unlike section 2.42.20 comet analysis was carried out immediately after treatment (rather than after cells were exposed to drug for 48 hrs) as when using radiation, a spike in ROS occurs immediately after irradiation exposure and then begins to repair gradually (Zhang *et al*., 2018). Therefore, to quantify this spike in DNA damage a comet assay was carried out immediately following irradiation, 24 hrs after initial treatment and 48 hrs after initial treatment. This same time points were used for MMF alone and SCH3 treated cells, for SCH3 treatment the 0-hr time point was taken 24 hrs after MMF administration and immediately after these pre-exposed MMF cells were irradiated. This allowed for an analysis of cells exposed to radiation without MMF prior exposer and those with prior MMF exposure. MMF alone treated cells were exposed to MMF for 10 minutes (this is to allow for the time taken to irradiate cells using X-irradiator and carry cell back to a cell culture hood for harvesting).

2.4.21 Comparison of DNA fragmentation at 0hr, 24hr and 48hr- Analysis of DNA repair

Figure 2.28 represents the median tail moment (AU) as a percentage of the control at 0 hrs post treatment, 24 hrs post treatment and 48 hrs post treatment. Treatments administered were RAD 2 Gy, MMF 2 μM or SCH3 combination of MMF 2 μM + RAD 2 Gy. Statistical analysis was carried out on these results using a one-way ANOVA with Bonferroni's correction, the results are detailed in Appendix Table 2.4.

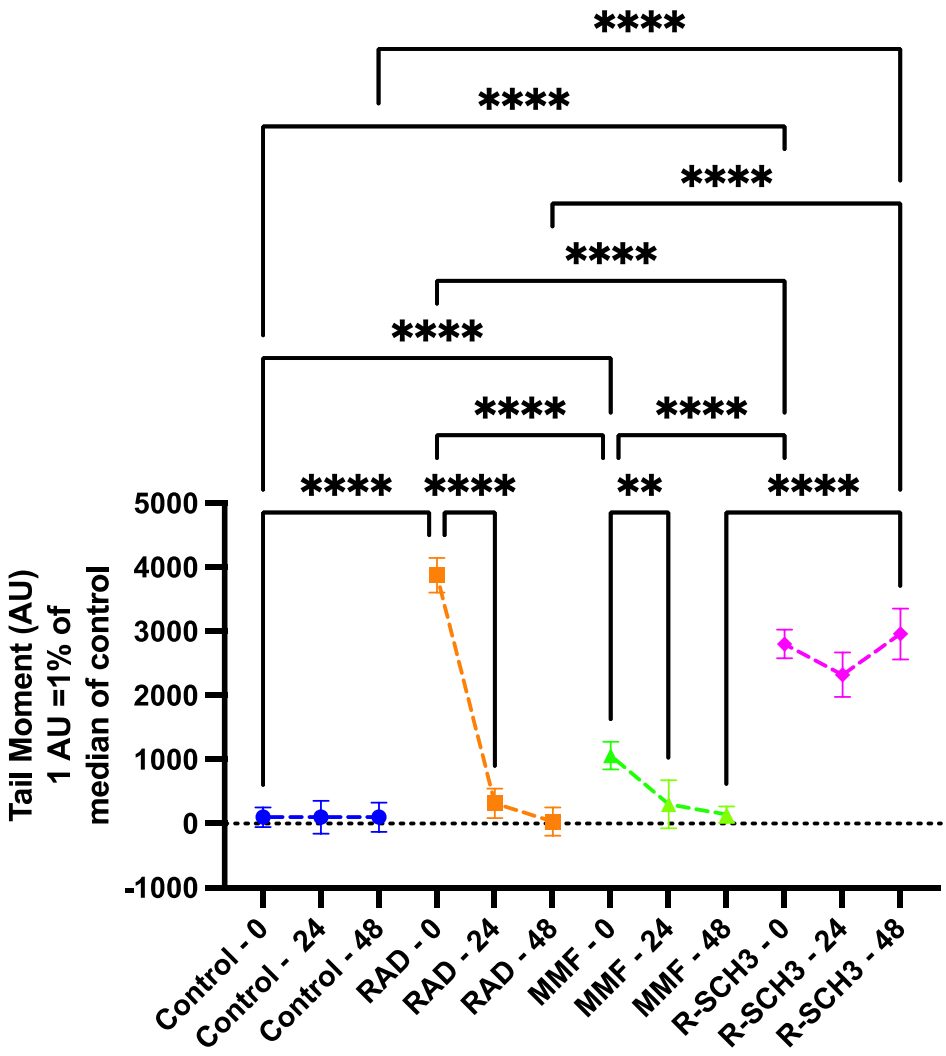

Figure 2. 28 The median DNA damage quantified as Tail Moment (AU) is displayed as a percentage of the control median.

RAD alone, MMF alone and combination SCH3M+R were the treatments used as described in section 2.4.7.1. 3 time points of 0hr post treatment, 24hrs post treatment and 48hrs post treatment are compared for each treatment, results are an average of 3 independent experiments carried out in triplicate, 70 comets per treatments group. Statistical analysis was carried out using a one-way ANOVA with Bonferroni's correction and are detailed in table 3. p>0.0001 ****, p>0.001 *** and p>0.01** (see Appendix 4).

Figure 2.28 reported that 0 hrs post treatment there was a statistically significant increase in the median tail moment of all treated cells when compared to the untreated control (all P<0.0001). There was a statistically significant increase in the median tail

moment 0 hrs post treatment when cells were treated with RAD alone and SCH3 compared to MMF alone (both P<0.000). 24 hrs post treatment there was a statistically significant increase in median tail moments when cells were treated with SCH3 compared to the untreated control and both single therapies RAD alone and MMF alone (all P<0.0001). This was the only statistical significance found when comparing any treated group to each other at the 24 hrs post treatment time point. 48 hrs post treatment there was a statistically significant increase in median tail moments of cells treated with SCH3 compared with the untreated control and the single therapies, RAD alone and MMF alone (all P<0.0001), again this was the only statistically significant change in median tail moments found 48 hrs post treatment when comparing any treated or untreated group to each other. There were no statistically significant changes in the median tail moment of cells treated with SCH3 when comping results from 0 hrs post treatment, 24 hrs post treatment and 48 hrs post treatment (all NS).

Overall. the results from Figure 2.28 suggest that between 0 hrs and 24 hrs tail moments decrease in cells treated with RAD alone and MMF alone, indicating cell repair of DNA strand breaks. This repair is maintained up to 48 hrs post treatment for RAD alone and MMF alone treated cells, these results are supportive of the findings from clonogenic analysis (Figure 2.11) and Annexin V, as it was found there were no statistically significant changes in the percentage of non-apoptotic cells 48 hrs post treatment, when cells were treated with RAD alone and MMF alone compared to the untreated control. Figure 2.28 suggests that the damage induced by SCH3 0 hrs post treatment, although not initially as great as the damage induced by RAD alone cells, was the only treatment group of cells that maintain the sustained median tail moments up to 48 hrs post treatment. These finding as supported by those in clonogenic assay (Figure 2.11) in which SCH3 treatment produced a statistically significantly lower survival fraction in cells when compared to the two single therapies RAD alone and MMF alone. The findings from the Annexin V assay in Figure 2.25 also support these results as SCH3 treated cells were the only treated cells to produce a statistically significant increase in apoptotic cells when compared to the untreated control and single therapies RAD alone and MMF alone.

2.5 Discussion

Doxorubicin

Clonogenic assays were carried out using DOX as this is the standard treatment of care for TNBC (Triple negative breast cancer | Cancer Research UK, 2020). When investigating novel treatments for cancer it is especially important to compare the results to the standard treatment of care as guidance by the National Institute for Health and Care Excellence (NICE) states that “all new treatments must be better than the current standard treatment of care as it would be unethical to give a patient a treatment that was not as effective as current therapies regardless of side effects” (Nice.org.uk. 2020).

In our experiments as expected, DOX successfully inhibited TNBC cell survival in (Figure 2.3) and results were dose dependant, as was seen in literature (Lovitt, Shelper and Avery, 2018). However, as we have discussed, the success of this standard treatment of care is limited as it is well documented that TNBC patients initially respond very well to chemotherapy, however, they eventually develop resistance and metastasis (Isakoff, 2010). The real issue is that TNBC has acquired resistance to the therapy, thus any development of novel therapies needs to fill that clinical space. To undertake meaningful experiments, we must therefore test any novel schemes in a range of cell lines with varying levels of resistance to existing therapies. To model this phenomenon within this project, resistant cells lines were developed and discussed in Chapter 4 by a process that was carried out by (McDermott *et al*., 2014). This also highlights the need for administering DOX at a lower dose in combination with a non-toxic agent to reduce unwanted side effects and this was the basis of investigating fumaric acids as a possible combination agent.

Radiation

Radiotherapy is currently used as part of the gold standard treatment of TNBC, patients normally receive radiotherapy post-surgical removal of tumour mass or mastectomy (Triple negative breast cancer (2023) Cancer Research UK). At present 2 Gy of radiation is the clinical dose and was the basis of using this dose to investigate potent combinations. As expected, radiation reduced MDA-MB-231 cell survival in a dose dependant manner from 0-10 Gy.

Dimethyl Fumarate (DMF)

Clonogenic assays were carried out to determine the toxicity of DMF which we hypothesised to be relatively low, as DMF is not a cytotoxic drug. However, it has been shown that high levels of DMF can induce apoptosis, due to DMF binding to all intracellular GSH inducing a stress response during which cells induce apoptosis because of glutathione depletion (De Nicola and Ghibeli 2014). DMF was selected for investigation due to its ability to sensitise and enhance cell death by inhibiting the synthesis of GSH, thus preventing the neutralisation of ROS (Mills *et* al 2018). In initial assays (Figure 2.5) DMF had no significant impact on MDA-MB-231 cells clonogenic survival. Evidence found by (Bennett and Saidu *et al.,* 2018), reported that lower concentration of DMF did not inhibit cell growth but enhanced it at concentrations of <25 μM. However, unlike Bennett *et al*., (2018) in our experiments the inhibition in cell growth was still not seen at concentrations above 25 μM. However, experiments carried out by (Bennett and Saidu *et al*., 2018) did not use MB-MDA-231 cells and therefore this is not a fair comparison. To our knowledge there have been no reports of the assessment of DMF on cell survival undertaken in MDA-MB-231 cells. This would suggest that DMF is a poor candidate for single therapy to treat TNBC.

Monomethyl Fumarate (MMF)

MMF was selected for investigation due to its ability to neutralise the antioxidant GSP and to inhibit the translocation of NRF2 and in-turn the production of antioxidants, this would sensitise cells to death through ROS activation, as previously detailed (Rostami-Yazdi, Clement and Mrowietz, 2010). However, much about this mechanism of action of MMF remains unknown and further investigations were carried out to clarify this mechanism of action. Unlike with DMF, there was a notable inhibition of cell survival following incubation of the cells with MMF treatment (Figure 2.6). At drug concentrations of 10 μM there was a statistically significant inhibition in cell survival ($P<0.0076$). These results suggest that unlike DMF, MMF had a significant effect on the survival fractions of MDA-MB-231 and is a suitable candidate to investigate in combination treatments.

Diroximel Fumarate (EMF)

EMF has been reported to have the same mechanism of action as DMF (Palte *et al*., 2019). It was developed to reduce gastrointestinal complications that MS patients experienced while taking DMF. As expected, similar results were seen in EMF (Figure 2.7) as in DMF (Figure 2.5) due to these two compounds having the same mechanism of action. No results were statistically significant when compared with the control. Given the scope of the project it was decided that as EMF was the least effective candidate at inhibiting cell growth and was not carried into combination therapy investigations.

As expected DMF and EMF had no significant inhibitory effects at any dose on MDA-MB-231 cell survival fraction after treatment. These results contradict those from (Bennett Saidu *et al*., 2018) as at administered concentrations above 25 μM DMF inhibited the growth of cancer cells including lung, uterine and ovarian. However, Bennet did not carry out investigations into its effect on breast cancer cells, and from the results in Figure 2.5 and 2.7, data would suggest that neither DMF nor EMF are effective therapies to treat TNBC alone. This supports the hypothesis that MMF is a more effective fumaric acid at investigating combination therapies than DMF, it may neutralise glutathione and down regulate translocation of NRF2 in MB-MDA-231 cells. However, as MMF is the active metabolite of DMF, it may be that in 2D culture MMF is more effective at inhibiting the translocation of NRF2 as DMF has to be hydrolysed by esterase to MMF to have any intracellular effects (Litjens *et al*., 2004). Due to data from others in the lab investigating glioma tumours and the effect these fumaric acids had on glioma cell survival, it was hypothesised that MMF is more effective at inhibiting cell growth *in vitro* than DMF. This supports the need for further investigation into the mechanisms of action of MMF which was carried out throughout this chapter.

Combination of Fumaric Acids and doxorubicin treatment on MDA-MB-231 cells

Due to the mechanism of action of DMF (inhibition of NRF2 nuclear translocation that prevents the synthesis of antioxidants such as GSH). It was hypothesised that combining fumaric acids with cytotoxic agents will be more effective than chemotherapy or radiotherapy alone. In theory the inhibition of the NRF2 pathway sensitises the cancer cell to damage by preventing the neutralisation of ROS

generated because of radio or chemotherapy, which in-turn can induce higher levels of DNA damage. Therefore, a lower dose of chemotherapy and the standard dose of 2 Gy radiation will be as effective at killing TNBC cells as if higher doses where used. This would in turn reduce the side-effects of TNBC treatments and would most importantly increase the patient's quality of life.

Thus, to test this hypothesis, cell survival of MDA-MB-231 cells was measured after combination treatment with either DMF or MMF and doxorubicin or radiation in 3 scheduled combinations. From Figure 2.9 it was evident that only one treatment combination gave rise to a statistically significant decrease in the survival fraction of MDA-MB-21 cells, the Schedule 3 DMF1st (100 μM) + DOX (0.02 μM) compared to the untreated control. However, when using MMF in scheduled combinations with doxorubicin it was seen in Figure 2.10 that SCH3 induced a statistically significant decrease in cell survival when compared with the control, and the single therapies alone MMF and DOX.

The scheduled combinations were continued when looking at Radiation (2 Gy) + DMF (100 μM) or MMF (2 μM). From Figure 2.11 it was found that the SCH3 (DMF1st+RAD) and SCH1 (DMF+RAD simultaneous administration), induced a statistically significant decrease in cell survival when compared to both the control and DMF alone. Figure 2.12 reported that using MMF and radiation in combination schedules, SCH3 most effectively reduced the cell survival of MDA-MB-231 cells compared to the control and single therapies, RAD alone and MMF alone. SCH3 was the only combination to induce a significant decrease in cell survival when compared to either radiation or MMF alone.

As hypothesised, SCH3 was the most effective combination at reducing cell survival, this may be due to MMF already being administered to the cell prior to chemotherapeutic damage or irradiation. As such, MMF has had time to carry out intracellular processes, inhibiting the translocation of NRF2, preventing the production of antioxidants. As a result, when the cell is damaged by ROS induced by DOX or irradiation, the cell is left defenceless as it is not able to produce antioxidants such as glutathione to protect the cell from DBS and SSB resulting in ultimately cell death.

Combination Index

Therefore, based on the results above MMF in combination with DOX at all three schedules was investigated to determine the combination index value to identify the most effective schedule. From Figure 2.12 it was shown that that at the lower administered doses of MMF (2 μM) and DOX (0.02) μM, the SCH3 combination was synergistic. Therefore, schedule 3 was used alongside single therapies to investigate mechanistic properties of MDA-MB-231 cells after treatment.

Cell Cycle analysis

All three treatments tested on MDA-MB-231 cells MMF, DOX and SCH3 M+D combination induced a change in cell cycle distribution of cells verses the control (Figure 2.12), immediately after treatment was removed and surprisingly MMF produced the greatest number of cells in G1, this was expected as it has been shown in literature that MMF causes accumulation of cells in G1 phase of the cell cycle (Takebe *et al*., 2006). There is some evidence in the literature that cells undergoing mitotic catastrophe are blocked at the G1 phase of the cell cycle, and this may be an explanation for the block seen in these treated cells (Fragkos and Beard, 2011). The results suggested that after treatment with MMF, MDA-MB-231 cells show a similar distribution of cells to that of the control 48 hrs post treatment, suggesting any disruption caused by MMF treatment has been resolved by the cells. SCH3 and DOX treated cells, show a significantly reduced percentage of cells in the G1 and G2/M phase of the cell cycle when compared to the control and MMF treated cells, 48hrs after treatment is removed. This may be due to SCH3, and DOX treated cells being unable to enter the cell cycle and cells within the cell interphase stage of the cell cycle are being inhibited by cell cycle checkpoints and are unable to enter G2/M phase to divide into two complete daughter cells. This may be due to an accumulation of DNA strand breaks. These results were expected as it has been shown that doxorubicin causes cell cycle arrest in G2/M in MDA-MB-231 cells (Sabzichi *et al*., 2019). This has been reported to be due to DOX inducing the synthesis of cyclin B and preventing its degradation, which would allow the cell to enter mitosis and divide into two identical daughter cells (Ohno *et al*., 2011). Additionally, SCH3 M+D combo treated MDA-MB-231 cells continually decrease their percentage of cells in G2/M over 48 hours, suggesting the percentage of cells completing mitosis was being inhibited by this combination treatment.

Annexin V

In a similar thought process to that of cell cycle analysis investigations, Annexin V analysis was carried out over 48 hours post treatment to investigate the cell death and repair process of MDA-MB-231 cells post treatment. MMF alone (2 μM), DOX alone (0.02 μM) and M+D SCH3 combinations were used to treat cells. As shown in Figure 2.15, all treatments reduced the percentage of non-apoptotic cells compared with the control, but only M+D SCH3 treatment induced a statistically significant decrease in the percentage of non-apoptotic cells compared with the control. This was the only treatment that failed to increase the percentage of viable cells 48 hours after treatment, therefore, it would suggest that this M+D SCH3 treatment was the most successful treatment at inducing apoptosis and inhibiting normal cell function. This hypothesis is supported by the evidence in cell cycle analysis (section 2.42.14) as it is known that apoptosis can occur in any phase of the cell cycle (Pucci *et al*., 2000) and as cells undergoing DNA replication and cell division are reduced after treatment with M+D SCH3, this may be due to SCH3 treated cells are entering apoptosis and thus being lost from the assay. These findings are also supported by the statistically significant reduction in survival fraction of MDA-MB-231 cells treated with SCH3 compared with the untreated control, MMF and DOX alone in section 2.4.7.

Glutathione

The results from Figure 2.17 supported the hypothesis that MMF can alter the intracellular levels of GSH as a single therapy and in combination. The data suggests that there was a significant reduction in GSH levels of MDA-MB-231 cells treated with D-SCH3. This may explain my D-SCH3 was shown to induce the highest percentage of apoptotic cells 48 hours post treatment as MMF bound to intracellular GSH and prevented its antioxidant activates on ROS that were generated from DOX treatment, it may also be possible that MMF treatment prevented the synthesis of new glutathione following the administration with DOX by inhibiting the nuclear translocation of NRF2 via the DJ-1 inhibition. This would allow the ROS generated from DOX treatment to cause SSB and DSB which when accumulated would result in the activation of caspase 3 and the cell death. Again, this data is supported by that significant increase in the percentage of apoptotic cells in Figure 2.16 and decrease

in survival fraction of cells following clonogenic analysis of SCH3 in Figure 2.8. However, further investigations are required to determine the change in activities of DJ-1, NRF2.

Autophagy

It appears from Figure 2.19 that autophagy was not the mechanism used by DOX alone, MMF alone or M+D SCH3 to cause a reduction in cell survival fraction as reported in section 2.42.1.2. There were no statistically significant results in Figure 2.19 and levels of absorbance 412 nm were relatively unchanged by any treatment tested. This investigation ultimately concluded that no further analysis of autophagy was necessary when investigating these treatments in MDA-MB-231 cells.

Comet Assay

As reported in Figure 2.21, treatment with DOX alone (0.02 μM), MMF alone (2 μM) and M+D SCH3 combination caused statistically significant increases in the median tail moments of cells compared with the control across all time frames. Much like all previous assays detailed above these comet assays were carried out over a 48-hour period to monitor both cell damage and cell repair following treatment. MMF, DOX and D-SCH3 all followed similar patterns of cells damage and repair. Many median tail moments were seen initially after treatment was removed; however, this median tail moment was reduced in all treated cells after 24 and 48 hours. SCH3 resulted in the highest median tail moments 48 hours post treatment than any other treated cell, this increase in median tail moment was statistically significant compared with the control MMF alone and DOX alone (all, $P>0.0001$). Additionally, the results from the comet assay may reflect ROS bursts (Zorov *et al.,* 2014). This process involves a burst of ROS after initial insult is given to cells (via DOX treatment in this case) which is captured 0 hrs post treatment. The cells treated with DOX alone then begin to repair, however the cells treated with SCH3 are unable to protect themselves from ROS generate by doxorubicin in the combination. This may be due to MMF binding to GSH; therefore, the median tail moments increase as the cell are unable to repair damage induced and the SSB and DSB accumulate resulting in apoptosis. It was hypothesised that the SCH3 combination would produce greater median tail moments (fragmented DNA) than DOX alone as MMF would have bound to GSH and potentially inhibited the nuclear translocation of NRF2 which prevents the cell from producing

antioxidants to protect from SSB and DSB caused by DOX administration, as was reflected in clonogenic data and Annexin V analysis.

Radiation + MMF combinations

Combination Index Analysis

Following the results from Figure 2.11, the data was analysed using combination index analysis to determine if any schedule of MMF and RAD induced synergistic cell kill. From Figure 2.21 at the lower concentration range tested (2 μM MMF + 2 Gy Rad), a synergistic CI value was reported for SCH3 MMF1st +RAD. SCH3 induced the lowest synergist value when treated with a higher concentration of MMF also. Therefore, given the synergistic effects determined from combination index analysis this scheduled combination was investigated by application of several mechanistic assays.

Cell Cycle Analysis

The results from Section 2.42.27, suggested that following treatment with MMF, RAD and SCH3 there was a change in the distribution of cell in each phase of the cell cycle. Results suggest that following treatment with RAD alone and SCH3, the decrease in cells in G1 phase of the cell cycle is maintained for all treated cells 48 hrs after treatment removal, this may be due to the significant increase in the percentage of cells in G2/M reported 24 hrs after treatment removal (Figure 2.23), these cells have now begun apoptotic processes and are prevented from re-entering the cell division process. The statistically significant decrease in the percentage of cells in S may be due to cells in G1 being inhibited by the G1 checkpoint, unable to progress into S phase 48 hrs after treatment removal., again this block may be an indicator of cells in militia catastrophe as is used previously. The percentage of cells in each phase of the cell cycle after treatment with SCH3 followed a similar pattern to that of RAD, however there was a significant decrease in G1 and increase in G2/M for SCH3 treated cells when compared to RAD alone. This may be due to MMF binding to glutathione and preventing the antioxidant from neutralising ROS, therefore ROS induced by radioactivation in the combination therapy, is able to induce SSB and DSB which will result in a G2/M checkpoint inhibition. This would prevent the cells from dividing into two daughter cells (Nikolakopoulou *et al.,* 2021). MMF treated cells show a similar distribution of cells in each phase of the cell cycle 48 hrs post treatment

removal to that of the untreated control, suggesting that these cells have recovered from any disruption caused by MMF treatment. The initial increase in the percentage of cells in G1 was expected as this was reported in the literature as described above in section 2.42.27. As cells treated with RAD and SCH3 still show significant differences in cell cycle distribution 48 hrs post treatment removal, this would suggest that these cells are still accumulating at checkpoints within the cell cycle and the damage caused by irradiation and the combination has not been fully repaired. These finding are supported by clonogenic data in Figure 2.11 which reported a statistically significant decrease in the survival fraction of cells treated with RAD alone and SCH3 compared to the untreated control. This may be due to an accumulation of DNA strand breaks, this resulting in the activation of apoptotic pathways.

Annexin V

After investigating the percentage of MDA-MB-231 cells undergoing apoptosis because of treatment with MMF (2 μM), RAD (2 Gy) and SCH3 M+R, the results for each treatment were vastly different (Figure 2.25). M+R SCH3 was the only treatment to induce a significant reduction in non-apoptotic cells compared with the control and both single treatments at all time points investigated. Immediately after treatments were removed, M+R SCH3 induced a significant decrease in the percentage of viable cells, as well as an increase in early and later apoptotic cells when compared to the untreated control and each single therapy. This significant reduction in the percentage of viable cells and increase in early apoptotic cells was continued 48 hrs post treatment when comparing SCH3 treated cells to the untreated control and each single therapy. This data supports the hypothesis that a SCH3 combination enhances the percentage of cell death in MDA-MB-231. This promising result may be a result of a MMF administration prior to radiation, binding to GSH and possibly inhibiting the nuclear translocation of NRF2 and preventing the synthesis of antioxidants. As a result, the ROS generated because of radiation induce SSB and DSBs which when accumulated activates the caspase 3 pathway leading to apoptosis, evident 48 hrs post treatment removal for SCH3 treated cells only (Figure 2.25C). These findings are supported by this in clonogenic assay and cell cycle analysis, in which SCH3 induced a significant decrease in the clonogenic survival of MDA-MB-231 cells and appears to induce cell cycle arrest in G2/M.

Glutathione

Results from Figure 2.26 supported the hypothesis that MMF treatment depletes GSH. Following treatment with SCH3 and radiation alone, the relative GSH levels decrease up until 48 hrs post treatment removal. 1 hr post treatment administration there is a significant decrease in the relative GSH when comparing SCH3 to radiation alone. This may be that normally 1 hr post radiation MDA-MB-231 cells are able to synthesis GSH to neutralise ROS generated by irradiation, visible in Figure 2.26. However, this significant decrease in relative GSH when comparing SCH3 to radiation, may be a result of prior MMF administration 24 before cells were irradiated and these SCH3 treated MDA-MB-231 cells are unable to utilise cellular GSH as MMF has bound to it, additionally these cells may be unable to synthesis due to the disruption of the NRF2 translocation caused by MMF treatment.

Autophagy

No results from Figure 2.27 were statistically significant compared with the control or any other treatment. These assays were carried out over a 48-hour time scale and there was very little variation in untreated MDA-MB-231 cells or cells treated with MMF 2 μM alone, Rad 2Gy or M+R SCH3. These results suggest that autophagy is not activated following treatment with any of these therapies.

Comet Assay

The median tail moments for MDA-MB-231 cells treated with MMF (2 μM), RAD (2 Gy) or M+R SCH3 were measured over a 48-hour time window (Figure 2.28). The results of RAD alone and MMF alone treated cells followed a similar pattern, an increase in median tail moments 0 hrs post treatment, which then decreases 24 and 48 hrs later, indicating cell repair. This was not the pattern of median tail moments in SCH3 treated cells, there was a significant increase in median tail moment of SCH3 treated cells 0 hrs post treatment when compared to the untreated control and MMF alone, which was maintained 48 hrs post treatment. This resulted in a significant increase in median tail moment of SCH3 treated cells when compared to all other treatment groups, suggesting that the repair capacity of the SCH3 treated cells was not well maintained up to 48 hrs after treatment. This maintained significant median tail moment is indicative that SCH3 treated cells are unable to repair the damage

induced by the combination. This supports the hypothesis that MMF administered prior to radiation can sensitise cells to radiation damage, this is due to the mechanism of action of MMF, binding to intracellular glutathione and preventing the neutralisation of ROS generated because of radiation treatment.

Summary

As M+R and M+D SCH3 induced the lowest survival fraction of cells when analysed using clonogenic assay, produced the highest percentage of cells in apoptosis, appears to have caused cell cycle arrest (from cell cycle analysis) and produced significant median tail moments up to 48 hrs post treatment when compared to any single treatment alone or control. From all these findings, it can be deduced that M+R and M+D SCH3 treatment are the most successful treatments tested to kill MDA-MB-231 cells. The original hypothesis that this schedule causes significantly more cell death single therapies alone was supported by the findings in this chapter.

As this combination treatment induces cell cycle arrest and apoptosis, it was continued into 3D investigations in Chapter 3. This will involve an investigation into change in spheroid sizes following treatment. These models are more representative of *in vivo* as they possess a hypoxic core and outer layer of proliferating cells that better mimics the conditions of a tumour. Having already determined that MB-MDA-231 cells successful form spheroids using the 96-well plate method, these spheroid models with be investigated using the single treatments of DMF, MMF, doxorubicin and radiation. Then the combinations of these drugs as used above (SCH3). This will allow for an analysis into how successful DMF and MMF in combination with cytotoxic therapies are at reducing spheroid size (mimicking tumour mass) and give us a more realistic view of their use in patients.

Chapter 3

Assessment of the efficacy of combination therapies using Doxorubicin and Radiation with DMF or MMF on multicellular tumour spheroids

3.1 Introduction

Despite recent advances in some cancer therapies, breast cancer remains a major problem worldwide, with 40% of patients developing metastasis following gold standard treatment (Anastasiadi *et al.* 2019). Many of the issues faced with developing new therapies is that the models used to investigate potential therapies are not reflective of a patient's tumour. As such, multicellular tumour spheroid models (MTS) have shown promise for the development of cancer treatments (Nath and Davi., 2016). MTS more closely mimic cell-cell interactions, heterogeneity, gene expression patterns and signalling pathways present in tumours *in vivo.*

Following on from clonogenic experiments on 2-dimensional (2D) monolayers, MDA-MB-231 cells were cultured as 3D MTS. Assessment of the efficacy of a proposed combination therapy on MTS enables longitudinal monitoring of any investigational interventions. Once grown to the desired size (around 350 µm), spheroids reflect the heterogeneity of *in vivo* tumours as they are composed of an outer proliferating layer of cells, a quiescent inner layer, and an inner hypoxic core (Thakuri *et al* 2019). This model therefore better mimics the environment of a tumour *in vivo* (Huang *et al 2020)*.

3.2 Aims

The aims of this chapter were:

- To investigate the effects of single therapy treatments; Doxorubicin, Radiation, DMF and MMF on spheroid growth via measurement of the change in spheroid volume over time.

- To investigate the effects of scheduled combination therapies utilising combinations of DOX+DMF/ MMF and RAD+DMF/MMF, on spheroid growth via measurement of the change in spheroid volume over time.

3.3 Materials and methods

3.3.1 Spheroids

Spheroids were grown using 96 well ultra-low attachment plates (Corning, Fisher Scientific UK). Cell suspensions were prepared as detailed in chapter 2. The cells were counted using a haemocytometer (Jenson UK) and the volume of cell suspension required for 700 cells was then calculated and resuspended in complete DMEM for a total volume of 200 µL. This 200 µL cell suspension was then added to each well of the 96-round bottomed well plate. The outer surrounding wells were filled with 200 µL of PBS to keep cells in the inner wells hydrated. The plate was then incubated at 37 ^{o}C in a 5% CO_2 environment and media was refreshed 2 times per week by drawing out 50 µL of media and replacing this with 50 µL of fresh complete media. Spheroids were then imaged every 3 days. Spheroids were incubated with the desired treatments after around 7 days or once optimum size was reached (350 µm) dependant on desired characteristics (hypoxic core/ outer proliferating layer). Spheroids were sized utilizing IMAGEJ software, and the average sizes calculated for each column. For each spheroid two orthogonal diameters, d_{max} and d_{min} (µm) were measured using IMAGEJ. Spheroid volume (V) was calculated as described by Jensen (Jensen *et al*., 2008 and Boyd *et al.,* 2002) using Equation 1. Spheroids were measured for a total of 21 days as control MDA-MB-231 cells grew exponentially and due to their large size, this prohibited further measurement of spheroids.

$$V = \frac{1}{2}(d_{max} \times (d_{min})^2)$$

Equation 1: Equation used to calculate the MTS volume where d_{max} is the maximum diameter and d_{min} is the minimum diameter.

Change in spheroid volume (V/V_0) was calculated by dividing the spheroid volume (V) at each time point by the initial spheroid volume (V_0). Data was reported as V/V_0, as an average of three independent experiments and each therapy was carried out in triplicate.

The area under the curve was calculated for Log V/V_0 against time using the trapezoidal approximation using GraphPad prism 9.2.1 to evaluate the overall change in spheroid volume following each treatment.

Results:

3.4. Single treatment of TNBC MTS using Doxorubicin, Radiotherapy, Dimethyl Fumarate or Monomethyl Fumarate

3.4.1. Effect of Doxorubicin on growth of MDA-MB-231 spheroids

The effect of administration of DOX alone on MDA-MB-231 spheroid growth was measured following incubation of the spheroids with a concentration range of 0.02 μM – 0.1 μM DOX. Results are shown in Figure 3.1 below.

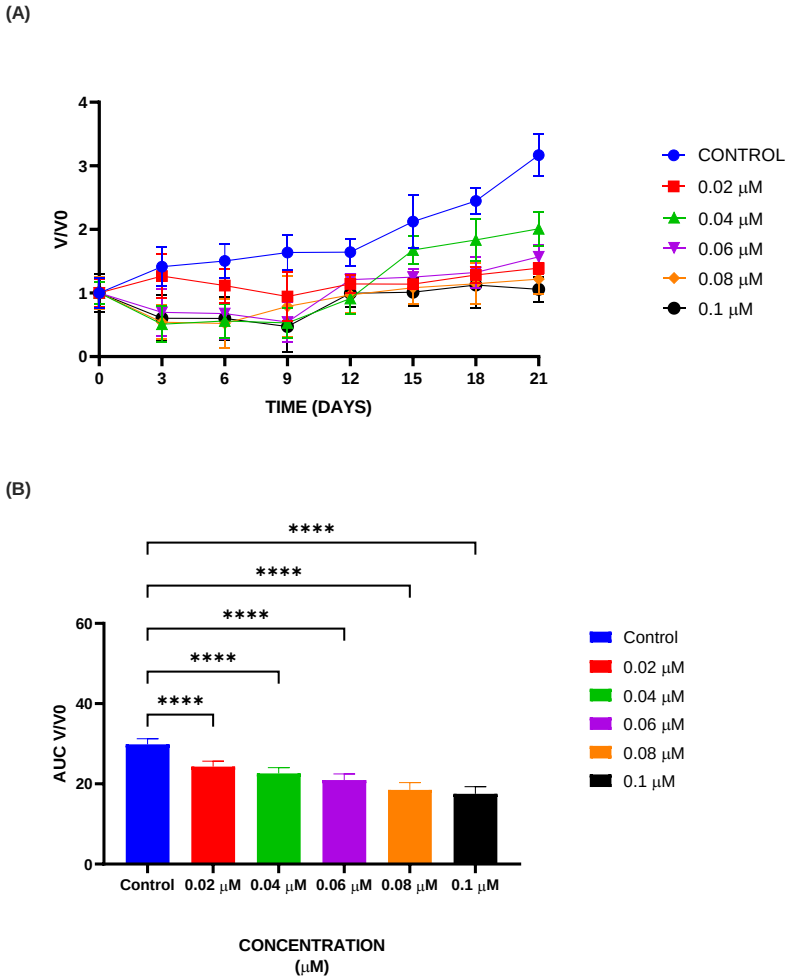

Bonferroni's multiple comparisons test	V/V0 Summary	Adjusted P Value	AUC Summary	Adjusted P Value
CONTROL vs. 0.02 μM	*	0.0120	****	<0.0001
CONTROL vs. 0.04 μM	**	0.0081	****	<0.0001
CONTROL vs. 0.06 μM	**	0.0022	****	<0.0001
CONTROL vs. 0.08 μM	***	0.0004	****	<0.0001
CONTROL vs. 0.1 μM	***	0.0002	****	<0.0001

Figure 3. 1 The effect of administration of DOX at varying concentrations on the growth of MDA-MB-231 spheroids.

(A) MDA-MB-231 spheroids were incubated with DOX at a concentration range from 0.02 μM-0.1 μM continually for 21 days and images captured every 2-4 days, results are an average of 3 independent experiments carried out in triplicate with 36 spheroids per treatment group. Spheroid volumes were calculated and the average fold increase from initial V/V0 +/- S.D, is presented on a linear scale, (B)The area under the curve (AUC) +/- S.D. was also calculated using one-way ANOVA analysis with Bonferroni's testing for multiple comparisons, results displayed in (C). Statistical analysis was carried out on the data using GraphPad prism 9.2.1, determined by the. P<0.05=*, P<0.01=**, P<0.001=***, P<0.0001=**** when compared with the control (applicable to Figure 3.1-3.16).

In MDA-MB-231 MTS treated with concentrations of 0.02 μM to 0.1 μM DOX, there was a statistically significant reduction in spheroid growth (V/V_0) after incubation of the spheroids with all concentrations of DOX versus the untreated control (Figure 3.1C). When reviewing the area under the curve analysis (Figure 3.1B) of this spheroid volume data, it was clear that all concentrations of DOX induced a statistically significant reduction in the area under the curve values when compared with the control area under the curve value, Figure 3.1(B) (P<0.0001 for all concentrations tested). This data therefore supports the use of 0.02 μM DOX in combination with DMF or MMF in scheduled combination therapies of MTS as this was the concentration of DOX used in 2D culture (Chapter 2), the use of this concentration in 3D studies would allow for an accurate comparison of combination results.

3.4.2 Effect of Radiotherapy on growth of MDA-MB-231 spheroids

In Figure 3.2, MDA-MB-231 spheroids were exposed to various radiation doses (0-10Gy Gy) to determine the change in volume over time of each treatment group. This is shown in figure 3.2.

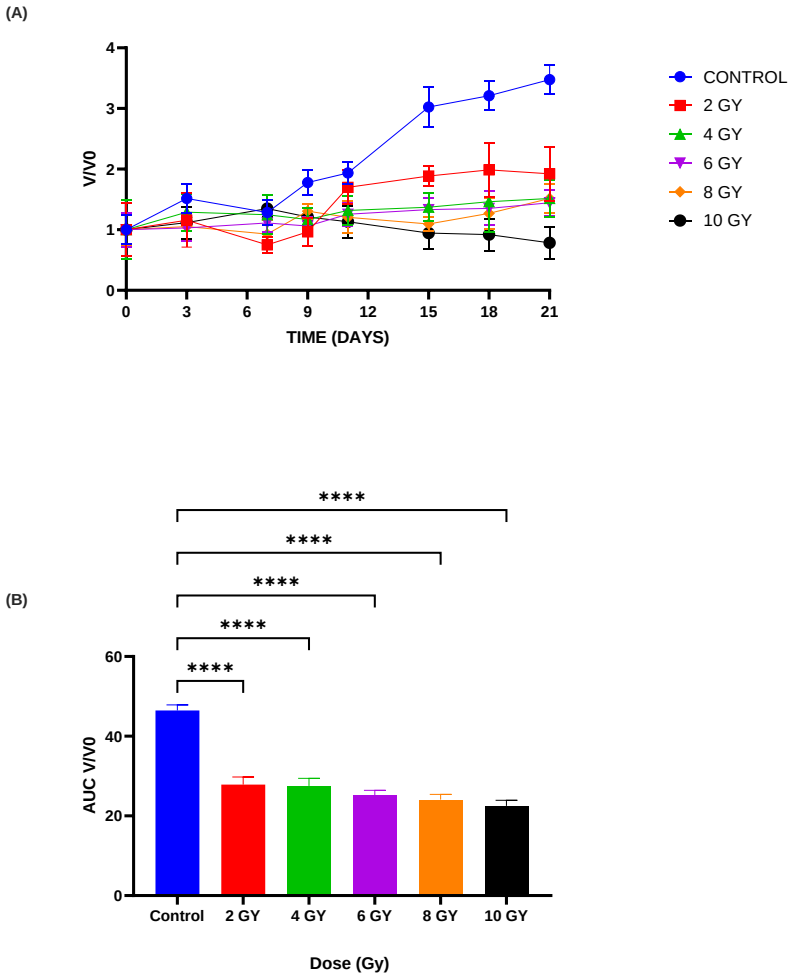

(C)

Bonferroni's multiple comparisons test	V/V0 Summary	Adjusted P Value	AUC Summary	Adjusted P Value
CONTROL vs. 2 GY	**	0.0019	****	<0.0001
CONTROL vs. 4 GY	**	0.0061	****	<0.0001
CONTROL vs. 6 GY	**	0.0015	****	<0.0001
CONTROL vs. 8 GY	**	0.0010	****	<0.0001
CONTROL vs. 10 GY	***	0.0002	****	<0.0001

Figure 3. 2 The effect of administration of radiation at varying Gy on the growth of MDA-MB-231 spheroids.

Results from Figure 3.2 suggest that MDA-MB-231 spheroids treated with all doses of radiation had a statistically significantly reduction the growth (V/V_0) compared with the untreated control as expected (see Figure 3.2C). In Fig 3.2B, all treated spheroids had a statistically significant reduced area under the curve values when compared with the control (all, $P<0.0001$). Given the similar reduction in the AUC for all radiation doses we have chosen 2Gy to be used in scheduled combination therapies involving irradiation and DMF or MMF. This dose of radiation will be comparable to the dose

used in 2D culture (Chapter 2) and was selected as this is the clinical dose of radiation administered to patients.

3.4.3 Effect of Dimethyl Fumarate on growth of MDA-MB-231 spheroids

The effect of administration of DMF alone on MDA-MB-231 spheroid growth was measured following incubation of the spheroids with a concentration range of 20 μM – 100 μM DMF. Results are shown in Figure 3.3 below.

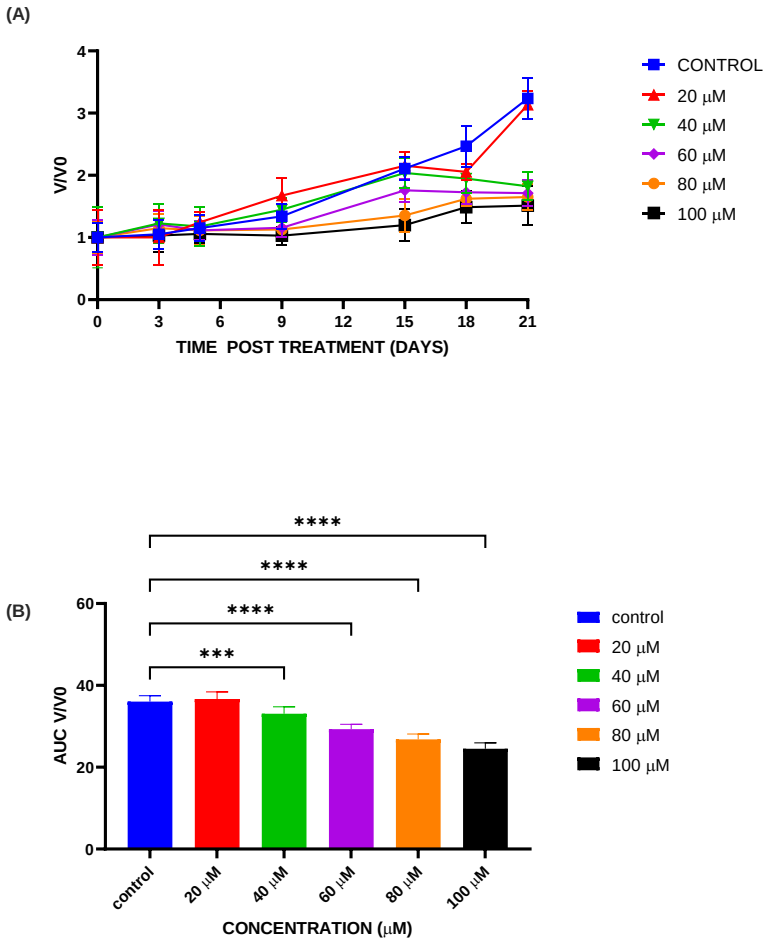

Bonferroni's multiple comparisons test	V/V0 Summary	Adjusted P Value	AUC Summary	Adjusted P Value
CONTROL vs. 20 μM	ns	>0.9999	****	<0.0001
CONTROL vs. 40 μM	ns	>0.9999	****	<0.0001
CONTROL vs. 60 μM	ns	>0.9999	****	<0.0001
CONTROL vs. 80 μM	ns	>0.9999	****	<0.0001
CONTROL vs. 100 μM	ns	0.7807	****	<0.0001

Figure. 3 The effect of DMF at varying concentrations on the growth of MDA-MB-231 spheroids.

From Figure 3.3 we can see that there was no statistically significant reduction in growth of spheroids treated with any dose of DMF. However, in Figure 3.3B Spheroids treated with 40 μM, 60 μM, 80 μM, 100 μM of DMF induced a statistically significantly reduction in AUC values when compared to the untreated control (all, $P<0.0001$).

This data therefore suggests that DMF alone is not a suitable treatment to reduce the growth of MDA-MB-231 spheroids. This data also supports the use of 100 μM DMF in scheduled combinations using MTS as it is the concentration that reduced the growth of spheroids and produced the lowest AUC value recorded. As this concentration was used in 2D investigations (Chapter 2) 100 μM will be the concentration of DMF used in combination therapies in this chapter.

3.4.4 Effect of Monomethyl Fumarate on growth MDA-MB-231 spheroids.

In Figure 3.4, MDA-MB-231 spheroids were exposed to varying concentrations of MMF (0-10 μM) only to determine the change in volume of time of each treatment group. This is shown in Figure 3.4 below.

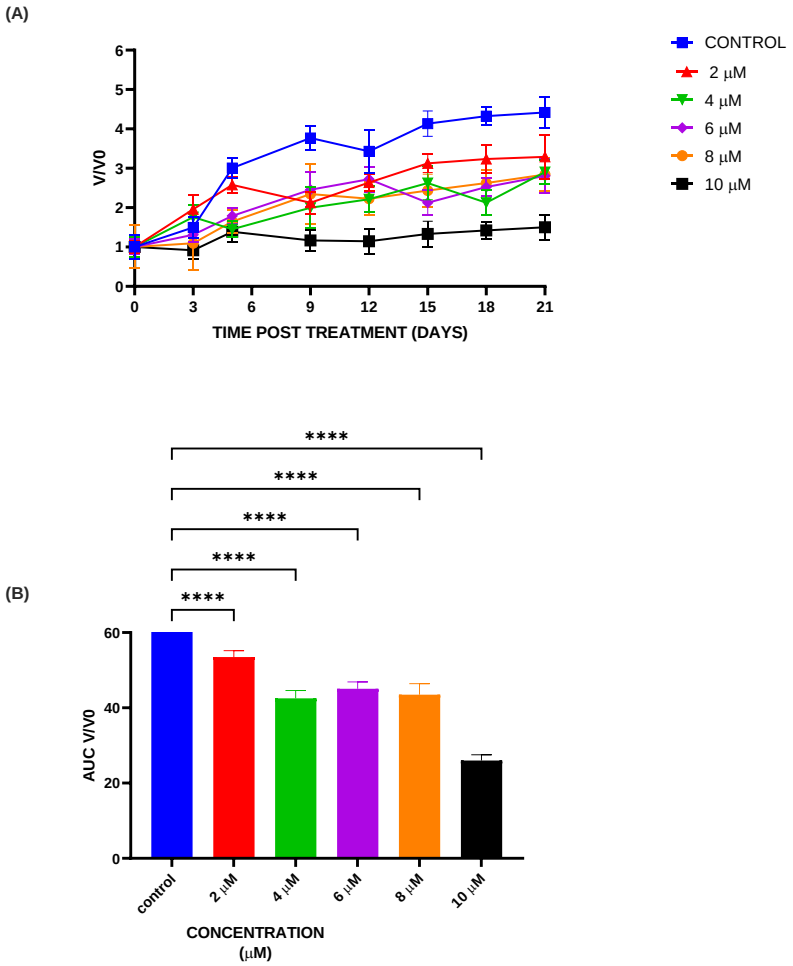

(C)

Bonferroni's multiple comparisons test	V/V0 Summary	Adjusted P Value	AUC Summary	Adjusted P Value
CONTROL vs. 2 μM	ns	>0.9999	****	<0.0001
CONTROL vs. 4 μM	ns	0.0592	****	<0.0001
CONTROL vs. 6 μM	ns	0.1039	****	<0.0001
CONTROL vs. 8 μM	ns	0.0664	****	<0.0001
CONTROL vs. 10 μM	***	0.0001	****	<0.0001

Figure 3. 4 The effect of MMF at varying concentrations on the growth of MDA-MB-231 spheroids.

Results from Figure 3.4A suggest that the only dose of MMF that statistically significantly reduced the growth of MDA-MB-231 spheroids when compared to the untreated control was 10 μM MMF (P=0.0001). The area under the curve value of spheroids treated with all concentrations of MMF, 2 μM 4 μM, 6 μM, 8 μM and 10 μM produced statistically significantly reduced AUC values compared with the control AUC value (all, P<0.0001). This data supports the use of 2 μM MMF to be used in scheduled combination therapies to treat MTS. This concentration of MMF was used

in 2D investigations and combination investigation from this chapter will be more accurately comparable to Chapter 2 findings.

3.4.5 Effect of Doxorubicin given in combination with Dimethyl Fumarate on growth of MDA-MB-231 spheroids.

- ***Scheduling of Treatment administration***

Following on from single treatment investigations, the change in spheroid volume over time was investigated after treatment of the spheroids with combination therapies. These combinations therapies were scheduled the same as those used 2D investigations (Chapter 2) and are detailed in section 2.3.6.

By following the same treatments schedules, and concentrations of drugs, it allowed for an accurate comparison between 2D and 3D effects that combination therapies had on MBA-MB-231 cells.

Firstly, the effects of a schedule 1 (SCH1) combination involving DOX + DMF on the growth of MDA-MB-231 spheroids over time was assessed, as seen below in Figure 3.5. DMF at 100 μM was chosen as this was the concentration of DMF used to investigate 2D models and will allow for a more accurate comparison of the effects of DMF in 2D vs 3D culture. These doses of treatment were also used to investigate 2D cells in Chapter 2 Section 2.4. DOX at 0.02 μM was chosen as this is the lowest concentration of DOX that was able to reduce the AUC value of spheroids statistically significantly, this is also the dose of DOX used in Chapter 2, 2D investigations.

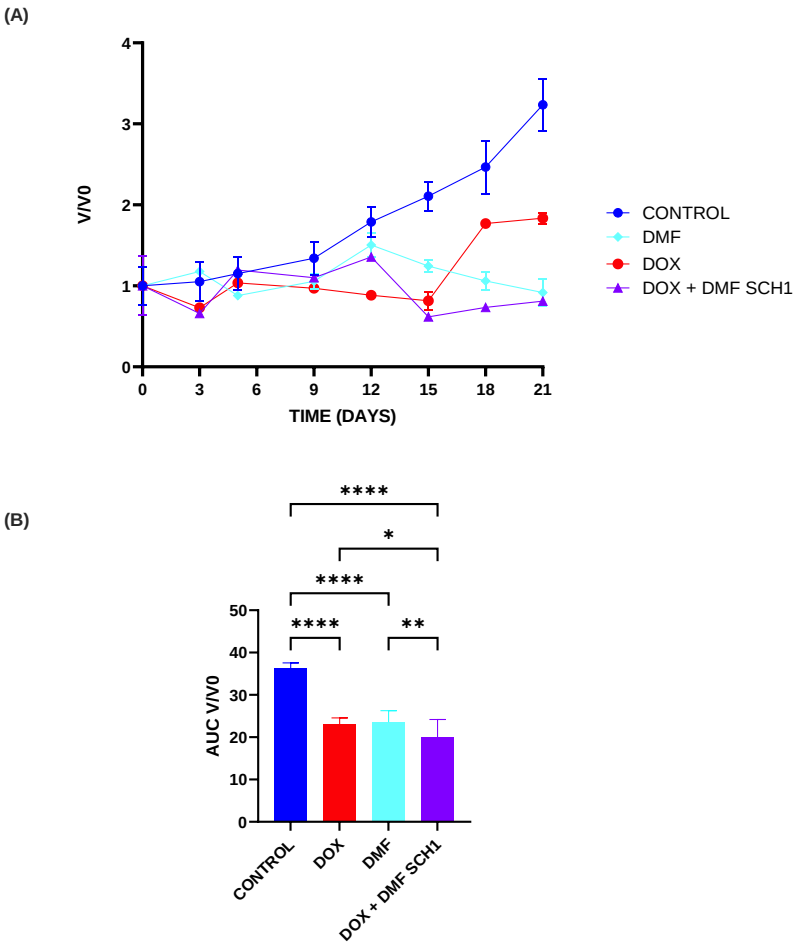

(C)

Bonferroni's multiple comparisons test	V/V0 Summary	Adjusted P Value	AUC Summary	Adjusted P Value
CONTROL vs. DOX	ns	0.0960	****	<0.0001
CONTROL vs. DMF	ns	0.0711	****	<0.0001
CONTROL vs. SCH1	**	0.0081	****	<0.0001
DOX vs. DMF	ns	>0.9999	ns	>0.9999
DOX vs. SCH1	ns	>0.9999	*	0.0154
DMF vs. SCH1	ns	>0.9999	**	0.0015

Figure 3. 5 The effect of DOX and DMF simultaneous schedule 1 combinations on the growth of MDA-MB-231 spheroids.

Results from Figure 3.5A with respect to V/V0 analysis, suggest that treatment of spheroids in a SCH1 combination of DOX 0.02 μM + DMF 100 μM statistically significantly reduce the growth of MDA-MB-231 spheroids when compared to the untreated control (P=0.0081, Figure 3.5A), this was the only statistically significant changes in V/V0 found. When reviewing AUC data however (Fig 3.5B), all treated spheroids gave rise to an AUC that was statistically significantly smaller that the AUC of the control spheroids (P>0.0001) as was seen with the experiments using individual

drugs. The SCH1 combination produced a statistically significant reduction in AUC value when compared to DOX alone and DMF alone AUC value (DOX P=0.0154, DMF P=0.0015). This data therefore suggests that SCH1 treatment is more effective at reducing the growth of MDA-MB-231 spheroids than DOX and DMF alone. These results are reflective of the findings in Chapter 2 Section 2.42.1.2. This data does not however support our hypothesis that DMF sensitises MDA-MB-231 cells to death via doxorubicin treatment.

Following on from SCH1 investigations, Schedule 2 (SCH2) combinations were investigated using MDA-MB-231 spheroids as seen in Figure 3.6. This was investigated to assess this combination's ability to reduce the growth of spheroids than the single therapies alone and to determine if this schedule was a more appropriate method of treatment administration than SCH1 more effectively.

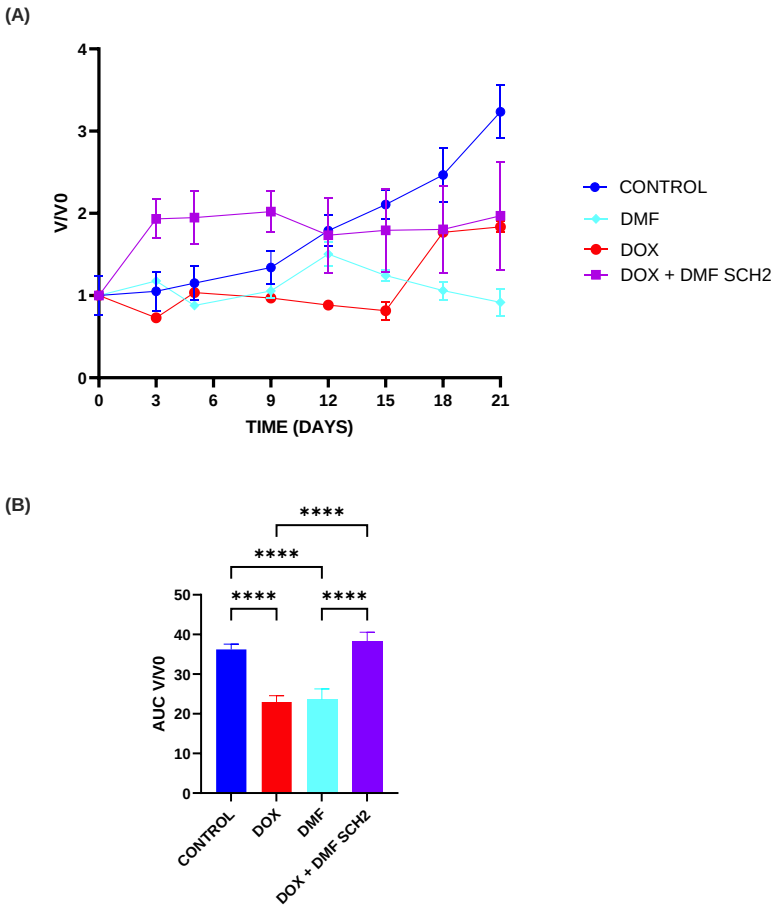

(C)

Bonferroni's multiple comparisons test	V/V0 Summary	Adjusted P Value	AUC Summary	Adjusted P Value
CONTROL vs. DOX	ns	0.1162	****	<0.0001
CONTROL vs. DMF	ns	0.0871	****	<0.0001
CONTROL vs. SCH2	ns	>0.9999	ns	0.0339
DOX vs. DMF	ns	>0.9999	ns	>0.9999
DOX vs. SCH2	ns	0.1060	****	<0.0001
DMF vs. SCH2	ns	0.0792	****	<0.0001

Figure. 3. 6 The effect of DOX 1st and DMF schedule 2 combinations on the growth of MDA-MB-231 spheroids.

Results from Figure 3.6 with respect to V/V0 analysis suggests no combination treatment produced spheroids that where statistically significantly smaller than untreated control spheroids or any other treated group when assessing the V/V0 Figure 3.6A. When looking at AUC Figure 3.6B, it was seen that spheroids treated with DMF alone and DOX alone produced statistically significantly smaller AUC values, compared with the control (both, P<0.0001). SCH2 failed to produce a statistically significantly smaller AUC value when compared to the untreated control,

DOX alone or DMF alone. This therefore suggests that doxorubicin and DMF administered in a SCH2 combination is not a more appropriate administration of combination therapies than SCH1 combination therapy (Figure 3.5) as this treatment method is not more effective at reducing the growth of MDA-MB-231 spheroids than the single therapies alone. This data is reflective of that in Chapter 2 Section 2.42.1.2. This data supports our hypothesis that DMF administered after cellular damage has been induced by DOX, is unable to mediate intracellular mechanisms and prevent the activation of protective cellular responses.

Next a SCH3 (DMF1st + DOX) combination therapy was investigated as seen in Figure 3.7. This figure details the findings of spheroid investigations involving a SCH3 combination of DOX + DMF, Dox alone and DMF alone on MDA-MB-231 spheroids.

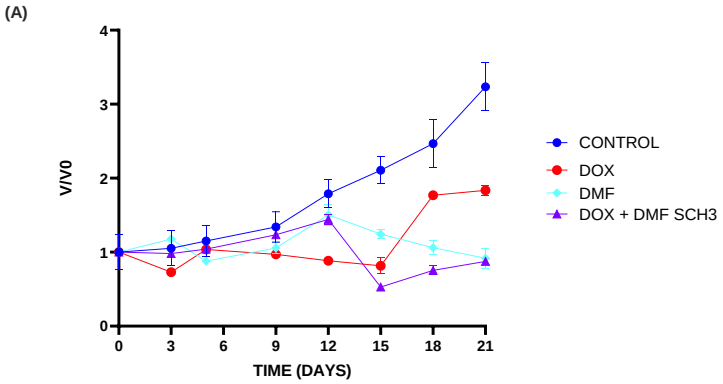

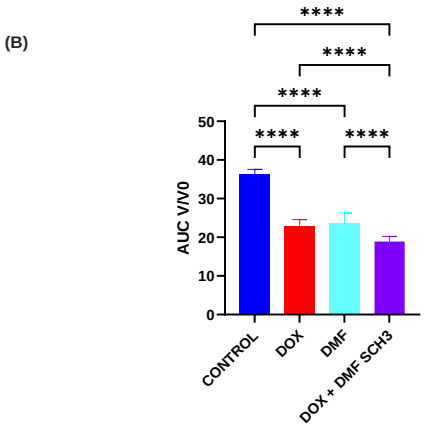

(C)

Bonferroni's multiple comparisons test	V/V0 Summary	Adjusted P Value	AUC Summary	Adjusted P Value
CONTROL vs. DOX	ns	0.1153	****	<0.0001
CONTROL vs. DMF	ns	0.0863	****	<0.0001
CONTROL vs. SCH3	*	0.0193	****	<0.0001
DOX vs. DMF	ns	>0.9999	ns	>0.9999
DOX vs. SCH3	ns	>0.9999	****	<0.0001
DMF vs. SCH3	ns	>0.9999	****	<0.0001

Figure 3. 7 The effect of DOX and DMF 1st, schedule 3 combinations on the growth of MDA-MB-231 spheroids.

Figure 3.7A shows that with respect to V/V0 assessment there was a statistically significant decrease in spheroid growth curve when spheroids were treated with SCH3 compared to the untreated control (P=0.0193, Figure 3.7C). When assessing AUC Figure 3.7B, once again all treated groups produced AUCs that were statistically significantly smaller than the AUC produced by untreated control spheroids (all, P<0.0001). SCH3 combination treated also statistically significantly reduced the AUC values when compared to DOX alone and DMF alone (P<0.0001 for both). These

results suggest that SCH3 administration of DOX + DMF SCH3 was the most appropriate combination schedule as it was shown that only this combination produced statistically significantly reduced AUC values when compared to the individual therapies alone. This again supports findings in Chapter 2 Section 2.42.1.1 that suggested SCH3 scheduling was the most appropriate method of administration to reduce the growth of MDA-MB-231 cells in 2D culture. These findings support our hypothesis that the administration of DMF prior to the induction of ROS damage, induced by DOX, induces a higher degree of cell kill.

Following on from DMF investigations, MMF was investigated in the same 3 scheduled administrations in combination with DOX as detailed in section 3.42.2.

3.4.6 Effect of Doxorubicin given in combination with Monomethyl Fumarate on MDA-MB-231 spheroids.

Figure 3.8 details the findings from 3D spheroid investigations into the change in volume over time of SCH1 treated MDA-MB-231 spheroids with a combination of 0.02 μM and MMF 2 μM. DOX at a concentration of 0.02 μM was chosen as this was the lowest concentration that induced a statistically significant reduction in the AUC value of the spheroids, additionally was the dose of DOX used in Chapter 2, 2D investigations. 2 μM MMF was chosen as this was the lowest concertation of MMF that was able to reduce the AUC values of MDA-MB-231 spheroids statistically significantly. This is also the dose of MMF used to investigate 2D combination therapies in Chapter 2.

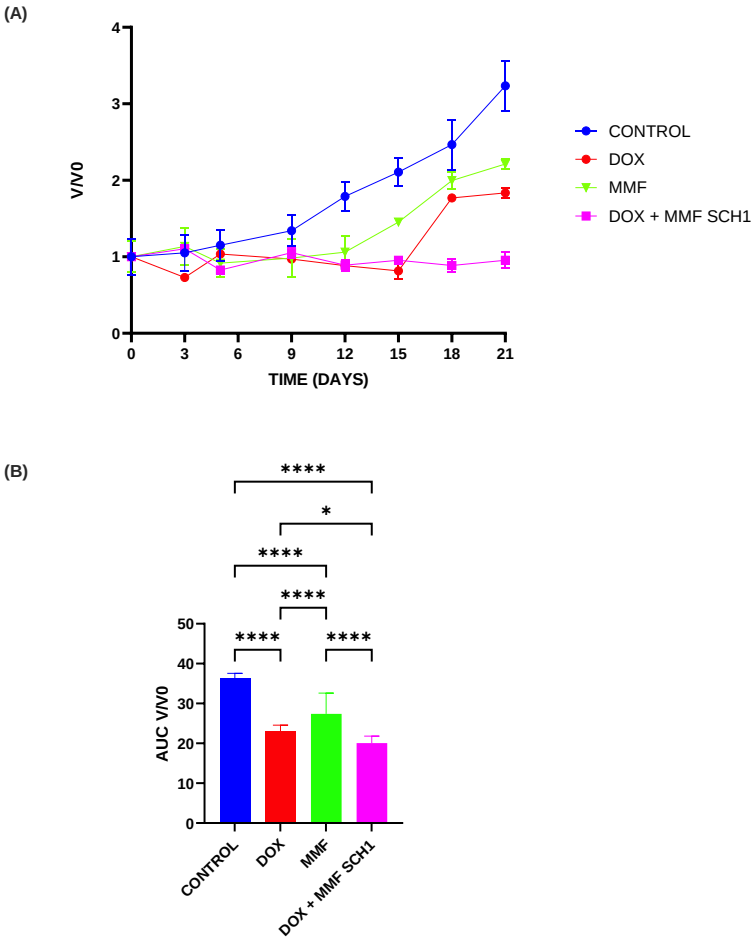

(C)

Bonferroni's multiple comparisons test	V/V0 Summary	Adjusted P Value	AUC Summary	Adjusted P Value
CONTROL vs. DOX	ns	0.0960	****	<0.0001
CONTROL vs. MMF	ns	0.9609	****	<0.0001
CONTROL vs. SCH1	*	0.0112	****	<0.0001
DOX vs. MMF	ns	>0.9999	***	0.0008
DOX vs. SCH1	ns	>0.9999	*	0.0264
MMF vs. SCH1	ns	0.9079	****	<0.0001

Figure. 8 The effect of DOX and MMF simultaneous schedule 1combinations on the growth of MDA-MB-231 spheroids.

Results from Figure 3.8A with respect to V/V0 analysis show that only SCH1 treated spheroids produced a statistically significant decrease in the spheroids growth curve when compared to the untreated control (P=0.01122, Figure 3.8C). When looking at AUC (Figure 3.8B), all treated spheroids produced AUC that was statistically significantly smaller than that of the control (P<0.0001). SCH1 treated spheroids statistically significantly reduced the AUC value compared to the AUC value of DOX alone (P=0.0264) and MMF alone (P <0.0001). These results suggest that MMF given

in a SCH1 is a more effective combination at reducing the growth of MDA-MB-231 cells, than the individual therapies alone. These results support our hypothesis that MMF can inhibit intracellular protective mechanisms that would be upregulated following damage induced by DOX, and as a result increase cell death compared to DOX alone therapy. This data is reflective of that in Chapter 2 Section 2.41.1.2.

A SCH2 combination using doxorubicin and MMF was investigated to determine the ability to inhibit the growth of MDA-MB-231 spheroids, as seen in Figure 3.9.

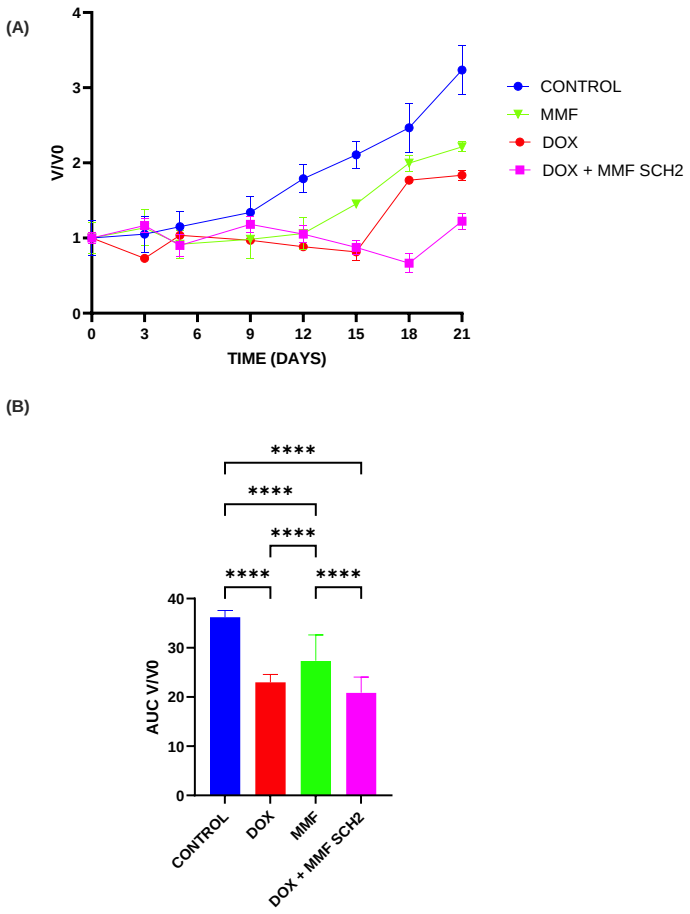

(C)

Bonferroni's multiple comparisons test	V/V0 Summary	Adjusted P Value	AUC Summary	Adjusted P Value
CONTROL vs. DOX	ns	0.1162	****	<0.0001
CONTROL vs. MMF	ns	>0.9999	****	<0.0001
CONTROL vs. SCH2	*	0.0272	****	<0.0001
DOX vs. MMF	ns	>0.9999	***	<0.0001
DOX vs. SCH2	ns	>0.9999	ns	0.2403
MMF vs. SCH2	ns	>0.9999	****	<0.0001

Figure 3. 9 The effect of DOX and MMF simultaneous schedule 2 combinations on the growth of MDA-MB-231 spheroids.

Results from Figure 3.9A with respect to V/V0 analysis show only SCH2 treated spheroid produced a statistically significant decrease in the spheroid growth curve when compared to the control (P=0.0272, Figure 3.9C). When reviewing AUC data Fig 3.9B, all treated spheroids statistically significantly reduced the AUC values compared with the untreated control AUC value (all P>0.0001). SCH2 treatment also statistically significantly reduced the AUC values of spheroids compared with MMF alone (P<0.0001). DOX only treated spheroids produced a statistically significantly

reduction in AUC value when compared with MMF treated spheroids ($P<0.0001$). This data suggests that a SCH2 combination treatment of DOX + MMF can reduce the growth of MDA-MB-231 spheroids more effectively than MMF alone treatment but not more effectively than Doxorubicin alone. This data supports our hypothesis that MMF administered after DOX is unable to mediate the intracellular protective mechanisms and enhance cell death compared to the single doxorubicin therapy alone. The protective mechanisms have already been activated in response to DOX damage and administration of MMF to inhibit these pathways is too late to as the damage has already been mediated. This data is reflective of that in Chapter 2 Section 2.42.1.2.

A SCH3 combination of Dox 0.02 μM + MMF 2 μM was carried out as seen in Figure 3.10 to investigate the ability to reduce the growth of MDA-MB-231 spheroids.

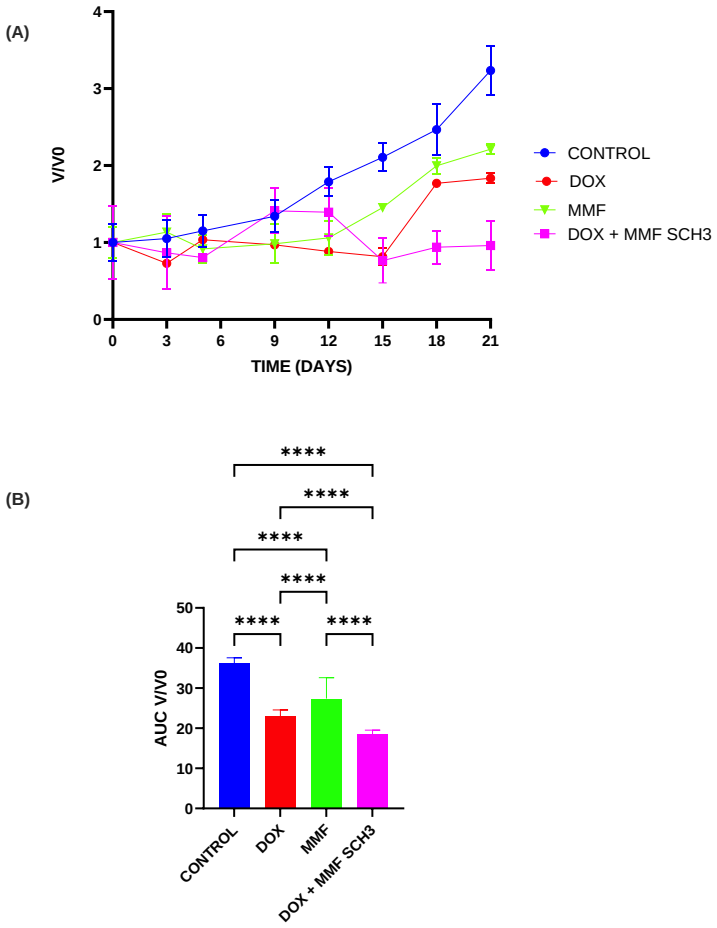

(C)

Bonferroni's multiple comparisons test	V/V0 Summary	Adjusted P Value	AUC Summary	Adjusted P Value
CONTROL vs. DOX	ns	0.1153	****	<0.0001
CONTROL vs. MMF	ns	>0.9999	****	<0.0001
CONTROL VS. SCH3	*	0.0304	****	<0.0001
DOX vs. MMF	ns	>0.9999	****	<0.0001
DOX vs. SCH3	ns	>0.9999	****	<0.0001
MMF vs. SCH3	ns	>0.9999	****	<0.0001

Figure 3. 10 The effect of DOX and MMF simultaneous schedule 3 combinations on the growth of MDA-MB-231 spheroids.

Results from Figure 3.10A suggests that with respect to V/V0 analysis, there was a statistically significant reduction in the change in spheroid volume when spheroids were treated with SCH3 compared to the untreated control (P=0.0304, Figure 3.10C). When reviewing AUC (Fig 3.10B) there was a statistically significantly reduction in the AUC values for all treated spheroids, when compared with the untreated control AUC value (all P>0.0001). SCH3 treated spheroids also reported a statistically significantly reduced AUC value when compared to MMF alone and Dox alone (both P<0.0001).

This data suggests that a SCH3 administration was the most effective combination when reducing the growth of 3D MDA-MB-231 cells. This SCH3 combination is the only DOX combination that statistically significantly reduced the AUC values of treated spheroids compared with the single therapy treated spheroids AUC values. These findings support those in Chapter 2 that suggested a SCH3 administration was the most appropriate treatment combination at reducing the growth of 2D MDA-MB-231 cells. This supports our hypothesis that administration of MMF before ROS damage can inhibit intracellular processes that protect the cell from damage and result in a higher degree of cell kill.

3.4.7 Effects of Radiotherapy given in combination with Dimethyl Fumarate on MDA-MB-231 spheroids

Following on from radiation combination investigations carried out in 2D cell culture, spheroids were used to investigate these scheduled combinations as described in Section 2.42.1.2. Exposure to 2 Gy irradiation was chosen as the clinical dose used is approximately 2.7 Gy (Lilley and Murray 2023). 100 μM DMF was chosen as concentration was used to investigate 2D cells and is shown to have some use at inhibiting the growth of spheroids, as detailed in Figure 3.3. These doses of therapy were also used to investigate 2D cells in Chapter 2 Section 2.42.

Figure 3.11 details the results from investigations involving MDA-MB-231 spheroids treated with a SCH1 combination involving RAD (2 Gy) and DMF (100μM).

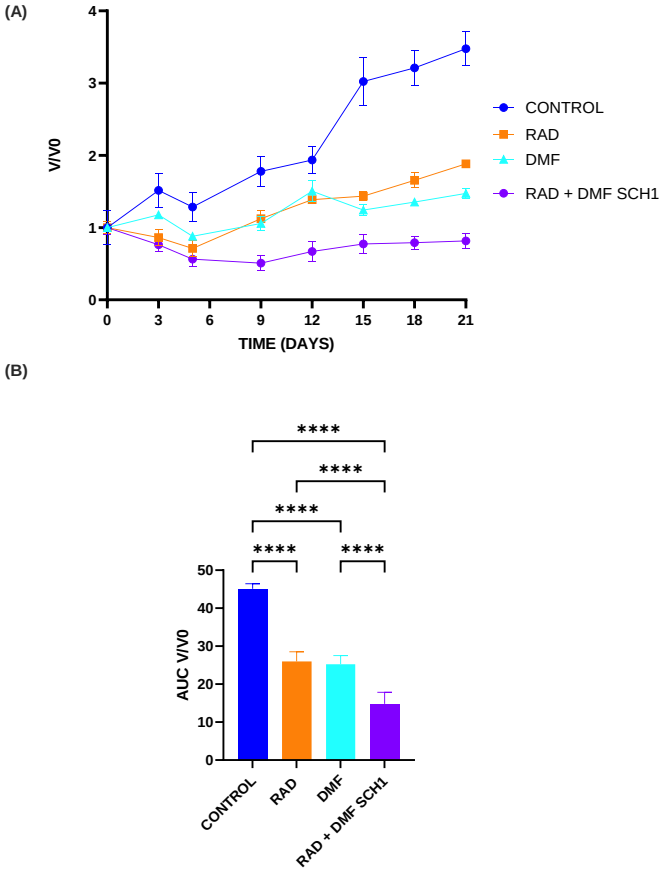

(C)

Bonferroni's multiple comparisons test	V/V0 Summary	Adjusted P Value	AUC Summary	Adjusted P Value
CONTROL vs. RAD	*	0.0190	****	<0.0001
CONTROL vs. DMF	**	0.0062	****	<0.0001
CONTROL vs. SCH1	****	<0.0001	****	<0.0001
RAD vs. DMF	ns	>0.9999	ns	>0.9999
RAD vs. SCH1	ns	0.5996	****	<0.0001
DMF vs. SCH1	ns	0.9002	****	<0.0001

Figure 3. 11 The effect of RAD and DMF simultaneous schedule 1 combinations on the growth of MDA-MB-231 spheroids.

When investigating Figure 3.11A, with respect to V/V0 analysis, there was a statistically significant reduction in the growth of spheroids when treated with SCH1, RAD and DMF compared with the untreated control (Figure 3.11C). However, there was no statistically significant decrease in the change in the volume of spheroids treated with RAD, DMF or SCH1 compared with each other (Figure 3.11C). When reviewing AUC (Figure 3.11B) values, all treatments induced a statistically significantly smaller AUC values than that of the untreated control (all, P<0.0001).

SCH1 treated spheroids also had statistically significantly smaller AUC value when compared to RAD alone ($P<0.0001$) and DMF alone ($P<0.0001$).

These results suggest that SCH1 is a suitable schedule to reduce the growth of MDA-MB-231 spheroids. SCH1 reduced the growth of spheroids more effectively than the single therapies alone. This supports our hypothesis that DMF administration can inhibit intracellular mechanisms and sensitise the cell to death via ROS damage induced by radiation. These results are reflective of those in Chapter 2 Section 2.42.1.2.

Fig 3.12 reports the effect single therapies DMF, RAD and SCH2 combination therapy on MDA-MB-231 spheroids.

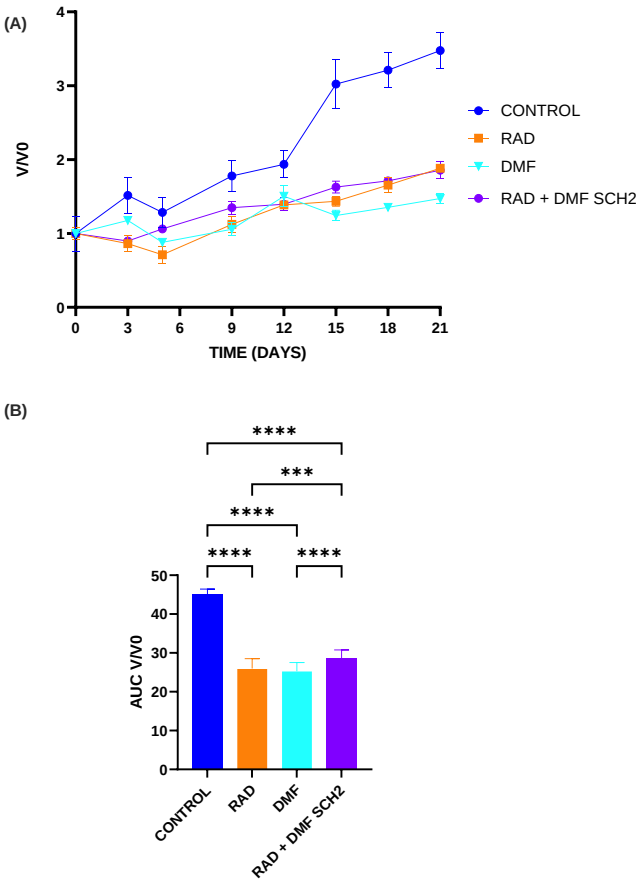

(C)

Bonferroni's multiple comparisons test	V/V0 Summary	Adjusted P Value	AUC Summary	Adjusted P Value
CONTROL vs. RAD	*	0.0141	****	<0.0001
CONTROL vs. DMF	**	0.0082	****	<0.0001
CONTROL vs. SCH2	*	0.0465	****	<0.0001
RAD vs. DMF	ns	>0.9999	ns	>0.9999
RAD vs. SCH2	ns	>0.9999	***	0.0007
DMF vs. SCH2	ns	>0.9999	****	<0.0001

Figure 3. 12 The effect of RAD and DMF simultaneous schedule 2 combinations on the growth of MDA-MB-231 spheroids.

Results from Figure 3.12A suggests that with respect to V/V0 analysis, there was a statistically significant decrease in the change in spheroids volume when spheroids were treated with RAD alone, DMF alone and SCH2 (Figure 3.12C) compared to the untreated control. There was however no statistically significant decrease in the change in spheroid volume results when comparing the growth of any treated spheroids to each other (Figure 3.12C). When reviewing AUC data, all treated spheroids had AUC values that were statistically significantly smaller than that of the control AUC value, (all P<0.0001). As expected for the SCH2 combination, where

radiation was administered first, followed by DMF (RAD1st+DMF) there was not statistically significantly reduction in AUC values when compared with the single therapies alone, however there was a statistically significantly greater AUC value when compared to DMF alone (P=0.0048) and RAD (P=0.0007).

These results suggest that SCH2 administration of RAD + DMF is not a suitable combination schedule to reduce the growth of MDA-MB-231 spheroids. This schedule enhanced the growth of the spheroids when compared to the single therapy treated spheroids alone. These results reflect that of 2D findings in Chapter 2 Section 2.4.

Fig 3.13 investigates the effects of DMF alone, Rad alone and SCH3 on change in spheroid volume over time.

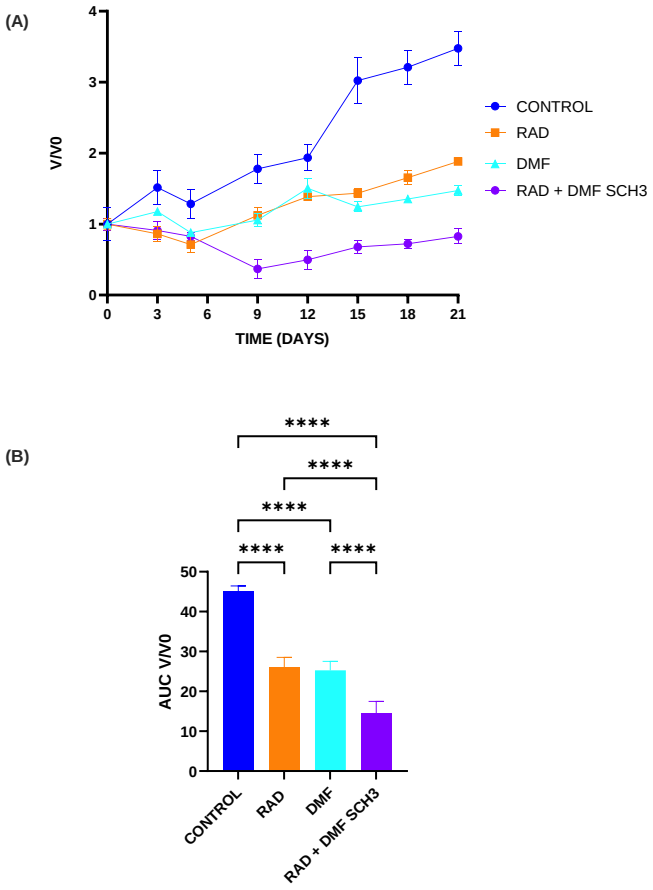

(C)

Bonferroni's multiple comparisons test	V/V0 Summary	Adjusted P Value	AUC Summary	Adjusted P Value
CONTROL vs. RAD	*	0.0107	****	<0.0001
CONTROL vs. DMF	**	0.0061	****	<0.0001
CONTROL vs. SCH3	****	<0.0001	****	<0.0001
RAD vs. DMF	ns	>0.9999	ns	>0.9999
RAD vs. SCH3	ns	0.5603	****	<0.0001
DMF vs. SCH3	ns	0.8447	****	<0.0001

Figure. 13 The effect of RAD and DMF simultaneous schedule 3 combinations on the growth of MDA-MB-231 spheroids.

Figure 3.13A suggests that with respect to V/V0 analysis there was a statistically significant decrease in the change in spheroid volume when spheroids were treated with RAD alone, DMF alone and SCH3 combination when compared to the untreated control (Figure 3.13C). Furthermore, there was no statistically significant decrease in the change in spheroid volume when comparing any treated spheroid group to each other (Figure 3.13C). When reviewing the AUC values, all treated spheroids showed statistically significantly smaller AUC values than untreated control spheroids (all,

P>0.0001). The SCH3 combination also produced statistically significantly reduced AUC values when compared with RAD alone (P<0.0001) and DMF alone (P<0.0001).

This data suggests that SCH3 is a suitable treatment schedule to reduce the growth of MDA-MB-231 spheroids and is more suitable than the single therapies alone. This supports our hypothesis that the administration of DMF prior to damage induced by ROS can prevent cellular protective mechanisms and result in enhanced cell death. These results support the findings of that in Chapter 2 Section 2.4.

3.4.8 Effects of Radiotherapy given in combination with Monomethyl Fumarate on MDA-MB-231 spheroids

This investigation using 3D spheroids was continued, MMF (2 μM) was used in combination with radiation (2 Gy). The radiation dose of 2 Gy was chosen as the clinical dose used is approximately 2.7 Gy (Lilley and Murray., 2023). 2 μM MMF was chosen as this was the lowest concertation of MMF that was able to reduce the AUC values of MDA-MB-231 spheroids statistically significantly. This was also the dose of MMF, and radiation used to investigate 2D combination therapies in Chapter 2. The 3 scheduled combinations as described in section 3.4.5.

Fig 3.14 reports the effects of RAD alone, MMF alone and SCH1 combination therapy.

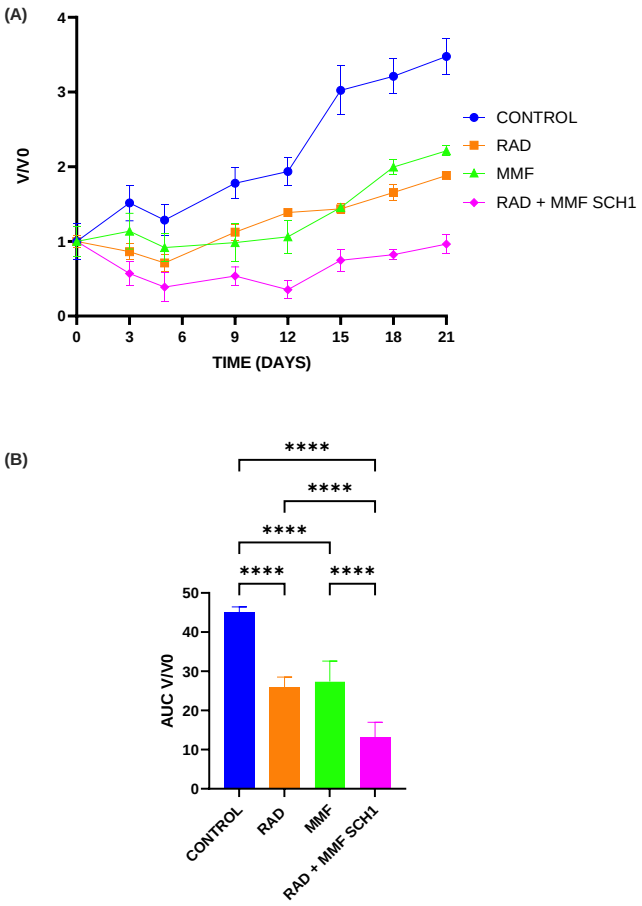

(C)

Bonferroni's multiple comparisons test	V/V0 Summary	Adjusted P Value	AUC Summary	Adjusted P Value
CONTROL vs. RAD	*	0.0109	****	<0.0001
CONTROL vs. MMF	*	0.0308	****	<0.0001
CONTROL vs. SCH1	****	<0.0001	****	<0.0001
RAD vs. MMF	ns	>0.9999	ns	>0.9999
RAD vs. SCH1	ns	0.3325	****	<0.0001
MMF vs. SCH1	ns	0.1363	****	<0.0001

Figure 3. 14 The effect of RAD and MMF simultaneous schedule 1 combinations on the growth of MDA-MB-231 spheroids.

Results from Figure 3.14A report that with respect to V/V0 analysis there was a statistically significant decrease in the change in spheroid volume of spheroids treated with RAD alone, MMF alone and SCH1 combination when compared to the untreated control (Figure 3.14C). However, there was no statistically significant decrease in the change in spheroid volume of any treated spheroid compared with each other (Figure 3.14C). When reviewing the AUC data, all treated spheroids had AUC values that were statistically significantly smaller than untreated control spheroids (all, P<0.0001). SCH1 also statistically significantly reduced the AUC values when compared with

RAD alone ($P<0.0001$) and MMF alone treated spheroids ($P<0.0001$). These results suggest that SCH1 administration of MMF + RAD is a suitable combination therapy at reducing the growth of MDA-MB-231 spheroids and is more effective as reducing cell growth than the individual therapies alone. These results support the hypothesis that MMF can inhibit intracellular processes that protect cells from ROS damage induced by radiation and result in cell death. These findings are reflective that in Chapter 2 Section 2.4.

Figure 3.16 reports the results of spheroids treated with RAD alone, MMF alone and MMF + RAD SCH2 combination therapy.

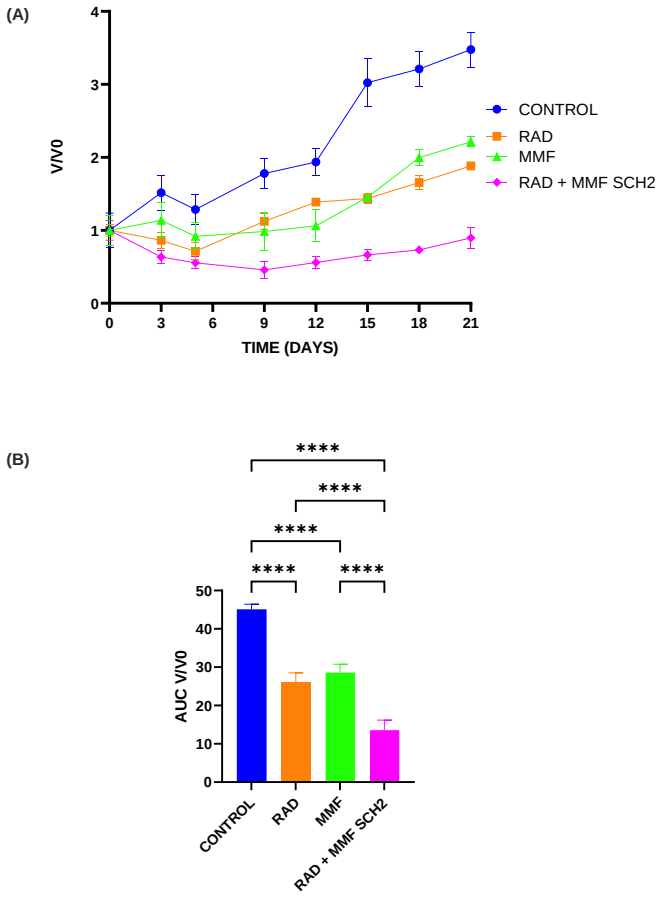

(C)

Bonferroni's multiple comparisons test	V/V0 Summary	Adjusted P Value	AUC Summary	Adjusted P Value
CONTROL vs. RAD	*	0.0141	****	<0.0001
CONTROL vs. MMF	*	0.0384	****	<0.0001
CONTROL vs. SCH2	****	<0.0001	****	<0.0001
RAD vs. MMF	ns	>0.9999	ns	>0.9999
RAD vs. SCH2	ns	0.4343	****	<0.0001
MMF vs. SCH2	ns	0.1861	****	<0.0001

Figure 3. 15 The effect of RAD and MMF simultaneous schedule 2 combinations on the growth of MDA-MB-231 spheroids.

Results from Figure 3.15A suggest that with respect to V/V0 analysis there was a statistically significant decrease in the change in spheroid volume when spheroids were treated with RAD alone, MMF alone and SCH2 combination, compared with the untreated control (Figure 3.15C). However once again There was no statistically significant decrease in the change in spheroid volume when comparing any treated group to each other (Figure 3.15C). When investigating the AUC values (Figure 3.15B) all treated spheroids had statistically significantly reduced AUC values when compared with the control (all P<0.0001). SCH2 treated spheroids had a statistically

significantly smaller AUC values when compared with RAD alone (P>0.0001) and MMF alone (P>0.0001). These results do not support the hypothesis that MMF administered after RAD is unable to inhibit intracellular protective mechanisms and as such the cells are able to prevent damage caused by ROS and prevent cell death. These results are supportive of the findings of that in Chapter 2, Section 2.4.

Figure 3.16 reports the effects of MMF, RAD and SCH3 combination on MDA-MB-231 spheroids.

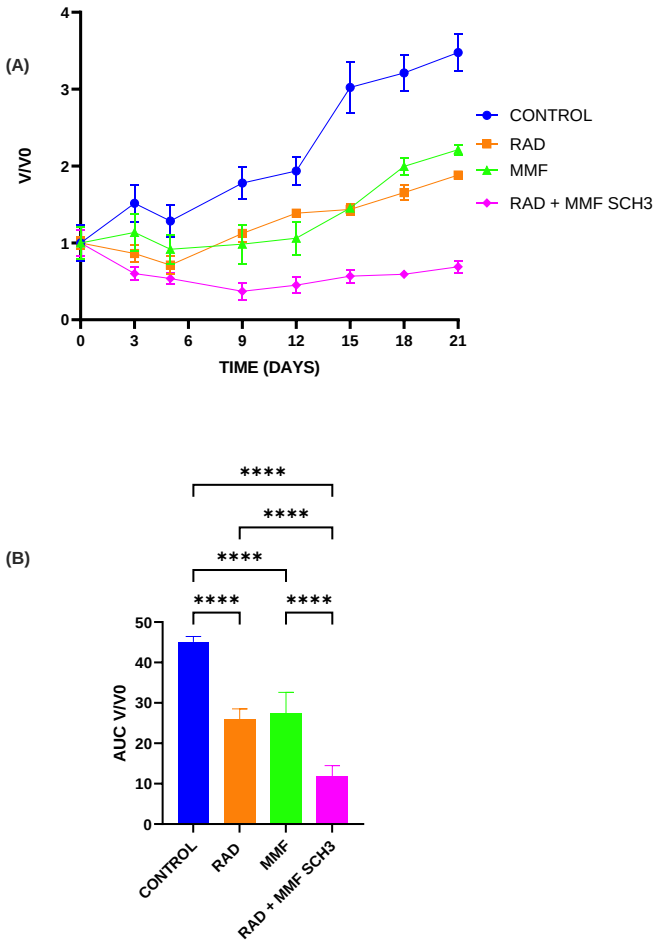

Bonferroni's multiple comparisons test	Summary	Adjusted P Value	AUC Summary	Adjusted P Value
CONTROL vs. RAD	*	0.0107	****	<0.0001
CONTROL vs. MMF	*	0.0302	****	<0.0001
CONTROL vs. SCH3	****	<0.0001	****	<0.0001
RAD vs. MMF	ns	>0.9999	ns	>0.9999
RAD vs. SCH3	ns	0.1599	****	<0.0001
MMF vs. sch3	ns	0.0620	****	<0.0001

Figure 3. 16 The effect of RAD and MMF simultaneous schedule 3 combinations on the growth of MDA-MB-231 spheroids.

Results from Figure 3.16A suggest that with respect to V/V0, there was statistically significant decrease in the change in spheroid volume of spheroids treated with RAD alone, MMF alone and SCH3, compared to the untreated control (Figure 3.16C). There was also a statistically significant reduction in spheroids growth when comparing any treated spheroids to each other. When analysing AUC there was a statistically significant decrease in AUC values in all treated spheroids when compared with the control ($P>0.0001$). There was also a statistically significant reduction in AUC values in SCH3 treated spheroids when compared with RAD alone ($P<0.0001$) and MMF alone ($P<0.0001$). These results support the hypothesis that MMF administered prior to RAD can inhibit intracellular processes that protect the cell from damage caused by ROS. These findings are reflective of that in Chapter 2 Section 2.4.

3.5 Discussion

Doxorubicin

Administration to MDA-MB-231 MTSs of the concentration range of 0.02 μM-1 μM of Dox reduced the size of treated spheroids in a dose dependent manner (Figure 3.1); it was found that all concentrations of DOX statistically significantly reduced the growth of spheroids over time. All concentrations used also induced a statistically significant reduction in the AUC value when compared to the untreated MDA-MB-231 control spheroids (Figure 3.1B). As 0.02 μM was the concentration used in 2D investigations, it would allow for a more accurate comparison of the effects of DOX on MDA-MB-231 2D and 3D models. It had been shown that this concentration reduced the growth of spheroids significantly when compared to the untreated control, this was therefore the concentration of doxorubicin that was chosen to investigate combination therapies.

Radiation

To measure the effect that different Gy of radiation had on MDA-MB-231 cells, a dose response investigation was carried out as seen in Figure 3.2. All doses of radiation produced significantly reduced the change in spheroid growth and the AUC values when compared with the control (Figure 3.3B). At present the current dose of radiation TNBC patients receive is approximately 2.7 Gy per treatments session (Lilley and

Murray., 2023). This can be given up to 5 days a week and last for 5-7 weeks, totalling 50 Gy per round of radiation therapy. 2 Gy of radiation was therefore the dose carried out for future combination therapies. Furthermore, this was the dose of radiation that was used in combination therapies in Chapter 2 section 2.4.7. However, recent evidence has been published from a study 'FAST-Forward' which was carried out in the UK and undertaken by Brunt *et a*l., (2020). This investigated the effect that 26 Gy of radiation administered over 1 week was just as effective for breast cancer patients. The progress of this clinical trial was monitored, and it was published that patients treated with the 26 Gy over one week (5.1 Gy per day) had results that were comparable to those treated with 50 Gy over 6-7 weeks. This study is still ongoing and patient outcomes are still being monitored. However, it does provide an interesting result so far in that the dose of radiation administered to patients seems to have little effect alone compared to results and patient quality of life. This study will be critical in designing combination therapies as higher doses may be able to be administered along with combination therapies, the results from this phase III trial may lead to changes in the standard practice in the UK ((fast-forward) (2022) Cancer Research UK 2022)).

Dimethyl Fumarate

The aim of these experiments was to determine the effect that DMF had on spheroid growth, to demonstrate the effect on MTS with a heterogeneous population of cells including proliferating cells, the quiescent middle layers, and inner hypoxic/necrotic cells. From Figure 3.3 DMF alone did not inhibit the growth of MDA-MB-231 spheroids. However, given the published mechanism of action of DMF (inhibiting the production of antioxidants that protect cells from ROS damage) it was hypothesised that administration of DMF prior to ROS damage induced by doxorubicin or radiation, would result in increased cell death. This is because the normal protective antioxidant mechanisms would be inhibited, therefore SSB and DSB would induce cell death via Caspase 3 mechanism. Therefore, DMF was investigated in combination with current standard therapies Doxorubicin or Radiation to determine if the correct scheduled combination would enhance the percentage of cell death compared to single therapies alone (Rostami-Yazdi, Clement and Mrowietz, 2010). This hypothesis is supported by the findings of Saidu *et al* in (2018), who reported that the concentration of DMF was critical in inducing cancer cell death. This hypothesis was investigated in Section 3.4.

Monomethyl Fumarate

Spheroids treated with concentrations of MMF (2 μM-10 μM) in Figure 3.4 induced a dose dependent reduction of spheroid growth over time. The only significant reduction in change in spheroid growth was found when MDA-MB-231 spheroids were treated with 10 μM MMF (P=0.0001), however there was a significant decrease in the AUC values of MMF at all concentrations compared to the untreated control. As MMF is the active metabolite of DMF, it is expected that it would be more potent at enhancing cancer cell death. MMF binds to intracellular glutathione, preventing it from neutralizing ROS generated by DOX or radiation. It also inhibits NRF2 translocation to the nucleus which inhibits the transcription of antioxidants such as GSH (Saidu *et al*., 2017). Consequently, cells are unable to protect themselves from damage induced by reactive oxygen species (ROS) such as double strand breaks (DSB) and single strand breaks (SSB) which will then accumulate leading to the activation of Caspase 3 and resulting in cell death. Given this mechanism of action, the same hypothesis was given to combination therapies involving MMF as combinations involving DMF. To induce the greatest MDA-MB-231 cell death, MMF requires administration prior to ROS damage induced by chemotherapeutic agents or radiation. This allows time for the drug to bind to glutathione and potentially inhibit NRF2 nuclear translocation and inhibits the production of cellular protective antioxidants, thereby sensitizing the cell to damage by ROS. This hypothesis was investigated in 3D spheroids in Section 3.4.4.

Cytotoxic effects of combination therapy using Doxorubicin with Fumaric Acids on MDA-MB-231 spheroids.

When reviewing the results from DOX combination therapies it was found that the scheduled combinations SCH1 and SCH3 of DOX + DMF induced a statistically significant decrease in the change in the growth spheroids compared with the untreated control spheroids (Figure 3.5-7). These findings were more encouraging than that of the results from section 2.4.7 where it was reported no scheduled combination of DMF + DOX statistically significantly reduced the survival of MDA-MB-231 cells in clonogenic analysis, compared to the control. As these results were not reflected in 3D investigations, this may be due to the differences in the cell phenotypes

and interactions that are found in spheroids. As they are heterogeneous models, they contain not only proliferating cells but quiescent non dividing cells and a hypoxic core. The formation of spheroids is facilitated through membrane proteins called integrins, and extracellular matrix proteins, and binding between neighbouring cells allows for tight connections between allowing for cell-cell interactions that is different from that in 2D models (Kitel *et al*., 2013). These findings are particularly interesting as DOX and RAD target rapidly proliferating cells thus it is not surprising that spheroid volume was not reduced as significantly as 2D models, chemotherapy and radiotherapy have been shown to be less efficient at killing hypoxic cells (Muz *et al.,* 2015).This significant decrease in change in spheroid volume may be due to these heterogeneous cell types within the spheroid, as hypoxic cells have been shown to induce the production of components required for intracellular synthesis of GSH (Semenza, 2016), therefore it may be that DMF is binding to these ROS and in-turn these hypoxic cells are more sensitive to ROS damage. This therefore suggests that DMF in combination with DOX is not a more suitable treatment option than the current gold standard of doxorubicin alone when investigating 3D models (Rouzier *et al* 2005).

The same is true for DOX given in combination with MMF (Figure 3.8-10). At no time schedule combination did DOX + MMF significantly reduced the spheroid growth when compared to the control spheroids and each single therapy treatment. These results support the findings from Chapter 2 section 2.4.7 showed that SCH3 scheduled combinations of DOX + MMF statistically significantly reduced the clonogenic survival of MDA-MB-231 cells compared with the untreated control cells. However again in 3D investigation this significant decrease in change in spheroid volume was seen using at scheduled treatments, this may be due to the above stated reasons, hypoxic cells are known to upregulate intracellular synthesis of glutathione (Semenza, 2016), therefore inhibiting this may be sensitising these cells to death via doxorubicin.

Furthermore section 2.4.10 reported a significant increase in apoptotic cells when treated with SCH3 DOX + MMF when compared with the control and both single treatment therapies. These findings that in 3D culture both DMF and MMF in combination with DOX significantly reduce spheroid growth of MDA-MB-231 spheroids supports these findings. It is imperative that these investigations be carried out before progressing into more complex *in vivo* investigations such as the Chick

Embryo Model (CEM, Chapter 5) model or murine tumour models. Spheroids can help compliance with the 3Rs (replacement, reduction, and refinement) by reducing the number of procedures undertaken in animals through filtering out unpromising experimental parameters at an earlier stage. This is important as it reduces the cost of *in vivo* investigations by refining the number of mice required and the number of therapies being investigated will be reduced. The current issues faced when translating 2D results into 3D models were reviewed by Huang *et al* (2020), the authors demonstrated that in 3D culture these models exhibited an increase in resistance to antitumour compounds such as DOX. As TNBC tumour resistance to doxorubicin is a well-documented issue with the current gold standard of treatment, the authors found that these spheroid models accurately reflected this resistance that is often found in patients, strengthening the reliability of this model to investigate potential compounds to treat TNBC (Paramanantham *et al* 2021).

Cytotoxic effects of combination therapy using Radiation with Fumaric Acids on MDA-MB-231 spheroids.

MDA-MB-231 spheroid investigations involving a combination of radiation, DMF and MMF in scheduled combinations showed some promising results. SCH1, SCH2 and SCH3 using MMF or DMF all produced significantly reduced changes in spheroid volumes when compare with the control spheroid (Figure 3.11, 3.12 and 3.13). These combinations however did not produce spheroids that were significantly smaller than spheroids treated with radiation alone or DMF alone or MMF alone when looking at change in spheroid volume over time. When reviewing AUC data this statistical significance in reduced spheroid volume was mirrored in AUC values. Both SCH1, SCH2 and SCH3 treated spheroids had significantly smaller AUC values when compared with the control and notably a significant decrease in AUC when comparing SCH1 and SCH3 to the radiation alone and DMF alone treated spheroids AUC values. This was partially reflective of the findings in Chapter 2 Sections 2.4.7, as SCH 1 (Simultaneous administration of Radiation and DMF) and SCH3 (Radiation administered after DMF) combination produced a statistically significant reduction in clonogenic survival of MDA-MB-231 cells when compared with the control cells and DMF alone treated cells. SCH 2 (Radiation administered before DMF) did not produce any significant results when compared to the untreated control or any other treatment group in Figure 3.12 and likewise in clonogenic assays (Section 2.4.1). These results

supported the hypothesis that administration of DMF prior to damage caused by radiation or doxorubicin would result in an increased cell kill. This is due to the mechanism of action of DMF, by binding to GSH, preventing it from neutralising ROS generated by DOX or radiation therapy, and potentially by inhibiting NRF2 which prevents the synthesis of antioxidants. Which in turn results in ROS, generated from radiation or DOX therapy, causing SSB and DSB which when accumulated result in cell death via caspase 3 pathway (Wang *et al.,* 2018, Musaogullari *et al.,* 2020). As SCH2 requires that DMF/MMF is administered after radiation or DOX therapy, the lack of cell growth or 3D spheroid growth inhibition reported supports this hypothesis as the inhibition of antioxidant generation is being induced after the initial spike in ROS therefore there is no mediation of this protective mechanism at the time of initial insult to the cell. Thus, SCH1 and SCH3 are both promising candidates at treating TNBC and these results support our hypothesis that DMF administered prior to damage induced by ROS can inhibit the production of antioxidants that would protect cells from SSB and DSB, ultimately resulting in higher cell kill. This prompts further investigations and supports the use of *in vivo* investigations into these 2 schedules, potential in murine models or the Chick Embryo Model (CEM). Investigations into these therapies on the CEM is limited however if these combination therapies were investigated using an *in vivo* model it would provide a deeper insight into their effects on a larger tumour mass with developed angiogenesis (Ribatti., 2022).

Results from investigations involving radiation in scheduled combinations with MMF also produced reflective results as those found in 2D investigations (Chapter 2, sections 2.4.). Figures 3.14-16 show that SCH1, SCH2 and SCH3 combinations of radiation and MMF produced significant reductions in spheroid growth when compared with the control spheroids. When investigating the AUC values, again these scheduled treatments all produced statistically significantly reduced AUC values when compared with the control AUC, radiation and MMF alone. This suggested that RAD given in any investigated scheduled combination with MMF is a more effective treatment to treat TNBC spheroids than the current gold standard of radiation alone. This supports the findings in Section 2.4.15 as it was found in combination index that SCH3 MMF1st (2 μM) + RAD (2 Gy) produced a synergistic CI value. This means that the sum of both therapies when given alone is greater than that of the individual therapies (Duarte and Vale., 2022). This SCH3 combination (radiation administered after MMF) also significantly increased the percentage of apoptotic cells compared to

control cells, radiation alone treated cells or MMF alone treated cells (sections 2.4. 17). This SCH3 (radiation administered after MMF) combination also gave rise to a significant increase in tail moments when compared to control cells and MMF alone treated cells as seen in comet analysis in section 2.4.21. Suggesting that this decrease in spheroid volume we have seen in Figures 3.14-3.16 is reflective of the increase percentage of cells undergoing apoptosis because of this combination therapy detailed in Chapter 2, 2D investigations.

The findings of Figure 3.16 are encouraging as they support the results found in Section 2.4, further strengthening the evidence that radiation + MMF in a schedule 3 combination (Radiation administered after MMF) could potentially be a more effective therapy to treat TNBC patients than radiation alone. As such this would be the ideal candidate to take forward into additional 3D investigations such as CEM model and the most encouraging combination to investigate when overcoming therapy resistance in Chapter 4. Based on the results from Chapter 2 and 3 the combination therapy investigated in Chapter 4, when trying to overcome therapy resistance will be SCH 3 combination involving: DOX + MMF and RAD + MMF combinations.

Chapter 4

The development of Doxorubicin resistant MDA-MB-231 cells, Radiotherapy resistant MDA-MB-231 cells and Radiotherapy + Doxorubicin resistant MDA-MB-231 cells.

4.1 Introduction

Tumour resistance is one of the main issues faced when treating TNBC. Historically patients respond well to initial therapies, including the chemotherapeutic agent doxorubicin which is the current gold standard therapy. Radiotherapy is also used frequently as part of a multidisciplinary approach to treat TNBC, often after surgery (Clarke *et al.* 2005). However, tumour recurrence is common, the 10-year survival rate for TNBC is 66%, compared with other types of breast cancer where the ten-year survival rate is 76% (Breast cancer statistics (2023)). Often metastasis is found in the brain and lung of TNBC patients, and it is thought that the reason for this recurrence is due to therapy resistance (Nedeljković *et al.,* 2022). Therefore, to overcome cancer recurrence, it is important to use the correct model to investigate potential therapies for therapy resistant cells. The next phase of my project involved the development of MDA-MB-231 therapy resistant cells which I developed over a year. This involved the method used by McDermott, M. *et al.* (2014), cells were seeded and treated with the desired therapy. The colonies that survived where harvested and the treatment process repeated. Cells were exposed to 3 rounds of therapy and after this a resistance test was carried out via clonogenic assay was to determine sensitivity of these cells compared with the parental lines and round 1 and 2 of resistance therapy. For doxorubicin treatment, the cells were named after each round of treatment D1, D2 and D3. The same method of naming applies to radioresistant cells and radiotherapy + doxorubicin resistant cells.

Although MDA-MB-231 cells were killed effectively by radiation as detailed in Chapter 2 and 3, the issues arise when resistance develops (Kyndi *et al*., 2008). There are well documented issues with TNBC radio-resistance and as such this topic was a focus of this chapter (He *et al*., 2018). The use of a non-toxic agent (fumaric acids) to be given in combination with radiation and provide a potentially more effective synergistic cell kill was the basis of combination experiments. Using the same method, a Doxorubicin resistant cell line was also developed and, radiation resistant cell lines were also developed as well as a combination of both, Radiation + Doxorubicin resistance cells. This is discussed in Chapter 4.

4.2 Aims

The aims of this chapter were to.

- Develop MDA-MB-231 cells resistant to.
    - Doxorubicin
    - Radiotherapy
    - Doxorubicin and radiotherapy

- Investigate the identified combination therapy that was most successful in treating MDA-MB-231 resistant cells in 2D and 3D culture

- Investigate the mechanisms involved in each resistant cell clonal population after treatment to determine any differences.

4.3 Materials and methods

4.3.1 Development of resistant cells

MDA-MB-231 cells were plated in T25 cm^2 flasks (Fisher Scientific, UK) at a density of 200,000 cells/flask, in complete DMEM media (Fisher Scientific, UK) and placed in an incubator at 37 ^oC in a 5% CO_2 environment for 48 hrs as this is the cells doubling time. Cells were treated with either 1500 μL of 0.02 μM doxorubicin (Tocris Bioscience) in complete DMEM media or dosed with 2 Gy radiation or MDA-MB-231 cells were treated with 1500 μL doxorubicin in complete DMEM media AND then irradiated with a dose of 2 Gy. Cells were then left for 48 hrs in an incubator set to 37 ^oC in a 5% CO_2 environment before counting using a hemocytometer (Jenson, UK). 700 MDA-MB-231 cells were then seeded into 60 mm petri dishes (Fisher Scientific, UK) with 5 mL of complete DMEM media, in triplicate. Dishes were then incubated for 14 to 21 days until colonies of more than 50 cells were visible. Visible colonies were then isolated using a sterile PYREX cloning cylinder smeared on the bottom edge with sterile Vaseline (Fisher Scientific, UK). 10 μL of 0.05 % trypsin was placed in each cylinder and left for 10 minutes to remove cells from the surface of the petri dish. After this the cells in suspension were placed into a 96-well flat bottom plate containing 200 μL of complete DMEM. The plate was then placed into the incubator for 48 hrs or until the bottom of the 96 well was 90% confluent. At this point cells were detached with trypsin and seeded into a 24 well plate containing 500 μL of DMEM and incubated until the bottom of the 24 well plate was 90% confluent. This process of seeding into increasingly larger TC vessels was continued until a confluent T25 flask was obtained from which a single cell suspension was made via the addition of trypsin, then media and gentle passage of the cell suspension through a sterile 25 mm needle (BD Microlance). Three new T75 cm^2 flasks containing 20 mL of complete DMEM medium were then seeded with various volumes of the cell suspension (1 mL, 3 mL, and 5 mL) to maintain stock levels of viable cells of varying confluence. Some flasks were frozen down to keep as stock and stored at -80^0C for 2 weeks before transfer to liquid nitrogen.

This process was repeated twice more exactly as described above. After the third round a resistance test was carried out using a clonogenic assay (as described in Section 4.3.6) at 3 doses of the relevant therapy. Following this the clonal derived

flasks that had highest survival fraction from clonogenic analysis were chosen to investigate potential combination therapies and maintained in the same method as parent MDA-MB-231 cells (as described in Section 4.3.2). Cells were routinely tested for the presence of mycoplasma via a PCR test (Minerva Biolabs GmbH, 56-1010 and 11-1050).

4.4 Results.

4.4.1 Cytotoxicity of Combination therapy using Doxorubicin and Dimethyl Fumarate on Doxorubicin Resistant cells

- 2D cell culture

Doxorubicin resistant cells were developed as described in sections 4.3.13. After three rounds of resistance selection cells were tested to determine resistance via a clonogenic assay after incubation with different concentrations of doxorubicin (1μM, 2μM and 3μM) as seen in figure 4.1. Results are displayed as an average of 3 independent experiments.

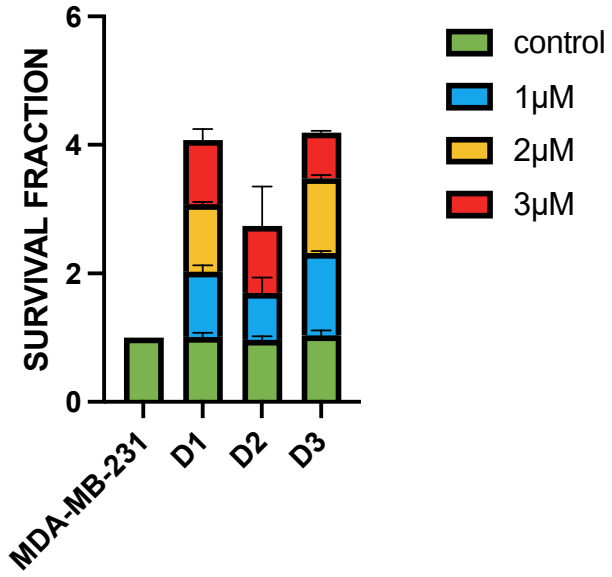

Figure 4. 1 Resistance test for doxorubicin exposed cells.

MDA-MB-231 cells that had undergone various rounds of DOXexposure treatment were tested for clonogenic survival after exposure to Doxorubicin at concentrations of 1,2 and 3 μM. Data shown is an average of at least three independent experiments

performed in triplicate +/- standard deviation and graphed using GraphPad Prism Version 9.

It can be seen in Figure 4.1 that all three doxorubicin resistant cells tested showed clonogenic survival at all 3 concentrations of drug tested except for D2. D3 was selected as the cell line to carry on and develop spheroids and test combination therapy on as this cell line showed the highest survival after incubation with 1μM doxorubicin where and reported clonogenic survival at all concentrations of drug tested. After incubation with 1μM Dox a survival fraction of (1.27) and IC_{50} value was 0.99 μM was observed which in comparison to the IC50 value of the parent MDA-MB-231 cells which was 0.06 μM (section 2.24.1 and Figure 4 below).

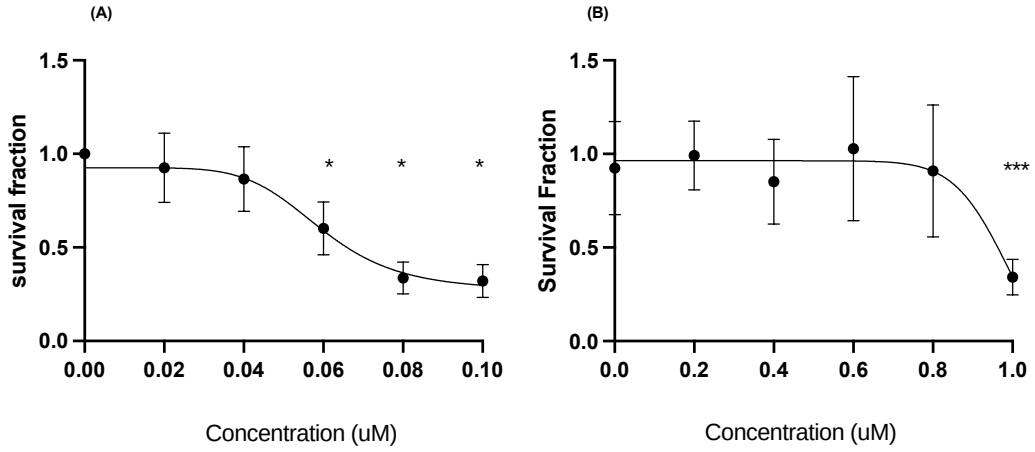

Figure 4. 2 D3 cells investigated using varying concentrations of doxorubicin.
(A) Parental MDA-MB-231 cells clonogenic survival when exposed to varying concentrations of doxorubicin 0.02μM – 0.1μM and (B) D3 cells which were exposed to varying concentrations of doxorubicin (0.2μM -1μM). Results are displayed as an average of 3 independent experiments performed in triplicate and results graphed using GraphPad Prism version 9.2.1. A 1-way ANOVA with Bonferroni post testing was performed using GraphPad Prism 9.2.1 software, with p-values of 0.05 = * and p=0.001 *** reported as significant difference of the treated group compared to the untreated control.

When investigating D3 cells it was decided that the concentration range of doxorubicin would be increased by a factor of ten as the initial resistance test results showed clonogenic survival at 1μM (Figure 4.1). From Figure 4.2B it was found that the IC_{50} of D3 cells when exposed to doxorubicin was 0.99μM. This is approximately 16 times greater than the IC_{50} found in Figure 4.2A when investigating the parental MDA-MB-231 cells. These finding show that D3 cells can survive up to 50% higher concentrations of doxorubicin and as such investigations into 3D culture and mechanistic actions of this cell line were investigated. We can therefore conclude that we had developed a doxorubicin resistant cell line.

To determine if the fumaric acids investigated in 2D culture (Chapter 2) had any potential use in overcoming resistance of D3 cells, the administration of Doxorubicin and MMF in scheduled combinations were investigated. The aim of these experiments using clonogenic assays were to determine if adding MMF in the most appropriate time schedule would re-sensitise the resistant cells potentially leading to a higher cell kill than the initial treatment that these cells developed resistance to. The outcome of these experiments is reported in Figure 4.3.

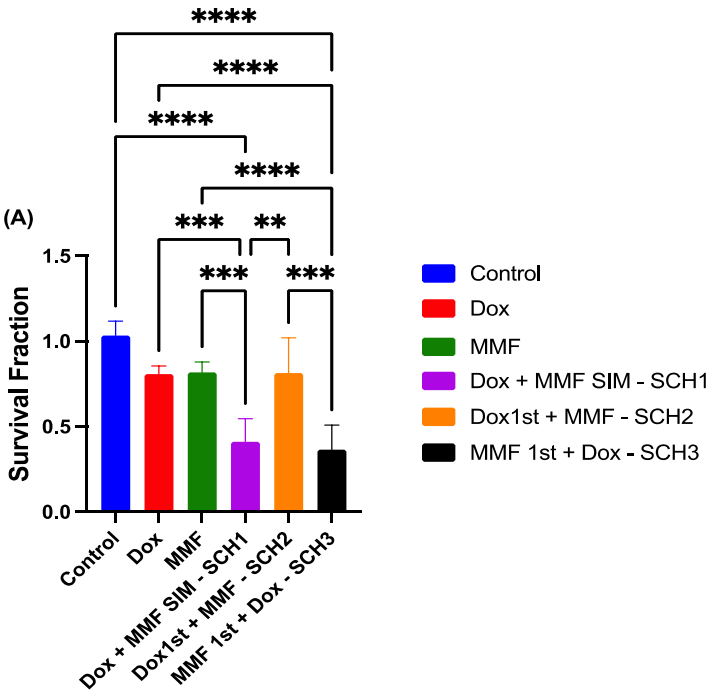

(B)

Bonferroni's multiple comparisons test	Summary	Adjusted P Value
Control vs. SCH1	****	<0.0001
Control vs. SCH3	****	<0.0001
MMF vs. SCH1	***	0.0002
MMF vs. SCH3	****	<0.0001
Dox vs. SCH1	***	0.0002
Dox vs. SCH3	****	<0.0001
SCH1vs. SCH2	**	0.0011
SCH2vs. SCH3	***	0.0002

Figure 4. 3 Clonogenic survival of D3 cells treated with MMF (2μM) scheduled combinations with doxorubicin 0.2 μM on D3 cells.

Survival fraction of DOX 0.2μM, MMF 2μM and the combination of three schedules of administration on D3 (DOX resistant) cells. Data shown is the average of three independent experiments carried out in triplicate +/- SD. (B) A 1-way ANOVA with Bonferroni's post-test was performed using GraphPad Prism 9.2.1 software, P <0.005 = *, <0.001= **, <0.0001= ***, <0.00001=**** reported as significant when compared with the control with all results compares to the control and each other.

From the Figure 4.3 we can see that with SCH1 and SCH3 combinations, the survival fraction of D3 cells was statistically significantly reduced when compared with the untreated control (Both, P<0.0001, Figure 4.3B), as well as Dox and MMF alone (Dox: SCH2 P=0.0002 and SCH3 P<0.0001, Figure 4.3B; MMF SCH2 P=0.0002, SCH3 P<0.0001, Figure 4.3B). There was also a statistically significant decrease in the

survival fraction of D3 cells when treated with SCH1 and SCH3 compared with SCH2 treated cells (SCH1 P=0.0011 and SCH3 P=0.0002, Figure 4.3B). There was however no statistically significant decrease in the survival fraction of cells treated with SCH1 compared with SCH3 treated cells (P>0.9999, Figure 4.3B).

These findings from Figure 4.3 support the hypothesis that MMF administered in combination with DOX to Doxorubicin resistant cells (D3), can statistically significantly reduce the clonogenic survival of cells more effectively than Doxorubicin alone, when MMF is administered before Doxorubicin. Therefore, this data supports the possible use of MMF in combination as a potential therapy for TNBC patients with developed resistance to doxorubicin chemotherapy.

4.4.2 Assessment of combination of Doxorubicin and MMF In 3D spheroid models of therapy resistant cells

Doxorubicin resistant cells were then investigated in 3D MTS. DOX alone, MMF alone and each combination of MMF, DOX, SCH1, SCH2 and SCH3 was used to investigate the change in spheroid growth over time. The results are detailed in Figure 4.4. Concentrations of drugs used were MMF 2 μM, DOX 0.2μM, SCH1 (MMF 2 μM + DOX 0.2 μM - simultaneous administrations), SCH2 (DOX 0.2 μM 1^{st} + MMF 2 μM) and SCH3 (MMF 2 μM 1^{st} + DOX 0.2 μM).

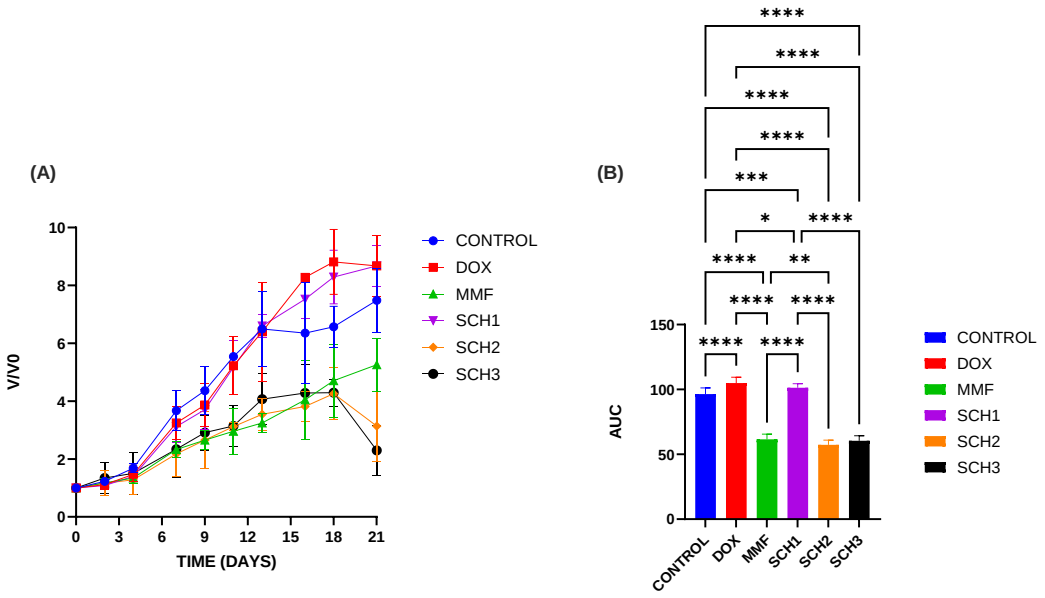

(C)

Bonferroni's multiple comparisons test	V/V0 Summary	Adjusted P Value	AUC Summary	Adjusted P Value
CONTROL vs. DOX	ns	>0.9999	****	<0.0001
CONTROL vs. MMF	ns	>0.9999	****	<0.0001
CONTROL vs. SCH1	ns	>0.9999	****	<0.0001
CONTROL vs. SCH2	ns	>0.9999	***	0.0010
CONTROL vs. SCH3	ns	0.8753	****	<0.0001
DOX vs. MMF	ns	>0.9999	****	<0.0001
DOX vs. SCH1	ns	0.4312	****	<0.0001
DOX vs. SCH2	ns	>0.9999	*	0.0341
DOX vs. SCH3	ns	0.3688	****	<0.0001
MMF vs. SCH1	ns	>0.9999	****	<0.0001
MMF vs. SCH2	ns	>0.9999	****	<0.0001
MMF vs. SCH3	ns	>0.9999	****	<0.0001
SCH1 vs. SCH2	ns	0.6175	****	<0.0001
SCH1 vs. SCH3	ns	>0.9999	ns	>0.9999
SCH2 vs. SCH3	ns	0.5318	****	<0.0001

Figure 4. 4 The effect of DOX and MMF simultaneous schedule 1,2 and 3 combinations on the growth of D3 spheroids.

(A) D3 spheroids were incubated with drugs continually for 21 days and images captured every 2-4 days. Spheroid volumes were calculated and the average fold increase from initial V/V0 +/- S.D, is presented on a linear scale, (B)The area under the curve (AUC) +/- S.D. was also calculated using one-way ANOVA analysis with Bonferroni's testing for multiple comparisons, results displayed in (C). Results are an average of three independent experiments with 36 spheroids per treatment, statistical analysis was carried out on the data using GraphPad prism 9.2.1, determined by the. P<0.05=*, P<0.01=**, P<0.001=***, P<0.0001=**** when compared with the control.

From Figure 4.4A none of the changes in spheroid volume as measured by V/V0 analysis where statistically significantly different compared with the control group or any other group measured (all P>0.9999). Surprisingly the V/V0 for SCH3 treated spheroids appears to be not statistically significant when compared to any other treated or untreated spheroid group when analysing the data using a one-way ANOVA with Bonferroni multiple comparison. With this statistical analysis only the significance between each point within the linear curve is compared. Clearly in Figure 4.4 the AUC data for SCH3 was statistically significant when compared to the untreated control, DOX, MMF and SCH2 (Figure 4.4C) as AUC considers the full area under each of the linear curves for the V/V0.

The results from AUC analysis (Figure 4.4B) suggest that there was statistically significant decrease in AUC values of all spheroids when treated with DOX compared with the untreated control (P<0.0001). There was also a statistically significant decrease in the AUC value of D3 spheroids treated with MMF, SCH1, SCH2 and SCH3 when compared to the untreated control (MMF, SCH1 and SCH3 P<0.0001, SCH2 P=0.001, Figure 4.4C) and Dox (MMF, SCH1 and SCH3 all P<0.0001, SCH2 P=0.034, Figure 4.4C).There was a statistically significant decrease in the AUC values of D3 spheroids treated with SCH1 and SCH3 when compared to MMF alone treated spheroids (both, P<0.0001, Figure 4.4C). There was a statistically significant decrease in the AUC values of D3 spheroids treated with SCH1 and SCH3 compared with SCH2 treated spheroids (both P<0.0001, Figure 4.4C). There was no statistically significant change in the AUC values of spheroids treated with SCH1 compared with SCH3 treated spheroids.

This data from Figure 4.4 is reflective of the findings in Figure 4.3, supporting the hypothesis that MMF administered in combination with DOX to Doxorubicin resistant MTS can significantly reduce the growth of spheroids more effectively than Doxorubicin alone, when MMF is administered before Doxorubicin. Therefore, this data supports the possible use of MMF in combination as a potential therapy for TNBC patients with developed resistance to doxorubicin chemotherapy.

Overall, our results support the hypothesis that MMF administered prior to doxorubicin administration can increase D3 (doxorubicin resistant) cell death. This may be due to the mechanism of action by which MMF binds to intracellular glutathione and prevents

the antioxidant from neutralising ROS generated from DOX treatment, it may also be causing the inhibition of nuclear NRF2 translation preventing the synthesis of antioxidants. As such, this SCH3 combination will be investigated at a mechanistic level.

4.4.3 Combination Index analysis of Combination therapy Doxorubicin and Monomethyl Fumarate on Doxorubicin Resistant cells

The principle behind combination index and equations used are detailed in chapter 2 section 2.4.8.

Figure 4.5 is a representation of the data in Figure 4.3 that has been analysed using the Calcucyin Software.

(A)

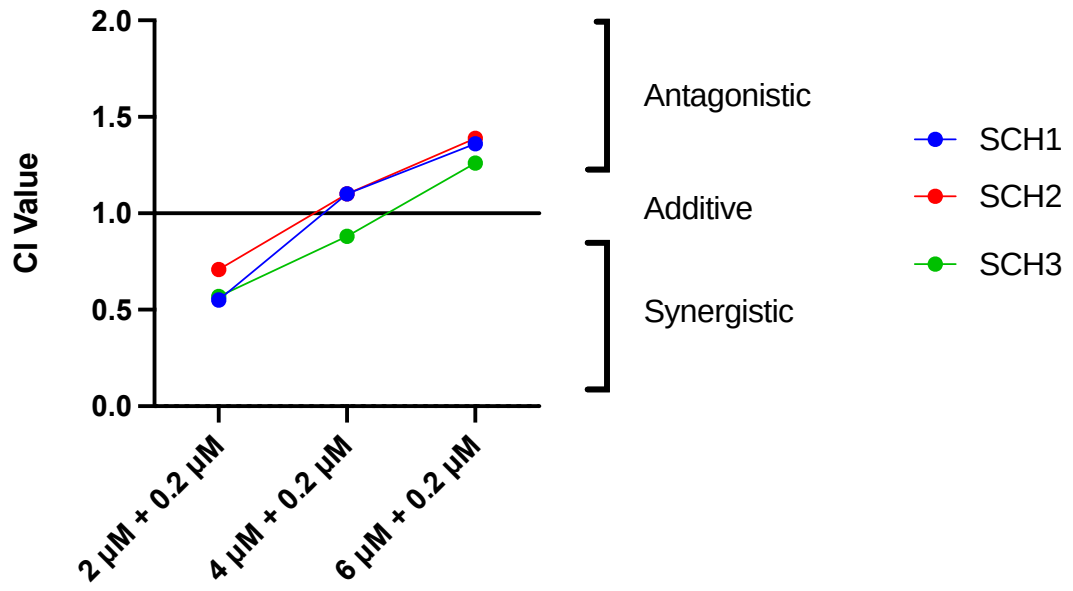

(B)

Drug Concentrations	Combination Index Values		
	SCH1	SCH2	SCH3
MMF 2 µM + DOX 0.2 µM	0.55	0.71	0.57
MMF 4 µM + DOX 0.2 µM	1.1	1.1	0.88
MMF 6 µM + DOX 0.2 µM	1.36	1.39	1.26

Figure 4. 5 (A) Combination Index (CI) after D3 cells are incubated with DOX and MMF in the 3 treatments Schedules.
Antagonistic <1.1, Additive = .9-1.1 and Synergistic > 0.9. Each point represents three independent experiments. (B) Values of CI plotted in (A).

From Figure 4.5 we can conclude that at administered concentration of 2 µM MMF + 0.2 µM DOX at all schedules there is our synergistic CI values (0.55, 0.71 and 0.57, Figure 4.5B) which suggest that at these concentrations DOX + MMF has a combined effect that is greater to that predicted from their individual survival fractions. However, SCH 3 is the only combination to produce synergistic CI value when using a higher concentration of 4 µM MMF + 0.2 µM Dox (0.88, Figure 4.5B). All CI values produced when investigating a concentration range of 6 µM MMF + 0.2 µM Dox were all antagonistic. These results support the use of SCH3 as a combination therapy to treat D3 cells as this combination produced synergistic CI values at 2 concentrations of drug tested, and therefore the results are concentration dependant.

4.4.4 Cell cycle analysis of D3 cells after combination treatment with Doxorubicin and Monomethyl Fumarate

As describes in Section 4.3.4, a Cell Cycle Analysis assay was carried out to investigate the effect each treatment has on the percentage of cells in each phase of the cell cycle. After 48 hours (cell doubling time) of incubation with respective treatments the media containing these therapies was removed and cells washed using PBS. Cells were harvested for treatment as described in Section 2.42.14.

Cells in Figure 4.6 were treated with Dox alone, MMF alone and the SCH3 dox combination (MMF1st 2 μM +Dox 0.2 μM, 24 hours after 1st therapy administration) and harvested immediately following treatment completion.

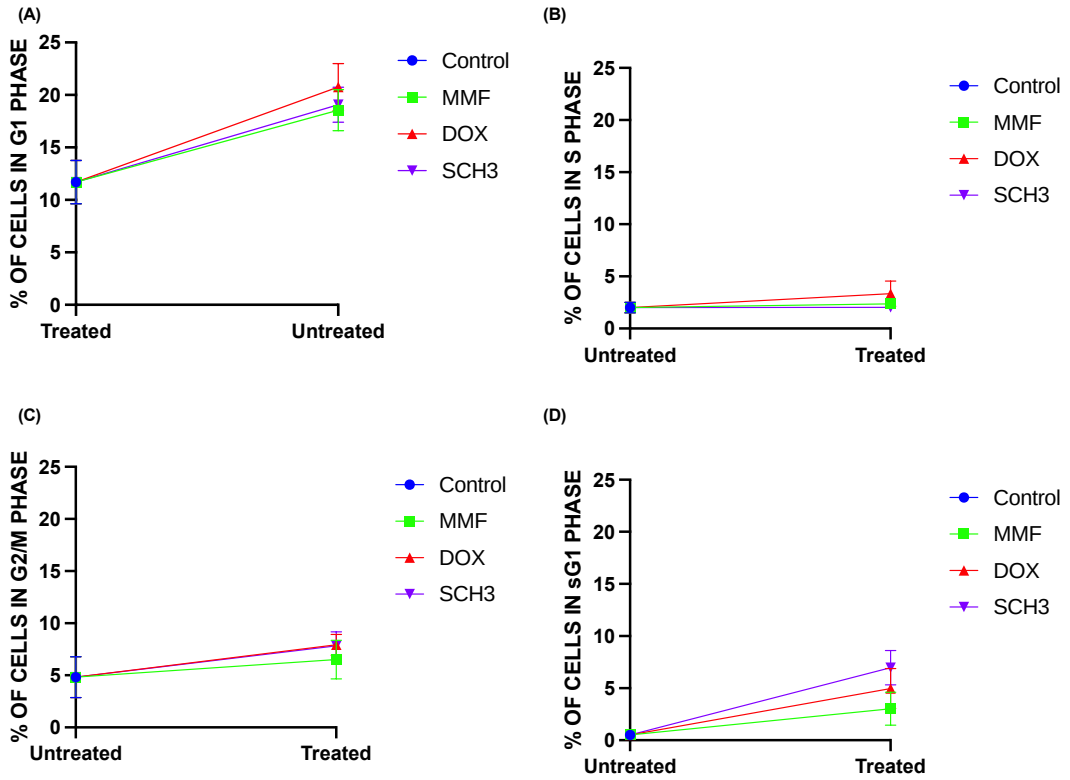

(E)

Bonferroni's multiple comparisons test	G1 - P Value	S – P Value	G2/M – P Value	sG1 – P Value
CONTROL vs. MMF	0.0185	>0.9999	>0.9999	0.4417
CONTROL vs. DOX	0.0033	0.2917	0.2657	0.0402
CONTROL vs. SCH3	0.0120	>0.9999	0.3032	0.0045
MMF vs. DOX	>0.9999	0.7657	>0.9999	0.9295
MMF vs. SCH3	>0.9999	>0.9999	>0.9999	0.0746
DOX vs. SCH3	>0.9999	0.3135	>0.9999	0.8396

Figure 4. 6 Shows the cell cycle distribution of untreated D3 cells and treated D3 cells 0hrs post treatment removal, with M+D SCH3, 0hr post treatment removal.

(MMF 2 μM, DOX 0.2 μM SCH3 – MMF2μM1st+ DOX 0.2 μM 24hours later). The figure above represents the percentage of cells in each phase of the cell cycle, results are an average of three independent experiments were carried out in triplicate, (A) – sG1, (B)- S, (C)- G1and (D)- G2/M. (E) A One-way ANOVA test was utilized to compare the means of the cell cycle phases after treatment cells versus untreated control cells and demonstrated in the above Tables where, *P<0.05, **P<0.01, ***P<0.001 and ****P<0.0001 (applicable for Figures 4.6 – 4.8).

.

Figure 4.6 reported a statistically significant increase in the percentage of cells in G1 phase of the cell cycle when cells were treated with MMF alone, DOX alone and SCH3 compared with the untreated control (MMF P=0.0185, DOX P=0.0033, SCH3 P-0.0120, Figure 4.6E). There were no statistically significant changes in the percentage of cells in S phase or G2/M of the cell cycle 0hrs post treatment removal when cells were incubated with any of the treatments compared to the untreated control or any other treatment group. There was a statistically significant increase in the percentage of cells in sG1 phase of the cell cycle when cells were treated with DOX alone and SCH3 compared to the untreated control (Dox P=0.0402 and SCH3 P=0.0045, Figure 4.6E).

In summary, treatment with a SCH3 combination of MMF + DOX in D3 cells may be inducing cell cycle arrest in G1 and an accumulation of cells in sG1. This may be due to ROS damaging D3 cells and causing a cell cycle blockade preventing the cells from entering the S phase of the cell cycle, as well as DOX and SCH3 inducing apoptosis which is associated with an accumulation of cells in subG1 (Plesca *et al*., 2008), however a more in-depth analysis of apoptosis is required to support this.

Figure 4.7 shows the cell cycle distribution of D3 cells 24 hrs post treatment removal, following treatment with DOX alone, MMF alone and the SCH3 dox combination (MMF1st 2 μM +DOX 0.2 μM) 24 hours after 1st treatment administration).

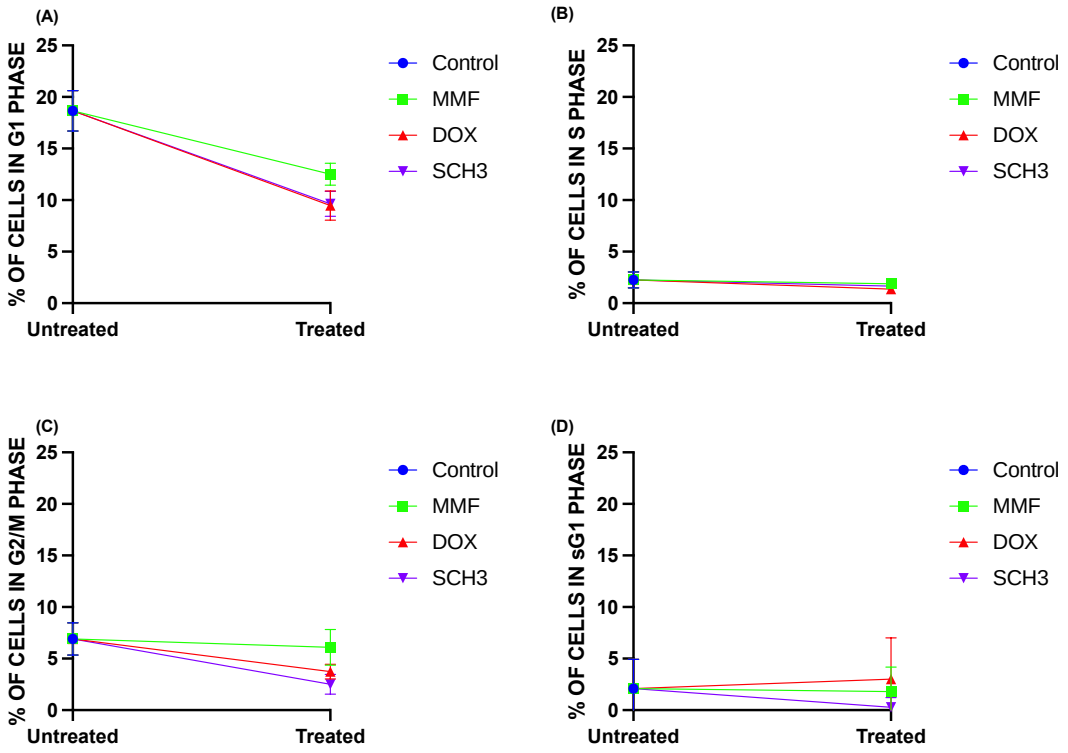

(E)

Bonferroni's multiple comparisons test	G1 - P Value	S – P Value	G2/M – P Value	sG1 – P Value
CONTROL vs. MMF	0.0052	>0.9999	>0.9999	>0.9999
CONTROL vs. DOX	0.0003	0.1659	0.1108	>0.9999
CONTROL vs. SCH3	0.0004	0.6632	0.0210	>0.9999
MMF vs. DOX	0.2011	0.9881	0.3611	>0.9999
MMF vs. SCH3	0.2479	>0.9999	0.0628	>0.9999
DOX vs. SCH3	>0.9999	>0.9999	>0.9999	>0.9999

Figure 4. 7 Shows the cell cycle distribution of untreated D3 cells and treated D3 cells with M+D SCH3, 24 hrs post treatment removal.

Results from Figure 4.7 reported that in contrast to 0hr where the percent of cells in G1 increase at 24 hrs, there was a statistically significant decrease in the percentage of cells in G1 phase of the cell cycle when D3 cells were treated with all treatments (MMF P=0.0052, Dox P=0.0003, SCH3 P=0.0004, Figure 4,7E). There were again no statistically significant changes in the percentage of cells in the S phase of the cell cycle 24hrs after treatment removal when comparing any treatment group to each other (Figure 4.7B and E). However, there was a statistically significant decrease in

the percentage of cells in G2/M phase of the cell cycle following treatment with SCH3 compared to the untreated control cells (P=0.0210, Figure 4.7E). This was the only statistically significant change in the percentage of cells in the G2/M phase of the cell cycle 24hrs post treatment removal. There were no statistically significant changes in the percentage of cells in sG1 phase of the cell cycle when comparing any treated or untreated group to each other (Figure 4.7D or E).

In summary, SCH3 treatment of D3 cells 24 hrs post treatment removal may be inducing a blockade at G1 and G2/M, we do see a redistribution of cells in different phases, but it cannot be supported from the findings above that this is exactly what is happening without further experiments into each phase of the cell cycle. The redistribution of cells may depend on what phase the cells were in during treatment (Hill *et al* 2023). An accumulation of cells in G1 was found at 0 hrs post treatment (Figure 4.6), however the percentage of cells in G1 is significantly depleted 24 hrs after treatment removal (Figure 4.7) and there is no significant increase in SCH3 treated cells in any other phase of the cell cycle. Therefore, it may be that these SCH3 treated cells have been damaged by ROS and are unable to enter the cell division cycle.

Figure 4.8 shows the cell cycle distribution of D3 cells treated with Dox alone, MMF alone and the SCH3 dox combination (MMF1st 2 μM +DOX 0.2 μM) 24 hours after 1st therapy administration) 48 hours post treatment removal.

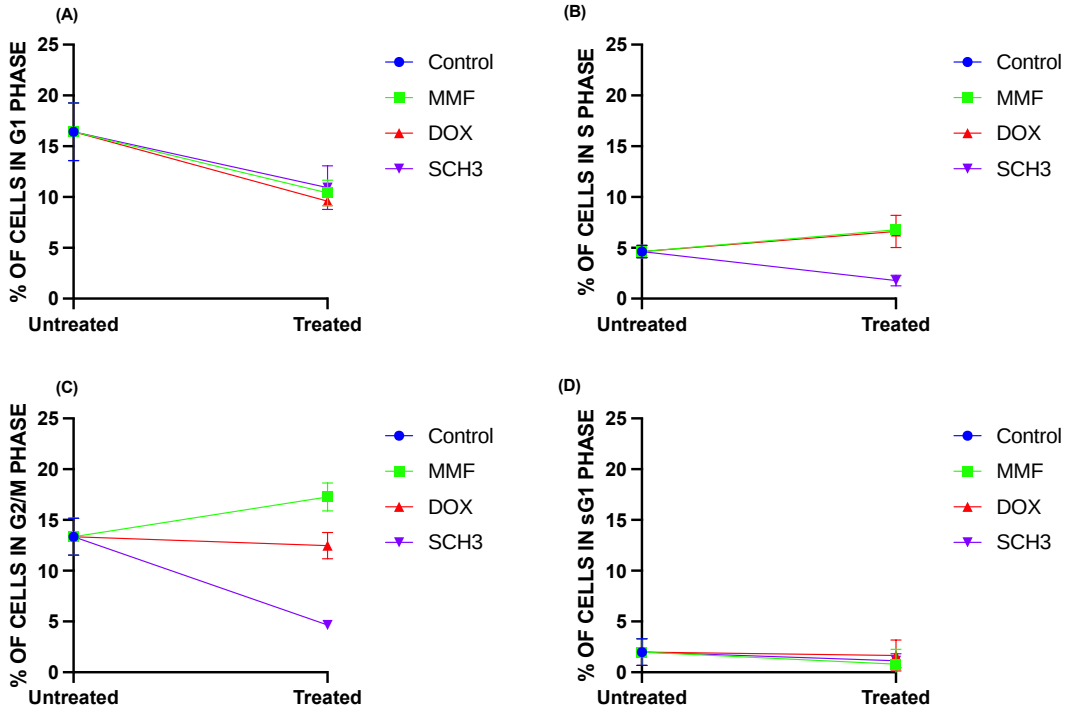

(E)

Bonferroni's multiple comparisons test	G1 - P Value	S – P Value	G2/M – P Value	sG1 – P Value
CONTROL vs. MMF	0.0273	0.1158	0.0382	>0.9999
CONTROL vs. DOX	0.0135	0.1646	>0.9999	>0.9999
CONTROL vs. SCH3	0.0443	0.0267	0.0002	>0.9999
MMF vs. DOX	>0.9999	>0.9999	0.0125	>0.9999
MMF vs. SCH3	>0.9999	0.0008	<0.0001	>0.9999
DOX vs. SCH3	>0.9999	0.0010	0.0005	>0.9999

Figure 4. 8 Shows the cell cycle distribution of untreated D3 cells and treated D3 cells, M+D SCH3, 48 hrs post treatment removal.

Interestingly as can be seen form Figure 4.8A, at 48 hrs after treatment of D3 cells with schedule 3 we are not seeing a resolution of cell distribution to that of the untreated cells as was seen previously with parental cells (Section 2,42.14). Instead, we observed that there was a statistically significant decrease in the percentage of cells in G1 phase of the cell cycle when treated with MMF, DOX or SCH3 compared with the untreated control (MMF P=0.0273, DOX P=0.0135 and SCH3 P=0.0443, Figure 4.8E). There were no statistically significant changes in the percentage of cells in G1 phase of the cell cycle when comparing any other of the treated groups of cells to each other (Figure 4.8A and E) suggesting all treated cells have similar effects on

the percentage of cells in G1 phase of the cell cycle 48 hrs post treatment removal. There was however a statistically significant increase in the percentage of cells in S phase of the cell cycle when cells were incubated with MMF alone, DOX alone or the untreated control cells when compared to SCH3 treated cells (MMF P=0.0008, DOX P=0.0010 and control P-0.0267, Figure 4.8E) where a large reduction in the percentage of cells in the S phase was observed. There were no other statistically significant changes in the percentage of cells in S phase of the cell cycle when comparing any other treated or untreated group to each other (Figure 4.8E). Similarly there was a statistically significant decrease in the percentage of cells in the G2/M phase of the cell cycle when treated with SCH3 compared with MMF alone, DOX alone and the untreated control (MMF P<0.0001, Dox P=0.0005 and control P=0.0002, Figure 4.8E) suggesting that the combination treatment induces changes in the cell cycle distribution of cells that are completely different to that seen with single treatments. There was a statistically significant increase in the percentage of cells in G2/M phase of the cell cycle when cells were treated with MMF and DOX alone compared to the untreated control cells (control P=0.0382 and DOX P=0.0125, Figure 4.8E). There were no statistically significant changes in the percentage of cells in sG1 phase of the cell cycle when comparing any treated or untreated group of cells (Figure 4.8E).

In summary, 48 hrs following treatment removal, SCH3 treated D3 cells had a significantly reduced percentage of cells in G1, S and G2/M phases of the cell cycle compared to the untreated control and single therapies. This data suggests that this combination alters cell cycle distribution perhaps through induction of cell cycle blocks to try and repair more combination damage. This may be due to ROS damaging the cell following DOX treatment, as MMF has bound to glutathione and ROS are able to induce damage on DNA strands which when accumulated prevents from completing the cell division process as they are too damaged to replicate into identical daughter cells.

4.4.5 Apoptosis/Necrosis quantification of Doxorubicin Resistant MDA-MB-231 cells after combination treatment with Doxorubicin and Monomethyl Fumarate

To investigate the percentage of doxorubicin resistant cells that undergo apoptosis following treatment with MMF, Doxorubicin or combination SCH3 MMF +DOX an Annexin V apoptotic detection assay was caried out (as described in section 4.3.5). D3 cells were treated for 48 hours (cells doubling time) with either DOX 0.2 μM alone, MMF 2 μM alone or the schedule 3 combination of MMF 2μM 1st + DOX 0.2 μM 24 hours later. After the 48-hr treatment, cells were harvested at different time points. For 0 hr, immediately following treatment removal, for 24 hr and 48 hr time points, cells were covered in fresh treatment free DMEM media until time of harvest (Ochs and Kaina, 2000).

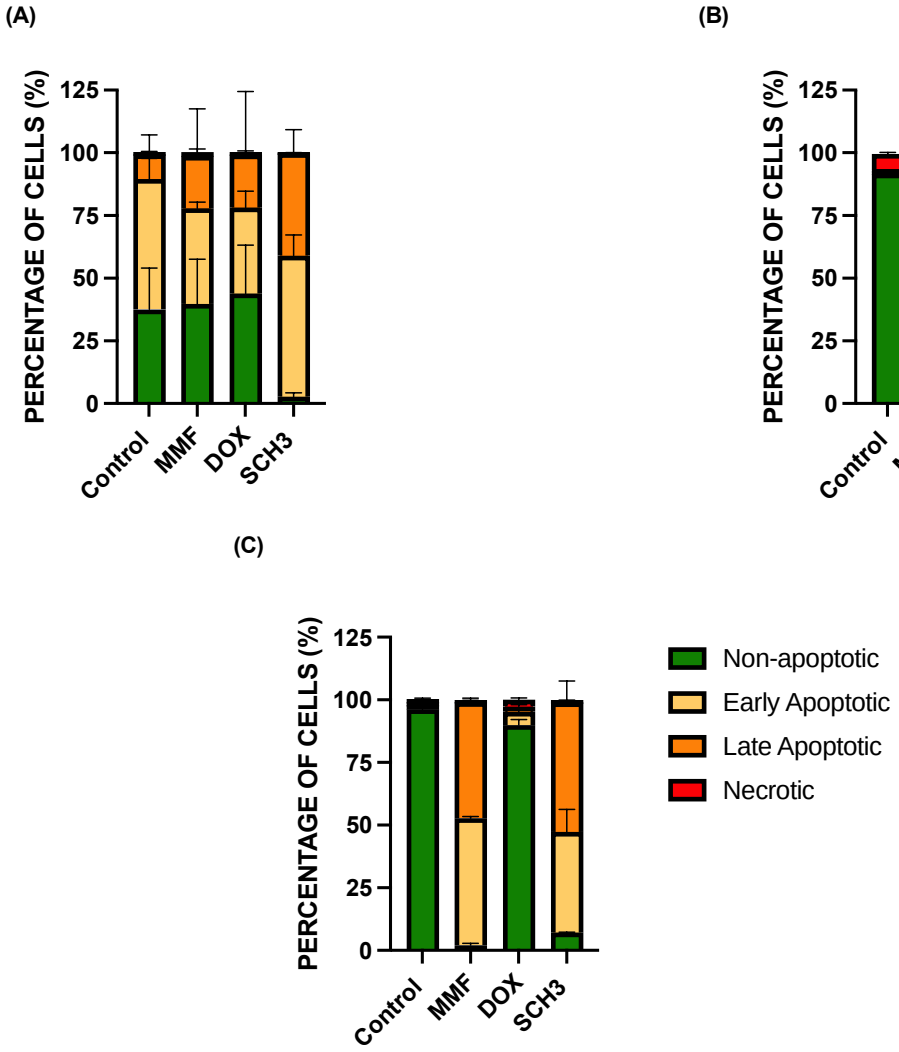

Figure 4. 9 The effect of DOX 0.2 μM, MMF 2 μM and SCH3 M1st 2 μM + D 0.2 μM on the different phases of apoptosis in D3 cells are shown.
Three different time points were used post treatment removal; (A) 0hr, (B) 24hr and (C) 48hr. Data is expressed as mean+/- SD of 3 individual experiments performed in triplicate at each time point, statistical Analysis was carried out using two-way ANOVA followed by Bonferroni's multiple comparison testing comparing each apoptotic phase separately between all each apoptotic phase separately between all treatments (see appendix 5).

As reported in Figure 4.9 there are differences in the percentage of cells in early apoptosis, late apoptosis, and necrosis, between treatments. At 0 hrs there was a statistically significant difference in the percentage of non-apoptotic cells observed when comparing with control cells, MMF treated cells and DOX treated cells with SCH3 (control P=0.0155, MMF P=0.0093 and DOX P=0.0036) with only SCH3 having

a lower percentage of viable cells than any other treatment group (P=0.0155). The only other statistically significant changes in percentage of apoptotic cells were found when comparing the percentage of cells in late apoptosis. There was a statistically significant increase in the percentage of cells in late apoptosis after treatment with SCH3 compared with the control cells (P=0.0375), this suggests that the combination even at this early time point is having a profound effect on cell viability that is greater than each individual component.

Figure 4.9B reports the percentage of cells in each phase of apoptosis 24 hrs post treatment removal. There was a statistically significant decrease in the percentage of non-apoptotic cells compared with the control when treated with MMF (P<0.0001), DOX (P<0.0001) and SCH3 (P<0.0001). There was also a statistically significant decrease in the percentage of non-apoptotic cells when treated with SCH3 compared with MMF alone (P<0.0001) and DOX alone (P=0.0003). When reviewing the percentage of cells in early apoptosis there was a statistically significant increase in the percentage of cells in early apoptosis compared with the untreated control, when treated with DOX only (P=0.0165) and SCH3 (P=0.0286). There were also a statistically significant differences in the percentage of cells in late apoptosis (Figure 4.9B). There was also a statistically significant increase in the percentage of cells in late apoptosis when treated with MMF (P=<0.0001), DOX (P<0.0001) and SCH3 (P<0.0001) when compare with the control cells. There was also as statistically significant increase in the percentage of late apoptotic cells when treated with SCH3 compared with MMF alone (P<0.0001) and DOX alone (P<0.0001). Therefore, at 24 hrs there was a large reduction in cell viability for all treatments verses the control, this was not surprising concentrations of drugs were chosen to kill a small percent of D3 cells. However again much greater in combination better than individuals so schedule killing these resistant cells more effectively than the individual therapies alone.

From Figure 4.9C the percentage of cells in each phase of apoptosis was reported 48 hrs post treatment removal. There was a statistically significant decrease in the percentage of non-apoptotic cells when treated with MMF (P<0.0001) and SCH3 (P<0.0001) when compared with the control cells. There was also a statistically significant decrease in the percentage of non-apoptotic cells when treated with SCH3 when compared with DOX alone (P<0.0001). When reviewing early apoptotic cells, it

was found that there was a statistically significant increase in the percentage of cells in early apoptosis when treated with MMF ($P<0.0001$) and SCH3 ($P<0.0001$) when compared with the control. There was also a statistically significant increase in the percentage of cells in early apoptosis when treated with SCH3 compared with DOX only ($P<0.0001$). Furthermore, there was a statistically significant increase in the percentage of cells in late apoptosis when comparing MMF only ($P<0.0001$) and SCH3 ($P<0.0001$) to the control. There was also a statistically significant increase in the percentage of late apoptotic cells when treated with SCH3 combination and DOX only treated cells ($P<0.0001$).

In summary Figure 4.9 reports a significant increase in apoptosis in D3 cells treated with SCH3 (DOX + MMF). This significant increase in apoptotic cells following SCH3 treatment is maintained up to 48 hrs post treatment. These results are supportive of Figure 4.8, that showed a significant decrease in the percentage of SCH3 treated cells in G1, S and G2/M phases of the cell cycle. As apoptosis can occur at any point in the cell cycle, it may be that SCH3 treated cells are becoming apoptotic and unable to enter or are removed from the cell cycle. These results support the hypothesis that MMF administered prior to DOX treatment in doxorubicin resistant cells can enhance the percentage of cells that killed compared to the single therapies alone.

4.4.6 Analysis of Glutathione levels in Doxorubicin resistant MDA-MB-231 cells after combination treatment with Doxorubicin and Monomethyl Fumarate

To investigate the effects monomethyl fumarate has on the glutathione (GSH) levels in D3 cells, a Glutathione assay was carried out, as described in Section 4.3.6. This analysis was also carried out on parent MDA-MB-231 cells in section 2.42.17.

GSH levels were assessed at 1 hour post treatment administration (for combination 1 hr after second therapy administered), immediately after the treatment was complete (48 hr incubation) 0 hr, 24 hrs after the treatments were removed and 48 hours after the treatment were removed. Results are shown in Figure 4.10

(A)

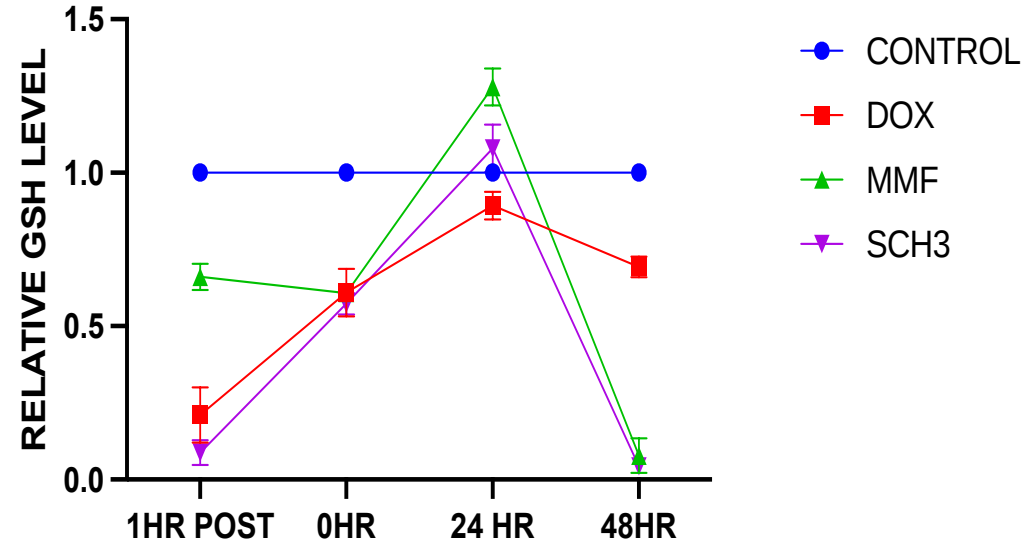

(B)

Bonferroni's multiple comparisons test	P Value 1 HR post	P Value 0HR	P Value 24HR	P Value 48HR
CONTROL vs. DOX	<0.0001	<0.0001	0.2548	<0.0001
CONTROL vs. MMF	0.0003	<0.0001	0.0014	<0.0001
CONTROL vs. SCH3	<0.0001	<0.0001	0.6619	<0.0001
DOX vs. MMF	<0.0001	>0.9999	0.0001	<0.0001
DOX vs. SCH3	0.1365	>0.9999	0.0178	<0.0001
MMF vs. SCH3	<0.0001	>0.9999	0.0115	>0.9999

Figure 4. 10 The effect single therapies DOX 0.2 μM and MMF 2 μM, and combination therapy SCH3 MMF 2 μM 1st + DOX 0.2 μM 24 hours later.
Data reported is an average of three independent experiments performed in triplicate. (B) A one-way ANOVA with Bonferroni multiple comparison testing was performed using GraphPad prism 9.2.1 comparing each treated and untreated group to each other, *P<0.05, **P<0.01, ***P<0.001 and ****P<0.0001.

From Figure 4.10, there was a statistically significant reduction in relative GSH levels in DOX, MMF and SCH3 treated D3 cells, compared with the control 1hr post treatment administration (DOX P<0.0001, MMF P=0.0003 and SCH3 P<0.0001, Figure 4.10B). DOX alone and SCH3 treated D3 cells also had a statistically significant decrease in when compared to MMF alone treated cells (both P<0.0001, Figure 4.10B). 0 hrs post treatment removal, DOX and SCH3 treated D3 cells had a statistically significant reduction in relative GSH levels, compared with the control (all P value <0.0001, Figure 4.10B). 24 hrs post treatment there was also a statistically

significant increase in the relative GSH levels of D3 cells when treated with MMF compared to the untreated control, DOX and SHC3 (control P=0.0014, DOX P=0.0003 and SCH3 P=0.0115, Figure 4.10B). There was also a statistically significant increase in relative GSH levels when cells were treated with SCH3 compared to DOX alone treated D3 cells (PP=0.0178, Figure 4.10B). 48 hrs post treatment there was statistically significantly reduced relative GSH level when D3 cells were treated with DOX, MMF and SCH3 when compared to the untreated control cells (all P value of <0.0001, Figure 4.10B). MMF and SCH3 treated D3 cells also reported a statistically significantly reduced relative GSH level when compared to DOX alone (both P values of <0.0001, Figure 4.10B).

In summary, the findings of Figure 4.10 support the hypothesis that SCH3 treatment of doxorubicin resistant D3 cells, caused a significant reduction in the levels of intracellular glutathione. The data show that relative GSH levels in D3 cells are significantly lower than control and DOX alone treated D3 cells, 48 hrs after treatments are removed. Although an increase in relative GSH is reported 24 hrs post treatment removal, the synthesis of GSH is not able to be maintained by SCH3 treated cells. These results also support the findings of Figure 4.9 that report a significant increase in apoptotic cells following D3 treatment up to 48 hrs post treatment. It may be that as GSH levels are not able to be maintained, ROS is left unchecked and able to induce SSB and DSB that when accumulated 48 hrs post treatment removal has induce apoptosis of D3 cells significantly more than control D3 cells or DOX alone treated D3 cells.

4.4.7 Detection of Autophagic Doxorubicin resistant cells after combination treatment with Doxorubicin and Monomethyl Fumarate

To investigate the percentage of cells that have died via autophagy because of treatment, an Autophagy assay was carried out as it was previously detailed that in the literature that when some cells become resistant, they can start to induce autophagy (Ho and Gorski, 2019). Doxorubicin resistant cells were treated with DOX alone 0.2μM, MMF alone 2μM and the SCH3 combination of MMF1st+DOX.This assay was carried out in triplicate at 3 different time points to co-inside with the Cell Cycle analysis data (Section 4.42.4), results are detailed in Figure 4.11.

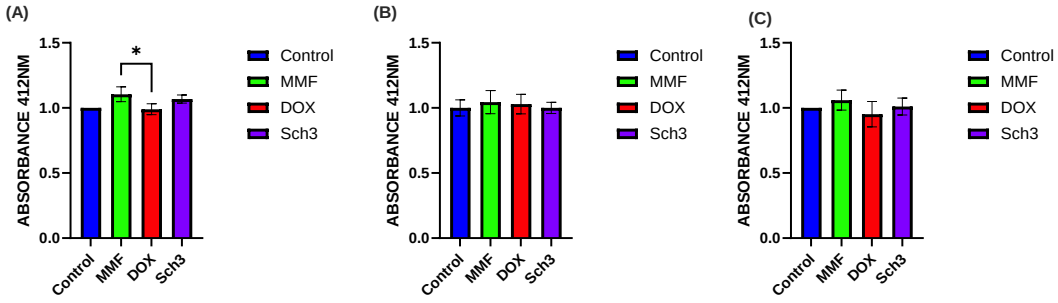

Figure 4. 11 The effect of; DOX alone 0.02μM, MMF alone 2μM or Schedule 3 combination MMF1st 2μM+ Dox 0.2μM 24 hours later, on Green Detection Reagent. Data is expressed relative to the control. Cells were measure on a fluorescent microplate reader at 412nm. (A) 0 hours after treatment removed. (B) 24 hours after treatment removed. (C) 48 hours after treatment removed. All graphs are displayed as mean and standard deviation of 3 individual experiments carried put in triplicate. One -way ANVOA was carried out with Bonferroni's correction.

From Figure 4.11A the only statistically significant changes in absorbance measurements were found when comparing MMF alone and DOX alone. There was a statistically significant increase in absorbance reading of MMF only treated cells compared with DOX only treated cells (P=0.0390). This suggests that in D3 cells treated with MMF there was a slight increase in autophagic vesicles 0 hrs post treatment removal. There were no statistically significant changes in absorbance readings of cells in Figure 4.12B, measured 24 hours or 48 hrs post treatment removal. This would suggest that autophagy was not significantly induced or inhibited by any treatment tested over a 48-hr window.

Overall, this data suggests that D3cells are not undergoing autophagy when treated with DOX alone, MMF alone or DOX + MMF SCH3 combination.

4.4.8 Quantification of DNA damage and repair using Comet Assay, of Doxorubicin resistant cells after combination treatment with Doxorubicin and Monomethyl Fumarate

To investigate the effects MMF, DOX and the SCH3 combination of M+D have on D3 cells DNA damage, single cell gel electrophoresis or Comet assay was carried out as described seen in Section 2.4.12.

- Comparison of DMA fragmentation at 0hr, 24hr and 48hr – Analysis of DNA repair

D3 cells were treated as described in section 4.42.81. As D3 cells were analysed following treatment at 3 different time points, DNA damage and repair was able to be analysed. Figure 4.13 describes the median tail moment (AU) as a percentage of the untreated control at 0hrs post treatment, 24hrs post treatment and 48hrs post treatment.

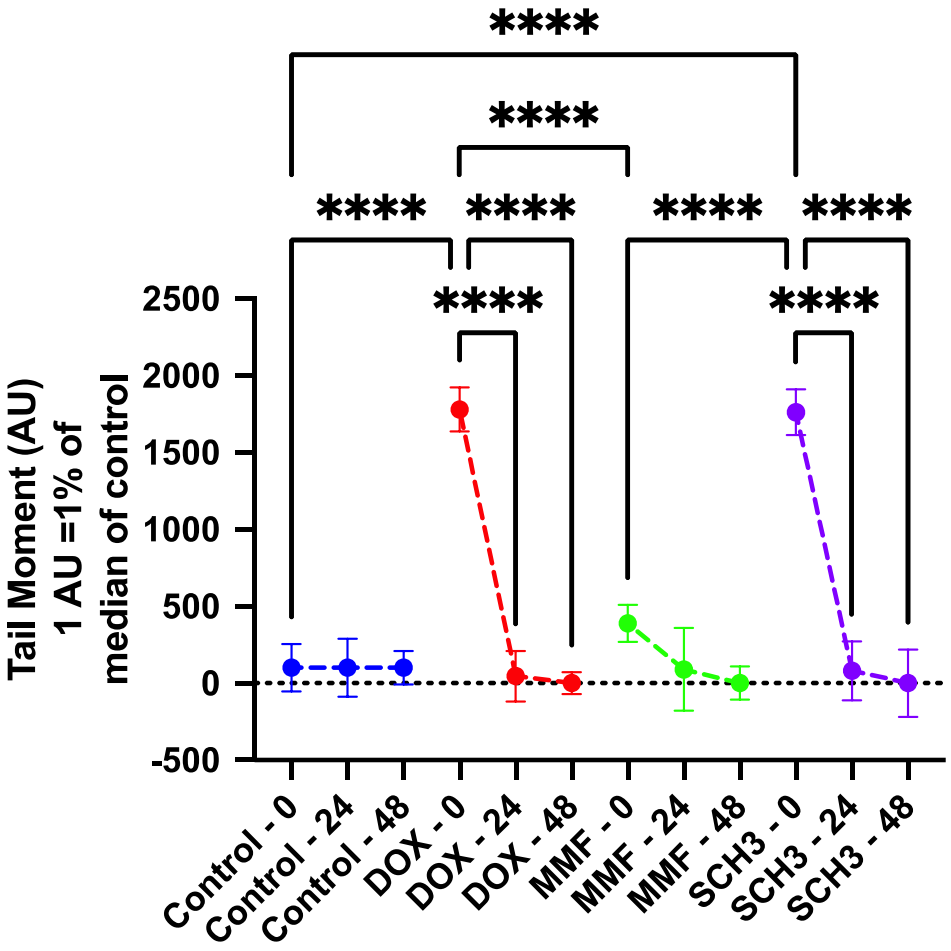

Figure 4. 12 The median DNA damage quantified as Tail Moment (AU) is displayed as a percentage of the control median.

DOX alone, MMF alone and combination SCH3M+D (DOX 0.2 μM, MMF 2 μM), were the treatments used as described in Figure 2.18. 3 time points of 0hr post treatment, 24hrs post treatment and 48hrs post treatment are compared for each treatment, each experiment was caried out in triplicate and a total of 70 comets per experiment. Statistical analysis was carried out using a one-way ANOVA with Bonferroni's correction and are detailed in table 3. P>0.0001 ****, P>0.001 ***, P>0.01** and P>0.1 *, (see appendix 6)

Results from Figure 4.13 suggest that there is a statistically significant increase in the median tail moment 0 hrs post treatment removal of D3 cells treated with DOX alone and SCh3 compared to the untreated control (all <0.0001). There were no statistically significant changes in any treated D3 cells median tail moments compared to the

untreated control cells at 24 hr or 48hr post treatment. All treated cells showed a statistically significant decrease in median tail moments at 24- and 48-hours post treatments compared to their relevant 0 hrs post treatment median tail moment value. suggesting that damage has been repaired or that damaged cells have expired and are no longer in the assay. There was no statistically significant change in the median tail moments of any treated cell when comparing each treatment 24 hr post treatment median tail moment to that treatment groups 48 hr median tail moment.

This data supports the hypothesis that SCH3 treatment can induce more DNA damage than DOX alone treatment in doxorubicin resistant cells. It does appear that the DNA damage induced begins to repair 24 hrs and 48 hrs post treatment removal when comparing all treated groups to each other and the control cells. These results are surprising as results from Annexin V suggested that significant DNA damage would be present in SCH3 treated cells 48 hrs post treatment. The lack of tail moments, however, may be explained by the presence of hedgehog comets, which can occur when DNA is incredibly fragmented in processes such as apoptosis, it has been reported in the literature that comet analysis is not the most effective assay at determining DNA damage caused by apoptosis (Lorenzo *et al*., 2013).

4.4.9 Cytotoxicity of Combination therapy Radiotherapy and Dimethyl Fumarate on Radiotherapy resistant cells

- 2D Cell Culture

Radiation resistant cells were developed as described in Section 4.1. MDA-MB-231 cells were exposed to 2 Gy radiation, and the surviving colonies were harvested. Some cells were frozen down, and the rest were re dosed with 2 Gy radiation and the process repeated until 3 rounds of treatment were undergone. These cells were then all tested using a clonogenic assay to determine the cytotoxicity of various doses of radiation as seen in Figure 4.14.

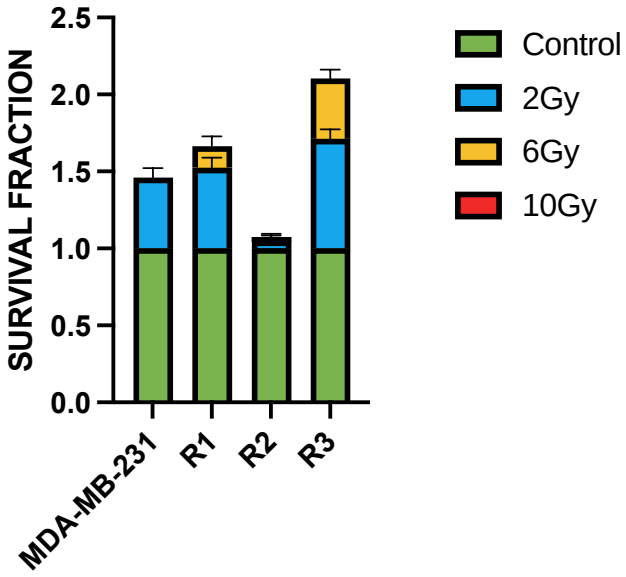

Figure 4. 13 Results of clonogenic assay on resistance test for radiation exposed cells.

MDA-MB-231 cells that had undergone 3 rounds of radiation exposure, cells were tested for toxicity using clonogenic assays. Radiation 2 Gy, 6 Gy and 10 Gy were used to test this. Results are displayed as an average of 3 independent experiments carried out in triplicate and graphed using GraphPad Prism Version 9.2.1.

Figure 4.13 suggests that MDA-MB-231 cells only showed survival at 2 Gy dose of radiation, in all other doses tested 100% clonogenic cell death was observed. R3

showed the highest survival fraction of cells exposed to both 2 Gy radiation and 6 Gy radiation (0.61 SD+/-0.288 and 0.39 SD+/- 0.18 respectively). Given that survival was seen in R3 cells at 6 Gy radiation and parental cells showed 100% cell death at this administered dose this data suggested that R3 had developed a level of resistance to radiation so the R3 cell line was used to investigate potential combination therapies to overcome radiotherapy resistance found in TNBC patients.

To determine the ability of fumaric acids DMF and MMF to re-sensitise radiation resistant cells to cells death via irradiation, clonogenic assays were carried out.

Based on the results of Chapter 2 section 2.4.6, Radiation administered in a SCH1 (simultaneous) and SCH3 (radiation after DMF) combination with DMF, demonstrated a statistically significant reduction in survival fraction of MDA-MB-231 cells, when compared to the untreated control (P=0.0039 SCH1 and P=0.0066 SCH3). Therefore, to assess if DMF given in combination with radiation using scheduled administration decreased the survival fraction of radiation resistant cells, a clonogenic assay was carried out using DMF 100 μM in scheduled combinations, SCH1 (simultaneous) SCH2 (radiation before DMF), and SCH3 (radiation after DMF) with radiation at 2 Gy and results are detailed in Figure 4.14.

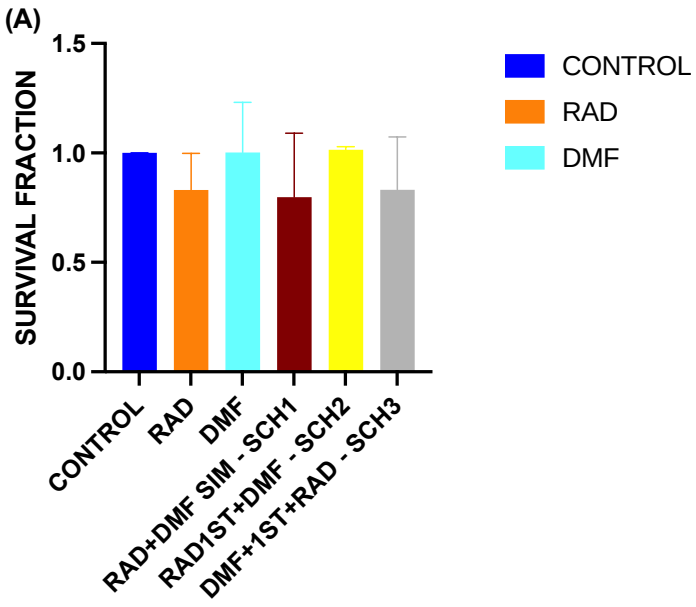

Figure 4. 14 A comparison between the survival fraction of RAD 2 Gy, DMF 100 μM and the combination of three schedules of administration on R3 cells.
Data shown is the average of three independent experiments carried out in triplicate +/- SD. (B) 1-way ANOVA with Bonferroni correction was performed using GraphPad Prism 9.2.1 software.

Results from Figure 4.14 suggests that there were no statistically significant changes in the survival fraction of radiation resistant (R3) cells when treated with 2 Gy radiation, 100 μM DMF or any of the combination therapies; SCH1 (simultaneous), SCH2 (radiation before DMF) or SCH3 (radiation after DMF) when compared to the untreated control or when comparing any other treated group to each other.

This data therefore suggests that DMF is not a suitable drug to be administered in combination with radiation to re-sensitise radiation resistant cells to cell death via irradiation. These results do not support the findings in Chapter 2 Section 2.4.6 where the clonogenic data supported the use of DMF in combination with radiation would statistically significantly decrease the survival fraction of MDA-MB-231 cells. It is clear from Figure 4.14 that these results are not translated over when investigating these combinations using R3 cells. It was decided based upon these findings in Figure 4.14 that DMF would not be carried forward into mechanistic or 3D spheroid investigation.

MMF was also investigated for its potential to re sensitise R3 cells to death via irradiation due to the findings of Chapter 2 Section 2.4.6. It was found that MMF administered in combination with irradiation at all 3 scheduled combinations produced a statistically significant reduction in survival fraction of MDA-MB-231 cells when compared to the untreated control. Therefore, it was decided that MMF administered in combination with radiation may have to potential to re-sensitise radiation resistant R3 cells to cell death. MMF at 2 μM and radiation at a dose of 2 Gy were used in scheduled combinations SCH1 (simultaneous) SCH2 (radiation before MMF), and SCH3 (radiation after MMF) and results are detailed in Figure 4.15.

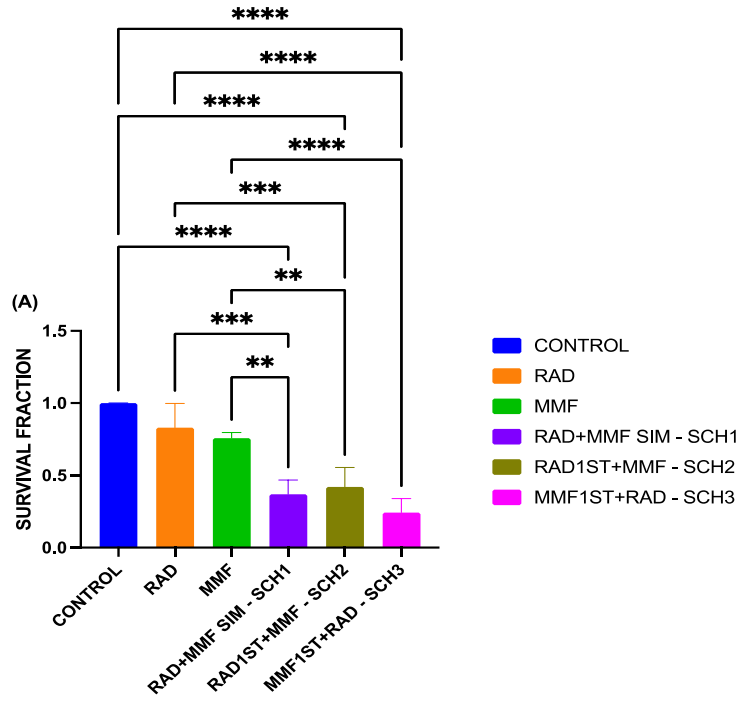

(B)

Bonferroni's multiple comparisons test	Summary	Adjusted P Value
CONTROL vs. SCH1	****	<0.0001
CONTROL vs. SCH2	****	<0.0001
CONTROL vs. SCH3	****	<0.0001
RAD vs. SCH1	***	0.0004
RAD vs. SCH2	***	0.0005
RAD vs. SCH3	****	<0.0001
MMF vs. SCH1	**	0.0030
MMF vs. SCH2	**	0.0039
MMF vs. SCH3	****	<0.0001

Figure 4. 15 This is a comparison between the survival fraction of RAD 2 Gy, MMF 2 μM and the combination of three schedules of administration on R3 cells.
Data shown is the average of three independent experiments carried out in triplicate +/- SD. (B) 1-way ANOVA with Bonferroni correction was performed using GraphPad Prism 9.2.1 software, with p-values of <0.005 = *, <0.001= **, <0.0001= ***, <0.00001=**** reported as significant when compared with the control with all results compares to the control and each other.

It was observed in Figure 4.15 that SCH1, SCH2 and SCH3 all produced statistically significant decreased in R3 cell survival when compared with the untreated control (all P<0.0001, Figure 4.16B). SCH1, SCH2 and SCH3 scheduled combinations also produced a statistically significant decrease in the survival fraction of R3 cells when

compared with radiation alone treated cells (SCH1 P=0.0004, SCH2 P=0.0005 and SCH3 P<0.0001, Figure 4.15B). Furthermore, SCH1, SCH2 and SCH3 scheduled combinations produced a statistically significant decrease in survival fraction of R3 cells when compared with MMF alone (SCH1 P=0.0030, SCH2 P=0.0039 and SCH3 P<0.0001, Figure 4.15B). There was however no statistically significant change in the survival fraction of R3 cells when comparing any of the combination therapies to each other (Figure 4.15B).

These results therefore support the findings in Chapter 2 Section 2.4.6 as MMF administered in all 3 scheduled combinations also produced a statistically significant reduction in radiation resistant cells as was seen in chapter 2 using MDA-MB-231 cells. As all three scheduled combinations also decrease the survival fractions of R3 cells significantly more that the single therapies, MMF and radiation alone, it was decided that all three of these scheduled combinations would be investigated using 3D spheroid model.

4.4.10 Assessment of combination of Radiation and MMF In 3D spheroid models of therapy resistant cells

Given the data in Section 4.43.1, MMF was the fumaric acid chosen to be investigated in combination with radiation using all three scheduled combination therapies. Using this 3D spheroid model for reasons described above in Chapter 1 Section 1.13. Radiation at a dose of 2 Gy, MMF 2 μM and combinations using these doses were administered in scheduled combinations; SCH1 (simultaneous), SCH2 (radiation before MMF) and SCH3 (radiation after MMF), results are detailed in Figure 4.16.

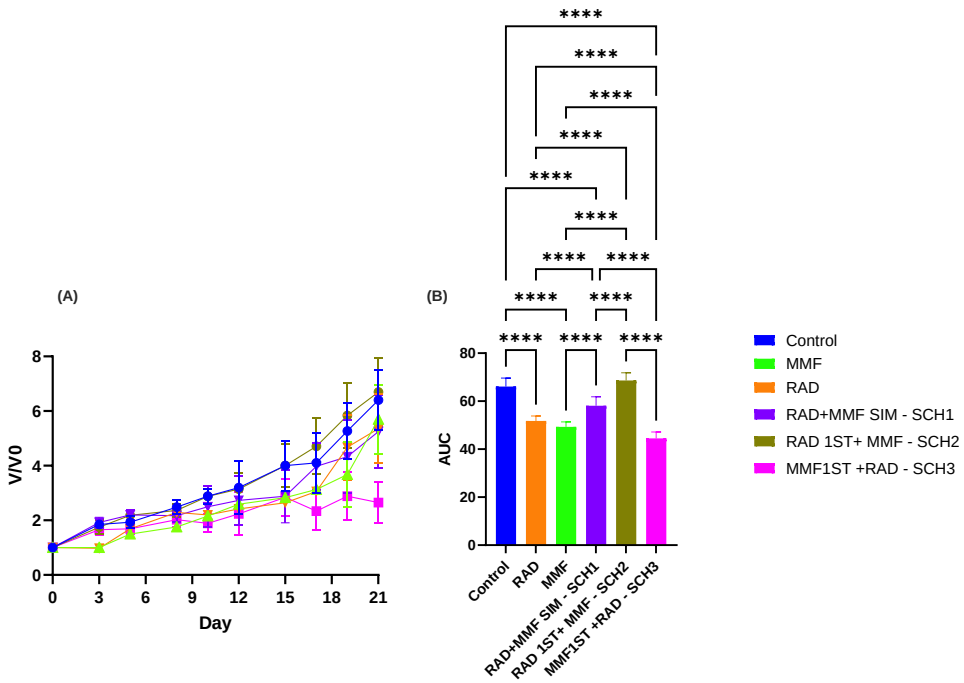

(C)

Bonferroni's multiple comparison test	V/V0 Summary	Adjusted P Value	AUC Summary	Adjusted P Value
Control vs. RAD	ns	>0.9999	****	<0.0001
Control vs. MMF	ns	>0.9999	****	<0.0001
Control vs. SCH1	ns	>0.9999	****	<0.0001
Control vs. SCH2	ns	>0.9999	ns	0.0512
Control vs. SCH3	ns	0.9953	****	<0.0001
RAD vs. MMF	ns	>0.9999	ns	0.0704
RAD vs. SCH1	ns	>0.9999	****	<0.0001
RAD vs. SCH2	ns	>0.9999	****	<0.0001
RAD vs. SCH3	ns	>0.9999	****	<0.0001
MMF vs. SCH1	ns	>0.9999	****	<0.0001
MMF vs. SCH2	ns	>0.9999	****	<0.0001
MMF vs. SCH3	ns	>0.9999	****	<0.0001
SCH1 vs. SCH2	ns	>0.9999	****	<0.0001
SCH1 vs. SCH3	ns	>0.9999	****	<0.0001
SCH2 vs. SCH3	ns	0.6079	****	<0.0001

Figure 4. 16 The effect of RAD and MMF in schedule 1,2 and 3 combinations on the growth of D3 spheroids.

(A) R3 spheroids were incubated with drugs continually for 21 days and images every 2-4 days. Spheroid volumes were calculated and the average fold increase from initial V/V0 +/- S.D, is presented on a linear scale, (B)The area under the curve (AUC) +/- S.D. was also calculated using one-way ANOVA analysis with Bonferroni's testing for multiple comparisons, results displayed in (C). Results are reported as an average of three independent experiments carried out using 36 spheroids per treatment, statistical analysis was carried out on the data using GraphPad prism 9.2.1, determined by the. P<0.05=*, P<0.01=**, P<0.001=***, P<0.0001=**** when compared with the control.

As suggested in Figure 4.16A with respect to V/V_0, there was no statistically significant results when comparing the change in volume of any spheroid group over time, as previously seen in section 4.4.2 (Figure 4.16A and C). There were however statistical differences when reviewing the AUC of these values as seen in Figure 4.16B. Radiation alone, MMF alone, SCH1 and SCH3 all produced statistically significantly decreased AUC values when compared to the untreated control AUC value (all $P<0.0001$, Figure 4.16B). There were however no statistically significant changes in AUC values when comparing SCH2 to the untreated control. SCH3 was the only treated group to produce a statistically significant decrease in the AUC value when compared to radiation alone and MMF alone (both $P<0.0001$, Figure 4.16B). SCH3 also produced a statistically significant reduction in AUC values when compared to SCH1 and SCH3 (both $P<0.0001$, Figure 4.16B). SCH1 and SCH3 both produced a statistically significant increase in AUC values when compared to radiation alone and MMF alone (all, $P>0.9999$, Figure 4.16B).

These results therefore support the hypothesis that MMF administered prior to irradiation can increase cell death. This may be due to MMF binding to glutathione which prevents the neutralisation of ROS induced by radiation therapy, it may also be caused by the inhibition of nuclear NRF2 translation preventing the synthesis of antioxidants such as glutathione. As such, the mechanisms underpinning the observed toxicity will be investigated as described in section 4.4.11- 4.4.16.

4.4.11 Combination Index analysis of Combination therapy Radiotherapy and Dimethyl Fumarate on Radiotherapy Resistant cells

As detailed in sections 4.42.13 combination index analysis was carried out on R3 cells to determine if any of the 3 scheduled combination therapies produced synergistic, additive, or antagonistic results, detailed in Figure 4.17.

(A)

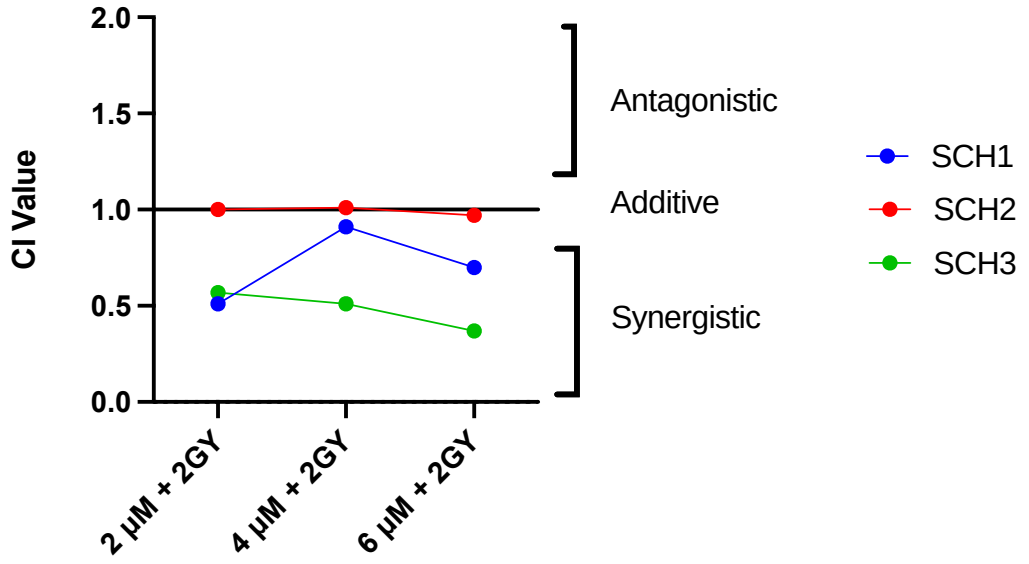

(B)

Drug Concentrations	Combination Index Values		
	SCH1	SCH2	SCH3
MMF 2 µM + RAD 2 GY	0.51	1	0.57
MMF 4 µM + RAD 2 GY	0.91	1.01	0.51
MMF 6 µM +RAD 2 GY	0.7	0.97	0.37

Figure 4. 17 (A) Combination Index (CI) after R3 cells are incubated with RAD and MMF in the 3 treatments Schedules.
Antagonistic <1.1, Additive = 0.9-1.1 and Synergistic > 0.9. Each point represents three independent experiments, N=9. (B) Values of CI plotted in (A).

Results from Figure 4.18 report that SCH1 produced all synergistic CI values at all concentrations tested (0.51, 0.91 and 0.7, Figure 4.14B). SCH2 produced additive CI values at the concentration 2 μM MMF + 2 Gy RAD (1), antagonistic CI value at 4 μM MMF + 2 Gy RAD and synergistic CI value at the highest concentrations tested, 6μM MMF + 2Gy RAD (0.97). SCH3 produced all synergistic CI values (0.57, 0.51) including the lowest CI recorded in Figure 4.18 (0.37) after treatment with 6 μM MMF + 2 Gy Rad.

These results support the use of SCH3 as a combination therapy to treat R3 cells. This combination produced synergistic CI values at all concentrations of therapies tested.

4.4.12 Cell cycle analysis of R3 cells after combination treatment with Radiation and Monomethyl Fumarate

The distribution of radiation resistant R3 cells in each phase of the cell cycle (G1, S, G2/M, sG1) was investigated using a Flow Cytometry assay. Cells following treatment with either single therapies (RAD and MMF) or combination therapy (RAD SCH3) were investigated using this assay to determine any disparities found between treatments. Cells were collected after treatment with single agents or combination therapies as described in section 4.4.1. SCH3 MMF was selected as this combination schedule was the only one that produced a statistically significant reduction in R3 cell survival when compared to the untreated control cells, RAD alone and MMF alone. All concentrations used as the same as those in Figures 4.18-20.

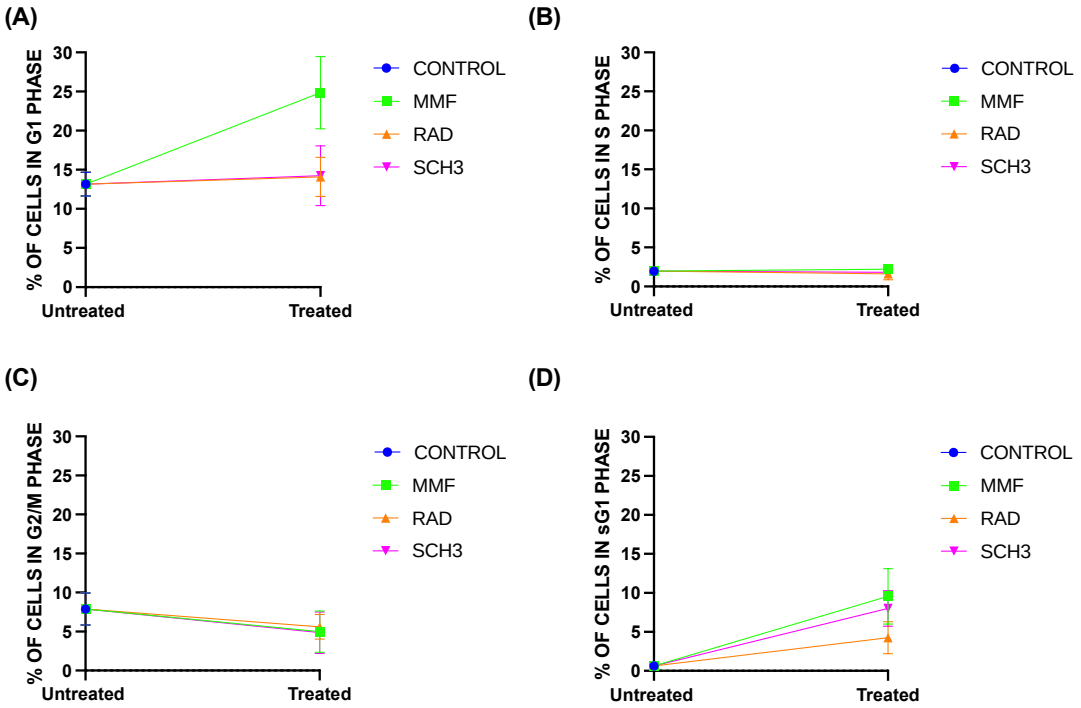

(E)

Bonferroni's multiple comparisons test	G1 P Value	S P Value	G2/M P Value	sG1 P Value
CONTROL vs. MMF	0.0162	>0.9999	0.9637	0.0099
CONTROL vs. RAD	>0.9999	>0.9999	>0.9999	0.5753
CONTROL vs. SCH3	>0.9999	>0.9999	0.8662	0.0299
MMF vs. RAD	0.0258	>0.9999	>0.9999	0.1482
MMF vs. SCH3	0.0278	>0.9999	>0.9999	>0.9999
RAD vs. SCH3	>0.9999	>0.9999	>0.9999	0.5239

Figure 4. 18 The cell cycle distribution of untreated R3 cells and treated R3 cells, M+R SCH3, 0 hrs post treatment removal.

(MMF 2μM, RAD 2 Gy, SCH3 – MMF 2 μM 1st+ Rad 2 Gy 24hours later). The figure above represents the percentage of cells in each phase of the cell cycle, results are displayed as an average of three independent experiments carried out in triplicate. (A) – G1, (B)- S, (C)- G2/M and (D)- sG1. (E) A One-way ANOVA test was utilized to compare the means of the cell cycle phases after treatment cells versus untreated control cells and demonstrated in the above Tables where, *P<0.05, **P<0.01, ***P<0.001 and ****P<0.000.1 (applicable for Figures 4.18 – 4.20).

Figure 4.18 demonstrates the percentages of cells in each phase of the cell cycle 0 hours post treatment removal. Figure 4.18A suggests that there is a statistically significant increase in the percentage of cell in G1 phase of the cell cycle following treatment with MMF compared to the untreated control cells, Rad alone and MMF alone (Control P=0.0162, Rad P=0.0258 and MMF P=0.0278, Figure 4.18E). This was the only statistically significant change in the percentage of cells in G1 phase of the cell cycle 0hrs after treatment removal when comparing any other group to each other. Results from Figure 4.18B show that there was no statistically significant change in the percentage of cells in the S phase of the cell cycle when comparing any of the treated or untreated groups (P>0.9999, Figure 4.18E). Results from Figure 4.18C suggest that there were no statistically significant changes in the percentage of cells in the G2/M phase of the cell cycle when comparing any treated or untreated group to each other. Results from Figure 4.18D show that there was a statistically significant increase in the percentage of cells in sG1 phase of the cell cycle when cells were treated with MMF and Radiation compared with the untreated control (MMF P=0.0099 and Rad P=0.029, Figure 4.18E). This was the only statistically significant change in the percentage of cells in sG1 phase of the cell cycle when comparing any treated or untreated group.

This data therefore suggests that treatment of R3 cells with SCH3 is increasing the percentage of cells in sG1 which might suggest that cells treated with SCH3 combination are unable to undertake cell division immediately following treatment removal and could be an indication of the induction of apoptosis.

Following this, cells were harvested 24hrs after treatment was removed and analysed for cell cycle distribution. Figure 4.19 depicts the percentage of cells found in each phase of the cell cycle after treatment with RAD 2 Gy alone, MMF 2 μM alone and the SCH3 RAD combination (MMF1st 2 μM +RAD 2 Gy 24 hours after 1st therapy administration) 24hrs after treatment was removed.

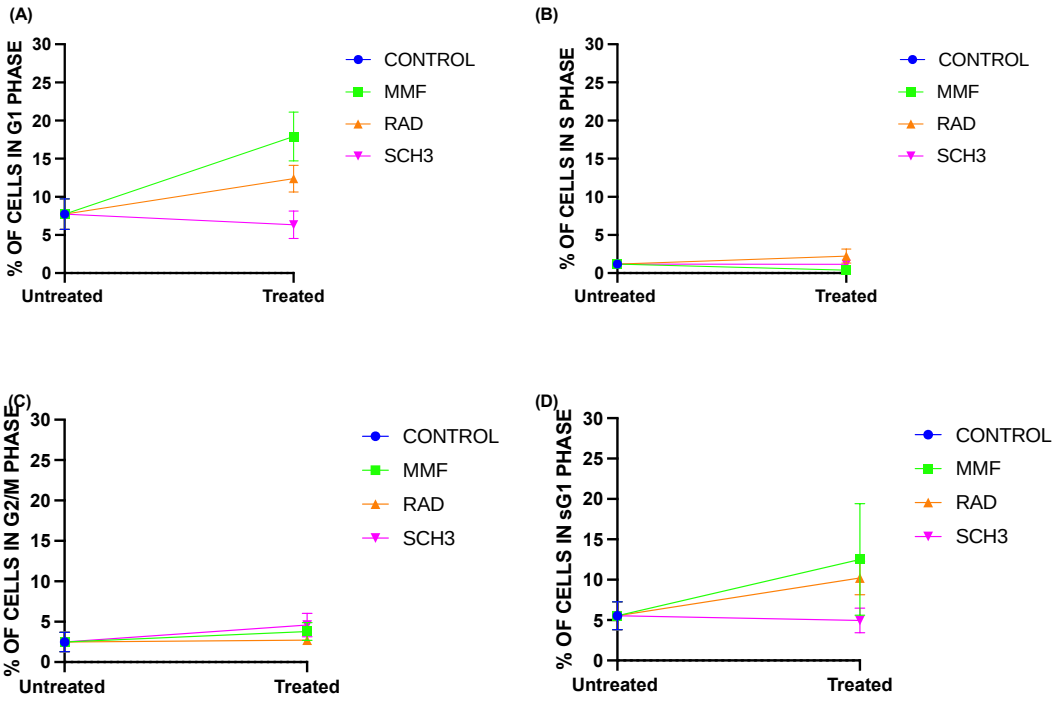

(E)

Bonferroni's multiple comparisons test	G1 P Value	S P Value	G2/M P Value	sG1 P Value
CONTROL vs. MMF	0.0035	0.7883	>0.9999	0.3264
CONTROL vs. RAD	0.2189	0.3378	>0.9999	>0.9999
CONTROL vs. SCH3	>0.9999	>0.9999	0.3021	>0.9999
MMF vs. RAD	0.1047	0.0269	>0.9999	>0.9999
MMF vs. SCH3	0.0015	0.8269	>0.9999	0.2423
RAD vs. SCH3	0.0690	0.3215	0.4336	0.7607

Figure 4. 19 The cell cycle distribution of untreated R3 cells and treated R3 cells, M+R SCH3, 24 hrs post treatment removal.

Figure 4.19A shows that there was a statistically significant increase in the percentage of cells in the G1 phase of the cell cycle when cells were treated with MMF alone compared to the untreated control and SCH3, as expected (MMF alone P=0.0035 and SCH3 P=0.0015. Figure 4.19E). This was the only statistically significant change in the percentage of cells in G1 phase of the cell cycle 24 hours after treatment removal. Figure 4.19B demonstrates that there was a statistically significant increase in the percentage of cells in the S phase of the cell cycle when treated with radiation alone,

compared to MMF alone (P=0.0269, Figure 4.19E). This was the only statistically significant change in the percentage of cells in S phase of the cell cycle when comparing treated or untreated groups (Figure 4.19E). Figure 4.19C and 4.19D both show that there was no statistically significant change in the percentage of cells in G2/M or sG1 phase of the cell cycle when comparing any treated or untreated group.

This data therefore suggests that there is a reduction in the percentage cells treated with SCH3 that can being the cell division cycle 24hrs after treatment removal.

Following this, cells were harvested 48hrs after treatment was removed and analysed for cell cycle distribution. Figure 4.20 depicts the percentage of cells found in each phase of the cell cycle after treatment with RAD 2 Gy alone, MMF 2 μM alone and the SCH3 RAD combination (MMF1st 2 μM +RAD 2 Gy 24 hours after 1st therapy administration) 48hrs after treatment was removed.

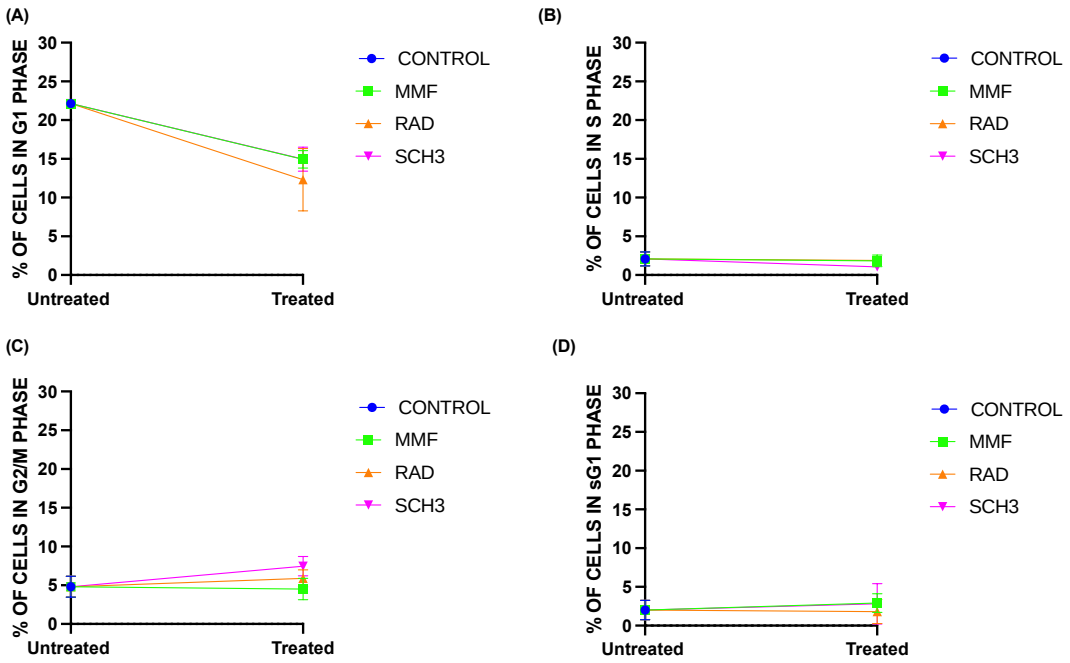

(E)

Bonferroni's multiple comparisons test	G1 P Value	S P Value	G2/M P Value	sG1 P Value
CONTROL vs. MMF	0.0273	>0.9999	>0.9999	>0.9999
CONTROL vs. RAD	0.0043	>0.9999	>0.9999	>0.9999
CONTROL vs. SCH3	0.0279	0.5387	0.2155	>0.9999
MMF vs. RAD	>0.9999	>0.9999	>0.9999	>0.9999
MMF vs. SCH3	>0.9999	>0.9999	0.1393	>0.9999
RAD vs. SCH3	>0.9999	0.9253	>0.9999	>0.9999

Figure 4. 20 The cell cycle distribution of untreated R3 cells and treated R3 cells, M+R SCH3, 48 hrs post treatment removal.

Figure 4.20A suggests that there was a statistically significant decrease in the percentage of cells in G1 phase of the cell cycle when treated with MMF alone, Rad alone and SCH3 compared with the untreated control (MMF P=0.027, Rad P=0.0043 and SCH3 P=0.02789, Figure 4.20E). This was the only statistically significant change in the percentage of cells in G1 phase of the cell cycle when comparing any treated or untreated group (Figure 4.20E). Figure 4.21B, 4.21C and 4.21D all reported that there were no statistically significant changes in the percentage of cells in the S, G2/M

or sG1 phase of the cell cycle when comparing any treated or untreated group (Figure 4.20E).

This data therefore suggests that up to 48hrs after treatment removal there is a maintained decrease in the percentage of cells progressing to subsequent phases of the cell cycle when cells are treated with SCH3. This is the only treatment group that reports a statistically significant decrease in the percentage of cells in G1 phase of the cell cycle at all three time points measured.

4.4.13 Apoptosis/Necrosis quantification of Radiotherapy Resistant MDA-MB-231 cells after combination treatment with Radiotherapy and Monomethyl Fumarate

As previously described in section 2.3.10, an investigation into Apoptosis induction in radiation resistant cells was investigated, however no chemotherapeutic agent was used in combination with MMF in this section but the effects of radiation at a dose of 2Gy was investigated. This section investigated the percentage of cells that undergo apoptosis following 48-hr treatment both MMF 2 μM and Radiation alone (2 Gy) but also as a combination SCH3 MMF 2 μM +RAD 2 Gy. The same Annexin V apoptotic detection assay was caried out as described in section 2.42.25 and section 4.3.5.

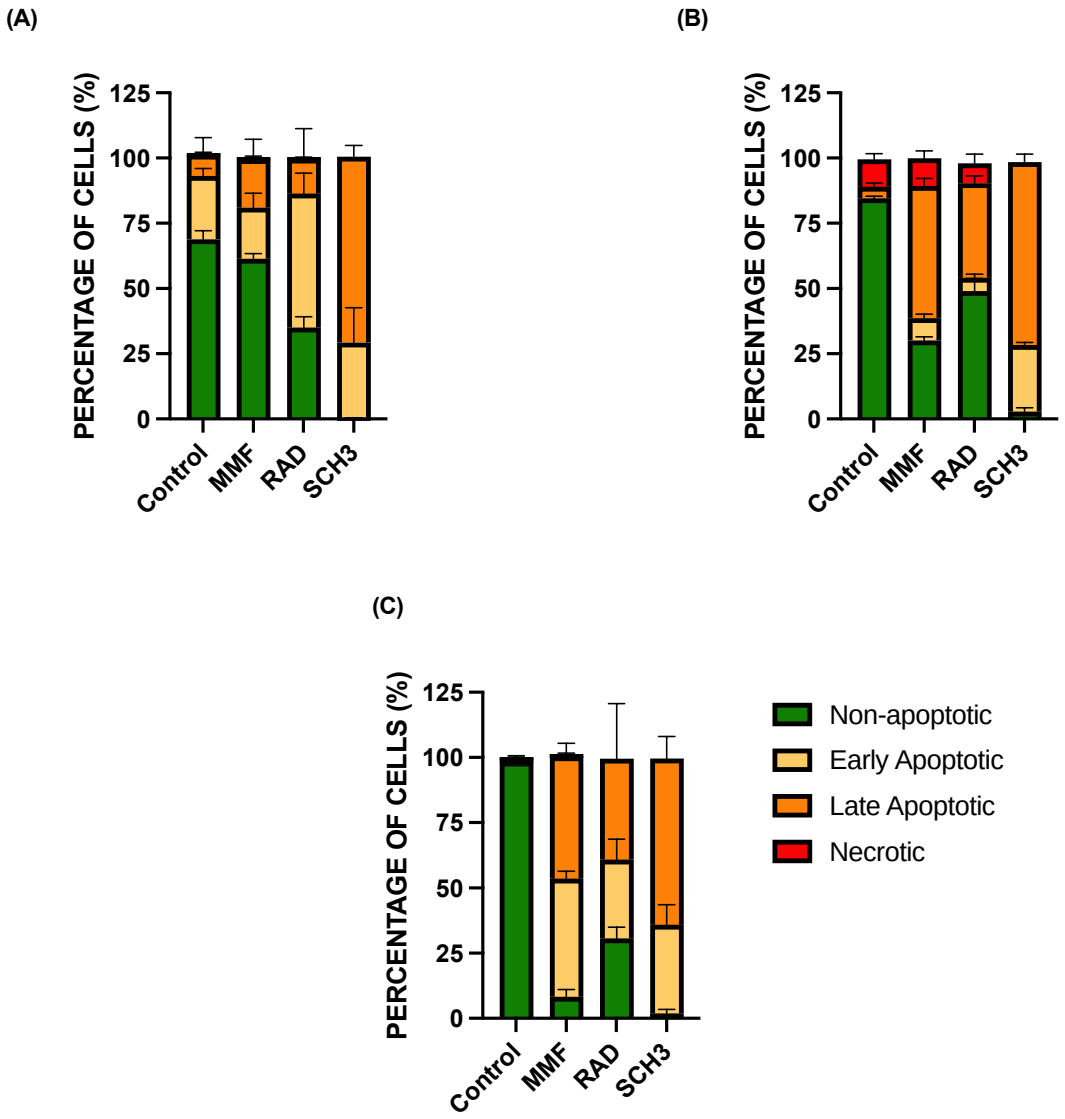

(D)

Figure 4. 21 The effect of RAD 2 Gy, MMF 2 μM and SCH3 M1st 2 μM +R 2 Gy on the different phases of apoptosis in R3 cells are shown.

Three different time points were used post treatment removal; (A) 0hr, (B) 24hr and (C) 48hr. Data is expressed as mean+/- SD of 3 individual experiments at each time point, carried out in triplicate. (D) Statistical Analysis carried out using two-way ANOVA followed by Bonferroni's post hoc testing, comparing each apoptotic phase separately between all treatments (see appendix 7).

Figure 4.21A suggests that there was a statistically significant decrease in the percentage of non-apoptotic cells when R3 cells were treated with Radiation and SCH3 compared with the untreated control and MMF alone (control vs. RAD

P=0.0002, control vs. SCH3 P<0.0001, MMF vs. RAD P=0.0025 and MMF vs. SCH3 P<0.0001). There was also a statistically significant decrease in the percentage of non-apoptotic cells when cells were treated with SCH3 compared with RAD alone (P+0.0001). There was a statistically significant increase in the percentage of early apoptotic cells when R3 cells were treated with RAD compared to the untreated control, MMF and SCH3 (control P=0.0019, MMF P=0.0004, SCH3 P=0.0097).There was also a statistically significant increase in late apoptotic cells when cells were treated with SCH3 compared with the RAD alone, MMF alone and the untreated control (all P<0.0001).

Figure 4.21B shows the percentage of cells in each phase of apoptosis 24 hrs post treatment removal. When reviewing the percentage of cells that were non-apoptotic it was found that all treated cells produced a statistically significant reduction in the percentage of viable cells when compared to the control and MMF alone (all, P<0.0001). There was also a statistically significant decrease in the percentage of non-apoptotic cells treated with SCH3 when compared with cells treated with MMF alone and RAD alone (all, P<0.0001). There was a statistically significant increase in the percentage of cells in early apoptosis when treated with MMF alone and SCH3 compared with the control (MMF, P=0.006 and SCH3 P<0.0001). There was also a statistically significant increase in the percentage of cells in early apoptosis when treated with SCH3 compared with MMF alone and RAD alone (both P<0.0001). The percentage of cells in late apoptosis statistically significantly increased when cells were treated with MMF alone, RAD alone and SCH3 compared with the control (all, P<0.0001). There was also a statistically significant increase in the percentage of cells in late apoptosis when treated with SCH3 compared with MMF alone and RAD alone (both, P<0.0001).

Figure 4.21C shows the percentage of cells in each phase of apoptosis 48 hrs post treatment removal. There was a statistically significant decrease in the percentage of non-apoptotic cells when treated with MMF, RAD and SCH3 when compared with the control cells (all, P<0.0001). There was also a statistically significant decrease in the percentage of non-apoptotic cells when treated with SCH3 when compared to RAD alone (P=0.0006). All treated cells produced a statistically significant increase in the percentage of cells in early apoptosis when treated with; MMF, RAD and SCH3, when compared to the control cells (MMF, P<0.0001, RAD, P=0.0012, and SCH3

P=0.0001). When comparing late-stage apoptotic cells there was a statistically significant increase in the percentage of cells when treated with MMF alone, RAD alone and SCH3 when compared with the control cells (all, P<0.0001). There was also a statistically significant increase in the percentage of cells in late apoptosis when treated with SCH3 combination, compared with RAD only treated cells (P=0.0023).

These results suggest that SCH3 treatment significantly increased the percentage of cells that enter apoptosis when compared to the untreated control, radiation alone and MMF alone up to 48hrs post treatment removal. This suggests that when radiation resistant cells are treated with the SCH3 combination of MMF administered before radiation, a higher percentage of cells are killed via apoptosis. These findings support the hypothesis that when MMF is administered before radiation, it could bind to glutathione, preventing the neutralisation if ROS generated from radiotherapy and may also be inhibiting the NRF2 nuclear translocation, so the cell is unable to synthesis antioxidants. This allows for ROS generated from irradiation to cause DSB and SSB triggering cell death via the caspase 3 pathway in radiation resistant cells.

4.4.14 Analysis of Glutathione levels Radiotherapy resistant MDA-MB-231 cells after combination treatment with Radiotherapy and Monomethyl Fumarate

As previously described in section 2.3.10 a Glutathione Assay was carried out to investigate the relative glutathione levels in samples after treatment. As SCH3 was the only combination that produced statistically significant reduction in cell survival compared with the control and radiation only treated cells both 2D and 3D, this was the scheduled combination investigated.

Cells were harvested so GSH levels could be measured; 1 hr after therapy was administered (for combination 1 hr after second therapy administered), immediately after the treatment was removed (following 48 hr treatment) 0 hr 24 hrs after the treatments were removed and 48 hrs after the treatment were removed and results detailed in Figure 4.22, doses used were Rad 2 Gy and MMF 2 μM.

(A)

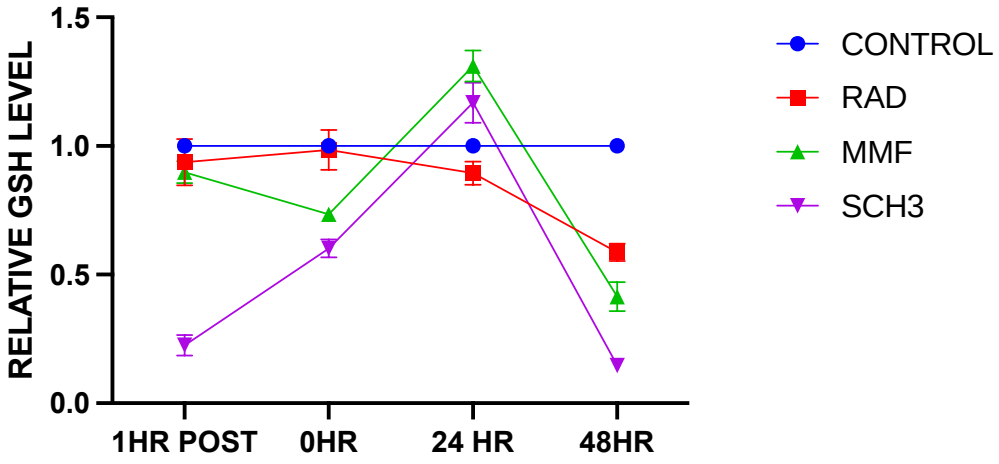

(B)

Bonferroni's multiple comparisons test	P Value 1 HR post	P Value 0HR	P Value 24HR	P Value 48HR
CONTROL vs. RAD	>0.9999	>0.9999	0.2594	<0.0001
CONTROL vs. MMF	0.2966	0.0004	0.0007	<0.0001
CONTROL vs. SCH3	<0.0001	<0.0001	0.0317	<0.0001
RAD vs. MMF	>0.9999	0.0006	<0.0001	0.0014
RAD vs. SCH3	<0.0001	<0.0001	0.0016	<0.0001
MMF vs. SCH3	<0.0001	0.0325	0.0720	<0.0001

Figure 4. 22 The effect single therapies RAD 2 Gy and MMF 2 μM, and combination therapy SCH3 MMF 2 μM 1st + RAD 2 Gy 24 hours later.

Data reported is an average of three independent experiments carried out in triplicate. (B) A one-way ANOVA with Bonferroni post testing was performed using GraphPad prism 9.2.1 comparing each treated and untreated group to each other, *P<0.05, **P<0.01, ***P<0.001 and ****P<0.0001.

As reported in Figure 4.22, in SCH3 treated R3 cells there was statistically significant reduction in relative GSH levels when compared with untreated control, RAD and MMF at 1 hr post treatment administration (all P <0.0001, Figure 4.22B). 0 hrs post treatment, SCH3 treated R3 cells had a statistically significantly reduced relative GSH levels when compared with the control cells, RAD alone and MMF alone (all P<0.0001, Figure 4.22B). 0 hrs post treatment there was a statistically significant decrease in relative GSH levels in R3 cells treated with MMF alone and SCH3 when compared to the untreated control (MMF P=0.0003, SCH3 P<0.0001, Figure 4.22B). There was also a statistically significant decrease in the relative GSH levels when R3 cells were treated with MMF and SCH3 compared to RAD alone 0 hrs post treatment

removal (MMF P=0.0006 and SCH3 P<0.0001, Figure 4.22B). There was also a statistically significant decrease in relative GSH levels when R3 cells were treated with SCH3 compared to MMF alone treated cells (P=0.035, Figure 4.22B). 24 hrs post treatment removal there was a statistically significant increase in relative GSH level when cells were treated with MMF and SCH3 when compared to the control (MMF P=0.0007 and SCH3 P=0.0317, Figure 4.23B). There was a statistically significant increase in relative GSH levels 24 hrs post treatment removal when R3 cells were treated with MMF and SCH3 compared to RAD alone treated cells (MMF P<0.0001 and SCH3 P=0.0016, Figure 4.22B). 48 hrs post treatment there was a statistically significantly reduction in relative GSH level when comparing SCH3, MMF and RAD to the control (all P<0.0001, Figure 4.22B). There was a statistically significant reduction in relative GSH when R3 cells were treated with MMF compared to RAD alone (P=0.0014, Figure 4.22B). There was also a statistically significantly reduced relative GSH level when comparing SCH3 with RAD and MMF alone (both P<0.0001, Figure 4.22B).

In summary, the findings of Figure 4.22 support the hypothesis that SCH3 treatment of radiation resistant MDA-MB-231 cells significantly reduced the synthesis of intracellular glutathione. GSH levels of R3 cells are significantly lower than control and RAD alone treated R3 cells, 48 hrs after treatment is removed. Although an increase in relative GSH is reported 24 hrs post treatment removal, the synthesis of GSH is not able to be maintained by SCH3 treated cells. These results also support the findings of Figure 4.21 that report a significant increase in apoptotic cells following R3 treatment up to 48 hrs post treatment. It may be that as GSH levels are not able to be maintained, ROS is left unchecked and able to induce SSB and DSB that when accumulated 48 hrs post treatment removal has induce apoptosis of R3 cells significantly more than control cells or RAD alone treated R3 cells.

4.4.15 Detection of Autophagic Radiation resistant cells after combination treatment with Radiation and Monomethyl Fumarate

As previously described in section 2.4.11 an autophagy assay was used to investigate the percentage of cells that autophaged because of treatment. However, this section investigated the radiation resistant cells that were treated with MMF 2μM alone radiation at 2Gy as well as the schedule 3 combination of MMF2μM + Rad 2Gy. This assay was carried out at 3 different time points to coincide with the Cell Cycle analysis data (Section 4.44.4) and results are detailed in Figure 4.24.

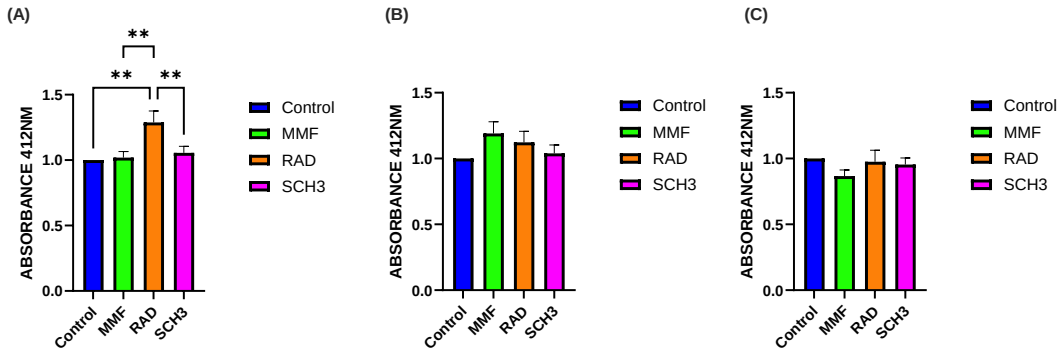

Figure 4. 23 The effect of; RAD alone 2Gy, MMF alone 2μM or Schedule 3 combination MMF1st 2μM+ Rad 2Gy 24 hours later, on Green Detection Reagent. Data is expressed relative to the control. Cells fluorescence was measure on a fluorescent microplate reader at 412nm. (A) 0 hours after treatment removed. (B) 24 hours after treatment removed. (C) 48 hours after treatment removed. All graphs are displayed as mean and standard deviation of 3 individual experiments caried out in triplicate. One -way ANVOA was carried out with Bonferroni's correction.

As reported in figure 4.23A, 0 hours post treatment removal, there was a statistically significant increase in the absorbance values of cells treated with RAD alone and when compare with the control (P=0.0013), MMF alone (P=0.0010) and SCH 3 (P=0.0052). This was the only statistically significant result reported when investigating the absorbance of all cells at all three-time time points measured.

Overall, this data suggests that R3 cells are not undergoing autophagy when treated with radiation alone, MMF alone or RAD + MMF SCH3 combination. This suggests that autophagy is not a mechanism that has been adapted by therapy resistant cells, this was an important investigation as it has been reported in the literature that when some cells become resistant, they can start to induce autophagy (Ho and Gorski, 2019).

4.4.16 Quantification of DNA damage and repair using Comet Assay, of MDA-MB-231 cells after combination treatment with Radiation and Monomethyl Fumarate

A comet assay was used to quantify the DNA damage induced by radiation alone at 2Gy, MMF alone at 2μM and the SCH 3 combination of M+R. This assay was previously described in Section 2.3.12.

- Comparison of DNA fragmentation at 0hr, 24hr and 48hr – Analysis of DNA repair

The median tail moment (AU) was calculated for each treatment; RAD 2 Gy, MMF 2 μM or SCH3 combination of MMF 2 μM +RAD 2 Gy. This was determined for each time point measured, 0 hrs post treatment, 24 hrs post treatment and 48 hrs post treatment. Statistical analysis was carried out on these results using a one-way ANOVA with Bonferroni's correction, the results are detailed in appendix 8. Unlike section 4.4.8, the comet analysis was carried out immediately after treatment (rather than after cells were exposed to drug for 48 hrs) as when using radiation, a spike in ROS occurs immediately after irradiation exposure. To quantify this spike in DNA damage, a comet assay was carried out immediately following this, 24 hrs after initial treatment and 48 hrs after initial treatment. This same time points were used for MMF alone and SCH3 treated cells, for SCH3 treatment the 0-hr time point was taken 24 hrs after MMF administration and immediately after these pre-exposed MMF cells were irradiated. This allowed for an analysis of cells exposed to radiation without MMF prior exposer and those with prior MMF exposure. MMF alone treated cells were exposed to MMF for 10 minutes (this is to allow for the time taken to irradiate cells using X-irradiator and carry cell back to a cell culture hood for harvesting).

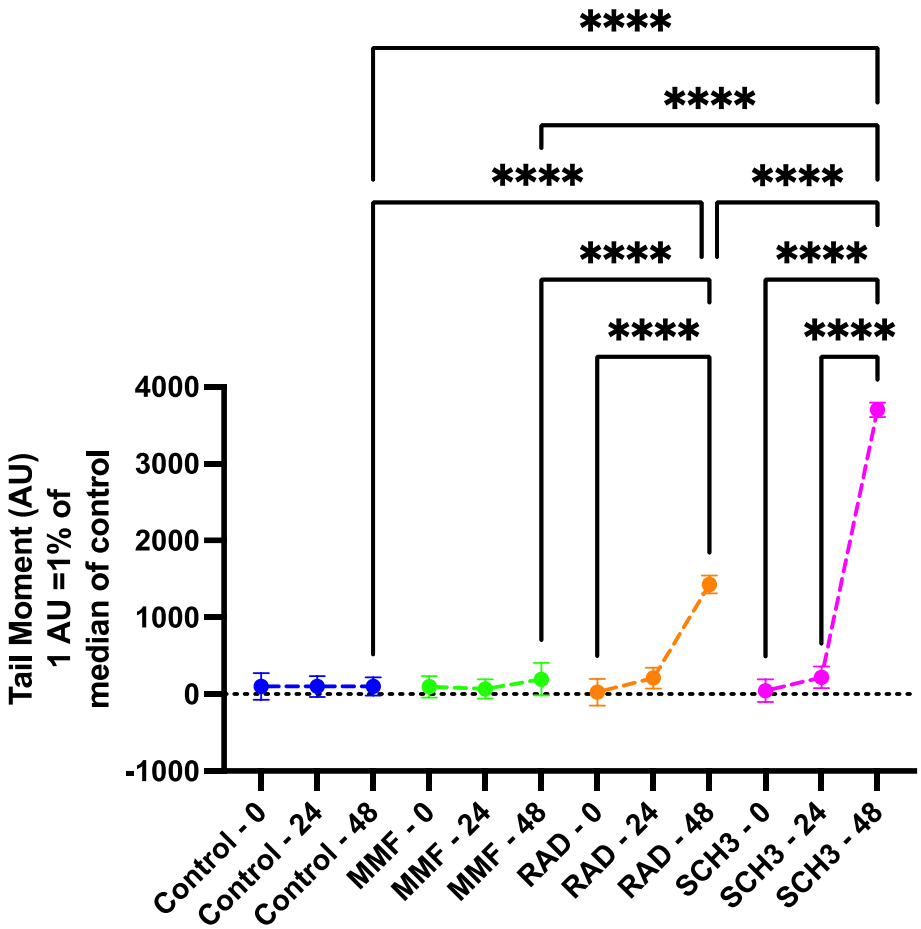

Figure 4. 24 The median DNA damage quantified as Tail Moment (AU) is displayed as a percentage of the control median.

RAD alone, MMF alone and combination SCH3M+R were the treatments used as described in Figure 4.26 time points of 0hr post treatment, 24hrs post treatment and 48hrs post treatment are compared for each treatment, results are displayed as an average of 3 independent experiments carried out using 70 comets per sample. Statistical analysis was carried out using a one-way ANOVA with Bonferroni's correction and are detailed in appendix 4D, table 3. P>0.0001 ****, P>0.001 ***, P>0.01** and P>0.1 *(see appendix 8).

Figure 4.26 suggest that there is a statistically significant increase in median tail moment of R3 cells treated with SCH3 compared with MMF alone and RAD alone, 48 hrs post treatment (all P<0.0001). The only other statistically significant increase in median tail moment was found when R3 cells were treated with RAD alone compared to the untreated control and MMF alone, 48 hrs post treatment (P<0.0001). As expected, due to its mode of action, MMF did not induce any statistically significant increase in median tail moments compared with the untreated control or any other treatment group. Both RAD alone and SCH3 treated cells had a statistically significant increase in median tail moments when comparing 24 hrs post treatment to 48 hrs post treatment within the relevant treatment group (P<0.0001).

In summary the findings in Figure 4.24 suggest that both RAD and SCH3 induce significant DNA damage to R3 cells 48 hrs post treatment, however the damage seen in that of SCH3 treated cells is greater. This supports the hypothesis that MMF in combination with radiation can induce a higher cell kill than single therapies alone. This may be due to MMF binding to glutathione, which is inhibited from neutralising ROS generated because of radiation. These finding also support that of clonogenic survival assay, in which SCH3 induced significant reductions in survival fractions of R3 cell, and Annexin V assay in which there was a statistically significant percentage of SCH3 treated cells in various stages of apoptosis. This induction of apoptosis may be causing SSB and DSB to accumulate and we can see the increase in DNA fragmentation above in Figure 4.21.

4.4.17 Cytotoxicity of Combination therapy Doxorubicin, Radiation and Monomethyl Fumarate on Doxorubicin + Radiotherapy Resistant cells

- 2D Cell Culture

Radiation and Doxorubicin resistant cells were developed as described in Section 4.1. MDA-MB-231 cells were exposed to 2 Gy radiation + 0.02 μM Dox, and the surviving colonies were harvested. Some cells were frozen down, and the rest were re dosed with 2Gy radiation + 0.02 μM Dox and the process repeated until 3 rounds of treatment were undergone. These cells were then all tested using a clonogenic assay to determine the toxicity of various doses of radiation as seen in Figure 4.25.

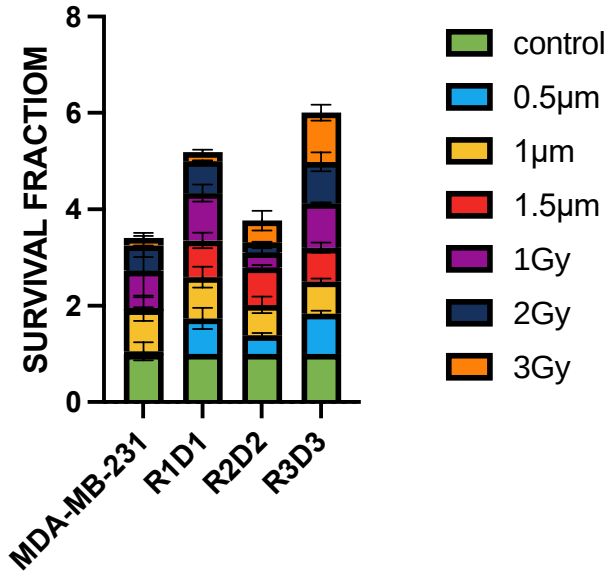

Figure 4. 25 Analysis of clonogenic survival in R3D3 resistant cell lines following exposure to radiotherapy + doxorubicin. MDA-MB-231 cells that had undergone 3 rounds of radiation + doxorubicin exposure, cells were tested for toxicity using clonogenic assays. Radiation 1Gy, 1Gy and 3Gy and doxorubicin concentrations 0.5 µM, 1 µM and 1.5 µM. Results are displayed as an average of 3 independent experiments carried out in triplicate, and graphed using GraphPad Prism Version 9.2.1

Results from Figure 4.25 suggest that R3D3 cells were the only tested resistant cell line to show any clonogenic survival at all concentrations of both Radiation and Doxorubicin tested. At the highest doxorubicin dose tested (1.5µM), the survival fraction reported was 0.70 SD+/- 0.10 and at the highest dose of radiation tested (3 Gy) the survival fraction was 1.02 SD+/- 0.16. Compared with the MDA-MB-231 parent cell line, the survival fraction at 1.5 µM was 0.019 SD+/- 0.01 and the survival fraction at radiation dose 3Gy was 0.15 SD+/- 0.04. Therefore, this demonstrated that R3D3 cells were more resistant to both radiation and doxorubicin than R1D1 or R2D2 cells lines.

To determine the cytotoxicity of MMF in combination with either Radiation or Doxorubicin on R3D3 cells, 3 scheduled combinations were used to determine if order of drug administration impacted cell survival fractions, results are detailed in Figure 4.26.

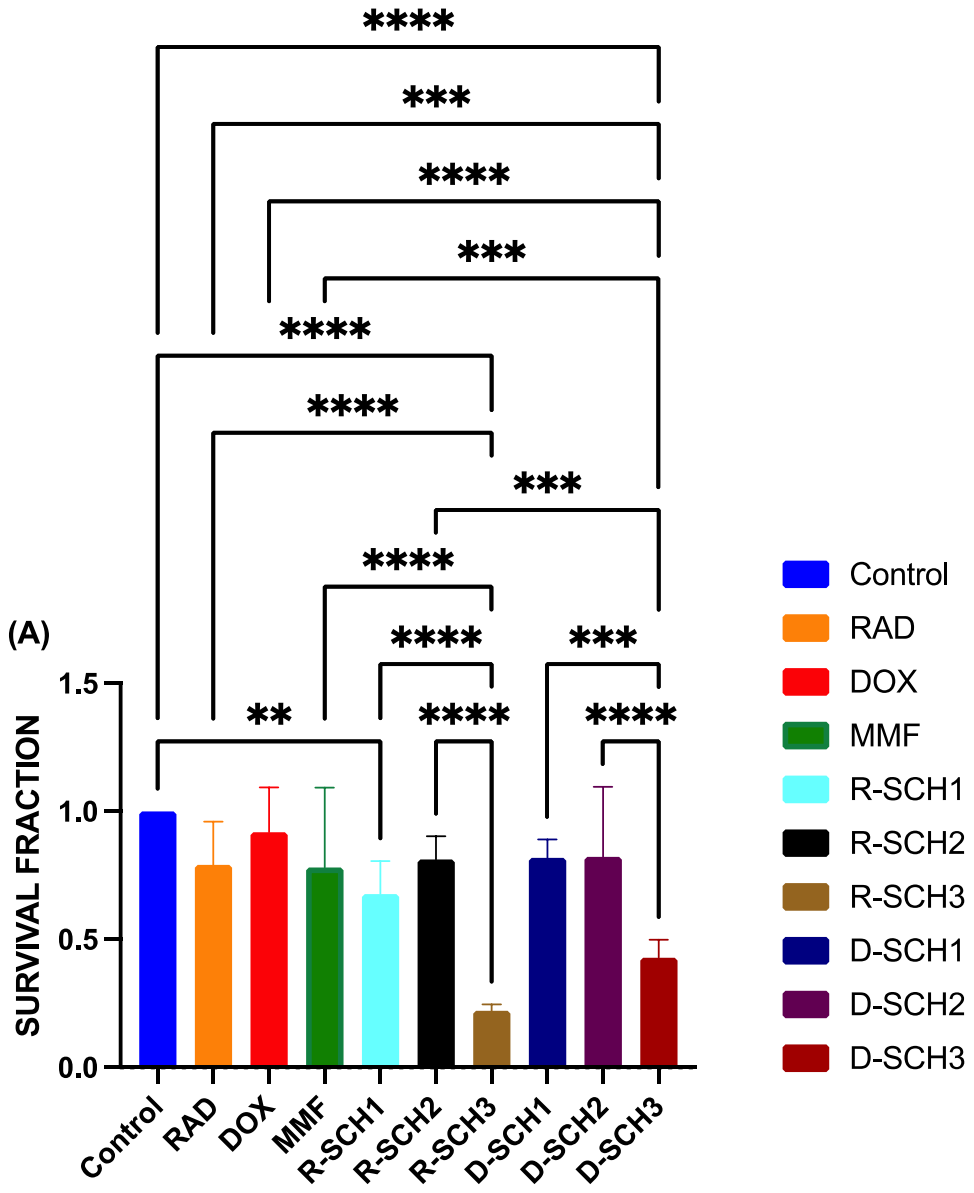

(B)

Bonferroni's multiple comparisons test	Summary	Adjusted P Value
Control vs. R-SCH1	**	0.0032
Control vs. R-SCH3	****	<0.0001
Control vs. D-SCH3	****	<0.0001
RAD vs. R-SCH3	****	<0.0001

RAD vs. D-SCH3	***	0.0005
DOX vs. R-SCH3	****	<0.0001
DOX vs. D-SCH3	****	<0.0001
MMF vs. R-SCH3	****	<0.0001
MMF vs. D-SCH3	***	0.0007
R-SCH1 vs. R-SCH3	****	<0.0001
R-SCH2 vs. R-SCH3	****	<0.0001
R-SCH2 vs. D-SCH3	***	0.0002
R-SCH3 vs. D-SCH1	****	<0.0001
R-SCH3 vs. D-SCH2	****	<0.0001
D-SCH1 vs. D-SCH3	***	0.0001
D-SCH2 vs. D-SCH3	****	<0.0001

Figure 4. 26 A comparison between the survival fraction of R3D3 cells treated with RAD 2 Gy, DOX 0.2 μM, MMF 2 μM and the combination of three schedules of: Rad 2 Gy +MMF 2 μM and Dox 0.2 μM + MMF 2 μM administration on R3D3 cells.
Data shown is the average of three independent experiments carried out in triplicate +/- SD, (B) results of a 1-way ANOVA with Bonferroni and Dunn's post hoc testing was performed using GraphPad Prism 9.2.1 software, with p-values of <0.01 = *, <0.001**, <0.0001***, <0.0001**** reported as significant when compared with the control with all results compares to the control and each other.

From Figure 4.26A we can conclude that there was a statistically significant decrease in the survival fraction of cells treated with R-SCH1, R-SCH3 and D-SCH3 when compared to the untreated control (R-SCH1 P=0.0032, R-SCH3 P<0.0001 and R-SCH3 P<0.0001, Figure 4.26B). There was also a statistically significant decrease in the survival fraction of R3D3 cells when treated with R-SCH3 and D-SCH3 compared with Rad alone treated cells (R-SCH3 P<0.0001, D-SCH3P=0.0005, Figure 4.26B). There was a statistically significant decrease in the survival fraction of R3D3 cells treated with D-SCH3 and R-SCH3 when compared to DOX alone treated cells (P<0.0001, Figure 4.26B). There was a statistically significant decrease in the survival fraction of R3D3 cells treated with D-SCH3 and R-SCH3 when compared to MMF alone treated cells (R-SCH3 P<0.0001, D-SCH3 P=0.0007 Figure 4.26B). There was a statistically significant decrease in the survival fraction of R3D3 cells treated with R-SCH3 compared with R-SCH1 and R-SCH2 (both P<0.0001, Figure 4.26B). There was a statistically significant decrease in the survival fraction of cells treated with D-SCH3 compared with R-SCH2 (P<0.0001, Figure 4.26B). Finally, there was a statistically significant decrease in the survival fraction of cells treated with D-SCH3 when compared to D-SCH1 and D-SCH2 treated cells (SCH1 P<0.0001 and SCH2 P=0.0001, Figure 4.26B).

These result support the hypothesis that MMF administered before DOX or RAD may be inhibiting the NRF2 nuclear translocation preventing the synthesis of antioxidants such as glutathione. This in turn will allow ROS to cause DSB and SSB ultimately leading to cell death via the caspase 3 pathway.

Following on from 2D clonogenic investigations, 3D spheroids were used to investigate the how the combination therapies of radiation 2 Gy + MMF 2 μM and doxorubicin 0.2 μM + MMF 2 μM, in a schedule 3 administration affects the growth of radiation + doxorubicin resistant (R3D3) cells, as detailed in Figure 4.27.

4.4.18 Assessment of combination of Radiation or Doxorubicin and MMF In 3D spheroid models of therapy resistant cells.

As it was decided that MMF was the more promising fumaric acid to re-sensitise resistant MDA-MB-231 cells to radiotherapy and doxorubicin chemotherapy, this was the fumaric acid investigated using a 3D spheroid model. All three times schedules were used to investigate the potential of MMF on R3D3 spheroids and results are detailed in Figure 4.27. Doses used were RAD 2 Gy, DOX 0.2 μM, MMF 2 μM and the combination of three schedules of: Rad 2 Gy +MMF 2 μM and DOX 0.2 μM + MMF 2 μM administration on R3D3 cells.

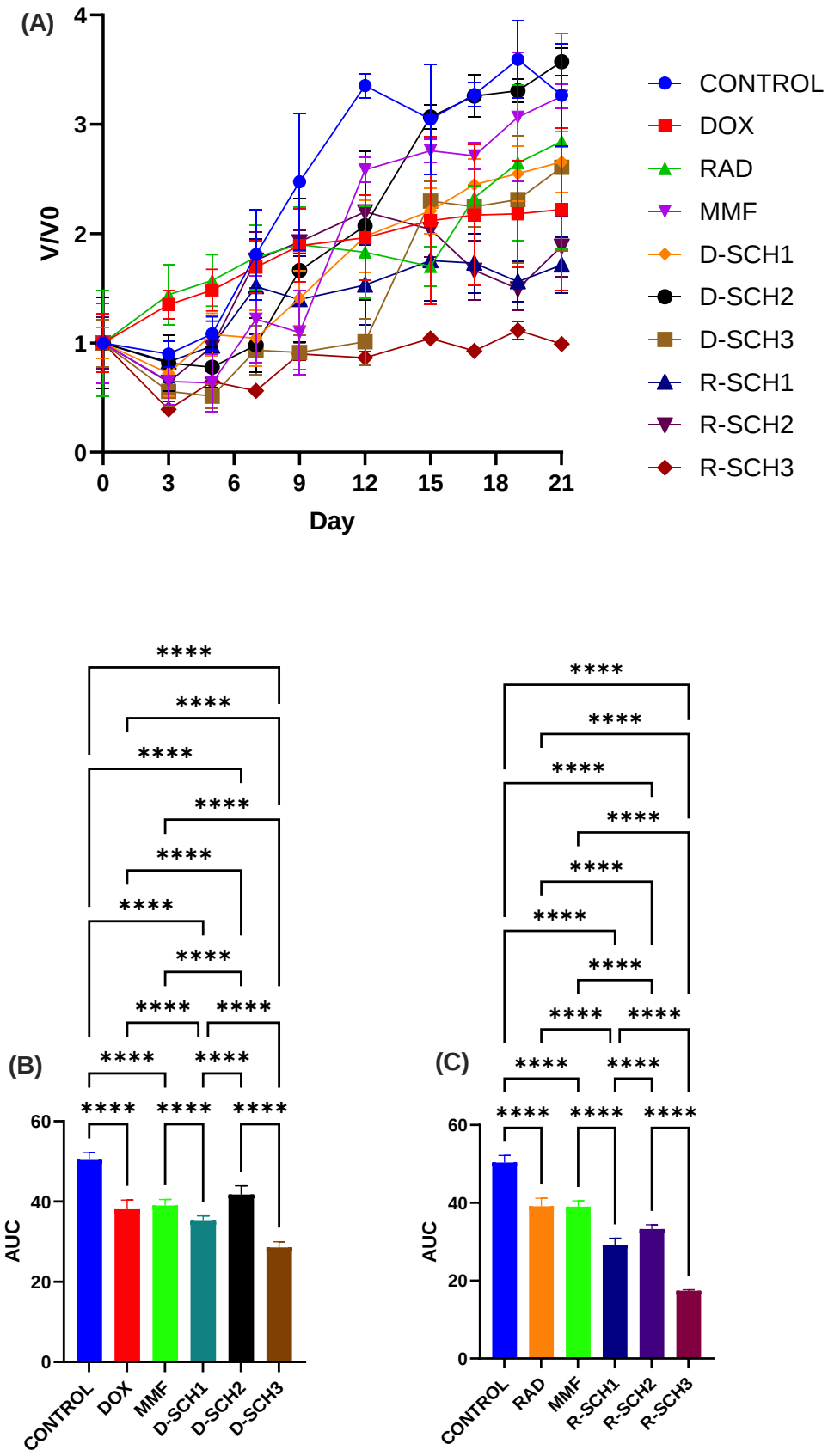
(A)
V/V0
Day
CONTROL
DOX
RAD
MMF
D-SCH1
D-SCH2
D-SCH3
R-SCH1
R-SCH2
R-SCH3
(B)
AUC
(C)
AUC
****

(D)

Bonferroni's multiple comparisons test	V/V0 Summary	Adjusted P Value	AUC Summary	Adjusted P Value
CONTROL vs. DOX	ns	>0.9999	****	<0.0001
CONTROL vs. RAD	ns	>0.9999	****	<0.0001
CONTROL vs. MMF	ns	>0.9999	****	<0.0001
CONTROL vs. D-SCH1	ns	>0.9999	****	<0.0001
CONTROL vs. D-SCH2	ns	>0.9999	****	<0.0001
CONTROL vs. D-SCH3	ns	0.3071	****	<0.0001
CONTROL vs. R-SCH1	ns	0.2198	****	<0.0001
CONTROL vs. R-SCH2	ns	0.7884	****	<0.0001
CONTROL vs. R-SCH3	***	0.0008	****	<0.0001
DOX vs. RAD	ns	>0.9999	NS	NS
DOX vs. MMF	ns	>0.9999	NS	0.9509
DOX vs. D-SCH1	ns	>0.9999	****	<0.0001
DOX vs. D-SCH2	ns	>0.9999	****	<0.0001
DOX vs. D-SCH3	ns	>0.9999	****	<0.0001
RAD vs. MMF	ns	>0.9999	NS	>0.9999
RAD vs. R-SCH1	ns	>0.9999	****	<0.0001
RAD vs. R-SCH2	ns	>0.9999	****	<0.0001
RAD vs. R-SCH3	ns	0.1084	****	<0.0001
MMF vs. D-SCH1	ns	>0.9999	****	<0.0001
MMF vs. D-SCH2	ns	>0.9999	****	<0.0001
MMF vs. D-SCH3	ns	>0.9999	****	<0.0001
MMF vs. R-SCH1	ns	>0.9999	****	<0.0001
MMF vs. R-SCH2	ns	>0.9999	****	<0.0001
MMF vs. R-SCH3	ns	0.1164	****	<0.0001
D-SCH1 vs. D-SCH2	ns	>0.9999	****	<0.0001
D-SCH1 vs. D-SCH3	ns	>0.9999	****	<0.0001
D-SCH2 vs. D-SCH3	ns	>0.9999	****	<0.0001
D-SCH2 vs. R-SCH1	ns	>0.9999	NS	NS
D-SCH2 vs. R-SCH2	ns	>0.9999	NS	NS
D-SCH2 vs. R-SCH3	*	0.0272	NS	NS
D-SCH3 vs. R-SCH1	ns	>0.9999	NS	NS
D-SCH3 vs. R-SCH2	ns	>0.9999	NS	NS
D-SCH3 vs. R-SCH3	ns	>0.9999	NS	NS
R-SCH1 vs. R-SCH2	ns	>0.9999	****	<0.0001
R-SCH1 vs. R-SCH3	ns	>0.9999	****	<0.0001
R-SCH2 vs. R-SCH3	ns	>0.9999	****	<0.0001

Figure 4. 27 The effect of RAD + MMF and DOX + MMF in schedule 1,2 and 3 combinations on the growth of D3 spheroids.

(A) R3D3 spheroids were incubated with drugs continually for 21 days and images every 2-4 days. Spheroid volumes were calculated and the average fold increase from initial V/V0 +/- S.D, N= 36, is presented on a linear scale, (B-C) The area under the curve (AUC) +/- S.D. was also calculated using one-way ANOVA analysis with Bonferroni's testing for multiple comparisons, results displayed in (D). Results are shown as an average of 3 independent experiments carried out using 36 spheroids per treatment, statistical analysis was carried out on the data using GraphPad prism 9.2.1, determined by the. P<0.05=*, P<0.01=**, P<0.001=***, P<0.0001=**** when compared with the control.

Figure 4.27A suggests that there was a statistically significant decrease in the change in spheroid growth with respect to V/V0 when R3D3 cells were treated with R-SCH3 compared to the untreated control (P=0.0008, Figure 4.27D). There was also a statistically significant decrease in the change in spheroid volume when R3D3 spheroids were treated with R-SCH3 compared with D-SCH2 (P=0.0272, Figure 4.27D). This suggests that R-SCH3 is the most suitable therapy tested at reducing the growth of resistant spheroid, this may be due to MMF inhibiting glutathione and allowing ROS to induce DNA damage, resulting in a higher percentage of cell death, however further mechanistic analysis will be carried out to investigate this.

Figure 4.27B shows that there was a statistically significant decrease in the AUC value of all R3D3 treated spheroids compared with the untreated control spheroids (all P<0.0001, Figure 4.27B and C). There was also a statistically significant decrease in AUC value of R3D3 spheroids treated with D-SCH1, D-SCH2 and D-SCH3 compared with DOX alone and MMF alone (all P<0.0001, Figure 4.27B) and R3D3 spheroids treated with D-SCH3 compared with D-SCH1 and D-SCH2 (all, P<0.0001, Figure 4.27B)

Figure 4.27C reported that there was a statistically significant decrease in AUC when R3D3 spheroids were treated with R-SCH1, R-SCH2 and R-SCH3 compared with radiation alone and MMF alone (all, P<0.0001, Figure 4.27C) and R3D3 spheroids treated with R-SCH3 when compared to R-SCH1 and R-SCH2 (all, P<0.0001, Figure 4.27C).

Overall, the findings from Figure 4.27 suggest that radiation in a SCH3 combination with MMF, was the most successful therapy at reducing the growth of radiation + doxorubicin resistant cells, as is supported by the clonogenic analysis of the survival fraction of R3D3 treated cells. Thus R-SCH3 was also found to significantly reduce the growth of R3D3 cells in both 3D models and 2D models.

4.4.19 Combination Index analysis of Combination therapy Doxorubicin, Radiation and Monomethyl Fumarate on Doxorubicin + Radiotherapy Resistant cells

As described in Sections 4.42.13, combination index analysis was carried out to investigate the synergistic capabilities of R3D3 cells treated with scheduled combinations of MMF + Dox or MMF + Rad. Results from the analysis are detailed in Figure 4.28.

(A)

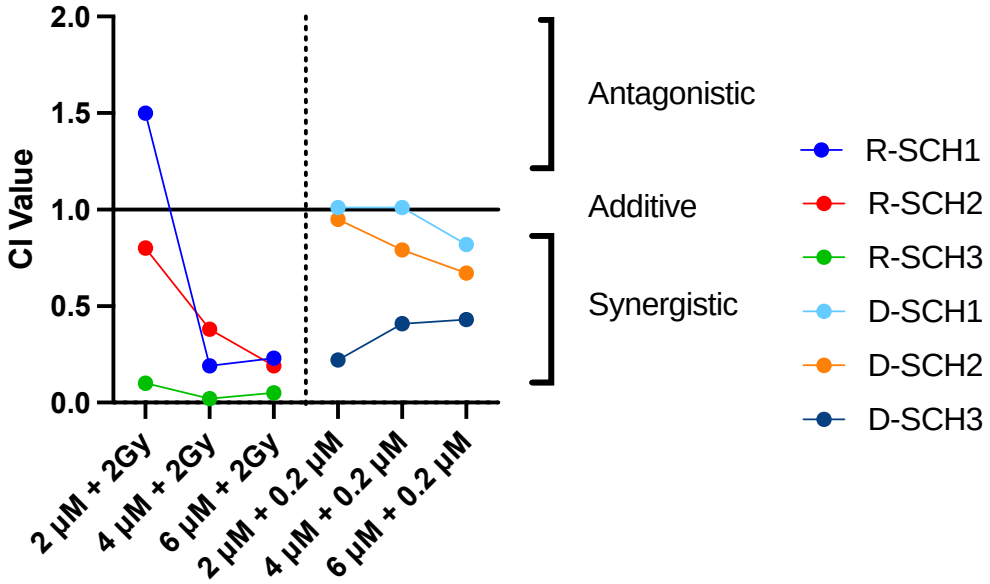

(B)

Drug Concentrations	Combination Index Values		
	SCH1	SCH2	SCH3
MMF 2 µM +RAD 2 Gy	1.5	0.8	0.1
MMF 4 µM + RAD 2 Gy	0.19	0.38	0.02
MMF 6 µM + RAD 2 Gy	0.23	0.19	0.05
MMF 2 µM + DOX 0.2 µM	1.01	0.95	0.22
MMF 4 µM + DOX 0.2 µM	1.01	0.79	0.41
MMF 6 µM + DOX 0.2 µM	0.82	0.67	0.43

Figure 4. 28 (A) Combination Index (CI) after R3D3 cells are incubated with DOX + MMF or RAD + MMF in the 3 treatments Schedules.

Antagonistic <1.1, Additive = .9-1.1 and Synergistic > 0.9. Each point represents three independent experiments carried out in triplicate. (B) Values of CI plotted in (A).

Results from Figure 4.28 report that all Radiation scheduled treatments at all concentrations produced synergistic CI values, except for R-SCH1 treated with 2 μM MMF + 2 Gy Rad. This combination produced an antagonistic CI value (1.5). D-SCH1 combination produced additive CI values when using 2 μM MMF + 0.2 μM Dox and 4 μM MMF + 0.2 μM DOX combinations (1.01, 1.01). at the highest concentration tested 6 μM MMF + 0.2 μM DOX D-SCH1 produced a synergistic CI value (0.82). D-SCH2 and D-SCH3 produced all synergistic CI values at all concentrations tested.

These results support the use of SCH3 combination therapies for both radiation and doxorubicin combinations in R3D3 cells. These results suggest that SCH3 is the most appropriate combination to use as it produced a synergistic (better than the sum of each agent) CI value at when investigating R-SCH3 and D-SCH3.

4.4.20 Cell cycle analysis of R3D3 cells after combination treatment with Doxorubicin, Radiation and Monomethyl Fumarate

As described in Section 2.3.9, Cell Cycle Analysis assay was carried out to investigate the effect each treatment has on the percentage of cells in each phase of the cell cycle. Cells were treated with DOX alone RAD alone, MMF alone, the SCH3 DOX combination D-SCH3 (MMF1st 2 μM +DOX 0.2 μM 24 hours after 1st therapy administration) and the SCH3 RAD combination, R-SCH3 (MMF1st 2 μM +RAD 2 Gy 24 hours after 1st therapy administration) (Figure 4.29).

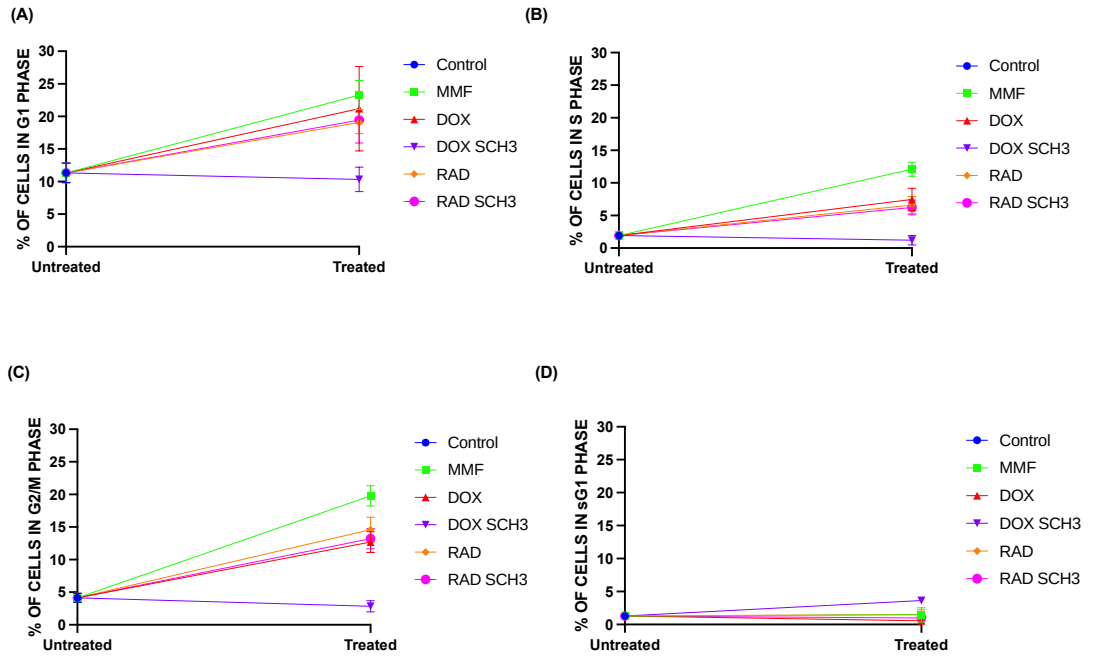

(E)

Bonferroni's multiple comparisons test	G1 P Value	S P Value	G2/M P Value	sG1 P Value
Control vs. MMF	0.0143	<0.0001	<0.0001	>0.9999
Control vs. DOX	0.0565	0.0012	0.0001	>0.9999
Control vs. DOX SCH3	>0.9999	>0.9999	>0.9999	0.0046
Control vs. RAD	0.2313	0.0050	<0.0001	>0.9999
Control vs. RAD SCH3	0.1829	0.0101	<0.0001	>0.9999
MMF vs. DOX	>0.9999	0.0050	0.0009	>0.9999
MMF vs. DOX SCH3	0.0076	<0.0001	<0.0001	0.0089
MMF vs. RAD	>0.9999	0.0012	0.0120	>0.9999
MMF vs. RAD SCH3	>0.9999	0.0006	0.0017	>0.9999
DOX vs. DOX SCH3	0.0291	0.0004	<0.0001	0.0004
DOX vs. RAD	>0.9999	>0.9999	>0.9999	0.9668
DOX vs. RAD SCH3	>0.9999	>0.9999	>0.9999	>0.9999
DOX SCH3 vs. RAD	0.1173	0.0014	<0.0001	0.0113
DOX SCH3 vs. RAD SCH3	0.0928	0.0026	<0.0001	0.0017
RAD vs. RAD SCH3	>0.9999	>0.9999	>0.9999	>0.9999

Figure 4. 29 The cell cycle distribution of untreated R3D3 cells and treated R3D3 cells, M+D and M+R SCH3, 0hr post treatment removal.

(MMF 2 μM, DOX 0.2 μM, RAD 2 Gy, D-SCH3 (MMF1st 2 μM +Dox 0.2 μM 24 hrs after 1st therapy administration), R-SCH3 (MMF 2 μM 1st+ RAD 2 Gy 24hrs later). The figure above represents the percentage of cells in each phase of the cell cycle, results are displayed as an average of 3 independent experiments carried out in triplicate (A) – G1, (B)- S, (C)- G2/M and (D)- sG1. (E) A two-way ANOVA test was utilized to compare the means of the cell cycle phases after treatment cells versus untreated control cells and demonstrated in the above Tables where, *P<0.05, **P<0.01, ***P<0.001 and ****P<0.000.1, (applicable to Figures 4.29 – 4.31).

From Figure 4.29A reported at there was a statistically significant decrease in the percentage of cells in the G1 phase of the cell cycle when R3D3 cells are treated with D-SCH3 compared with DOX alone and MMF alone (Dox P=0.0076 and MMF P=0.0291, Figure 4.29E). There was a statistically significant increase in the percentage of R3D3 cells in G1 phase of the cell cycle when cells were treated with MMF compared to the untreated control R3D3 cells (P=0.0143, Figure 4.29E).

Figure 4.31B reported that there was a statistically significant increase in the percentage of cells in S phase of the cell cycle when treated with MMF compared to the untreated control, Dox alone, D-SCH3, Rad alone and R-SCH3 (control P<0.0001, DOX P=0.0050, D-SCH3 P<0.0001, Rad alone P=0.0120 and R-SCH3 P=0.0017, Figure 4.29E). There was a statistically significant increase in the percentage of cells in S phase in the cell cycle when cells were treated with Dox alone and Rad alone when compared to the untreated control (Dox P=0.0012 and Rad P=0.0050, Figure 4.31E). There was a statistically significant decrease in the percentage of cells in the S phase of the cell cycle when cells were treated with D-SCH3 compared to MMF, Dox alone, Rad alone andR-SCH3 (MMF P<0.0001, Dox P=0.0004, Rad P=0.0014 and R-SCH3 P=0.0026, Figure 4.29E).

Figure 4.31C reported that there was a statistically significant decrease in the percentage of cells in the G2/M phase of the cell cycle when cells were treated with D-SCH3 compared to MMF alone, DOX alone, Rad alone and R-SCH3 (all P<0.0001, Figure 4.29E). There was a statistically significant increase in the percentage of cells in G2/M phase of the cells cycle when cells were treated with MMF, Dox alone, Rad alone and R-SCH3 (MMF P<0.0001, DOX P=0.0001, Rad P<0.0001, R-SCH3 P<0.0001, Figure 4.29E). There was a statistically significant increase in the percentage of cells in the G2/M phase of the cell cycle when cells were treated with MMF compared to Rad alone and R-SCH3 (Rad P=0.00120 and R-SCH3 P=0.0017, Figure 4.29E). Figure 4.29D reported that there was a statistically significant decrease in the percentage of cells in the sG1 phase of the cell cycle when cells were treated with D-SCH3 compared with the untreated control, MMF, Dox alone, Rad alone and R-SCH3 (control P=0.0046, Dox P=0.0089, MMF P=0.0004 Rad P=0.0113 and R-SCH3 P=0.0017, Figure 4.29E).

These results suggest that R3D3 cells treated with D-SCH3 are being stalled in sG1 phase of the cell cycle immediately after treatment is removed as cells fail to enter the cell division process, this is also supported by D-SCH3 treated cells being significantly decreased in all other phases of the cell cycle. This supports the hypothesis that MMF administered prior to DOX encourages cell death more than single therapies alone.

Following this, cells were harvested 24hrs after treatment was removed and analysed for cell cycle. Figure 4.30 depicts the percentage of cells found in each phase of the cell cycle after treatment with RAD 2 Gy alone, Dox alone 0.02 μM, MMF 2 μM alone, the SCH3 RAD combination (MMF1st 2 μM +RAD 2 Gy 24 hours after 1st therapy administration) and SCH3 dox combination (MMF 1st 2 μM + Dox 0.02 μM 24hrs after 1st therapy administration) 48hrs after treatment was removed.

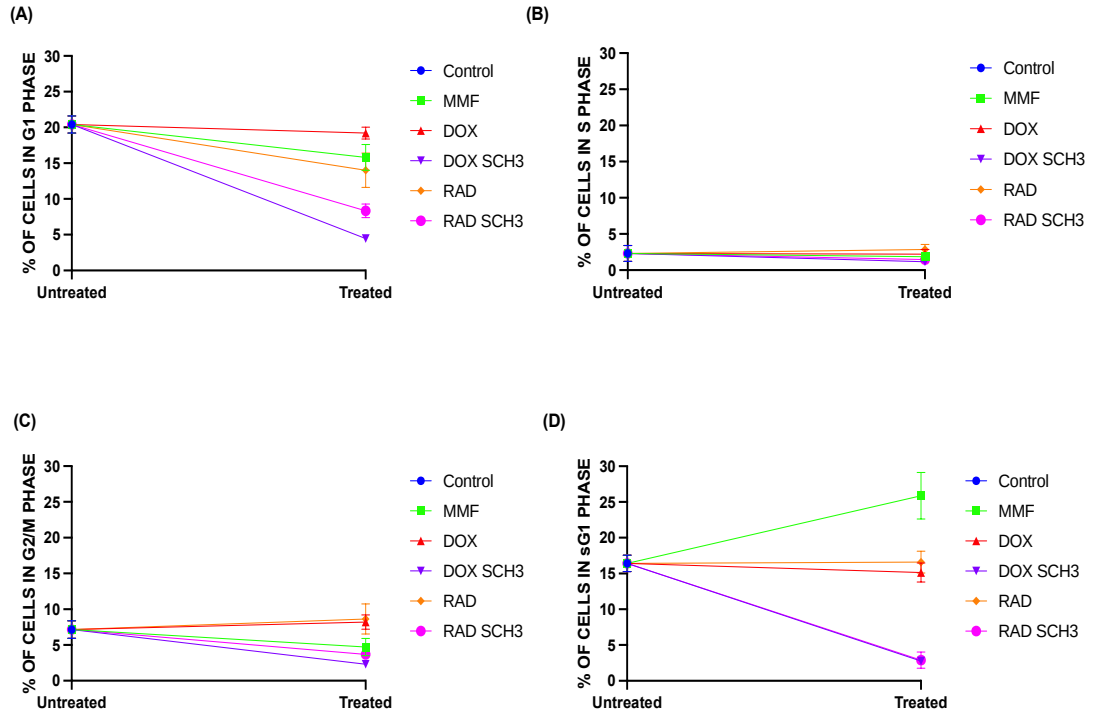

(E)

Bonferroni's multiple comparisons test	G1 P Value	S P Value	G2/M P Value	sG1 P Value
Control vs. MMF	0.0283	>0.9999	0.4103	0.0003
Control vs. DOX	>0.9999	>0.9999	>0.9999	>0.9999
Control vs. DOX SCH3	<0.0001	0.5521	0.0050	<0.0001
Control vs. RAD	0.0020	>0.9999	>0.9999	>0.9999
Control vs. RAD SCH3	<0.0001	>0.9999	0.0589	<0.0001
MMF vs. DOX	0.1883	>0.9999	0.0566	<0.0001
MMF vs. DOX SCH3	<0.0001	>0.9999	0.4680	<0.0001
MMF vs. RAD	>0.9999	0.9084	0.0254	0.0003
MMF vs. RAD SCH3	0.0005	>0.9999	>0.9999	<0.0001
DOX vs. DOX SCH3	<0.0001	0.8311	0.0009	<0.0001
DOX vs. RAD	0.0114	>0.9999	>0.9999	>0.9999
DOX vs. RAD SCH3	<0.0001	>0.9999	0.0087	<0.0001
DOX SCH3 vs. RAD	<0.0001	0.0683	0.0005	<0.0001
DOX SCH3 vs. RAD SCH3	0.0866	>0.9999	>0.9999	>0.9999
RAD vs. RAD SCH3	0.0056	0.2170	0.0041	<0.0001

Figure 4. 30 Shows the cell cycle distribution of untreated R3D3 cells and treated R3D3 cells, M+D and M+R SCH3, 24hr post treatment removal.

From Figure 4.30A reported a statistically significant decrease in the percentage of cells in the G1 phase of the cell cycle when cells were treated with MMF, D-SCH3, Rad only and R-SCH3 compared to the untreated control (MMF P=0.0283, D-SCH3 P<0.0001, Rad P=0.0020 and R-SCH3 P<0.0001, Figure 4.30E). There was a statistically significant decrease in the percentage of cells in the G1 phase of the cell cycle when cells were treated with R-SCH3 and D-SCH3 compared with MMF, Dox alone and Rad alone (MMF vs. D-SCH3 P<0.0001, MMF vs. R-SCH3 P=0.0005, Dox

both P<0.0001, Rad vs. D-SCH3 P<0.0001, Rad vs. R-SCH3 P=0.0056, Figure 4.30E). There were no statistically significant changes in the percentage of cells in the S phase of the cell cycle when comparing any treated or untreated group of R3D3 cells (Figure 4.30E).

There was a statistically significant increase in the percentage of cells in the G2/M phase of the cell cycle when cells were treated with Rad alone compared to MMF, D-SCH3 and R-SCH3 (MMF P=0.0254, D-SCH3 P=0.0005 and R-SCH3 P=0.0041, Figure 4.30E). There was a statistically significant decrease in the percentage of cells in the G2/M phase of the cell cycle when cells were treated with D-SCH3 compared with the untreated control and DOX alone (control P=0.0050 and Dox P=0.0009, Figure 4.30E). There was a statistically significant decrease in the percentage of cells in G2/M phase of the cell cycle when cells were treated with R-SCH3 compared with DOX alone and Rad alone (DOX P=0.0087 and Rad P=0.0041, Figure 4.30E).

There was a statistically significant decrease in the percentage of cells in the sG1 phase of the cell cycle when cells were treated with D-SCH3 and R-SCH3 compared to the untreated control, MMF, DOX alone and Rad alone (control both P<0.0001, DOX both P<0.0001, MMF P<0.0001 and Rad P<0.0001, Figure 4.30E). There was a statistically significant increase in the percentage of cells in sG1 phase of the cell cycle when cells were treated with MMF compared with the untreated control, DOX alone, MMF and Rad alone (control P=0.0003, Dox P<0.0001, Rad P=0.0003, Figure 4.30E).

These results support the hypothesis that MMF administered prior to radiation or doxorubicin increased the percentage of cell death. When cells are treated with D-SCH3 and R-SCH3 there is a significantly lower percentage of the cells in each phase of the cell cycle 24hrs after treatment is removed, suggesting less of the cells are entering the cell division process. This may be due to MMF binding to glutathione, preventing the neutralisation of ROS, which is induced by radiation or doxorubicin treatment, or potentially MMF could be inhibiting the nuclear translocation of NRF2, preventing the synthesis of antioxidants such as glutathione, in turn allowing radiation and doxorubicin to induce SSB and DSB, ultimately leasing to cell death via the caspase 3 pathway. These results highlight that the combination can disrupt the cell cycle distribution significantly more than single therapies alone.

Following this, cells were harvested 48hrs after treatment was removed and analysed for cell cycle. Figure 4.31 depicts the percentage of cells found in each phase of the cell cycle after treatment with RAD 2 Gy alone, Dox alone 0.2 μM, MMF 2 μM alone, the SCH3 RAD combination (MMF1st 2 μM +RAD 2 Gy 24 hrs after 1st therapy administration) and SCH3 dox combination (MMF 1st 2 μM + Dox 0.2 μM 24hrs after 1st therapy administration) 48hrs after treatment was removed.

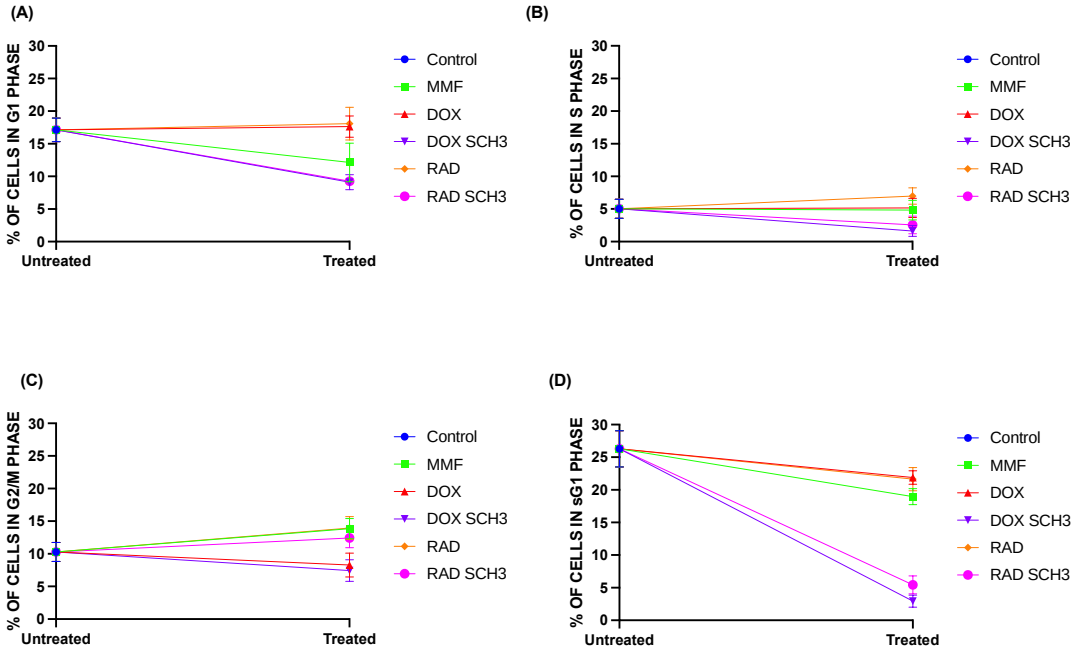

(E)

Bonferroni's multiple comparisons test	G1 P Value	S P Value	G2/M P Value	sG1 P Value
Control vs. MMF	0.1199	>0.9999	0.2999	0.0022
Control vs. DOX	>0.9999	>0.9999	>0.9999	0.1007
Control vs. DOX SCH3	0.0040	0.1329	0.7928	<0.0001
Control vs. RAD	>0.9999	>0.9999	0.2653	0.0716
Control vs. RAD SCH3	0.0048	0.6440	>0.9999	<0.0001
MMF vs. DOX	0.0673	>0.9999	0.0188	0.7432
MMF vs. DOX SCH3	>0.9999	0.1897	0.0062	<0.0001
MMF vs. RAD	0.0401	>0.9999	>0.9999	>0.9999
MMF vs. RAD SCH3	>0.9999	0.9069	>0.9999	<0.0001
DOX vs. DOX SCH3	0.0024	0.1066	>0.9999	<0.0001
DOX vs. RAD	>0.9999	>0.9999	0.0167	>0.9999
DOX vs. RAD SCH3	0.0028	0.5192	0.1360	<0.0001
DOX SCH3 vs. RAD	0.0015	0.0054	0.0055	<0.0001
DOX SCH3 vs. RAD SCH3	>0.9999	>0.9999	0.0419	>0.9999
RAD vs. RAD SCH3	0.0018	0.0240	>0.9999	<0.0001

Figure 4. 31 The cell cycle distribution of untreated R3D3 cells and treated R3D3 cells, M+D and M+R SCH3, 48hr post treatment removal.

Figure 4.31A reported that there was a statistically significant decrease in the percentage of cells in the G1 phase of the cell cycle when cells were treated with D-SCH3 and R-SCH3 compared to the untreated control, DOX alone and Rad alone (control vs. D-SCH3 P=0.0040, control vs. R-SCH3 P=0.0048, DOX vs. D-SCH3 P=0.0024, DOX vs. R-SCH3 P=0.0028, Rad vs. D-SCH3 P=0.0015 and Rad vs. R-SCH3 P=0.0018, Figure 4.31E). There was a statistically significant decrease in the

percentage of cells in the G1 phase of the cell cycle when cells were treated with MMF compared to Rad alone (P=0.0401, Figure 4.31E).

Figure 4.33B reported that there was a statistically significant decrease in the S phase of the cell cycle when cells were treated with D-SCH3 and R-SCH3 compared with Rad alone (D-SCH3 P=0.0054 and R-SCH3 P=0.0240, Figure 4.31E).

Figure 4.33C reported that there was no other statistically significant change in the percentage of cells in the S phase of the cell cycle when comparing any other treated or untreated group of R3D3 cells. There was however a statistically significant decrease in the percentage of cells in the G2/M phase of the cell cycle when cells were treated with D-SCH3 compared with MMF, Rad and R-SCH3 (MMF P=0.0062, Rad P=0.0053 and R-SCH3 P0.0419, Figure 4.31E). There was a statistically significant decrease in the percentage of cells in the G2/M phase of the cell cycle when cells were treated with DOX compared with MMF and Rad alone (MMF P=0.0188 and Rad P=0.0167, Figure 4.31E).

Figure 4.31D reported that there was a statistically significant decrease in the percentage of cells in the sG1 phase of the cell cycle when cells were treated with D-SCH3 and R-SCH3 compared with the untreated control, MMF, DOX alone and Rad alone (ALL P<0.0001, Figure 4.31E). There was also a statistically significant decrease in the percentage of cells in the sG1 phase of the cell cycle when cells were treated with MMF compared with the untreated control (P=0.0022, Figure 4.31E).

These results support the hypothesis that MMF given prior to doxorubicin or radiation can induce a higher percentage of cell death. This may be due to the scheduled combination therapies producing a significant decrease in the percentage of cells in G1, S and sG1 phases of the cell cycle suggesting that a larger percentage of these treated cells are prevented for completing the cell cycle and dividing. These result support the hypothesis that MMF is sensitizing R3D3 resistant cells to damage, this may be caused by a modulation in glutathione, however this will be investigated later in this chapter. The decrease in the distribution of R3D3 cells treated with SCH3 in each phase of the cell cycle may be an indication that this treatment may be causing cell cycle arrest in G1 and G2/M. These findings would support the idea that MMF

allows for an increase in DNA damage caused by doxorubicin and radiation and as such these strand breaks are inhibited by the G2/M checkpoint and cells are unable to fully divide into two identical daughter cells. An investigation into the apoptotic state of these cells will be discusses in section 2.3.10, this may highlight the proposed DNA damage that is suggested by cell cycle analysis of SCH3 treatments.

4.4.21 Apoptosis/Necrosis quantification of Doxorubicin + Radiotherapy Resistant MDA-MB-231 cells after combination treatment with Doxorubicin, Radiation and Monomethyl Fumarate

As previously described in section 2.3.10 an investigation into Apoptosis induction in radiation and doxorubicin resistant cells was investigated using; DOX 0.2 μM, RAD 2Gy in combination with MMF 2 μM.

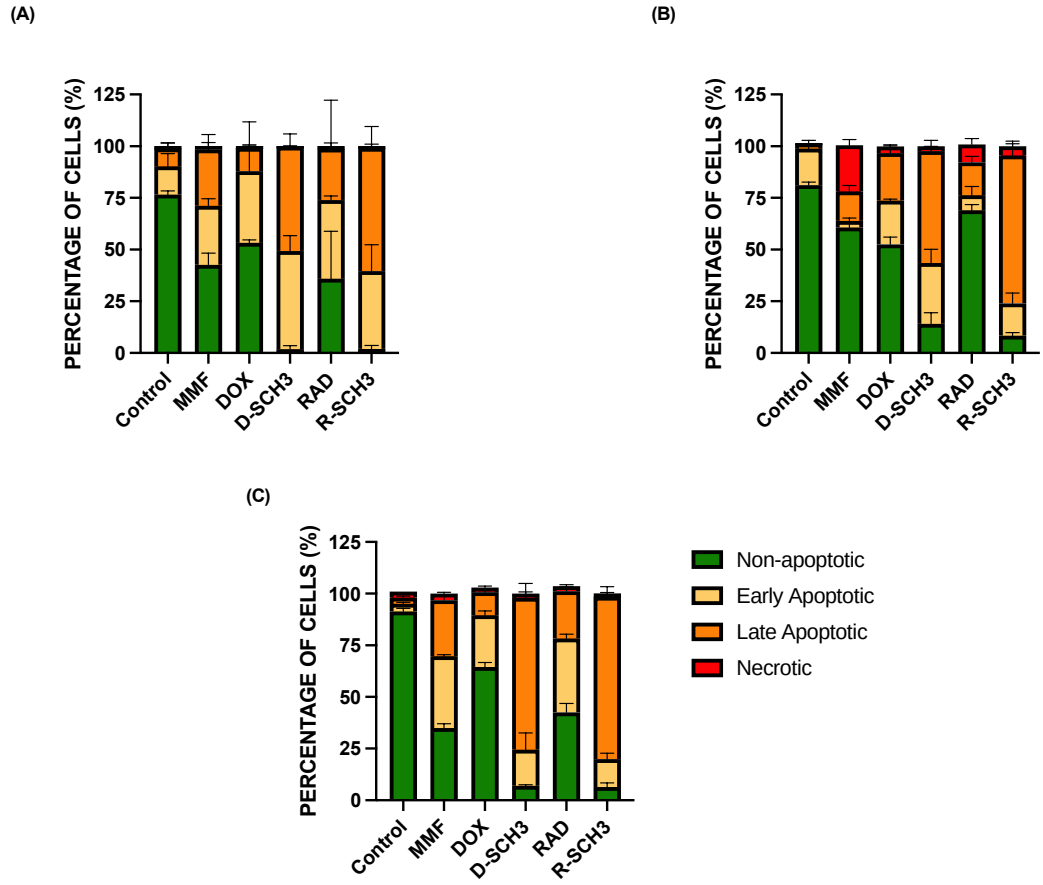

(D)

Figure 4. 32 The effect of DOX 0.2 μM, RAD 2 Gy, MMF 2 μM, DOX SCH3 and RAD SCH3 on the different phases of apoptosis in R3D3 cells are shown.
Three different time points were used post treatment removal; (A) 0hr, (B) 24hr and (C) 48hr. Data is expressed as mean+/- SD of 3 individual experiments at each time point, carried out in triplicate. Statistical Analysis carried out using two-way ANOVA followed by Bonferroni's post hoc testing, comparing each apoptotic phase separately between all treatments. *P<0.05, **P<0.01, ***P<0.001 and ****P<0.0001 (see appendix 9).

From Figure 4.32A, 0 hrs post treatment removal, there was a statistically significant decrease in the percentage of viable cells when treated with MMF alone, D-SCH3, RAD and R-SCH3 when compared with the control (MMF, P=0.0051, D-SCH3, P<0.0001, RAD, P=0.005 and R-SCH3 P<0.0001). There was also a statistically significant decrease in the percentage of viable cells when treated with D-SCH3, and R-SCH3 when compare with MMF alone (D-SCH3, P=0.0001and R-SCH3 P=0.0001).

DOX SCH3 also reported a statistically significantly reduced percentage of viable cells when compared with DOX alone (P<0.0001). R-SCH3 reported a statistically significant reduction in the percentage of viable cells when compared to RAD alone (P=0.0017). The only statistically significant result found in Figure 4.32A when comparing early apoptotic cells was found between D-SCH3 compared with the control (P=0.0017). When reviewing the percentage of cells in late apoptosis, there was a statistically significant increase in the percentage of late apoptotic cells when treated with D-SCH3 and R-SCH3 to the control (both P<0.0001). There was also a statistically significant increase in the percentage of cells in late apoptosis when treated with R-SCH3 compared with MMF alone (P=0.0031). D-SCH3 also produced a statistically significantly increased percentage of cells in late apoptosis when compared with DOX alone treated cells (P=0.0002). R-SCH3 also produced a statistically significantly increase percentage pf cells in late apoptosis when compared with RAD alone (P=0.0013).

Fig 4.32B reports the percentage of cells in each stage of apoptosis, 24 hrs after treatment removal. There was a statistically significant decrease in the percentage of viable cells in all treated cells when compared with the control; RAD alone, MMF alone, DOX alone, D-SCH3 and R-SCH3 (all P<0.0001 except for RAD alone P=0.0289). There was also a statistically significant decrease in the percentage of viable cells when treated with D-SCH3 and R-SCH3, compared with MMF alone treated cells (both P<0.0001). DOX SCH3 also produced a statistically significantly reduced percentage of viable cells when compared to DOX alone (P<0.0001). R-SCH3 reported a statistically significantly reduced percentage of viable cells when compared to RAD alone (P<0.0001). There was a statistically significant increase in the percentage of cells in early apoptosis when treated with D-SCH3 compared with the control (P=0.0166). There was also a statistically significant increase in the percentage of cells in early apoptosis when treated with D-SCH3 and R-SCH3 compared with MMF alone (D-SCH3 P<0.0001 and R-SCH3 P=0.0170). All treated cells reported a statistically significant increase in the percentage of cells in late apoptosis when treated with DOX, D-SCH3 and R-SCH3 compared with the control; (all P<0.0001). MMF and RAD treated cells also statistically significantly increased the percentage of cells in late apoptosis when compared to the untreated control (MMF P=0.0454 and RAD P=0.0142). There was a statistically significant increase in the percentage of late apoptotic cells when treated with D-SCH3 and R-SCH3

compared with MMF alone treated cells, (both P<0.0001). D-SCH3 also produced a statistically significant increase in late apoptotic cells compared with DOX alone (P<0.0001). R-SCH3 produced a statistically significant increase in late apoptotic cells compare to RAD alone (P<0.0001).

Figure 4.32C describes the percentage of cells in each phase of apoptosis 48 hrs post treatment removal. All treated cells reported a statistically significant decrease in viable cells when compared to the control group, (all P<0.0001). D-SCH3 and R-SCH3 treatments both produced a statistically significant decrease in viable cells when compare with MMF alone, (both P<0.0001). There was also a statistically significant decrease in the percentage of viable cells when treated with D-SCH3 and R-SCH3 compared with their relevant single therapies, (both P<0.0001). All treated cells also produced a statistically significant increase in the percentage of cells in early apoptosis when compared with the control (MMF, DOX and RAD P<0.0001, D-SCH3 P=0.0009 and R-SCH3 P=0.0365). Both D-SCH3 and R-SCH3 produced a statistically significant increase in the percentage of early apoptotic cells when compared to MMF alone (both P <0.0001). RAD alone produced a statistically significant increase in early apoptotic cells when compared with R-SCH3 (P<0.0001). When comparing the percentage of late apoptotic cells in Figure 4.32C, there was a statistically significant increase in the percentage of cells in late apoptosis when treated with MMF, D-SCH3, RAD and R-SCH3 compared with the control (all P <0.0001). There was a statistically significant increase in the percentage of cells in late apoptosis when treated with D-SCH3 and R-SCH3 compared with MMF alone (both P <0.0001). Finally, both D-SCH3 and R-SCH3 produced a statistically significant increase in the percentage of late apoptotic cells when compared to DOX alone and RAD alone (both P <0.0001). There were no statistically significant changes in the percentage of necrotic cells 48 hrs post treatment removal.

In summary the results from Figure 4.32 support the hypothesis that a SCH3 combination therapy of R-SCH3 or D-SCH3 is able in significantly increase apoptosis when compared to the individual therapies in R3D3 resistant cells. This may be due to the previously mentioned mechanisms in which the SCH3 combination therapy is working.

4.4.22 Analysis of Glutathione levels Doxorubicin + Radiotherapy resistant MDA-MB-231 cells after combination treatment with Doxorubicin, Radiation, and monomethyl Fumarate

The results shown in Figures 4.33 and 4.34 were gathered as described in Section 2.3.8. Cells were harvested so GSH levels could be measured; 25 hours into a 48hour treatment schedule or 1 hr after the second therapy was administered in the combination treatment, immediately after the treatment was removed (0HR), 24 hours after the treatments were removed and 48 hours after the treatment were removed as previously detailed in Section 2.3.6. All time points are an average of three independent experiments. The combination index results of R3D3 untreated control cells, 0.2 μM DOX, 2 μM MMF and SCH3 combination treated cells are detailed in Figure 4.33.

(A)

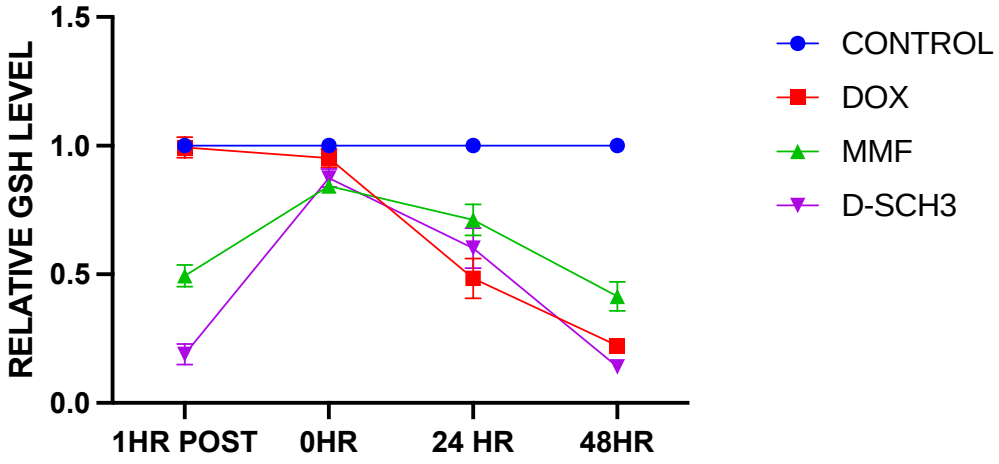

(B)

Bonferroni's multiple comparisons test	P Value 1 HR post	P Value 0HR	P Value 24HR	P Value 48HR
CONTROL vs. DOX	>0.9999	0.3011	<0.0001	<0.0001
CONTROL vs. MMF	<0.0001	0.0004	0.0030	<0.0001
CONTROL vs. SCH3	<0.0001	0.0018	0.0003	<0.0001
DOX vs. MMF	<0.0001	0.0047	0.0129	0.0003
DOX vs. SCH3	<0.0001	0.0333	0.3037	0.0568
MMF vs. SCH3	<0.0001	>0.9999	0.3835	<0.0001

Figure 4. 33 The affect single therapies DOX 0.2 μM and MMF 2 μM, and combination therapy SCH3 MMF 2 μM 1st + DOX 0.2 μM 24 hours later.

Data reported is an average of three independent experiments in triplicate. (B)A one-way ANOVA with Bonferroni post testing was performed using GraphPad prism 9.2.1 comparing each treated and untreated group to each other, *P<0.05, **P<0.01, ***P<0.001 and ****P<0.0001 (applicable for Figure 4.35 - 4.36).

Results from Figure 4.33 suggest that 1 hr post treatment administration, there was a statistically significant reduction in relative GSH levels when comparing D-SCH3 and MMF with the control, MMF, and DOX alone (all P<0.0001, Figure 4.33B). 0 hrs post treatment removal there was also a statistically significantly reduced relative GSH level when comparing D-SCH3 to the control and Dox (control, P=0.0018 and DOX P=0.033, Figure 4.33B). There was also a statistically significant reduction in relative GSH levels when comparing MMF to the control and Dox (control, P=0.0004 and DOX, P=0.0047, Figure 4.33B). 24 hrs post treatment there was a statistically significantly reduced relative GSH level when R3D3 cells were treated with DOX, MMF and D-SCH3, compared with the control (DOX P<0.0001, MMF P=0.003 and

SCH3 P=0.0003, Figure 4.33B). There was also a statistically significantly reduced relative GSH level when comparing DOX treated R3D3 cells and MMF treated R3D3 cells (P=0.012, Figure 4.33B). 48 hrs post treatment removal there was a statistically significant reduction in relative GSH levels when R3D3 cells were treated with DOX, MMF and D-SCH3 compared to the control (all P<0.0001, Figure 4.33B). There was also a statistically significant reduction in relative GSH levels when R3D3 cells were treated with DOX and D-SCH3 compared to MMF treated cells (DOX P=0.0003, D-SCH3 P<0.0001, Figure 4.33B).

Overall, these results suggest that D-SCH3 combination can significantly reduce the relative GSH levels in R3D3 cells. The data in Figure 4.33 supports the findings in Section 4.4.21 that suggest an increase in apoptotic cells following D-SCH3 treatment of R3D3 cells. We hypothesised that this increase in apoptotic cells was due to MMF inhibiting the nuclear translocation of NRF2 in R3D3 cell, thereby preventing the generation of GSH as seen in Figure 4.35. This supports the hypothesis that SCH3 treatment inhibits the production of GSH which prevents the neutralisation of ROS generated by doxorubicin treatment, allowing ROS generated to induce SSB and DSB, which induces apoptosis.

Figure 4.34 details the combination index analysis of R3D3 untreated control cells, Rad 2 Gy, MMF 2 μM and SCH3 combination treated R3D3 cells.

(A)

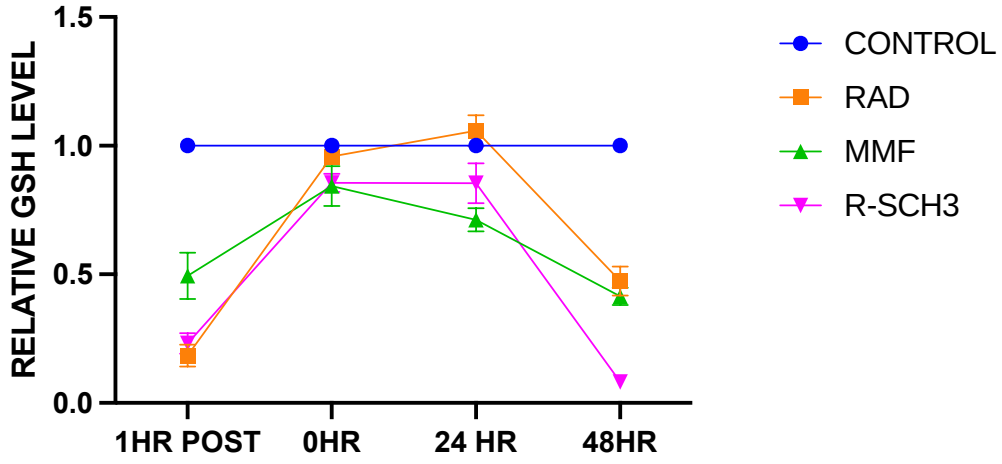

(B)

Bonferroni's multiple comparisons test	P Value 1 HR post	P Value 0HR	P Value 24HR	P Value 48HR
CONTROL vs. RAD	0.0002	>0.9999	>0.9999	0.0001
CONTROL vs. MMF	0.0024	0.2057	0.0430	<0.0001
CONTROL vs. SCH3	0.0002	0.2763	0.5410	<0.0001
RAD vs. MMF	0.0052	0.1785	0.0030	0.6321
RAD vs. SCH3	>0.9999	0.2704	0.0433	0.0001
MMF vs. SCH3	0.0123	>0.9999	0.1880	0.0003

Figure 4. 34 The affect single therapies RAD 2 Gy and MMF 2 μM, and combination therapy SCH3 MMF 2 μM 1st + RAD 2 Gy 24 hours later.

From Figure 4.34 it was reported that 1 hr post treatment removal there was a statistically significant reduction in relative GSH levels in R3D3 cells treated with RAD, MMF and R-SCH3 when compared to the control (RAD P=0.0002, MMF P=0.0024, R-SCH3 P=0.0002, Figure 4.34B). There was also a statistically significant reduction in relative GSH levels in R3D3 cells treated with RAD and R-SCH3 when compared with MMF alone (RAD P=0.0052, R-SCH3 P=0.0123, Figure 4.34B). 0 hrs post treatment there was no statistically significant changes in relative GSH levels in any R3D3 cells. 24 hrs post treatment there was a statistically significant reduction in relative GSH levels when comparing MMF treated R3D3 cells with the control and RAD (Control P=0.043, RAD P=0.003, Figure 4.34B). There was also a statistically significant reduction in the relative GSH levels of R3D3 cells when treated with R-SCH3 compared to RAD (P=0.0433, Figure 4.34B). 48 hrs post treatment removal there was a statistically significant reduction in the relative GSH levels of R3D3 cells treated with RAD, MMF and R-SCH3 compared with the control (all P<0.0001, Figure

4.34B). There was also a statistically significant reduction in the relative GSH levels of R3D3 cells treated with R-SCH3 compared with RAD and MMF (RAD P=0.0001 and MMF P=0.0003, Figure 4.34B).

In summary the results from Figure 4.34 suggest R-SCH3 combination can significantly reduce the relative GSH levels in R3D3 cells. The data in Figure 4.354 supports the findings in Section 4.4.21 that suggest an increase in apoptotic cells following R-SCH3 treatment of R3D3 cells for reasons detailed above.

4.4.23 Detection of Autophagic Radiation + Doxorubicin resistant cells after combination treatment with Doxorubicin, Radiation and Monomethyl Fumarate

As previously described in section 2.3.8 an autophagy assay was used to investigate the percentage of cells that had undergone autophagy because of treatment. This assay was carried out at 3 different time points to co-inside with the Cell Cycle analysis data (Section 4.4.20). This section investigated the radiation and doxorubicin resistant cells that were treated with MMF 2 μM alone, radiation at 2 Gy, DOX 0.2 μM as well as the schedule 3 combination of MMF 2 μM + Rad 2 Gy and MMF 2 μM +Dox 0.2 μM and results displayed in Figure 4.35.

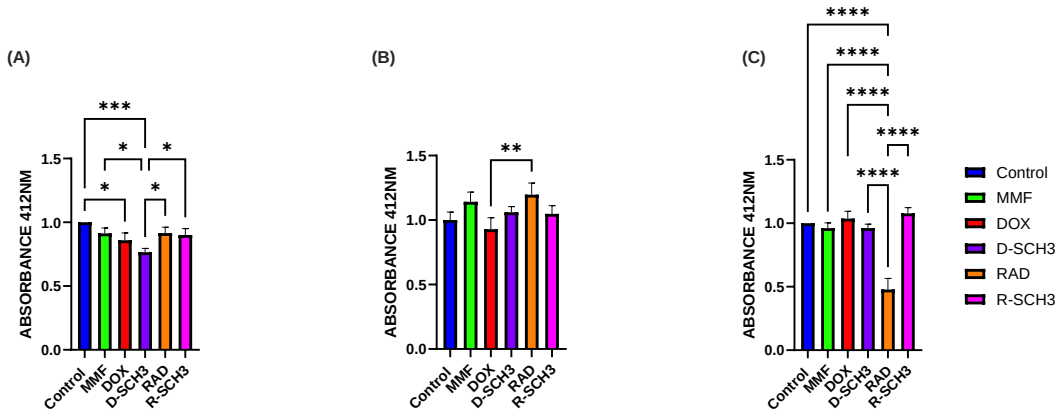

Figure 4. 35 The effect of; RAD alone 2 Gy, MMF alone 2 μM or Schedule 3 combinations of reagents on the induction of autophagy.
Data is expressed relative to the control. Cells were measure on a fluorescent microplate reader at 412nm. (A) 0 hours after treatment removed. (B) 24 hours after

treatment removed. (C) 48 hours after treatment removed. All graphs are displayed as mean and standard deviation of 3 individual experiments, in triplicate. One -way ANVOA was carried out with Bonferroni's correction.

As reported in Figure 4.35A the absorbance measured 0 hours post treatment removal showed some statistically significant results. There was a statistically significant decrease in absorbance of DOX alone (P=0.0221) and DOX SCH3 (P=0.0003) when compared with the control. There was also a statistically significant decrease in the absorbance of cells treated with DOX SCH3 compared with MMF alone (P=0.0152). Finally, there was a statistically significant decrease in the absorbance of cell treated with DOX SCH3 when compare with RAD SCH3 (P=0.0299).

The only statistically significant change in absorbance was found when comparing DOX and RAD 24 hours post treatment removal, (Figure 4.37B). There was a statistically significant increase in absorbance when cells were treated with RAD alone compared with DOX alone (P=0.0098).

There was a statistically significant decrease in absorbance of cells 48 hours post treatment (Figure 4.37C) when cells were treated with RAD alone compared with Control, MMF alone, DOX, D-SCH3 and R-SCH3, all produced P values of <0.0001.

These results suggest that RAD alone treated R3D3 cells may be producing a reduced autophagic signal 48 hrs following treatment. However, this was the only treated R3D3 group that produced a significant change in autophagic signals when compared to any other group. Therefore, it appears that the combination therapies D-SCH3 and R-SCH3 are not inducing cell death via an autophagic pathway.

4.4.24 Quantification of DNA damage and repair using Comet Assay, of MDA-MB-231 cells after combination treatment with Doxorubicin, Radiation and Monomethyl Fumarate

A comet assay was used to quantify the DNA damage induced by radiation alone at 2 Gy, MMF alone at 2 μM and the SCH 3 combination of R-SCH3as well as DOX 0.2 μM and D-SCH3 combination. This assay was previously described in Section 2.3.12. DOX treated R3D3 cells were exposed to treatment for 48 hrs before harvesting at 0 hrs post treatment removal, following this cell for collection at 24 hr and 48 hr time points were covered in drug free complete DMEM media until appropriate harvest time was reached.

There were differences in the harvest time points between DOX treated R3D3 cells and RAD treated R3D3 cells. For RAD treated R3D3 cells, comet analysis was carried out immediately after treatment (rather than after cells were exposed to drug for 48 hrs in DOX treated R3D3 cells) as when using radiation, a spike in ROS occurs immediately after irradiation exposure and in order to quantify this spike in DNA damage a comet assay was carried out immediately following this, 24 hrs after initial treatment and 48 hrs after initial treatment. This same time points were used for MMF alone and R-SCH3 treated cells, for R-SCH3 treatment the 0-hr time point was taken 24 hrs after MMF administration and immediately after these pre-exposed MMF cells were irradiated. This allowed for an analysis of cells exposed to radiation without MMF prior exposer and those with prior MMF exposure. MMF alone treated cells were exposed to MMF for 10 minutes (this is to allow for the time taken to irradiate cells using X-irradiator and carry cell back to a cell culture hood for harvesting).

- Comparison of DNA fragmentation of D-SCH3 combination at 0hr, 24hr and 48hr – Analysis of DNA repair

The median tail moment (AU) was calculated for each treatment; MMF 2 μM, DOX (0.2 μM), D-SCH3 combination as seen in Figure 4.36. This was determined for each time point measured, 0hrs post treatment removal, 24hours post treatment removal and 48hours post treatment removal. Statistical analysis was carried out on these results using a one-way ANOVA with Bonferroni's correction, the results are detailed in appendix 10 and 11.

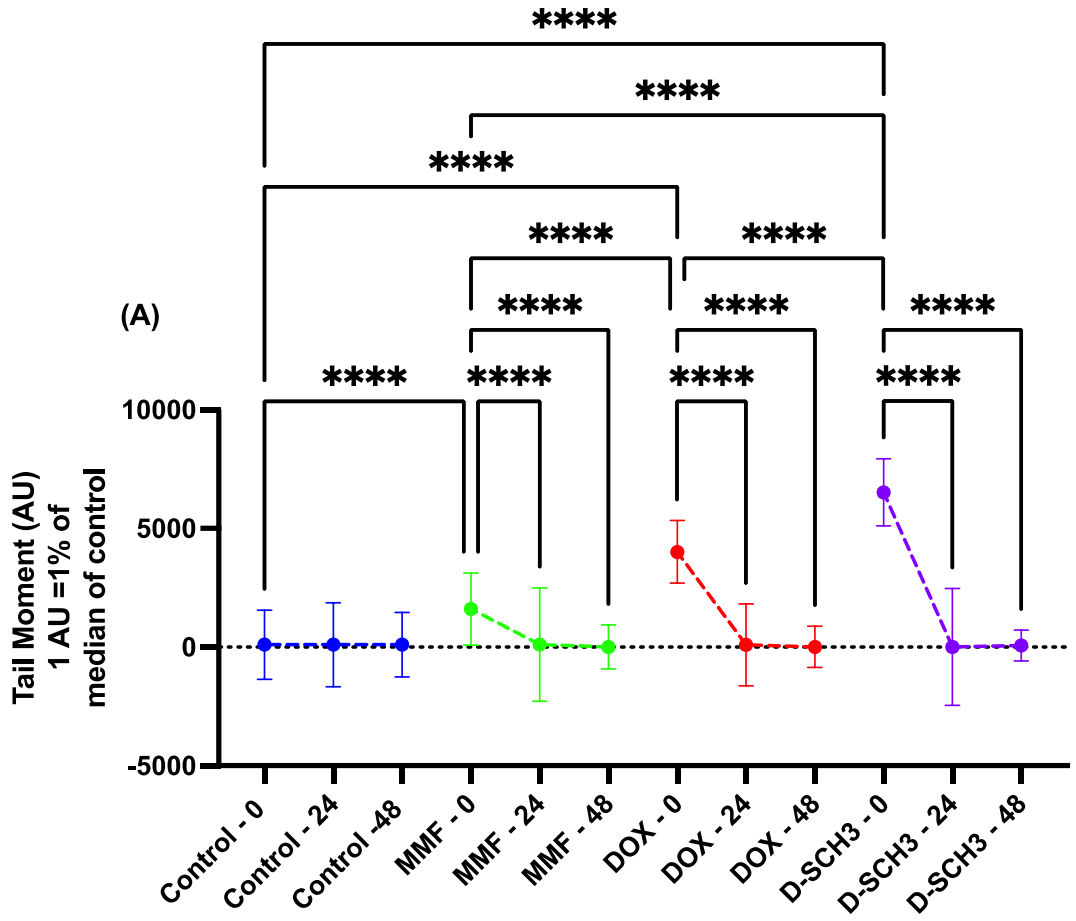

Figure 4. 36 The median DNA damage quantified as Tail Moment (AU) is displayed as a percentage of the control median.

MMF alone, DOX alone, D-SCH3 combination were the treatments used as described time points of 0hr post treatment removal, 24hrs post treatment removal and 48hrs post treatment removal are compared for each treatment. Results are displayed as an average of 3 independent experiments with 70 comets per treatments group. Statistical analysis was carried out using a one-way ANOVA with Bonferroni's correction and are detailed in Table 4.3. P>0.0001 ****, P>0.001 ***, P>0.01** and P>0.1 * (applicable to Figure 3.36 – 4.37) (see appendix 10 and 11).

The results from Figure 4.36 suggested, a statistically significant increase in 0hr median tail moments of cells treated with MMF, DOX and D-SCH3 at the 0-hr median tail moment, when compared with 0hr medial tail moment of the untreated control (all P<0.0001). There was a statistically significant increase in median tail moment of cells treated with MMF alone at 0hours post treatment removal compared with DOX 0 hr

post treatment removal (P<0.0001). There were statistically significant decreases in median tail moment when comparing MMF 0hr, DOX 0hr and D-SCH3 0hr, to their respective 24 hr and median tail moments (all P<0.0001). There was a statistically significant decrease in median tail moment when comparing MMF 0hr and DOX 0hr to their respective 48 hr and median tail moments (both P<0.0001). There was a statistically significant increase in 0 hr median tail moment of MMF alone treated R3D3 cell, when compared to the 0-hr median tail moment of D-SCH3 treated R3D3 cells (P<0.0001). There was a statistically significant increase in the 0-hr median tail moment of D-SCH3 treated R3D3 cells when compared to the 0-hr median tail moment of DOX alone treated R3D3 cells (P<0.0001).

Overall, these results suggest that treatment of cells with D-SCH3 initially results in a greater DNA fragmentation than DOX alone treated R3D3 cells. However, with all treatments tested, this DNA fragmentation did not continue 48 hrs after treatment. This may be due to R3D3 cells being able to repair DNA fragmentation efficiently or that because of treatment, the DNA is incredibly fragmented, causing hedgehog comets, as previously described. This comet data was surprising as there is a significant increase in apoptotic cells found after treatment with D-SCH3, therefore it was expected that a larger median tail moment would be visible following treatment of these cells. However, the results do support the hypothesis that D-SCH3 combination induced more DNA damage than DOX alone in R3D3 cells.

4.4.25 Comparison of DNA fragmentation of D-SCH3 combination at 0hr, 24hr and 48hr – Analysis of DNA repair

The median tail moment (AU) was calculated for each treatment; MMF 2 μM, RAD 2 Gy, R-SCH3 combination.

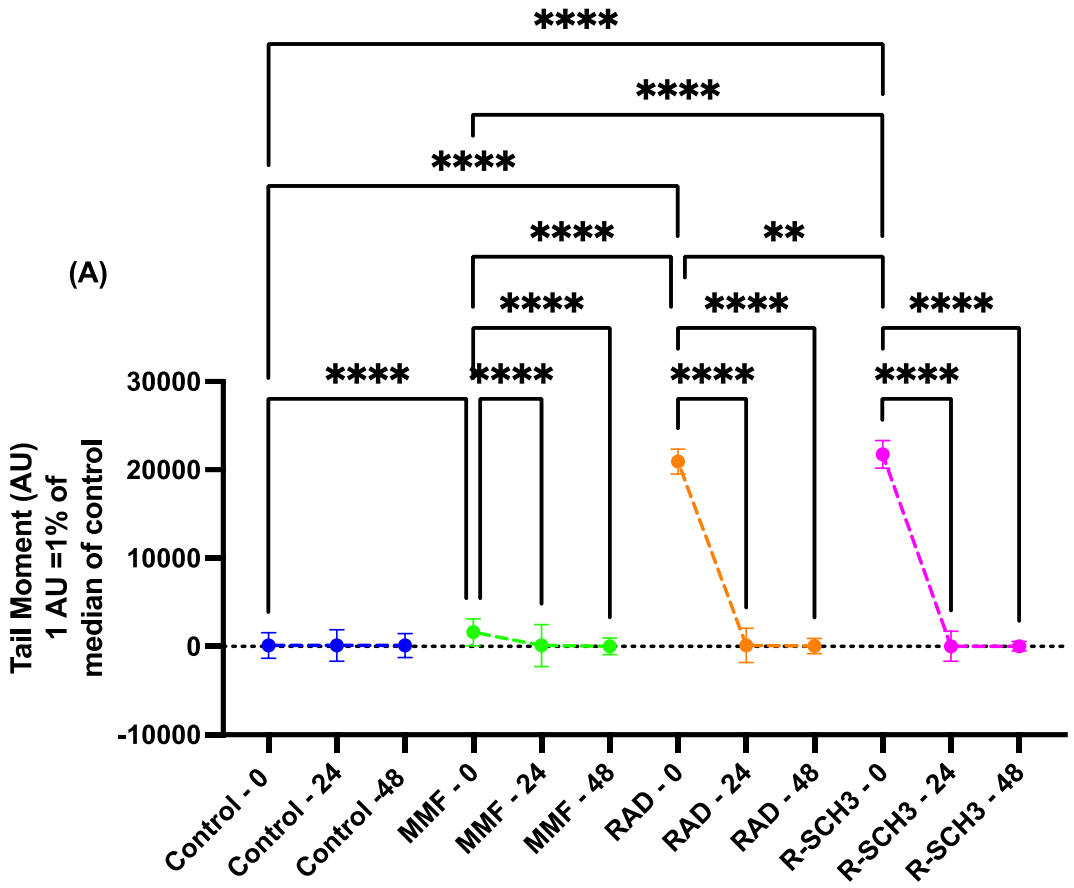

Figure 4. 37 The median DNA damage quantified as Tail Moment (AU) is displayed as a percentage of the control median.

The results from Figure 4.37 suggested that there is a statistically significant increase in 0 hr median tail moment of R3D3 cells treated with RAD alone and R-SCH3 when compared to the untreated control and MMF alone median tail moment at 0 hrs post treatment (both P<0.0001). There was a statistically significant increase in the median tail moment 0 hrs post treatment when R3D3 cells were treated with RAD alone and R-SCH3 compared to MMF alone treated cells (both, P<0.0001) and a statistically significant decrease in the median tail moments of R3D3 cells treated with RAD and R-SCH3 when comparing 0 hr post treatment to 24 hr and 48 hr post treatment median tail moments for respective therapies (all P<0.0001).

Overall, the data from Figure 4.37 supports the hypothesis that R-SCH3 can induce DNA damage, and this was found to be significantly greater DNA fragmentation than RAD alone induced. The DNA fragmentation of R3D3 treated cells also appears to be repaired 24 and 48 hrs after treatment following Rad alone and R-SCH3 treatment.

These results were surprising as the results from Annexin V reported a statistically significant percentage of apoptotic cells following RAD and R-SCH3 treatment in R3D3 cells. However, it may be that the initial DNA fragmentation found 0 hrs post treatment is able to induce the apoptotic pathway and even though this DNA fragmentation appears to be repairing from the comet data, the apoptosis is already underway and cell death pathway in R3D3 cells are already inducing, causing significant cell death. As previously stated, it is known that comet assays are not the most effective at visualising DNA fragmentation when analysing apoptotic cells, they can lead to the formation of hedgehog comets and results are often not fully representative of the damage induced by therapies.

4.5 Discussion

4.5.1 Doxorubicin resistant cells

Our derived D3 cell line has been shown to have therapy resistance to doxorubicin treatment, compared with parent MDA-MB-231 cells. After establishing this resistance, these cells were used to investigate the potential of MMF in scheduled combination to re-sensitise these cells to the treatment modalities that they had hitherto shown resistance to. It was found that SCH3 combination of MMF 1st +DOX was the combination therapy that produced a statistically significant reduction in cell survival compared to the control, MMF alone and DOX alone. This suggests that this SCH3 combination is the most effective therapy tested at killing D3 cells and could potentially be re-sensitising the D3 cells to death via doxorubicin. However, 3D models and mechanistic studies were carried out to determine what was happening to these cells on a mechanistic level after D-SCH3 treatment and if any differences were seen between single therapy and D-SCH3 combination in D3 cells.

Upon reviewing the data in section 4.4.1, it was found that with respect to spheroid growth, that AUC values of D3 resistant cells, D-SCH1 and D-SCH3 induced statistically significant decreased in AUC values compared with control D3 cells, and DOX only treated cells, D-SCH1 also demonstrated a statistically significant decrease in AUC value when compared with MMF alone. However, given that the 2D and 3D data suggests that the D-SCH3 combination is the most statistically significant combination that will induce cell death this was the schedule that was chosen to be investigated mechanistically.

Results from cell cycle analysis suggest that after treatment with DOX, MMF and D-SCH3 combination, for D3 cells at 0 hours post treatment removal there was cell cycle arrest in the G1 phase of the cell cycle (Figure 4.7). Cell cycle arrest in G1 phase of the cell cycle inhibits cells from progressing through the cell cycle and provides an opportunity for cells to carry our repair mechanisms or follow an apoptotic pathway (Murad *et al*., 2016). This coincides with the statistically significant decrease in percentage of viable cells when treated with D-SCH3, MMF and DOX alone in Figure 4.10A. 24 hours later (Figure 4.8) cell exhibit a different percentage of cells in each phase of the cell cycle. There is a decrease in the percentage of cells in G1 and G2/M

phase of the cell cycle when treated with D-SCH3, MMF and DOX compared with the percentage of control cells in G1 and G2/M phase of the cell cycle. This would suggest that there is a decrease in the percentage of cells that are progressing through the cell cycle, as well as cells potentially being trapped at the G2/M checkpoint, due to an accumulation of DNA strand breaks that are unable to be repaired. This is reflective of the findings in Figure 4.10B, there is a statistically significant increase in the percentage of cells in the late apoptotic phase of apoptosis when treated with MMF, DOX and D-SCH3 when compared with the control cells. Taken together these data supports the idea that cells treated with D-SCH3, MMF and DOX are being arrested in G1 phase of the cell cycle, where it is determined that these cells are unable to continue through the cell cycle process and enter the apoptotic pathway. It appears that some of the treated cells can overcome G1 cell cycle arrest and continue through the cell cycle as seen in Figure 4.9. Cells treated with DOX show a similar percentage of cells in G2/M and S phase compared with the control cells. This is reflective of the Annexin V data in Figure 4.10C as DOX treated cells show no significant difference in viable cells compared with the control, suggesting doxorubicin resistant cells can repair following treatment with doxorubicin alone. However, the opposite is seen in D-SCH3 treated D3 cells. From Figure 4.9, the cell cycle data indicates a reduced percentage of D-SCH3 treated cells in the S phase and G2/M phases compared with all other treated cells. This would suggest that a reduced percentage of D-SCH3 treated D3 cells are being allowed to progress through the cell cycle and divide. This idea is supported by the data in Figure 4.10C, where there is a statistically significant increase in the percentage of cells in late apoptosis when treated with D-SCH3 compared with the D3 control cells and DOX alone treated cells. Overall, the data from figure 4.7-4.10 suggest that D-SCH3 treated D3 cells are unable to progress through the cell cycle and are entering the apoptotic pathway, ultimately resulting in cell death. As this is not the case with DOX only treated doxorubicin resistant cells, where the data suggests initial cell cycle arrest, the treated cells are able to repair and continue through the cell cycle and do not result in death via apoptosis. These results suggest that the D-SCH3 combination of MMF 1st + DOX is effective at killing doxorubicin resistant D3 cells via apoptosis which is not seen in doxorubicin alone treated D3 cells. This idea is supported by the clonogenic data seen in Figure 4.3 where D-SCH3 treated D3 cells had a significantly reduced the survival fraction of 2D cells compared with control D3 cells, DOX only and MMF only treated D3 cells.

Following Glutathione analysis of D3 cells treated with MMF and D-SCH3 combination in Figure 4.10, there was no stabilising of the relative glutathione levels of D3 cells after treatment with these therapies 48 hrs post treatment removal, D-SCH3 treated D3 cells still had statistically significantly reduced relative GSH levels compared with the control and DOX alone treated D3 cells. This suggests that MMF can reduce the relative GSH levels of D3 cells up to 48 hrs post treatment removal and may explain why elevated apoptotic markers are present following D3 treatment with D-SCH3 combination therapy. This potentially could be due to the glutathione production in D3 cells being inhibited by MMF following treatment with D-SCH3 and the cells are failing to stabilise their relative glutathione levels post treatment, resulting in the cells being more susceptible to damage. In the case of treatment with D-SCH3 this is reflective of the findings in Figure 4.4 where the clonogenic analysis of D3 survival was statistically significantly reduced following treatment with SCH3 combination.

The results from Figure 4.11 suggest that the mechanism of action by which D3 cells are dying following treatment with D-SCH3 if not via autophagy. There was no significant increase in treated cells vs control cells at all 3 time points measured.

Upon reviewing the data in Figure 4.12 there was a significant increase in the median tail moment of D3 cells treated with D-SCH3 combination 0 hrs post treatment removal. However, at 24 hours and 48 hours post treatment there was no statistically significant increase in median tail moments when comparing the treated D3 cells tail moments to the control or any other treated cell. This suggests that although the damage is being induced in these D3 cells, they can repair cells 24 hours post treatment removal and that repair is sustained 48 hours later. These results are contradictory of those reported in the Annexin V and Cell Cycle analysis studies (Figures 4.6 and 7) and suggest that D3 cells are undergoing apoptosis following treatment with D-SCH3 combination. However, this has been reported in previous studies (Siles *et al.,* 1998, O'Callaghan *et al.,* 2001). These studies all demonstrated that although comet assays are useful in detecting DNA damage in cells, they are not adequate to detect modes of cell death and that in apoptotic or necrotic cells. In this case the DNA can be extremely fragmented and by using a comet assay in a comet assay the fragmented DNA is being electrophoresed out of the gel and therefore unable to be accurately measured.

4.5.2 Radiation resistant cells

Treatment of radiation resistant R3 cells caused an increase in the number of cells in the sG1 phase of the cell cycle, when they were treated with MMF, RAD and R-SCH3 compared with the untreated control R3 cells (Figure 4.18). This could indicate that cells are beginning apoptosis as cells with a decreased propidium iodide intensity are displayed in the sub G1 phase of the cell cycle (Rieger *et al.,* 2011). This can be useful in determining apoptotic cells; however, a more accurate assay is required such as the Annexin V assay. As such the results from Figure 4.20A show a statistically significant decrease in the percentage of viable cells when they were treated with R-SCH3, compared with the R3 untreated control, RAD only and MMF only treated R3 cells. There is also a statistically significant increase in the percentage of cells in late apoptosis when treated with R-SCH3 compared with the untreated control, MMF and RAD only. The percentage of cells in each phase of the cell cycle appear to be like that of the untreated control cells 24 hours following treatment removal (Figure 4.18). This is again reflected in Figure 4.19B (24 hr), investigating apoptosis as the percentage of viable cells when treated with MMF and RAD only increases when compared to Figure 4.18A (0 hr). However, R-SCH3 treated R3 cells still suggest a statistically significantly greater percentage of cells in late apoptosis when compared to all other R3 cells (Figure 4.21C). R-SCH3 is the only treated group of R3 cells that shows no statistically significant increase in viable cells 48 hours post treatment, suggesting that this treatment can induce R3 cells damage and prevent cell repair up to 48 hrs post treatment removal.

This is reflective of the data detailed in Figure 4.15, using a clonogenic assay to determine cell survival post treatment. R-SCH3 treated R3 cells were the only treated cells that showed a statistically significant decrease in cell survival fraction when compared to the untreated control R3 cells and MMF and RAD alone treated R3 cells. Similarly, in 3D analysis (Figure 4.16), R-SCH3 was the only scheduled combination to produce a statistically significant decrease in AUC values when compared to the untreated R3 control and RAD alone treated R3 cells.

Results from Figure 4.22 indicate that 48 hrs post treatment R3 cells treated with R-SCH3 and MMF have statistically significantly reduced relative glutathione levels. As hypothesised, this reduction in glutathione levels post treatment with MMF may be

reflective of the findings detailed above. As treatment with the R-SCH3 schedule is reducing the intracellular glutathione levels, this may be the explanation as to why clonogenic analysis, Annexin V and spheroids have a decrease in cell survival and upregulation of apoptosis following treatment with R-SCH3.This could be due to MMF inhibiting intracellular glutathione production and the cells are sensitized to irradiation with 2 Gy 24 hours following.

There are some statistically significant increases in absorbance at 412nm in 0hrs post treatment removal experimental groups, (Figure 4.30), compared to the untreated control R3 cells. This significant increase is however not found at any other time point and there is little difference in absorbance measure among treated R3 cells. This suggest that autophagy is not the mechanism by which R3 cells are being killed by R-SCH3 combination, with little change in the absorbance measured, which is a direct reflection of intracellular autophagic vessels.

The results from comet assays carried out to investigate DNA damage of R3 cells following treatment with MMF, RAD and the R-SCH3 combination, detailed in figure 4.24. The results suggest that 48 hours post treatment removal, R3 cells treated with R-SCH3 combination have a significant increase in median tail moments when compared with the untreated control R3 cells and all other treated R3 cells, Suggesting the R-SCH3 combination was inducing damage, and that damage was unable to be repaired 48 hours post treatment removal. This data supports the results from Annexin V, clonogenic assays and 3D spheroid result when treating R3 cells treated with R-SCH3.

4.5.3 Radiation and Doxorubicin resistant cells

Following development of radiation + Doxorubicin resistant cells (R3D3), R3D3 cells had the highest cell survival fraction when investigating survival after treatment with 1.5 μM Dox and 3 Gy dose of radiation (Section 4.4.17). R3D3 was therefore the R+D resistant cell line that was chosen to investigate potential combination therapies to overcome cell resistance and re-sensitize cells to death. R3D3 cells were used to investigate scheduled Radiation combination therapies and scheduled Doxorubicin combination therapies (Section 4.4.17). It was found that the R-SCH3 treatment was

the only scheduled combination therapy to significantly reduce the survival fraction of R3D3 cells when compared with single therapies (control, radiation and MMF). Treatment of the R3D3 cells with R-SCH3 also significantly reduced the survival fraction of R3D3 cells when compared to the other two scheduled radiation combination therapies investigated (R-SCH1 and R-SCH2), suggesting this therapy would be the most suitable Radiation combination candidate to investigate the underlying mechanistic properties. D-SCH3 was the only scheduled DOX combination to significantly reduce the survival fraction of R3D3 cells only when compared to single therapies (untreated control, DOX and MMF). D-SCH3 also significantly reduced the survival fraction when compared with the two other DOX scheduled combination therapies (D-SCH1 and D-SCH2). Therefore, D-SCH3 is the most appropriate candidate to investigate mechanistic properties of following doxorubicin combination therapy.

When investigating 3D spheroids, Figure 4.27 showed that treatment with R-SCH3 in R3D3 cells group to report a significantly decreased in spheroid volume over time, compared to the control. However, when investigating AUC values, R-SCH3 significantly reduced AUC values compared with single therapies (untreated control, Rad and MMF) and the two other scheduled radiation combinations (R-SCH1 and R-SCH2), suggesting that the results found in 2D clonogenic analysis (Figure 4.26) reflect the findings of 3D spheroid investigation. Thus, suggesting that R-SCH3 is the most appropriate radiation combination to investigate R3D3 mechanistic properties.

Figure 4.27 suggests that with respect to spheroid growth, D-SCH2 and D-SCH3 combination therapies significantly reduced AUC values when compared with single treatments (untreated control, DOX and MMF). The only difference between these two doxorubicin combination therapies was that D-SCH2 induced a significantly lower AUC value when compared to D-SCH3. These results are not entirely reflective of 2D clonogenic data in Figure 4.27, which reported D-SCH3 produced significantly lower survival fraction when compared with single therapies (untreated control, DOX and MMF). As well as the two other doxorubicin combination therapies (D-SCH1 and D-SCH2), suggesting that D-SCH3 was the most effective doxorubicin combination therapy at reducing survival fraction of R3D3 cells. This however may be due to be previously described differences between 2D and 3D investigations.

For both radiation and doxorubicin combinations, SCH3 induced the lowest CI values indicating synergy at all concentrations tested. Therefore, after evaluating clonogenic analysis and 3D spheroid and CI data, it was decided that R-SCH3 and D-SCH3 were the most appropriate radiation and doxorubicin combination therapies to use to investigate the mechanistic properties of R3D3 cells.

Cell cycle analysis (Figure 4.29 - 4.31) results indicated that R3D3 cells treated with D-SCH3 and R-SCH3 were the only treated cells to have a decreased percentage of cells in S, G1 and G2/M 24- and 48-hours following treatment removal. This suggest that less cells progress through the cell cycle when treated with D-SCH3 and R-SCH-3 compared with, doxorubicin, MMF, radiation untreated control R3D3. Cell cycle analysis showed that R-SCH3 and D-SCH3 treated cells had cell cycle arrest in the G1 phase of the cell cycle, which inhibits cells from progressing through the cell cycle and provides an opportunity for cells to carry our repair mechanisms or follow an apoptotic pathway (Murad *et al.,* 2016). SCH3 treatment may also be causing cell cycle arrest at the G2/M checkpoint, this would be explained by radiation and doxorubicin inducing DNA strand breaks, as ROS are not being neutralised by glutathione due to MMF administration. Therefore, the cells are unable to repair these DNA strand breaks and are unable to fully divide into two daughter cells. This is supported by the Annexin V data in Figure 4.32, in which D-SCH3 and R-SCH3 treated R3D3 cells were the only treated cells to show a significant decrease in the percentage of non-apoptotic cells when compared with the control, MMF, DOX and RAD, 0-, 24- and 48-hrs post treatment removal. D-SCH3 and R-SCH3 were the only treated R3D3 cells to show a significant increase in late apoptotic cells when compared to untreated control, MMF, DOX and RAD, 0-, 24- and 48-hrs post treatment removal. This data supports the clonogenic and spheroid data that suggested SCH3 combinations were effective at inducing R3D3 cells death.

Results from the glutathione assay (Figure 4.33 and 4.34) suggest that D-SCH3 treated R3D3 cells and R-SCH3 treated R3D3 cells show the lowest relative GSH levels of any treated or untreated R3D3 cell and that this reduction in glutathione is sustained 48 hrs following treatment removal. This could be due to the glutathione production in R3D3 cells being inhibited by MMF in SCH3 combinations and the cells are failing to stabilise the relative glutathione levels, resulting in the cells being more susceptible to damage. These relative GSH levels in R-SCH3 and D-SCH3 treated

R3D3 cells are failing to stabilise the relative glutathione levels 48 post treatment. This is reflective of the findings in Figure 4.26 where the clonogenic analysis of R3D3 survival was statistically significantly reduced following treatment with R-SCH3 and D-SCH3 combination therapies. These findings are supportive of those in the literature, as it is well established that depletion of glutathione is necessary for apoptosis (Franco *et al.,* 2007, Circ., 2009).

Once again, the data from Figure 4.35 suggest that autophagy is not the mechanism of action in which R3D3 cells are dying following treatment with R-SCH3 or D-SCH3. These findings were surprising, as previously mentioned it has been found that DMF is able to induce autophagy (Lee *et al.,* 2021). In addition to this there is evidence that in some therapy resistant cells autophagy can act as a pro-survival process, controlled increase in levels of autophagic vessels has been shown to improve cell viability, however the mechanisms in which this happens are not fully understood (Xinyu *et al.,* 2019).

There was a significant increase in median tail moment 0hrs post treatment in R3D3 cells treated with SCH3 combination therapies compared to the untreated control or any single therapies (Figure 4.36 and 4.37). This suggests that by administering MMF prior to radiation or doxorubicin the cells are sensitised to DNA damage as hypothesised. This DNA damage is repaired 24 and 48 hrs post treatment removal; however, this could be explained as detailed above when discussing D3 and R3 comet analysis 4.5.1. The limitations of comet assays have already been extensively discussed. Therefore, the median tail moments of R3D3 cells treated with SCH3 at the 24 and 48 hr time points may be too fragmented to produce an acceptable tail moment, this is supported by the significant increase in apoptosis found in Annexin V investigations Figure 4.32.

Chapter 5

Development of the Chick Embryo Tumour Model as a potential platform to investigate 3D tumours in vivo.

5.1 Introduction

At present the model used predominantly to bridge the gap from bench to clinic in cancer research is predominantly murine models. These models are essential to study tumour microenvironment, metastasis, and therapy toxicities, in 2022 there was approximately 800,000 experimental procedures carried out on animals in the UK, 12% of which were used for the purposed of cancer research (UK, Home office Statistics, 2022). There has however been a focus within the field of breast cancer research to address the issues surrounding the use of murine models to develop breast cancer treatments. A nation-wide database has been launched by the National Centre for Replacement, Refinement and Reduction (NC3Rs), to provide a platform for researchers to share details of *in vivo* investigations (-Breast, www.searchbreast.org). The aim of the database is to reduce the number of animal experiments and prevent unnecessary experiments that have already been detailed on the database, thereby reducing the number of *in vivo* investigations required (Morrissey *et al*., 2016).

There are many different types of *in vivo* investigations that can be carried out; however, the MDA-MB-231 cell line is frequently used in cell derived xerograph models (CDX) (Simmons *et al.,* 2012) and is the current model used in our lab, and as such issues surrounding this model are well characterised. The tumour grown in this model is derived from human cancerous cell and is unable to form a heterogeneous tumour *in vivo* (Hannah and Weinberg, 2011). Additionally, the murine species used as the hosts for human tumour grafts are immunocompromised and are unable to elicit any kind of immune response to the tumour or to investigative therapies, thereby limiting the information attainable as to the full effect on the entire system. Spontaneous metastasis is also difficult to replicate in these models preventing the study of metastatic cancer in these systems (Paschall and Liu, 2016). Given this absence of heterogeneity and metastases there is a direct need for another model to bridge the gap between *in vitro*, *in vivo,* and clinical studies. The Boyd Lab was awarded an NC3Rs grant in 2020 to establish and develop a Chick Embryo facility to support the development of a chicken embryo tumour model with the aim to reduce and refine murine in vivo studies.

5.1.2 Chick Embryo Model (CEM)

The CEM is comprised of a fertilised chicken egg and the choriallantoic membrane is the surface of the extraembryonic membrane of a chicken embryo, which is of great interest when using these models for investigations (Rabatti., 20212). The chorioallantoic membrane (CAM), also known as the chorioallantois, is a highly vascularised membrane found in the eggs of certain amniotes like birds and reptiles (Maugeri *et al*., 2022). It is formed by the fusion of the mesodermal layers of two extra-embryonic membranes – the chorion and the allantois and it is the avian homologue of the mammalian placenta (Kundeková *et al*., 2021). It is the outermost extra-embryonic membrane which lines the non-vascular eggshell membrane. Given the characteristics of this membrane, researchers have been investigating the use of the CAM for a variety of *in vivo* models which have the potential to reduce and replace procedures in rodents (Krutzke *et al*., 2020). The CAM model has a lower sentience than rodent models which reduces suffering and is a much cheaper alternative with a potentially higher throughput. There is also no requirement for a personal animal licence to work on these models as they are not covered by the Animal (Scientific Procedures) Act 1986 until 2/3 gestations or day 15 of embryo development.

The aim of this work was to create a facility to develop the chicken embryo tumour model as a potential *in vivo* model and alternative cancer model to mouse xenographs at the University of Strathclyde. This was done by transferring methods developed in the University of Liverpool, for growing CAM tumour models and using them to analyse cancer cells, tissue, the efficacy of combination therapies and drug gene delivery systems.

5.2 Aims

The aims of this chapter were to.

- Set up and development of Chick Embryo Model facility

- Determine the maximum dose of irradiation and concentration of cytotoxic drugs, CEM can sustain without death- to enable future tumour kill experiments

-Characterise tumours grown in CEM

5.3 Materials and methods

5.3.1 White Leghorn eggs

White leghorn chicken eggs were purchased from the Roslin Institute, University of Edinburgh, from the Dick School of Veterinary Sciences. Chickens used for egg laying were kept at Easter bush Farm in the Greenhouse building of the campus and were free roaming chickens. Eggs were collected via DHL delivery services and delivered to the University of Strathclyde within 24 hours of collection. Eggs were packaged in carboard egg cartons and wrapped in foam to avoid breakage.

5.3.2 Chick Embryo Model

Fertilised white leghorn chicken eggs were cleaned upon arrival from Roslin Institute (University of Edinburgh, Easter bush Farm, EH2 9HL) with disinfectant cleaner Safe4U. Eggs were placed in plastic trays, 4 to a row, to prevent egg rolling. The incubator (Easy advanced Incubator – Brinsea) was then set to 37.5 ^{o}C at 65% humidity and rotated at 45^{0}C every 45 minutes for the first 3 days. On day 3, the rotation was stopped, and the eggs were removed. To access the CAM, a small window was created in the eggshell. This was done by puncturing the egg (Semi-automatic pinhole egg piercer, IRYNA, Amazon UK.) and removing 3 mL of albumin using a 0.2 mm needle and 5 mL syringe. This was then covered with a piece of electrical tape to prevent leakage. Next a 2-inch piece of scotch tape was placed vertically over the egg and using fine scissors a 0.5 cm x 1 cm window in the egg was cut, leaving one end attached to create a window effect. The window was then sealed with another piece of scotch tape to prevent infection and prevent the eggs within from drying out. The eggs were then placed back in the incubator at 37.5 ^{0}C and 65 % humidity without rotation. The eggs were left until day 7 when cancer cells were implanted onto the CAM membrane. Cells were trypsinised to single cell suspension and centrifuged into a pellet at 1200g for 5 minutes. The pellet was gently washed with PBS and centrifuged again using the same conditions. The supernatant was removed at 5 µL of PBS + 5 µL of Matrigel was added to each pellet (2 million cells per egg). Once the cell pellet was prepared, viability of the embryos was assessed and if they were alive, sterile tissue paper was used to dry a small patch of CAM membrane and create trauma to membrane to ease cell implantation on the surface

of the CAM. The resulting cell pellet was added to the surface of the CAM, the window was then sealed using scotch tape and the egg was placed back into incubator. If the embryos were subject to any treatments, such as radiation, this occurred on day 10, otherwise eggs were left until day 14 and tumours dissected, and the embryo terminated using decapitation.

5.3.3 Extraction of tumour from CEM

On day 14 of the CEM cycle, the tumours present on the surface of the CAM were imaged using a fluorescent microscope (Zeiss, UK). After imaging, the tumour was dissected using fine scissors and a spatula to cut the tumour from the membrane. The tumour was then placed into 4% paraformaldehyde (PFA) (Fisher Scientific, UK) for 2 hours and then washed with PBS. The tumour sample was firstly placed into a IHC cassette (Fisher Scientific, UK) for dehydration and submerged in 70% ethanol (EtOH) 90% ETOH and 100% EtOH for 1 hour each then histoclear (Fisher Scientific, UK) for 1 hour. The tumour sample was then placed into molten wax (Fisher Scientific, UK) for 6 hours. Tumour samples were then removed and placed into wax moulds. Moulds were then set on the bench overnight and placed in the freezer until use for immunohistochemistry (IHC). Immunohistochemistry of these tumours has not yet been undertaken; analysis of tumour sections will be investigated in the next stage of the CEM project.

5.3.4 Treatments

Drugs used to test toxicity in CAM were common therapies previously used within the group; MMF (Sigma Aldrich, St. Louis, MO), stock solution 500 μM, was diluted in MEM to achieve working concentrations of 3 μM, 6 μM, 12 μM, 24 μM and 60 μM. Gemcitabine was dissolved to create a 500 μM stock solution of complete DMEM media and final concentrations of 1 μM, 2 μM, 3 μM, 4 μM and 5 μM were used. Doxorubicin was dissolved in PBS to create a 500 μM stock solution, complete DMEM media was used to create working solutions of 0.025 μM, 0.05 μM, 0.075 μM, 0.1 μM and 0.125 μM. Radiation was also applied to the chicken embryos to assess their viability post exposure. The eggs were irradiated in an XRAD225 (Precision X-ray Inc. N. Bradford, CT USA) irradiation cabinet at doses of 1 Gy radiation to 3 Gy irradiation with a dose rate of 2.3 Gy per minute.

5.4 Results

5.4.1 Set up of the CEF facility.

As the NC3Rs grant was awarded in 2020 during the COVID-19 pandemic, delivery of equipment and set up of the facility was challenging. However more critically to the project we were unable to travel to the University of Liverpool for a tech transfer with Dr Herman. One member of our team was able to travel to Liverpool and returned to Strathclyde to train the rest of the team one at a time due to restrictions. This was important for the team as we had to adapt to virtual training and problem solving due to the limited staff members allowed in the factify.

5.4.1 Initial development of the embryo model

Following set up of the CEF there were several issues faced such as control and optimisation of humidity and temperature of incubators. Maintaining the humidity of the incubators in the facility was difficult as the pumps in the Brinsea incubators had known faults and were unreliable. As a result, the CAM membranes were drying out and crusting over (Figure 5.1).

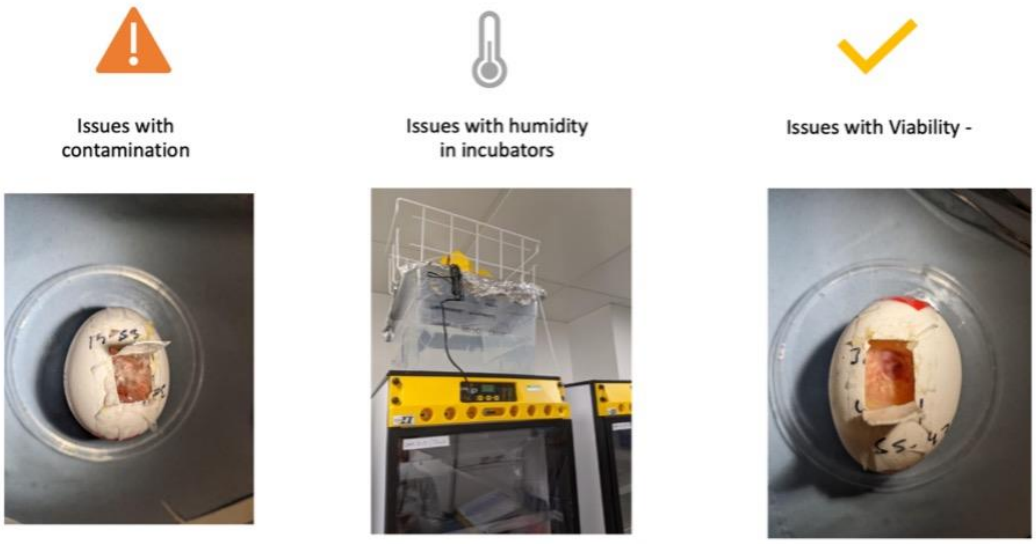

Figure 5. 1 Issues faced when setting up CEF facility.

To combat this, large basins of purified water were sealed and connected to the incubators to ensure humidity was well maintained. The humidity was also increased

from what some literature suggests, to 65% as even with optimised conditions the viability of the embryos was very low (Nowak-Sliwinska *et al*., 2014). In published papers to combat the drying out issue, authors may have required a reduced humidity as they were adding PBS to the CAM membrane every day to avoid membrane drying out. This however was not an ideal option as there were issues with embryo contamination, possibly due to the absence of a cell culture hood. Due to the pandemic, there were restrictions and availability leading to the hood being unable to be delivered and installed until 2021. Egg viability was also an issue as the nearest available facility that produced fertilised chicken eggs was in Edinburgh and required a courier to deliver the eggs. Some deliveries were left overnight in warehouses and in vans of unknown temperature which may have affected the viability of the eggs. The Roslin Institute also had issues with the fertility of their chicken as large numbers of eggs laid and which we received were infertile.

5.4.2 Development of Chick embryo tumour model

To assess the potential of the CAM model to for future study of therapy effects on various tumour types (TNBC, GBM and PANC-1), various therapeutics at a range of concentrations/doses were applied to the chick embryos. This was an essential step in developing the model as if the treatments alone killed the embryo, they would not be able to successfully continue to grow a tumour on the surface of the CAM and thus any effect of treatments on tumour growth would not be able to be measured. The investigation involved windowing and treating the CEM as previously described and visualised in Figure 5.2.

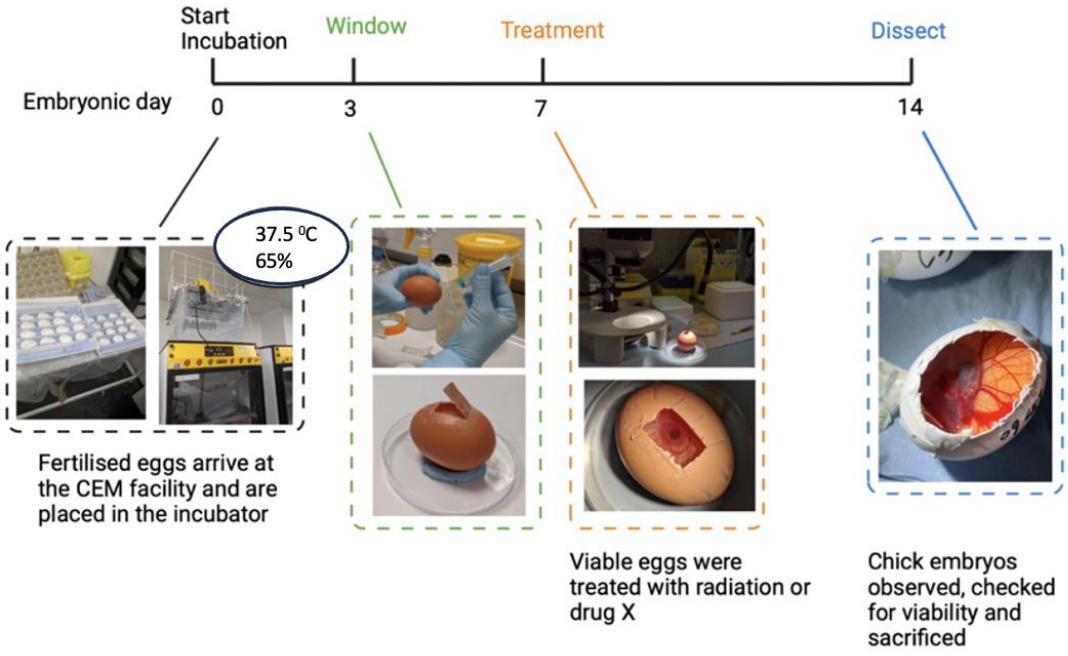

Figure 5. 2 A visual timeline of the CEM from embryonic day one to day 14.

Various therapies (Radiation, MMF, Gemcitabine and Doxorubicin) were investigated to determine their toxicity to the embryo containing eggs. If the use of these therapies alone induced CEM death, then these therapies would not be suitable candidates to investigate in this *in vivo* cancer tumour model.

CEMs were irradiated at doses of 1 Gy, 2 Gy and 3 Gy to determine if irradiation alone would kill the CEM. As radiation is a therapy that has been expensively investigated in Chapter 2,3 and 4, its potential as a therapeutic used to treat *in vivo* models had to be assessed. If radiation alone killed the CEM then this treatment would not be a

suitable option when investigating novel therapies using the chick embryo tumour model.

On embryonic day 10 the CEM were removed from the incubator and treated with the desired therapy. Figure 5.3 reports the results from irradiation of the CEM.

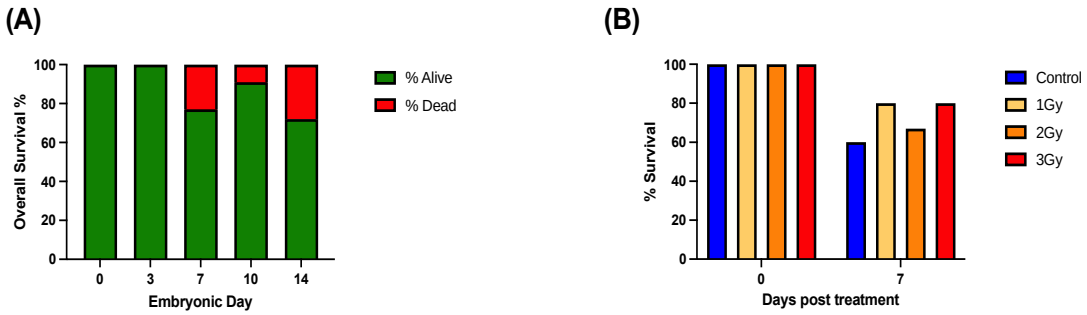

Figure 5. 3 Survival of CEMs post radiations treatment.
(A) Survival data post treatment of CEM with 0 Gy, 1 Gy, 2 Gy and 3 Gy radiation from embryonic day 0 to day 14. (B) Overall CEM survival preceding irradiation treatment until termination of embryo, 7 days post treatment (embryonic day 14) All results have an N=30.

The data from Figure 5.3 suggests that 100% of eggs that arrived were undamaged and placed in the incubator. On embryonic day 3, 100% of eggs in the incubator were viable, meaning that once windowed a live embryo was inside the egg. When investigating the survival of CEM on day 7 (treatment day) 77% of embryos were alive and any dead embryos were disposed. On day 10, 91% of these eggs were viable and on the final embryonic day 14, 72% of eggs were alive. When investigating how differing doses of radiation effected the embryos, the survival was broken down into percentage of live cells in each treatment group. As shown on the day of treatment, 100% of eggs that were treated were alive. On the final day, 7 days post treatment only 60% of control CEM were alive, 2 Gy treated CEM suggests that 67% alive and 1 Gy and 3 Gy CEM suggests 80% survival. Figure 5.8 reported no correlation between the dose of radiation administered and CEM survival, suggesting the survival or death of the embryo was determined by other factors and were not the radiation i.e., humidity or contamination of CEM.
To investigate the effects that the fumaric acid MMF has on CEM viability, a concentration range of this drug was used to investigate toxicity in the model as

detailed in Figure 5.4. MMF was selected as this drug was extensively investigated in Chapter 2,3 and 4 and was identified as a potential novel therapy to treat TNBC when administered in combination with radiation and doxorubicin. Therefore, the toxicity of MMF alone on the CEM was investigated by treating CEMs to a concentration range of 3, 6 μM, 12 μM, 24 μM, 60 μM MMF and the survival of CEM assessed and shown in Figure 5.4 below.

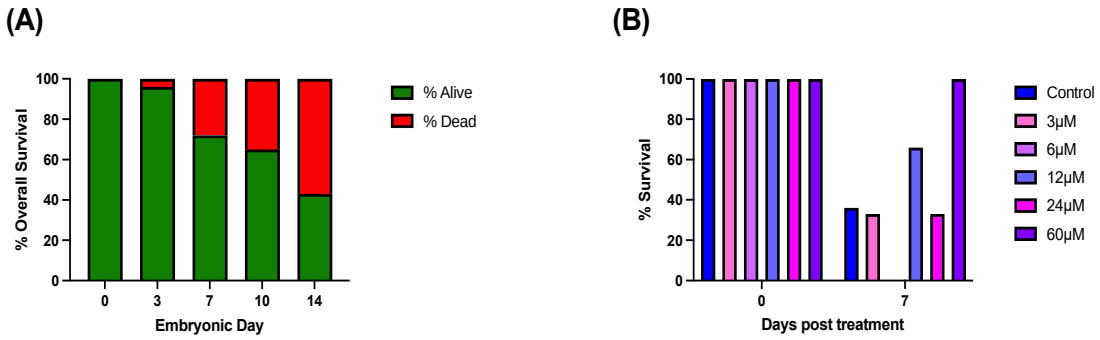

Figure 5. 4 Survival of CEMs post MMF treatment.

(A) Survival data post treatment of CEM with MMF at a concentration of 3, 6 μM, 12 μM, 24 μM, 60 μM, from embryonic day 0 to day 14. (B) Overall CEM survival preceding irradiation treatment until termination of embryo, 7 days post treatment (embryonic day 14) All results have an N=30.

From the data in Figure 5.4, 100 % of the eggs that arrived were undamaged and placed in the incubator. On embryonic day 3, 96% of eggs in the incubator were viable. When investigating the survival of CEMs on day 7 (treatment day) 72% of embryos were alive. Day 10 and 14 suggest 65% and 43% survival. When investigating how a concentration range of MMF affected the embryos, the survival was broken down into percentage of live cells in each treatment group. As shown in Figure 5.4, on the day of treatment 100% of eggs that were treated were alive. 7 days post treatment 36% of the untreated control CEM were alive, 3 μM treated CEM reported 32% alive and 0% of 6 μM treated CEM were alive on 7 days post treatment. However, 12 μM treated CEMs suggest 66% survival, 24 μM treated CEM reported 32% survival and 100% survival was seen in CEM treated with 60 μM MMF. Results

from Figure 5.4 suggest that there is no correlation between the dose of MMF used and the survival of CEM.

Gemcitabine (GEM) was chosen to investigate its toxicity as it is a common therapeutic to treat pancreatic cancer, with known therapy resistance documented in patients (Koltai *et al*., 2022). As this chemotherapy is known to induce resistance in cancer cells, it was selected for toxicity investigations in CEM model, to provide evidence should it be a candidate for future grant endeavours. Results from the survival of GEM treated CEM are detailed in Figure 5.5.

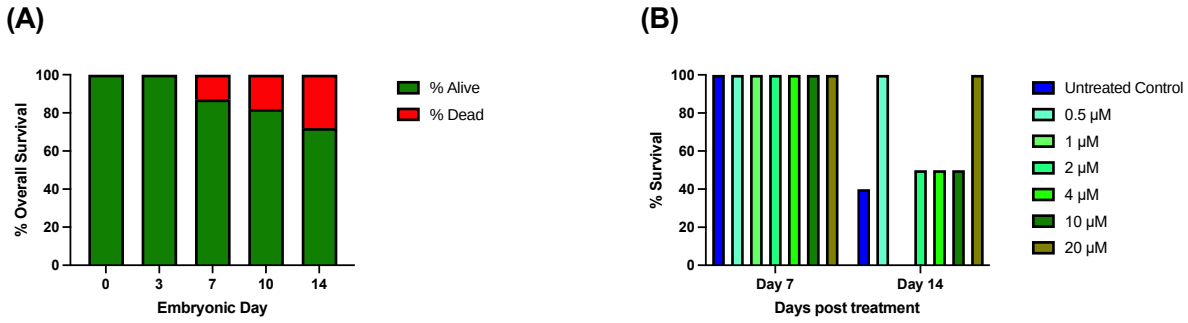

Figure 5. 5 Survival of CEMs post Gemcitabine treatment.
(A) Survival data post treatment of CEM with Gemcitabine at concentrations 0.5 µM, 1 µM, 2 µM, 4 µM, 10 µM, 20 µM from embryonic day 0 to day 14. (B) Overall CEM survival preceding irradiation treatment until termination of embryo, 7 days post treatment (embryonic day 14) All results have an N=30.

The results from Figure 5.5 detail that 100 % of eggs that arrived were undamaged and placed in the incubator. On embryonic day 3, 100% of eggs in the incubator were viable. On day 7, 87% of CEM were alive and on the final day (Day 14) there was 72% survival was reported. This again suggests no corelation between the dose of GEM used and the survival of CEM, these findings suggest that CEM death may be caused by other factors such as, contamination, change in humidity or temperature.

Doxorubicin (DOX) was investigated as this is the current gold standard for TNBC treatment and as already described in Chapter 1. As this chemotherapeutic has been extensively investigated in Chapters 2, 3 and 4 it is a therapeutic drug that would be

of interest when investigating the possible treatments for TNBC. Therefore, its toxicity in a CEM *in vivo* model was investigated in Figure 5.6.

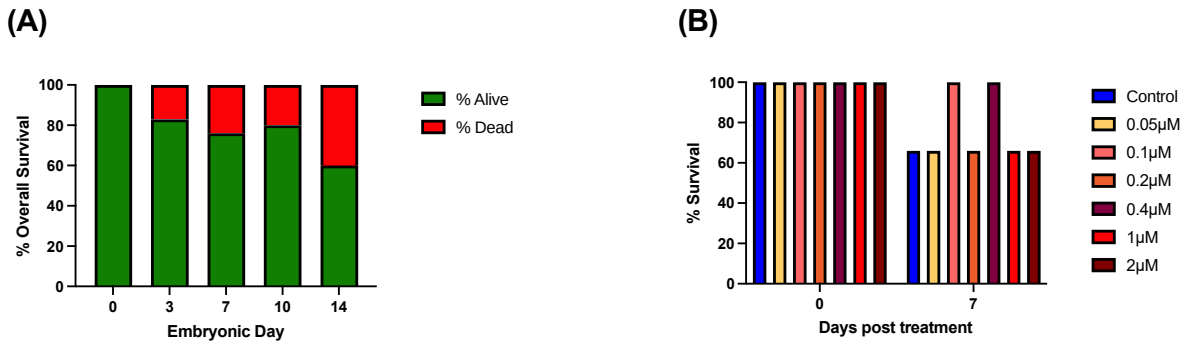

Figure 5. 6 Survival of CEMs post Doxorubicin treatment.
(A) Survival data post treatment of CEM with Doxorubicin at concentrations 0.5μM, 0.1μM, 0.2μM, 0.4μM, 1μM, 2μM from embryonic day 0 to day 14. (B) Overall CEM survival preceding irradiation treatment until termination of embryo, 7 days post treatment (embryonic day 14) All results have an N=30.

Figure 5.6 suggests 66 % survival for untreated CEM and CEM treated with DOX at 0.05 μM, 0.2 μM, 1 μM and 2 μM. 100% survival was found when CEF were treated with 0.01 μM and 0.04 μM DOX. Therefore, data from Figure 5.6 suggests that there is no correlation between the dose of DOX administered and the survival of CEM. The same survival rate was found when comparing the untreated control and the highest concentration of DOX administered (2 μM).

5.4.3 Development of Embryo Protocol

Initially cell lines investigated as potential candidates for use in the chick embryo tumour model were MDA-MB-231, U87, PANC and HT1080. Growth of these tumours using relative cell lines was carried out as described in section 5.3.6. However, without the addition of Matrigel or trypsin. Before this the success rate of growing a tumour in the CEM was around 10%. This then required a literature search to investigate potential cell lines to increase this tumour uptake rate. It was discovered that Matrigel is used when developing CEM tumour models in some published literature (Deryugina

& Quigley., 2008 and Mangir *et al*., 2018). They reported that by the addition of Matrigel to the cell pellet that the rate of successful tumour growth increased by 40%. Therefore, this became an essential aspect of the chick embryo tumour protocol.

Another aspect of designing the most effective chick embryo tumour model protocol required the investigation of the use of trypsin. From a literature review it was discovered that the addition of trypsin to the CAM increased pre addition of cells encouraged the growth of vasculature to the tumour (Swadi *et al.,* 2018). Initially 10 μL of 0.05% trypsin was added the surface of the CAM and left for 10 minutes before cell pellet was added. However, this results in tumours that grew under the surface of the membrane and were unable to be fully visualised, and of little use when imaging the CAM for tumour progression. After optimisation, the current protocol required the application of 10 μL 0.05% trypsin and then immediate addition of the cell pellet. This method was found to produce tumours with vascularised membranes that protruded above the CAM for effective imaging of the tumour.

5.4.4 Optimised Embryo Tumour Protocol

To determine the most effective uptake of cells to the CAM to form a tumour, there were several factors to consider. Therefore, after extensive literature review and investigation the most optimal method was designed. Figure 5.7 represents the current cell implantation process of CEM.

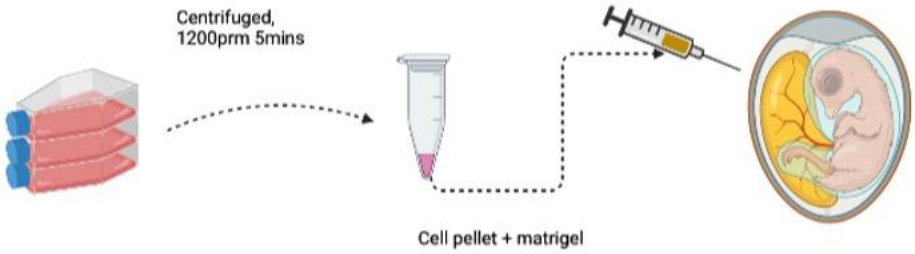

Figure 5. 7 The process of 2D culture cells trypsinised and spun into pellets before injecting onto the CAM membrane of the chick embryo model. Created using Biorender.

This optimised protocol involves using 2D cultured cells, to date the most suitable cell lines to form a tumour in the CEM are U87 – Glioma cells, MDA-MB-231 – TNBC cells and Panc-1, pancreatic cancer cell and HT1080, sarcoma cell line. The optimal number of cells per egg was determined to be $2x10^6$. Large T75 flasks of cells were trypsinised and counted to achieve $2x10^6$ cells. These cells were pelleted at 1200g for 5 minutes and washed with PBS before re-spinning. Once pellets were formed, the supernatant was removed and 5 µL of Matrigel and 5 µL PBS were added to the pellet.

After the cells were prepared as per section (5.3.3), the pellet containing 50:50 (v/v) PBS: Matrigel was mixed and added to the surface of the CAM post traumatisation of the CAM and addition of 5 µL of trypsin to the point where cells were added. Matrigel was used as it provides extra vascular growth factors and will encourage the growth of a tumour on the surface of the CAM (Pawlikowska *et al*., 2020). Figure 5.8 details the process of cell uptake to the CAM membrane.

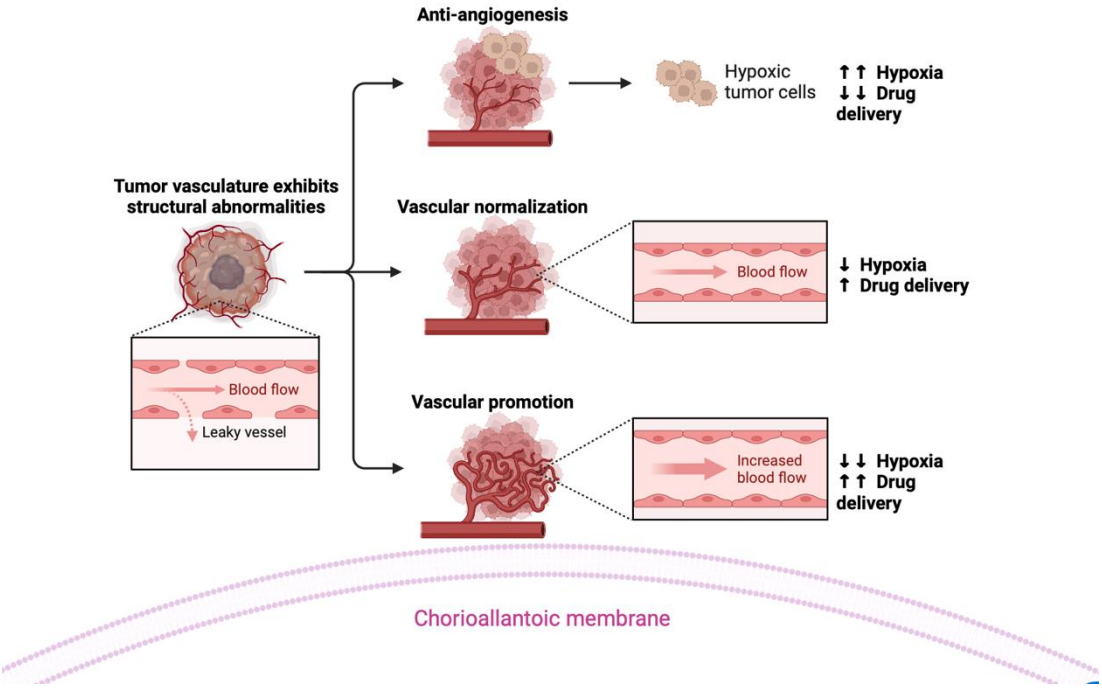

Figure 5. 8 The process of cell uptake to the chorioallantoic membrane, allowing the development of hypoxic core, drug delivery system and provides the tumor with a direct blood supply. Created using Biorender.

Before the addition of cell mixture, the surface of the CAM was lacerated using an autoclaved piece of paper tissue, the semi solid cell mixture was then pipetted onto the traumatised area of the CAM to encourage blood supply and metastasis of the cancer cells as depicted in Figure 5.8. Eggs were incubated until day 14 were images and samples of the CAM were taken as seen in Figure 5.9.

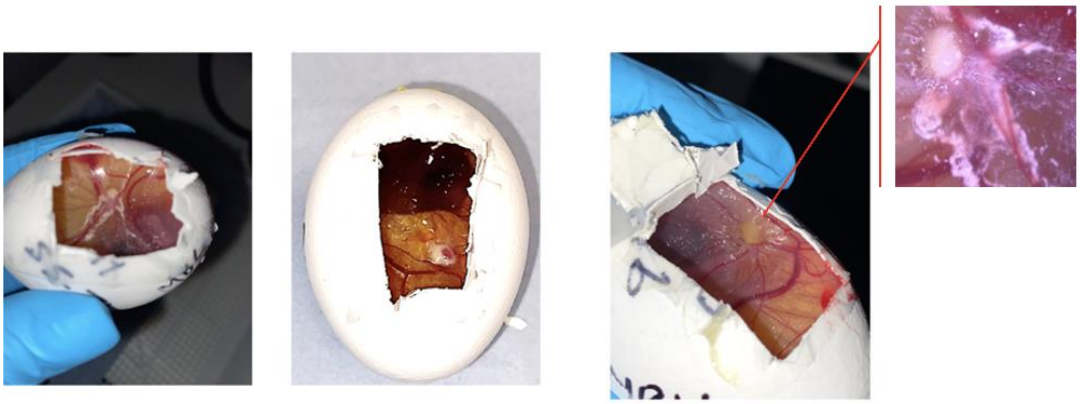

Figure 5. 9 Images of eggs on Day 14 of CEM with MDA-MB-231 cells.

5.5 Discussion

Having partially translated the methodology from Liverpool for establishment of the CAM tumour models, our next stage of the investigation will be to develop and adapt irradiation and chemotherapeutic methodologies in the chick embryo tumour model for single or combination treatment and to validate the model by comparison to our existing mouse xenograft data. Finally, we will screen for the efficacy of drugs or nanomaterials alone or in combination.

The success of designing a replicable chick embryo tumour protocol has great potential when investigating promising therapies in TNBC prior to murine *in vivo* experiments. The use of this model will reduce costs of *in vivo* experiments, reduce the number of mice required for animal experiments and refine potential therapies for their use as novel TNBC treatments as well as adhering to good practice and application of the principles of the 3Rs (Archiving best practice., 2023). For example, the combination therapy of MMF + radiation (investigated in Chapter 2 and 3) would be an ideal candidate to investigate in the chick embryo model. It has already been concluded from the findings in section 5.4.2 that these single agents do not induce CEM death alone at doses of therapy tested in Figure 5.8 and 5.9. This combination therapy reports promising data in 2D and 3D *in vitro* investigations and its efficacy in MDA-MB-231 chick embryo tumour model would allow for *in vivo* investigation into its potential as a treatment for TNBC patients, to assess the most promising schedules and thus reduce the number of experimental parameters that are utilised in murine tumour models.

Future studies using the chick embryo model may also include the validation of various cell lines that are reported in the literature to successfully grow chick embryo tumours, such as, Panc, HT1080 and A549 (Pawlikowska *et al.,* 2020, Chen *et al* 2021 and hu *et al*., 2022). With the generation of the optimised chick embryo protocol these cell lines can be investigated to identify their use in *in vivo* chick embryo tumour model. Additionally, there is the potential to utilise GFP transfected cancer cells to study the metastasis of cell in the chick embryo in future investigations as detailed by Augustine *et al.,* (2020). The authors of this paper injected GFP transfected cells directly into the heart of the embryo on embryonic day 3, on embryonic day 14 selected organs were then harvested and imaged under fluorescent microscopy for the prescience of GFP cells.

Chapter 6

Final Discussion

Due to time restrains on the project caused by critical time lost in the laboratory during the COIVD-19 pandemic, a complete characterisation of developed resistant cells was unable to be carried out in as much detail as originally planned. However, Table 6.1 summarises the critical findings between parental MDA-MB-231 cells and the resistant cells developed in-house.

	MDA-MB-231	D3	R3	R3D3
Clonogenic survival	DOX IC_{50} 0.0595 μM EC_{50} 1.45 Gy SCH3 most effective	DOX IC_{50} 0.99 μM D-SCH3 MMF most effective	RAD EC_{50} 2.03 Gy R-SCH3 MMF most effective	DOX $1C_{50}$ 0.42 μM RAD EC_{50} 3.36 Gy MMF in SCH3 administration most effective
Cell Cycle analysis- (Cell cycle arrest)	D-SCH3, treated cells begin to return to normal distribution, 48 hrs post. R-SCH3, G2/M cell cycle arrest, decrease in G1	D-SCH3, decrease in distribution of cells in G1 and G2/M, 48 hrs post treatment removal.	R-SCH3 maintained decrease in G1	D-SCH3 and R-SCH3 decrease in distribution of cells in G1 and G2/M, 48 hrs post treatment removal.
Annexin V (Apoptotic cells)	D-SCH3 and R-SCH3 significant increase in apoptotic cells, 48 hrs post treatment removal	D-SCH3 significant increase in apoptotic cells, 48 hrs post treatment removal	R-SCH3 significant increase in apoptotic cells 48 hrs post treatment removal	D-SCH3 and R-SCH3 significant increase in apoptotic cells, 48 hrs post treatment removal
Glutathione (Decrease in glutathione levels)	D-SCH3 and R-SCH3 maintained decrease of glutathione, 48 hrs post treatment.	D-SCH3 maintained decrease of glutathione, 48 hrs post treatment	R-SCH3 maintained decrease of glutathione, 48 hrs post treatment	D-SCH3 and R-SCH3 maintained decrease of glutathione, 48 hrs post treatment.
Autophagy (Increased autophagic markers)	D-SCH3 and R-SCH3 No autophagy	D-SCH3 No autophagy	R-SCH3 No autophagy	D-SCH3 and R-SCH3 No autophagy
Comet Assay	D-SCH3 and R-SCH3, significant increase in DNA damage NOT REPAIRED 48 hrs post treatment removal	D-SCH3 significant increase in DNA damage, but is REPAIRED 48 hrs post treatment removal	R-SCH3 significant increase in DNA damage but is NOT REPAIRED 48 hrs post treatment removal	D-SCH3 and R-SCH3, DNA damage induced but is REPAIRED 48 hrs post treatment removal
3D Spheroid Model	MMF in combination with RAD reduced spheroid growth most effectively	D-SCH3 most effective combination at reducing spheroid growth (not seen in MDA)	R-SCH3 MMF most effective at reducing spheroid growth	MMF in combination with RAD reduced spheroid growth most effectively

Table 6. 1 Comparison of key findings in the project between MDA-231, D3, R3 and R3D3 cells.

As we can see from Table 6.1, there was an increase in the cell survival capacity when R3, D3 and R3D3 cells were treated with DOX and RAD alone, compared to the parental cell line. These initial findings supported the use of these cells as potential cell lines to investigate therapy resistance in MDA-MB-231 cells. Clonogenic assay results all supported the hypothesis that MMF administered in a SCH3 combination with DOX or RAD in parental and all resistant cell lines was the most effective treatment at reducing the survival of cells. Both parental and resistant cells all showed similar patterns of cell cycle distribution following treatment with MMF SCH3 combination, a decrease in cells in G1 and G2/M, suggesting that cells are potentially struggling to repair damage induced by the combination therapy. In parental and resistant cells all data suggested that MMF SCH3 combination treatment induces apoptosis. All cells also showed that GSH levels were reduced following SCH3 treatment and that a decrease in GSH was maintained up to 48 hours post treatment removal. No cell line tested suggested that autophagy was a mechanism that was begin induced by any treatment tested. Results from parental cells comet assay suggested that MMF SCH3 was able to induce DNA damage that was unable to be repaired at the latest time point tested. However, this was not the case with D3 and R3D3 cells, in which a SCH3 combination induced DNA damage initially, however this damage was repaired. R3 resistant cells were the only resistant cells line tested where following treatment with SCH3, DNA damage occurred that was unable to be repaired by cells at the latest time point tested, similarly to that of the parental cells. When reviewing 3D data, it was found that MMF in a SCH3 combination induced a significant reduction in spheroid growth overtime, in parental cells, D3 cells, R3 cells and R3D3 cells.

Another main area of investigation that was not able to be conducted was to investigate the designed combination therapies on another TNBC cell type, such as MDA-MB-453. This would have been particularly interesting as this cell line is androgen receptor positive, unlike the cell line used in this thesis (MDA-MB-231) and would have given the project a more reflective scope of investigation. Investigating these potential combination therapies designed throughout this project in androgen receptor positive and negative cell lines would be of great interest as studies into the androgen receptors potential as a targeted therapy for TNBC patients has generated much interest in TNBC research in recent years. However, its potential role as a therapeutic target has yet to be fully understood (Kolyvas *et al*., 2022).

It is well established in the literature that DMF in non- cancerous cells can upregulate the NRF2 pathway thus elucidating a protective response in the cell, this is particularly useful in autoimmune diseases such as Multiple Sclerosis and Psoriasis, of which DMF is licenced to treat (Bomprezzi, 2015). However, in cancerous cells there is a phenomenon that has yet to be fully understood by researchers in that when DMF is administered in high concentrations (approximately > 25 μM) its function as an NRF2 activator is switched. Current literature suggests that this may be due to DMF binding to DJ-1 protein destabilising NRF2 and preventing its nuclear translocation and the synthesis of antioxidtive compounds such as GSH, sensitising the cell to damage via ROS (Saidu *et al*., 2017). As MMF is the direct metabolite of DMF it was thought that this drug has the same mechanism of action, however evidence from this project and that in the literature, suggest that there may be an alternative mechanism of action that MMF utilises intracellularly (Landeck *et al*., 2018). For example, DMF has been shown to induce more cytoprotective effects than MMF in neurons and astrocytes (Scannevin *et al.*, 2012). There has been very little research into the differences in mechanisms of action of DMF and MMF intracellularly. However, in order to gain a better understanding of potential alterations in mechanisms between the two drugs it would be of interest to use western blot techniques to determine levels of NRF2 and DJ-1 in TNBC cells treated with single doses of DMF/MMF as we all combinations of these fumaric acids with radiotherapy and chemotherapy.

Research into the role of NRF2 and cancer has generated much interest in recent years. A recent review article published by Lin *et al* (2023) highlights findings that the overexpression of NRF2 has been related to cancer progression and tumour metastasis. Conversely, reduced levels of NRF2 in turn leads to a decrease in antioxidant activity and increased sensitivity to ROS, inducing apoptosis in cancer cells.

Given the evidence from Chapter 3 of this thesis it would be of great interest to use additional 3D models to investigate combination therapies, following on from the results of this spheroid chapter. Once such potential model of interest would be 3D co-cultures, utilising extracellular matrix proteins that better reflect the *in vivo* condition, as this allows for cell-cell communication which is a better reflection of the tumour microenvironment (Asante *et al*., 2022). As this model can incorporate both

cancer cells and fibroblast cells, it would allow for a more representative model of *in vivo* tumours, providing a more robust investigation of MMF + DOX/RAD combination therapy. This model has been used successfully in published literature, a study conducted by Liu and Mac, (2022) demonstrated that by varying the density of cell populations within this co-culture authors were able to design a system that supported an environment that was more representative of a patient tumour with cells exhibiting more extended morphology.

In addition to these co-cultures, it would be of great interest to use the in-house develop resistant cells used in this thesis in such 3D models, D3, R3 and R3D3. This would provide a more substantial profile of these cells as at present there is a large are of research that requires investigation to treat resistant cancer cells. The mechanism of action in which cancer cells develop resistance is lacking information. However, as this thesis focused on mediating intracellular GSH levels, the literature surrounding GSH metabolism as a potential driver of cancer progression was used to support the hypothesis that generated resistant MDA-MB-231 cells (developed during this project), upregulate GSH as a resistance mechanism. It was found by Bansal and Simon, (2018) that excess GSH promoted tumour progression in bone, breast, colon and lung cancers, this is due to GSH exhibiting antioxidant mechanisms, neutralising ROS that would cause SSB and DSB that when accumulated result in cell death. Therefore, given the surrounding evidence, there is support for the investigation of mediation of GSH levels in resistant cells, given the findings of Chapter 4, further 3D models systems such as co-cultures could provide beneficial information of these resistant tumour microenvironments and how they interact with other cell types such as fibroblasts.

Overall, the SCH3 combinations tested against R3, D3 and R3D3 resistant cells provide some evidence to support the promise of this therapy as a novel approach to overcome resistance in MDA-MB-231 cells. The findings of this thesis support the hypothesis that MMF can inhibit action and potentially the synthesis of GSH via NRF2 pathway and when this occurs prior to DOX or irradiation administration, resistant cells are not able to neutralise ROS generated from toxic therapies. As a result, ROS can induce SSB and DSBs which when accumulated activate the caspase 3 pathway and result in cell death via apoptosis. This SCH3 combination therapy is therefore an

ideal candidate to investigate using a chick embryo tumour model or murine model to determine its capability *in vivo*.

Appendix

Bonferroni's multiple comparisons test	0HR - P Value	24HR – P Value	48hr – P Value
Non- Apoptotic (NA)			
CONTROL vs. DOX	0.0261	0.0100	0.3617
CONTROL vs. MMF	0.4112	>0.9999	0.4951
CONTROL vs. SCH3	0.0071	<0.0001	<0.0001
DOX vs. MMF	0.0005	0.0006	0.0641
DOX vs. SCH3	0.0003	0.0027	<0.0001
MMF vs. SCH3	<0.0001	>0.0001	0.0002
Early Apoptotic			
CONTROL vs. DOX	0.0655	>0.9999	>0.9999
CONTROL vs. MMF	>0.9999	0.1513	0.3398
CONTROL vs. SCH3	0.0241	0.0462	0.0201
DOX vs. MMF	0.0067	0.1529	0.3039
DOX vs. SCH3	0.3342	0.0463	0.0203
MMF vs. SCH3	0.0822	0.0331	0.0188
Late Apoptotic			
CONTROL vs. DOX	0.0773	0.0013	0.0936
CONTROL vs. MMF	<0.0001	<0.9999	0.4506
CONTROL vs. SCH3	0.2035	0.0034	0.0291
DOX vs. MMF	0.4290	0.0016	0.0332
DOX vs. SCH3	0.3193	0.0039	0.0230
MMF vs. SCH3	0.2695	0.0073	0.0258
Necrotic			
CONTROL vs. DOX	0.9274	<0.0001	>0.9999
CONTROL vs. MMF	>0.9999	>0.9999	>0.9999
CONTROL vs. SCH3	0.4783	0.1160	>0.9999
DOX vs. MMF	>0.9999	0.0073	>0.9999
DOX vs. SCH3	0.4170	0.0917	0.3315
MMF vs. SCH3	>0.9999	>0.9999	0.0842

Appendix 1. Statistical analysis of Figure 2.6 D.

Statistical Analysis carried out using two-way ANOVA followed by Bonferroni's post-testing, comparing each apoptotic phase separately between all treatments. *P<0.05, **P<0.01, ***P<0.001 and ****P<0.0001.

Bonferroni's multiple comparisons test	Summary	Adjusted P Value
Control - 0 vs. Control - 24	ns	>0.9999
Control - 0 vs. Control - 48	ns	>0.9999
Control - 0 vs. DOX - 0	****	<0.0001
Control - 0 vs. MMF - 0	****	<0.0001
Control - 0 vs. SCH3 - 0	**	0.0079
Control - 24 vs. DOX -24	ns	0.1168
Control - 24 vs. MMF - 24	ns	>0.9999
Control - 24 vs. SCH3 - 24	****	<0.0001
Control - 48 vs. DOX - 48	ns	>0.9999
Control - 48 vs. MMF - 48	ns	>0.9999
Control - 48 vs. SCH3 -48	****	<0.0001
DOX - 0 vs. DOX -24	****	<0.0001
DOX - 0 vs. DOX - 48	****	<0.0001
DOX - 0 vs. MMF - 0	**	0.0067
DOX - 0 vs. SCH3 - 0	****	<0.0001
DOX -24 vs. DOX - 48	ns	>0.9999
DOX -24 vs. MMF - 24	ns	0.4217
DOX -24 vs. SCH3 - 24	****	<0.0001
DOX - 48 vs. MMF - 48	ns	>0.9999
DOX - 48 vs. SCH3 -48	****	<0.0001
MMF - 0 vs. MMF - 24	**	0.0012
MMF - 0 vs. MMF - 48	****	<0.0001
MMF - 0 vs. SCH3 - 0	ns	0.4107
MMF - 24 vs. MMF - 48	****	<0.0001
MMF - 24 vs. SCH3 - 24	****	<0.0001
MMF - 48 vs. SCH3 -48	****	<0.0001
SCH3 - 0 vs. SCH3 - 24	****	<0.0001
SCH3 - 0 vs. SCH3 -48	****	<0.0001
SCH3 - 24 vs. SCH3 -48	****	<0.0001

Appendix 2. Statistical analysis results of Figure 2.20

Significance of DNA damage in MDA-MB-231 cells, caused my DOX 0.02μM, MMF2μM and SCH3 M+D, at 3 different time points, 0hr post treatment, 24hrs post treatment and 48hrs post treatments. This table is a summary of statistical analysis carried out in Figure 19, One-way ANOVA was carried out with Bonferroni's post-test and the comparisons of each median tail moment are displayed above P>0.0001 ****, P>0.001 ***, P>0.01** and P>0.1 *.

Bonferroni's multiple comparisons test	0HR - P Value	24HR – P Value	48hr – P Value
Non- Apoptotic (NA)			
CONTROL vs. RAD	0.1941	0.1157	0.3631
CONTROL vs. MMF	0.1685	0.3048	>0.9999
CONTROL vs. SCH3	0.0019	0.0015	0.0006
RAD vs. MMF	0.3997	0.3278	0.4058
RAD vs. SCH3	0.1276	0.0002	0.0032
MMF vs. SCH3	<0.0001	0.0011	0.0004
Early Apoptotic			
CONTROL vs. RAD	0.3369	0.5589	>0.9999
CONTROL vs. MMF	0.4732	0.1557	0.3398
CONTROL vs. SCH3	0.0037	0.4249	0.0260
RAD vs. MMF	0.4858	0.1632	0.3071
RAD vs. SCH3	0.1747	0.4317	0.0262
MMF vs. SCH3	0.0194	0.7242	0.0245
Late Apoptotic			
CONTROL vs. RAD	0.0422	0.0069	0.0520
CONTROL vs. MMF	<0.0001	>0.9999	0.4506
CONTROL vs. SCH3	0.0287	0.0491	0.0606
RAD vs. MMF	0.1184	<0.0001	0.0913
RAD vs. SCH3	0.0454	0.0569	0.0542
MMF vs. SCH3	0.0379	0.0493	0.0611
Necrotic			
CONTROL vs. RAD	0.4609	0.6850	>0.9999
CONTROL vs. MMF	0.8657	>0.9999	>0.9999
CONTROL vs. SCH3	0.6165	0.2490	>0.9999
RAD vs. MMF	0.9987	0.8515	>0.9999
RAD vs. SCH3	0.4121	>0.9999	>0.9999
MMF vs. SCH3	0.8144	0.5132	0.0779

Appendix 3. Statistical Analysis of Figure 2.25.

Carried out using two-way ANOVA followed by Bonferroni's post hoc testing, comparing each apoptotic phase separately between all treatments. *P<0.05, **P<0.01, ***P<0.001 and ****P<0.0001.

Bonferroni's multiple comparisons test	Summary	Adjusted P Value
Control - 0 vs. Control - 24	ns	>0.9999
Control - 0 vs. Control - 48	ns	>0.9999
Control - 0 vs. RAD - 0	****	<0.0001
Control - 0 vs. MMF - 0	****	<0.0001
Control - 0 vs. R-SCH3 - 0	****	<0.0001
Control - 24 vs. RAD - 24	ns	>0.9999
Control - 24 vs. MMF - 24	ns	>0.9999
Control - 24 vs. R-SCH3 - 24	****	<0.0001
Control - 48 vs. RAD - 48	ns	>0.9999
Control - 48 vs. MMF - 48	ns	>0.9999
Control - 48 vs. R-SCH3 - 48	****	<0.0001
RAD - 0 vs. RAD - 24	****	<0.0001
RAD - 0 vs. RAD - 48	****	<0.0001
RAD - 0 vs. MMF - 0	****	<0.0001
RAD - 0 vs. R-SCH3 - 0	****	<0.0001
RAD - 24 vs. MMF - 24	ns	>0.9999
RAD - 24 vs. R-SCH3 - 24	****	<0.0001
RAD - 48 vs. MMF - 48	ns	>0.9999
RAD - 48 vs. R-SCH3 - 48	****	<0.0001
MMF - 0 vs. MMF - 24	**	0.0043
MMF - 0 vs. MMF - 48	****	<0.0001
MMF - 0 vs. R-SCH3 - 0	****	<0.0001
MMF - 24 vs. R-SCH3 - 24	****	<0.0001
MMF - 48 vs. R-SCH3 - 48	****	<0.0000
R-SCH3 - 0 vs. R-SCH3 - 24	ns	0.7722
R-SCH3 - 0 vs. R-SCH3 - 48	ns	>0.9999
R-SCH3 - 24 vs. R-SCH3 - 48	ns	0.0556

Appendix 4. Statistical analysis of Figure 2.27.

Significance of DNA damage in MDA-MB-231 cells, caused my RAD 2GY MMF 2 μM and SCH3 M+R, at 3 different time points, 0 hr post treatment, 24 hrs post treatment and 48 hrs post treatments.

This table is a summary of statistical analysis carried out in Figure 2.27, One-way ANOVA was carried out with Bonferroni's correction and the comparisons of each median tail moment are displayed above.

Bonferroni's multiple comparisons test	0HR - P Value	24HR – P Value	48hr – P Value
Non-apoptotic (NA)			
CONTROL vs. MMF	>0.9999	<0.0001	<0.0001
CONTROL vs. DOX	>0.9999	<0.0001	0.8101
CONTROL vs. SCH3	0.0155	<0.0001	<0.0001
MMF vs. DOX	>0.9999	0.0031	<0.0001
MMF vs. SCH3	0.0093	<0.0001	>0.9999
DOX vs. SCH3	0.0036	0.0003	<0.0001
Early Apoptotic			
CONTROL vs. MMF	>0.9999	0.4486	<0.0001
CONTROL vs. DOX	0.7488	0.0004	>0.9999
CONTROL vs. SCH3	>0.9999	0.0165	<0.0001
MMF vs. DOX	>0.9999	0.0286	<0.0001
MMF vs. SCH3	0.5294	>0.9999	0.0595
DOX vs. SCH3	0.2510	0.2789	<0.0001
Late Apoptotic			
CONTROL vs. MMF	>0.9999	<0.0001	<0.0001
CONTROL vs. DOX	>0.9999	<0.0001	>0.9999
CONTROL vs. SCH3	0.0375	<0.0001	<0.0001
MMF vs. DOX	>0.9999	0.0015	<0.0001
MMF vs. SCH3	0.3770	<0.0001	0.9445
DOX vs. SCH3	0.3993	<0.0001	<0.0001
Necrotic			
CONTROL vs. MMF	>0.9999	0.0744	>0.9999
CONTROL vs. DOX	>0.9999	>0.9999	>0.9999
CONTROL vs. SCH3	>0.9999	>0.9999	>0.9999
MMF vs. DOX	>0.9999	0.0142	>0.9999
MMF vs. SCH3	>0.9999	0.0105	>0.9999
DOX vs. SCH3	>0.9999	>0.9999	>0.9999

Appendix 5. Statistical analysis of Figure 4.9.

Statistical Analysis was carried out using two-way ANOVA followed by Bonferroni's multiple comparison testing comparing each apoptotic phase separately between all each apoptotic phase separately between all treatments. *P<0.05, **P<0.01, ***P<0.001 and ****P<0.0001.

C-0 vs. M-0	ns	>0.9999
C-0 vs. C-24	ns	>0.9999
C-0 vs. C-48	ns	>0.9999
C-0 vs. D-0	****	<0.0001
C-0 vs. SCH3 -0	****	<0.0001
C-24 vs. M- 24	ns	>0.9999
C-24 vs. D-24	ns	>0.9999
C-24 vs. SCH3- 24	ns	>0.9999
C-48 vs. M-48	ns	>0.9999
C-48 vs. D-48	ns	>0.9999
C-48 vs. SCH3- 48	ns	>0.9999
M-0 vs. M- 24	ns	>0.9999
M-0 vs. M-48	ns	>0.9999
M-0 vs. D-0	****	<0.0001
M-0 vs. SCH3 -0	****	<0.0001
M- 24 vs. D-24	ns	>0.9999
M- 24 vs. SCH3- 24	ns	>0.9999
M-48 vs. D-48	ns	>0.9999
M-48 vs. SCH3- 48	ns	>0.9999
D-0 vs. D-24	****	<0.0001
D-0 vs. D-48	****	<0.0001
D-0 vs. SCH3 -0	ns	>0.9999
D-24 vs. SCH3- 24	ns	>0.9999
D-48 vs. SCH3- 48	ns	>0.9999
SCH3 -0 vs. SCH3- 24	****	<0.0001
SCH3 -0 vs. SCH3- 48	****	<0.0001
SCH3 – 24 vs. SCH3 - 48	Ns	>0.9999

Appendix 6. Statistical analysis of Figure 4,13.

Significance of DNA damage in D3 cells, caused by DOX 0.2μM, MMF2μM and SCH3 M+D, at 3 different time points, 0hr post treatment, 24hrs post treatment and 48hrs post treatments. This table is a summary of statistical analysis carried out in Figure 4.14, One-way ANOVA was carried out with Bonferroni's correction and the comparisons of each median tail moment are displayed above.

Bonferroni's multiple comparisons test	0hr P Value	24hr P Value	48hr P Value
Viable			
Control vs. MMF	>0.9999	<0.0001	<0.0001
Control vs. RAD	0.0002	<0.0001	<0.0001
Control vs. SCH3	<0.0001	<0.0001	<0.0001
MMF vs. RAD	0.0025	<0.0001	0.0149
MMF vs. SCH3	<0.0001	<0.0001	>0.9999
RAD vs. SCH3	0.0001	<0.0001	0.0006
Early Apoptotic			
Control vs. MMF	>0.9999	0.0060	<0.0001
Control vs. RAD	0.0019	0.1989	0.0012
Control vs. SCH3	>0.9999	<0.0001	0.0001
MMF vs. RAD	0.0004	0.8074	0.1829
MMF vs. SCH3	0.8235	<0.0001	0.4112
RAD vs. SCH3	0.0097	<0.0001	>0.9999
Late Apoptotic			
Control vs. MMF	0.5718	<0.0001	<0.0001
Control vs. RAD	>0.9999	<0.0001	<0.0001
Control vs. SCH3	<0.0001	<0.0001	<0.0001
MMF vs. RAD	>0.9999	<0.0001	>0.9999
MMF vs. SCH3	<0.0001	<0.0001	0.0585
RAD vs. SCH3	<0.0001	<0.0001	0.0023
Necrotic			
Control vs. MMF	>0.9999	>0.9999	>0.9999
Control vs. RAD	>0.9999	>0.9999	>0.9999
Control vs. SCH3	>0.9999	0.0003	>0.9999
MMF vs. RAD	>0.9999	>0.9999	>0.9999
MMF vs. SCH3	>0.9999	0.0003	>0.9999
RAD vs. SCH3	>0.9999	0.0073	>0.9999

Appendix 7. Statistical analysis of Figure 4.22.

Statistical analysis carried out using two-way ANOVA followed by Bonferroni's post hoc testing, comparing each apoptotic phase separately between all treatments. *P<0.05, **P<0.01, ***P<0.001 and ****P<0.0001.

C-0 vs. C-24	ns	>0.9999
C-0 vs. C-48	ns	>0.9999
C-0 vs. M-0	ns	>0.9999
C-0 vs. R-0	ns	>0.9999
C-0 vs. SCH3-0	ns	>0.9999
C-24 vs. M-24	ns	>0.9999
C-24 vs. R-24	ns	>0.9999
C-24 vs. SCH3-24	ns	>0.9999
C-48 vs. M-48	ns	>0.9999
C-48 vs. R-48	****	<0.0001
C-48 vs. SCH3- 48	****	<0.0001
M-0 vs. M-24	ns	>0.9999
M-0 vs. M-48	ns	>0.9999
M-0 vs. R-0	ns	>0.9999
M-0 vs. SCH3-0	ns	>0.9999
M-24 vs. M-48	ns	>0.9999
M-24 vs. R-24	ns	>0.9999
M-24 vs. SCH3-24	ns	>0.9999
M-48 vs. R-48	****	<0.0001
M-48 vs. SCH3- 48	****	<0.0001
R-0 vs. R-24	ns	>0.9999
R-0 vs. R-48	****	<0.0001
R-0 vs. SCH3-0	ns	>0.9999
R-24 vs. R-48	ns	>0.9999
R-24 vs. SCH3-24	ns	>0.9999
R-48 vs. SCH3- 48	****	<0.0001
SCH3-0 vs. SCH3-24	ns	>0.9999
SCH3-0 vs. SCH3- 48	****	<0.0001
SCH3-24 vs. SCH3- 48	****	<0.0001

Appendix 8. Statistical analysis of Figure 4.26.

Table 4. 1 Significance of DNA damage in R3 cells, caused my RAD 2 GY MMF 2 μM and SCH3 M+R, at 3 different time points, 0hr post treatment, 24hrs post treatment and 48hrs post treatments.

This table is a summary of statistical analysis carried out in Figure 4.26, One-way ANOVA was carried out with Bonferroni's correction and the comparisons of each median tail moment are displayed above.

Bonferroni's multiple comparisons test	0HR P Value	24HR P Value	48HR P Value
Viable			
Control vs. MMF	0.0051	<0.0001	<0.0001
Control vs. DOX	0.1426	<0.0001	<0.0001
Control vs. D-SCH3	<0.0001	<0.0001	<0.0001
Control vs. RAD	0.0005	0.0289	<0.0001
Control vs. R-SCH3	<0.0001	<0.0001	<0.0001
MMF vs. DOX	>0.9999	0.4653	<0.0001
MMF vs. D-SCH3	0.0001	<0.0001	<0.0001
MMF vs. RAD	>0.9999	0.4401	0.4241
MMF vs. R-SCH3	0.0001	<0.0001	<0.0001
DOX vs. D-SCH3	<0.0001	<0.0001	<0.0001
DOX vs. RAD	0.7220	0.0011	<0.0001
DOX vs. R-SCH3	<0.0001	<0.0001	<0.0001
D-SCH3 vs. RAD	0.0016	<0.0001	<0.0001
D-SCH3 vs. R-SCH3	>0.9999	0.9797	>0.9999
RAD vs. R-SCH3	0.0017	<0.0001	<0.0001
Early Apoptotic			
Control vs. MMF	>0.9999	0.0060	<0.0001
Control vs. DOX	0.2680	>0.9999	<0.0001
Control vs. D-SCH3	0.0017	0.0166	0.0009
Control vs. RAD	0.1022	0.1253	<0.0001
Control vs. R-SCH3	0.0574	>0.9999	0.0365
MMF vs. DOX	>0.9999	0.0003	0.0880
MMF vs. D-SCH3	0.2929	<0.0001	<0.0001
MMF vs. RAD	>0.9999	>0.9999	>0.9999
MMF vs. R-SCH3	>0.9999	0.0107	<0.0001
DOX vs. D-SCH3	>0.9999	0.2830	0.2806
DOX vs. RAD	>0.9999	0.0086	0.0436
DOX vs. R-SCH3	>0.9999	>0.9999	0.0095
D-SCH3 vs. RAD	>0.9999	<0.0001	<0.0001
D-SCH3 vs. R-SCH3	>0.9999	0.0008	>0.9999
RAD vs. R-SCH3	>0.9999	0.2703	<0.0001
Late Apoptotic			
Control vs. MMF	0.5261	0.0454	<0.0001
Control vs. DOX	>0.9999	<0.0001	0.2936
Control vs. D-SCH3	<0.0001	<0.0001	<0.0001
Control vs. RAD	0.9797	0.0142	<0.0001
Control vs. R-SCH3	<0.0001	<0.0001	<0.0001
MMF vs. DOX	0.9905	0.3480	0.0005
MMF vs. D-SCH3	0.0767	<0.0001	<0.0001
MMF vs. RAD	>0.9999	>0.9999	>0.9999
MMF vs. R-SCH3	0.0031	<0.0001	<0.0001
DOX vs. D-SCH3	0.0002	<0.0001	<0.0001
DOX vs. RAD	>0.9999	0.8966	0.0186
DOX vs. R-SCH3	<0.0001	<0.0001	<0.0001
D-SCH3 vs. RAD	0.0333	<0.0001	<0.0001
D-SCH3 vs. R-SCH3	>0.9999	<0.0001	>0.9999
RAD vs. R-SCH3	0.0013	<0.0001	<0.0001
Necrotic			
Control vs. MMF	>0.9999	<0.0001	>0.9999
Control vs. DOX	>0.9999	>0.9999	>0.9999
Control vs. D-SCH3	>0.9999	>0.9999	>0.9999
Control vs. RAD	>0.9999	0.3528	>0.9999
Control vs. R-SCH3	>0.9999	>0.9999	>0.9999
MMF vs. DOX	>0.9999	0.0002	>0.9999
MMF vs. D-SCH3	>0.9999	<0.0001	>0.9999
MMF vs. RAD	>0.9999	0.0107	>0.9999
MMF vs. R-SCH3	>0.9999	<0.0001	>0.9999

DOX vs. D-SCH3	>0.9999	>0.9999	>0.9999
DOX vs. RAD	>0.9999	>0.9999	>0.9999
DOX vs. R-SCH3	>0.9999	>0.9999	>0.9999
D-SCH3 vs. RAD	>0.9999	0.9824	>0.9999
D-SCH3 vs. R-SCH3	>0.9999	>0.9999	>0.9999
RAD vs. R-SCH3	>0.9999	>0.9999	>0.9999

Appendix 9. Statistical analysis of Figure 4.34.

Statistical analysis carried out using two-way ANOVA followed by Bonferroni's post hoc testing, comparing each apoptotic phase separately between all treatments. *P<0.05, **P<0.01, ***P<0.001 and ****P<0.0001.

Bonferroni's multiple comparisons test	Summary	Adjusted P Value
Control - 0 vs. Control - 24	ns	>0.9999
Control - 0 vs. Control -48	ns	>0.9999
Control - 0 vs. MMF - 0	****	<0.0001
Control - 0 vs. DOX - 0	****	<0.0001
Control - 0 vs. D-SCH3 - 0	****	<0.0001
Control - 24 vs. MMF - 24	ns	>0.9999
Control - 24 vs. DOX - 24	ns	>0.9999
Control - 24 vs. D-SCH3 - 24	ns	>0.9999
Control -48 vs. MMF - 48	ns	>0.9999
Control -48 vs. DOX - 48	ns	>0.9999
Control -48 vs. D-SCH3 - 48	ns	>0.9999
MMF - 0 vs. MMF - 24	****	<0.0001
MMF - 0 vs. MMF - 48	****	<0.0001
MMF - 0 vs. DOX - 0	****	<0.0001
MMF - 0 vs. D-SCH3 - 0	****	<0.0001
MMF - 24 vs. DOX - 24	ns	>0.9999
MMF - 24 vs. D-SCH3 - 24	ns	>0.9999
MMF - 48 vs. DOX - 48	ns	>0.9999
MMF - 48 vs. D-SCH3 - 48	ns	>0.9999
DOX - 0 vs. DOX - 24	****	<0.0001
DOX - 0 vs. DOX - 48	****	<0.0001
DOX - 0 vs. D-SCH3 - 0	****	<0.0001
DOX - 24 vs. D-SCH3 - 24	ns	>0.9999
DOX - 48 vs. D-SCH3 - 48	ns	>0.9999
D-SCH3 - 0 vs. D-SCH3 - 24	****	<0.0001
D-SCH3 - 0 vs. D-SCH3 - 48	****	<0.0001
D-SCH3 - 24 vs. D-SCH3 - 48	ns	>0.9999

Appendix 10. Statistical analysis of Figure 4.36.

Significance of DNA damage in R3D3 cells, caused by MMF 2 μM DOX 0.2 μM and D-SCH3, at 3 different time points, 0hr post treatment removal, 24hrs post treatment removal and 48hrs post treatment removal.

This table is a summary of statistical analysis carried out in Figure 4.39, One-way ANOVA was carried out with Bonferroni's correction and the comparisons of each median tail moment are displayed above. P>0.0001 ****, P>0.001 ***, P>0.01** and P>0.1 *.

Bonferroni's multiple comparisons test	Summary	Adjusted P Value
Control - 0 vs. Control - 24	ns	>0.9999
Control - 0 vs. Control -48	ns	>0.9999
Control - 0 vs. MMF - 0	****	<0.0001
Control - 0 vs. RAD - 0	****	<0.0001
Control - 0 vs. R-SCH3 - 0	****	<0.0001
Control - 24 vs. MMF - 24	ns	<0.9999
Control - 24 vs. RAD - 24	ns	>0.9999
Control - 24 vs. R-SCH3 - 24	ns	>0.9999
Control -48 vs. MMF - 48	ns	>0.9999
Control -48 vs. RAD - 48	ns	>0.9999
Control -48 vs. R-SCH3 - 48	ns	>0.9999
MMF - 0 vs. MMF - 24	****	<0.0001
MMF - 0 vs. MMF - 48	****	<0.0001
MMF - 0 vs. RAD - 0	****	<0.0001
MMF - 0 vs. R-SCH3 - 0	****	<0.0001
MMF - 24 vs. MMF - 48	****	<0.0001
MMF - 24 vs. RAD - 24	ns	>0.9999
MMF - 24 vs. R-SCH3 - 24	ns	>0.9999
MMF - 48 vs. RAD - 48	ns	>0.9999
MMF - 48 vs. R-SCH3 - 48	ns	>0.9999
RAD - 0 vs. RAD - 24	****	<0.0001
RAD - 0 vs. RAD - 48	****	<0.0001
RAD - 0 vs. R-SCH3 - 0	**	0.0034
RAD - 24 vs. RAD - 48	ns	>0.9999
RAD - 24 vs. R-SCH3 - 24	ns	>0.9999
RAD - 48 vs. R-SCH3 - 48	ns	>0.9999
R-SCH3 - 0 vs. R-SCH3 - 24	****	<0.0001
R-SCH3 - 0 vs. R-SCH3 - 48	****	<0.0001
R-SCH3 - 24 vs. R-SCH3 - 48	ns	>0.9999

Appendix 11. Statistical analysis of Figure 4.37.

Table 4. 2 Significance of DNA damage in R3D3 cells, caused by MMF 2 μM RAD 2 Gy and R-SCH3, at 3 different time points, 0hr post treatment, 24hrs post treatment and 48hrs post treatment.

This table is a summary of statistical analysis carried out in Figure 4.40, One-way ANOVA was carried out with Bonferroni's correction and the comparisons of each median tail moment are displayed above. P>0.0001 ****, P>0.001 ***, P>0.01** and P>0.1 *.

(A)

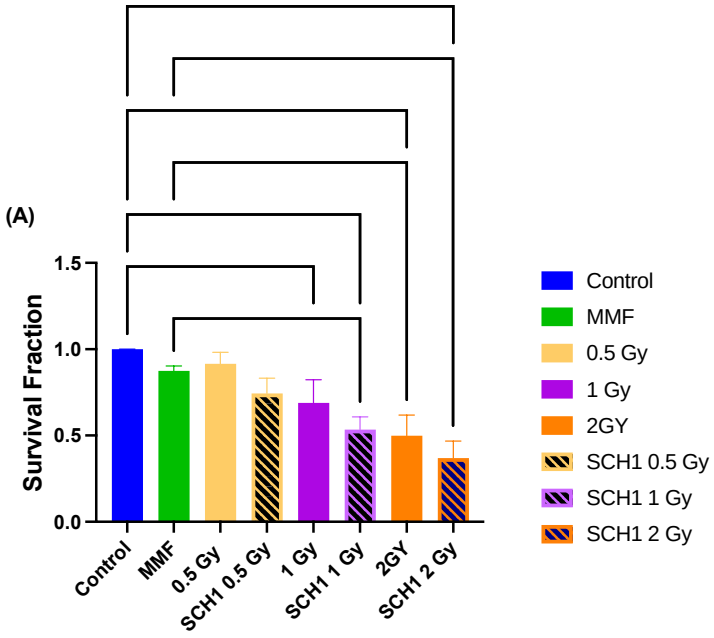

(B)

Bonferroni's multiple comparisons test	Summary	Adjusted P Value
Control vs. MMF	ns	>0.9999
Control vs. 0.5 Gy	ns	>0.9999
Control vs. 1 Gy	**	0.0042
Control vs. 2GY	****	<0.0001
Control vs. SCH1 0.5 Gy	ns	0.0553
Control vs. SCH1 1 Gy	****	<0.0001
Control vs. SCH1 2 Gy	****	<0.0001
MMF vs. 0.5 Gy	ns	>0.9999
MMF vs. 1 Gy	ns	0.9378
MMF vs. 2GY	**	0.0034
MMF vs. SCH1 0.5 Gy	ns	>0.9999
MMF vs. SCH1 1 Gy	*	0.0215
MMF vs. SCH1 2 Gy	***	0.0003
0.5 Gy vs. 1 Gy	ns	0.1380
0.5 Gy vs. 2GY	***	0.0002
0.5 Gy vs. SCH1 0.5 Gy	ns	>0.9999
0.5 Gy vs. SCH1 1 Gy	**	0.0021
0.5 Gy vs. SCH1 2 Gy	****	<0.0001
1 Gy vs. 2GY	ns	0.1893
1 Gy vs. SCH1 0.5 Gy	ns	>0.9999
1 Gy vs. SCH1 1 Gy	ns	>0.9999
1 Gy vs. SCH1 2 Gy	**	0.0070
2GY vs. SCH1 0.5 Gy	ns	0.0525
2GY vs. SCH1 1 Gy	ns	>0.9999
2GY vs. SCH1 2 Gy	ns	>0.9999
SCH1 0.5 Gy vs. SCH1 1 Gy	ns	0.3406
SCH1 0.5 Gy vs. SCH1 2 Gy	**	0.0026
SCH1 1 Gy vs. SCH1 2 Gy	ns	>0.9999

Appendix 12. MDA-MB-231 cell clonogenic assay investigating the survival fraction of cells treated with 0.5 Gy, 1 Gy,2 Gy radiation, 2 mM MMF and SCH1 combination using each Gy radiation and 2 mM MMF.

Data shown is the average of three independent experiments carried out in triplicate +/- SD. (B) 1-way ANOVA with Bonferroni post-test was performed using GraphPad Prism 9.2.1 software, P <0.005 = *, <0.001= **, <0.0001= ***, <0.00001=**** reported as significant when compared with the control with all results compares to the control and each other.

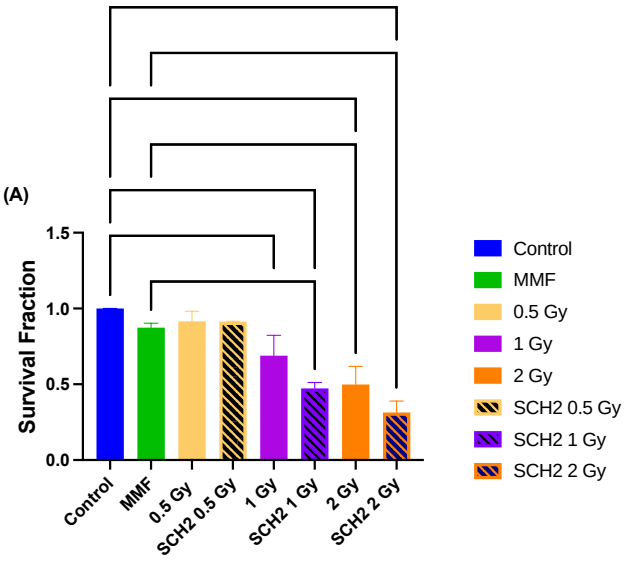

(B)

Bonferroni's multiple comparisons test	Summary	Adjusted P Value
Control vs. MMF	ns	>0.9999
Control vs. 0.5 Gy	ns	>0.9999
Control vs. 1 Gy	**	0.0017
Control vs. 2 Gy	****	<0.0001
Control vs. SCH2 0.5 Gy	ns	>0.9999
Control vs. SCH2 1 Gy	****	<0.0001
Control vs. SCH2 2 Gy	****	<0.0001
MMF vs. 0.5 Gy	ns	>0.9999
MMF vs. 1 Gy	ns	0.6232
MMF vs. 2 Gy	**	0.0014
MMF vs. SCH2 0.5 Gy	ns	>0.9999
MMF vs. SCH2 1 Gy	**	0.0017
MMF vs. SCH2 2 Gy	****	<0.0001
0.5 Gy vs. 1 Gy	ns	0.0745
0.5 Gy vs. 2 Gy	****	<0.0001
0.5 Gy vs. SCH2 0.5 Gy	ns	>0.9999
0.5 Gy vs. SCH2 1 Gy	***	0.0001
0.5 Gy vs. SCH2 2 Gy	****	<0.0001
1 Gy vs. 2 Gy	ns	0.1056
1 Gy vs. SCH2 0.5 Gy	ns	0.2041
1 Gy vs. SCH2 1 Gy	ns	0.1064
1 Gy vs. SCH2 2 Gy	***	0.0002
2 Gy vs. SCH2 0.5 Gy	***	0.0004
2 Gy vs. SCH2 1 Gy	ns	>0.9999
2 Gy vs. SCH2 2 Gy	ns	0.1247
SCH2 0.5 Gy vs. SCH2 1 Gy	***	0.0006
SCH2 0.5 Gy vs. SCH2 2 Gy	****	<0.0001
SCH2 1 Gy vs. SCH2 2 Gy	ns	0.6981

Appendix 13. MDA-MB-231 cell clonogenic assay investigating the survival fraction of cells treated with 0.5 Gy, 1 Gy,2 Gy radiation, 2 μM MMF and SCH2 combination using each Gy radiation and 2 μM MMF.

Data shown is the average of three independent experiments carried out in triplicate +/- SD. (B) 1-way ANOVA with Bonferroni post-test was performed using GraphPad Prism 9.2.1 software, P <0.005 = *, <0.001= **, <0.0001= ***, <0.00001=**** reported as significant when compared with the control with all results compares to the control and each other.

(A)

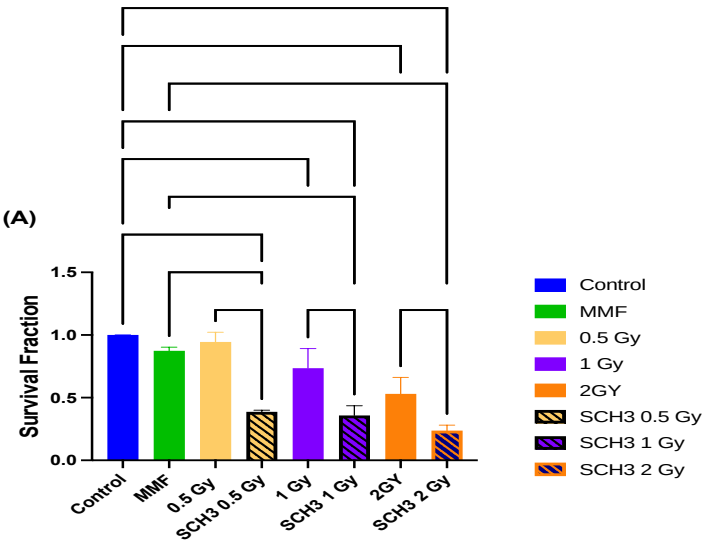

(B)

Bonferroni's multiple comparisons test	Summary	Adjusted P Value
Control vs. MMF	ns	>0.9999
Control vs. 0.5 Gy	ns	>0.9999
Control vs. 1 Gy	*	0.0235
Control vs. 2GY	****	<0.0001
Control vs. SCH3 0.5 Gy	****	<0.0001
Control vs. SCH3 1 Gy	****	<0.0001
Control vs. SCH3 2 Gy	****	<0.0001
MMF vs. 0.5 Gy	ns	>0.9999
MMF vs. 1 Gy	ns	>0.9999
MMF vs. 2GY	*	0.0124
MMF vs. SCH3 0.5 Gy	**	0.0026
MMF vs. SCH3 1 Gy	**	0.0013
MMF vs. SCH3 2 Gy	****	<0.0001
0.5 Gy vs. 1 Gy	ns	0.1645
0.5 Gy vs. 2GY	****	<0.0001
0.5 Gy vs. SCH3 0.5 Gy	****	<0.0001
0.5 Gy vs. SCH3 1 Gy	****	<0.0001
0.5 Gy vs. SCH3 2 Gy	****	<0.0001
1 Gy vs. 2GY	ns	0.0851
1 Gy vs. SCH3 0.5 Gy	*	0.0136
1 Gy vs. SCH3 1 Gy	**	0.0060
1 Gy vs. SCH3 2 Gy	****	<0.0001
2GY vs. SCH3 0.5 Gy	ns	>0.9999
2GY vs. SCH3 1 Gy	ns	>0.9999
2GY vs. SCH3 2 Gy	**	0.0055
SCH3 0.5 Gy vs. SCH3 1 Gy	ns	>0.9999
SCH3 0.5 Gy vs. SCH3 2 Gy	ns	>0.9999
SCH3 1 Gy vs. SCH3 2 Gy	ns	>0.9999

Appendix 14. MDA-MB-231 cell clonogenic assay investigating the survival fraction of cells treated with 0.5 Gy, 1 Gy,2 Gy radiation, 2 mM MMF and SCH3 combination using each Gy radiation and 2 mM MMF.

Data shown is the average of three independent experiments carried out in triplicate +/- SD. (B) 1-way ANOVA with Bonferroni post-test was performed using GraphPad Prism 9.2.1 software, P <0.005 = *, <0.001= **, <0.0001= ***, <0.00001=**** reported as significant when compared with the control with all results compares to the control and each other.

References

- *A Study of Novel Anti-cancer Agents in Patients with Metastatic Triple Negative Breast Cancer (BEGONIA)* (2023) *CTG Labs - NCBI*. Available at: https://www.clinicaltrials.gov/study/NCT03742102?cond=Triple+Negative+Breast+Cancer&rank=4 (Accessed: 28 July 2023).
- A trial looking at giving 1 week of radiotherapy for breast cancer (fast-forward) (2022) Cancer Research UK. Available at: https://www.cancerresearchuk.org/about-cancer/find-a-clinical-trial/a-trial-looking-giving-1-week-radiotherapy-breast-cancer-fast-forward#undefined (Accessed: 12 May 2023).
- *AAT Bioquest*. Available at: https://www.aatbio.com/resources/application-notes/mtt-assay (Accessed: April 11, 2023).
- Almeida M, Soares M, Ramalhinho AC, Moutinho JF, Breitenfeld L, Pereira L. The prognostic value of NRF2 in breast cancer patients: a systematic review with meta-analysis. Breast Cancer Res Treat. 2020 Feb;179(3):523-532. doi: 10.1007/s10549-019-05494-4. Epub 2019 Nov 19. PMID: 31745730.
- Anastasiadi Z, Lianos GD, Ignatiadou E, Harissis HV, Mitsis M. Breast cancer in young women: an overview. Updates Surg. 2017 Sep;69(3):313-317. doi: 10.1007/s13304-017-0424-1. Epub 2017 Mar 4. PMID: 28260181.
- Andreopoulou, E., Schweber, S., Sparano, J. and McDaid, H. (2015). Therapies for triple negative breast cancer. Expert Opinion on Pharmacotherapy, 16(7), pp.983-998
- *Archiving best practice* (2023) *NC3Rs*. Available at: https://nc3rs.org.uk/3rs-resources/breeding-and-colony-management/archiving-best-practice (Accessed: 15 August 2023).
- Arora G, Ghosh S, Chatterjee S. Understanding doxorubicin associated calcium remodeling during triple-negative breast cancer treatment: an *in silico*study. Explor Target Antitumor Ther. 2021;2(2):208-226. doi: 10.37349/etat.2021.00042. Epub 2021 Apr 30. PMID: 36046147; PMCID: PMC9400755.
- Asante EC, Pallegar NK, Viloria-Petit AM, Christian SL. Three-Dimensional Co-Culture Method for Studying Interactions Between Adipocytes, Extracellular Matrix, and Cancer Cells. Methods Mol Biol. 2022;2508:69-77. doi: 10.1007/978-1-0716-2376-3_7. PMID: 35737234.

- Ashburn TT, Thor KB. Drug Repositioning: Identifying and Developing New Uses for Existing Drugs. Nat. Rev. Drug Discov., 8, 2004, 673-83
- Augustine R, Alhussain H, Hasan A, Badie Ahmed M, C Yalcin H, Al Moustafa AE. A novel in ovo model to study cancer metastasis using chicken embryos and GFP expressing cancer cells. Bosn J Basic Med Sci. 2020 Feb 5;20(1):140-148. doi: 10.17305/bjbms.2019.4372. PMID: 31336058; PMCID: PMC7029200.
- Azoury, F. *et al*. (2022) "Role of radiation therapy in triple negative breast cancer: Current state and future directions—A narrative review," Precision Cancer Medicine, 5, pp. 3–3. Available at: https://doi.org/10.21037/pcm-21-9.
- Bai H., Z. Wang, K. Chen, *et al*., Influence of chemotherapy on EGFR mutation status among patients with non-small-cell lung cancer, J. Clin. Oncol. 30 (2012) 3077–3083.
- Bai X, Ni J, Beretov J, Wasinger VC, Wang S, Zhu Y, Graham P, Li Y. Activation of the eIF2α/ATF4 axis drives triple-negative breast cancer radioresistance by promoting glutathione biosynthesis. Redox Biol. 2021 Jul; 43:101993. doi: 10.1016/j.redox.2021.101993. Epub 2021 Apr 28. PMID: 33946018; PMCID: PMC8111851.
- Bai, X. *et al.* (2021) 'Triple-negative breast cancer therapeutic resistance: Where is the Achilles' heel?', *Cancer Letters*, 497, pp. 100–111. oi: 10.1016/j.canlet.2020.10.016.
- Balendiran, G.K., Dabur, R., and Fraser, D. (2004). The role of glutathione in cancer. Cell Biochem. Funct. *22*, 343–352.
- Ballatori N, Krance SM, Notenboom S, Shi S, Tieu K, Hammond CL. Glutathione dysregulation and the etiology and progression of human diseases. *Biol Chem.* 2009;390(3):191–214.
- Baranova A, Krasnoselskyi M, Starikov V, Kartashov S, Zhulkevych I, Vlasenko V, Oleshko K, Bilodid O, Sadchikova M, Vinnyk Y. Triple-negative breast cancer: current treatment strategies and factors of negative prognosis. J Med Life. 2022 Feb;15(2):153-161. doi: 10.25122/jml-2021-0108. PMID: 35419095; PMCID: PMC8999097.
- Beatty, A. *et al.* (2018) 'Metabolite profiling reveals the glutathione biosynthetic pathway as a therapeutic target in triple-negative breast cancer', *Molecular Cancer Therapeutics*, 17(1), pp. 264–275. doi: 10.1158/1535-7163.mct-17-0407.

- Beatty, A., Fink, L., Singh, T., Strigun, A., Peter, E., Ferrer, C., Nicolas, E., Cai, K., Moran, T., Reginato, M., Rennefahrt, U. and Peterson, J., 2017. Metabolite Profiling Reveals the Glutathione Biosynthetic Pathway as a Therapeutic Target in Triple-Negative Breast Cancer. Molecular Cancer Therapeutics, 17(1), pp.264-275.
- Bhamidipati, D., Haro-Silerio, J.I., Yap, T.A. *et al.* PARP inhibitors: enhancing efficacy through rational combinations. *Br J Cancer* (2023). https://doi.org/10.1038/s41416-023-02326-7
- Bianchini, G., Balko, J., Mayer, I., Sanders, M. and Gianni, L. (2016). Triple-negative breast cancer: challenges and opportunities of a heterogeneous disease. Nature Reviews Clinical Oncology, 13(11), pp.674-690.
- Blaquier JB, Cardona AF, Recondo G. Resistance to KRAS^{G12C} Inhibitors in Non-Small Cell Lung Cancer. Front Oncol. 2021 Dec 24; 11:787585. doi: 10.3389/fonc.2021.787585. PMID: 35004309; PMCID: PMC8739760.
- Bomprezzi R. Dimethyl fumarate in the treatment of relapsing-remitting multiple sclerosis: an overview. Ther Adv Neurol Disord. 2015 Jan;8(1):20-30. doi: 10.1177/1756285614564152. PMID: 25584071; PMCID: PMC4286944.
- Borrego-Soto, G., Ortiz-López, R. and Rojas-Martínez, A. (2015) 'Ionizing radiation-induced DNA injury and damage detection in patients with breast cancer', *Genetics and Molecular Biology*, 38(4), pp. 420–432. doi:10.1590/s1415-475738420150019.
- *BRCA*: The breast cancer gene - *BRCA* mutations & risks (2023) National Breast Cancer Foundation. Available at: https://www.nationalbreastcancer.org/what-is*BRCA*/#:~:text=What%20Is%20*BRCA*%3F,do%20not%20cause%20breast%20cancer. (Accessed: 27 June 2023).
- Breast cancer statistics (2023) Cancer Research UK. Available at: https://www.cancerresearchuk.org/health-professional/cancer-statistics/statistics-by-cancer-type/breast-cancer (Accessed: 13 May 2023).
- Brennan, M., Matos, M., Li, B., Hronowski, X., Gao, B., Juhasz, P., Rhodes, K. and Scannevin, R., 2015. Dimethyl Fumarate and Monoethyl Fumarate Exhibit Differential Effects on KEAP1, NRF2 Activation, and Glutathione Depletion In Vitro. PLOS ONE, 10(3), p.e0120254.
- Brunt, A., Haviland, J., Wheatley, D., Sydenham, M., Alhasso, A., Bloomfield, D., Chan, C., Churn, M., Cleator, S., Coles, C., Goodman, A., Harnett, A.,

Hopwood, P., Kirby, A., Kirwan, C., Morris, C., Nabi, Z., Sawyer, E., Somaiah, N., Stones, L., Syndikus, I., Bliss, J., Yarnold, J. and Group, F., 2020. FAST-Forward Phase III Randomised Controlled Trial of 1-Week Hypofractionated Breast Radiotherapy: 5-Year Results for Efficacy and Late Normal Tissue Effects. *SSRN Electronic Journal*,

- Bukowska B, Gajek A, Marczak A. Two Drugs Are Better Than One. A Short History of Combined Therapy of Ovarian Cancer. Contemp Oncol (Pozn) (2015) 19(5):350–3. doi: 10.5114/wo.2014.43975
- Byrski, T., Gronwald, J., Huzarski, T., Grzybowska, E., Budryk, M., Stawicka, M., *et al*. (2008). Response to neo-adjuvant chemotherapy in women with *BRCA*1-positive breast cancers. Breast Cancer Res. Treat. 108, 289–296. doi: 10.1007/s10549-007-9600-1
- C. Curtis, S.P. Shah, S.F. Chin, *et al*., The genomic and transcriptomic architecture of 2,000 breast tumours reveals novel subgroups, Nature 486 (2012) 346–352.
- Cancerresearchuk.org. 2020. Triple Negative Breast Cancer | Cancer Research UK. [online] Available at: <https://www.cancerresearchuk.org/about-cancer/breast-cancer/stages-types-grades/types/triple-negative-breast-cancer> [Accessed 17 June 2020].
- Cancerresearchuk.org. 2021. *Doxorubicin (Adriamycin)* | *Cancer drugs* | *Cancer Research UK*. [online] Available at: <https://www.cancerresearchuk.org/about-cancer/cancer-in-general/treatment/cancer-drugs/drugs/doxorubicin> [Accessed 27 July 2021].
- Cancerrxgene.org. 2021. *Drug: Doxorubicin - Cancerrxgene - Genomics of Drug Sensitivity in Cancer*. [online] Available at: <https://www.cancerrxgene.org/compound/Doxorubicin/1386/overview/ic50?tissue=PANCANCER&screening_set=GDSC1> [Accessed 6 July 2021].
- Canny, S., Cruz, Y., Southern, M. and Griffin, P. (2011). PubChem promiscuity: a web resource for gathering compound promiscuity data from PubChem. Bioinformatics, 28(1), pp.140-141.
- Chen H, Wu J, Zhang Z, Tang Y, Li X, Liu S, Cao S, Li X. Association Between *BRCA* Status and Triple-Negative Breast Cancer: A Meta-Analysis. Front Pharmacol. 2018 Aug 21; 9:909. doi: 10.3389/fphar.2018.00909. PMID: 30186165; PMCID: PMC6111442.

- Chen L, Wang S, Feng Y, Zhang J, Du Y, Zhang J, Ongeval CV, Ni Y, Li Y. Utilisation of Chick Embryo Chorioallantoic Membrane as a Model Platform for Imaging-Navigated Biomedical Research. Cells. 2021 Feb 22;10(2):463. doi: 10.3390/cells10020463. PMID: 33671534; PMCID: PMC7926796.
- Choi W, Lee ES. Therapeutic Targeting of DNA Damage Response in Cancer. Int J Mol Sci. 2022 Feb 1;23(3):1701. doi: 10.3390/ijms23031701. PMID: 35163621; PMCID: PMC8836062.
- Chou T, Martin N. **CompuSyn software**. CompuSyn for drug combinations: PC software and user's guide: a computer program for quantitation of synergism and antagonism in drug combinations, and the determination of IC_{50} and ED_{50} and LD_{50} values. ComboSyn Inc., Paramus, NJ. **2005**. https://www.combosyn.com (Website for registration and free download)
- Chou TC. Drug Combination Studies and Their Synergy Quantification Using the Chou-Talalay Method. Cancer Res (2010) 70(2):440–6. doi: 10.1158/0008- 5472.CAN-09-1947
- Chu PY, Koh AP, Antony J, Huang RY. Applications of the Chick Chorioallantoic Membrane as an Alternative Model for Cancer Studies. Cells Tissues Organs. 2022;211(2):222-237. doi: 10.1159/000513039. Epub 2021 Mar 29. PMID: 33780951; PMCID: PMC9153341.
- Circu ML, Aw TY. Glutathione and apoptosis. Free Radic Res. 2008 Aug;42(8):689-706. doi: 10.1080/10715760802317663. PMID: 18671159; PMCID: PMC3171829.
- Clarithromycin: Uses, dosage & side effects (no date) Drugs.com. Available at: https://www.drugs.com/clarithromycin.html# (Accessed: 28 June 2023).
- Clarke M, Collins R, Darby S, Davies C, Elphinstone P, Evans V, Godwin J, Gray R, Hicks C, James S, MacKinnon E, McGale P, McHugh T, Peto R, Taylor C, Wang Y; Early Breast Cancer Trialists' Collaborative Group (EBCTCG). Effects of radiotherapy and of differences in the extent of surgery for early breast cancer on local recurrence and 15-year survival: an overview of the randomised trials. Lancet. 2005 Dec 17;366(9503):2087-106. doi: 10.1016/S0140-6736(05)67887-7. PMID: 16360786.
- Comen, E., Davids, M., Kirchhoff, T., Hudis, C., Offit, K., and Robson, M. (2011). Relative contributions of *BRCA*1 and *BRCA*2 mutations to "triple-

negative" breast cancer in ashkenazi women. Breast Cancer Res. Treat. 129, 185–190. doi: 10.1007/s10549-011-1433-2

- Copyi
- Dagogo-Jack, I. and Shaw, A. (2017). Tumour heterogeneity and resistance to cancer therapies. *Nature Reviews Clinical Oncology*, 15(2), pp.81-94.
- De Nicola M, Ghibelli L. Glutathione depletion in survival and apoptotic pathways. Front Pharmacol. 2014 Dec 4; 5:267. doi: 10.3389/fphar.2014.00267. PMID: 25538619; PMCID: PMC4255488.
- Deo, S., Shukla, N., Gogia, A., Sharma, D., Jakhetiya, A., Muduly, D., Garg, P., Mathur, S. and Reenivas, V. (2017). A Comparative Study of Clinical Profile and Relapse Patterns in TRIPLE-NEGATIVE and Non-Triple-Negative Breast Cancer Patients Treated with Curative Intent. Indian Journal of Surgical Oncology, 8(3), pp.291-297.
- Deryugina EI, Quigley JP. Chick embryo chorioallantoic membrane model systems to study and visualize human tumor cell metastasis. Histochem Cell Biol. 2008 Dec;130(6):1119-30. doi: 10.1007/s00418-008-0536-2. Epub 2008 Nov 13. PMID: 19005674; PMCID: PMC2699943.
- Desouky, O., Ding, N. and Zhou, G., 2015. Targeted and non-targeted effects of ionizing radiation. *Journal of Radiation Research and Applied Sciences*, 8(2), pp.247-254.
- Diana Duarte, Nuno Vale, Evaluation of synergism in drug combinations and reference models for future orientations in oncology, Current Research in Pharmacology and Drug Discovery, Volume 3,2022,100110, ISSN 2590-2571,
- Drug repurposing: Advantages and key approaches (no date) Drug Discovery from Technology Networks. Available at: https://www.technologynetworks.com/drug-discovery/articles/drug-repurposing-advantages-and-key-approaches-344261 (Accessed: 28 June 2023).
- Drugbank.ca. (2020). Olaparib - DrugBank. [online] Available at: https://www.drugbank.ca/drugs/DB09074 [Accessed 8 Feb. 2020].
- Drugbank.ca. 2020. Diroximel Fumarate - Drugbank. [online] Available at: <https://www.drugbank.ca/drugs/DB14783#reference-A187532> [Accessed 19 June 2020].

- Fayaz S, Demian GA, El-Sherify M, Eissa H, *et al*. Triple negative breast cancer: 10-year survival update of the applied treatment strategy in Kuwait. *Gulf J Oncolog.* 2019;1(29):53–9.
- F.L. Sarmiento-Salinas, A. Delgado-Magallon, J.B. Montes-Alvarado, D. Ramirez- Ramirez, J.C. Flores-Alonso, P. Cortes-Hernandez, *et al*., Breast cancer subtypes present a differential production of reactive oxygen species (ROS) and susceptibility to antioxidant treatment, Front Oncol 9 (2019) 480.
- Fragkos, M. and Beard, P. (2011) 'Mitotic catastrophe occurs in the absence of apoptosis in p53-null cells with a defective G1 checkpoint', *PLoS ONE*, 6(8). doi:10.1371/journal.pone.0022946.
- Franco R, Panayiotidis MI, Cidlowski JA. Glutathione depletion is necessary for apoptosis in lymphoid cells independent of reactive oxygen species formation. J Biol Chem. 2007 Oct 19;282(42):30452-65. doi: 10.1074/jbc.M703091200. Epub 2007 Aug 27. PMID: 17724027; PMCID: PMC2267748.
- Frei E III, Karon M, Levin RH, *et al*. The effectiveness of combinations of antileukemic agents in inducing and maintaining remission in children with acute leukemia. Blood 1965; 26:642–56.
- Fu J, Sun H, Xu F, Chen R, Wang X, Ding Q, Xia T. RUNX regulated immune-associated genes predicts prognosis in breast cancer. Front Genet. 2022 Aug 26;13:960489. doi: 10.3389/fgene.2022.960489. PMID: 36092942; PMCID: PMC9459239.
- Garama DJ, Harris TJ, White CL, Rossello FJ, Abdul-Hay M, Gough DJ, Levy DE. A Synthetic Lethal Interaction between Glutathione Synthesis and Mitochondrial Reactive Oxygen Species Provides a Tumor-Specific Vulnerability Dependent on STAT3. Mol Cell Biol. 2015 Nov;35(21):3646-56. doi: 10.1128/MCB.00541-15. Epub 2015 Aug 17. PMID: 26283727; PMCID: PMC4589592.
- Garcia P, Wang Y, Viallet J, Macek Jilkova Z. The Chicken Embryo Model: A Novel and Relevant Model for Immune-Based Studies. Front Immunol. 2021 Nov 19; 12:791081. doi: 10.3389/fimmu.2021.791081. PMID: 34868080; PMCID: PMC8640176.
- Gewirtz DA. A critical evaluation of the mechanisms of action proposed for the antitumor effects of the anthracycline antibiotics adriamycin and

daunorubicin. *Biochem Pharmacol.* 1999; 57:727–741. [PubMed] [Google Scholar][Ref list]

- Gillies McKenna, W., Muschel, R., Gupta, A., Hahn, S. and Bernhard, E. (2003). The RAS signal transduction pathway and its role in radiation sensitivity. Oncogene, 22(37), pp.5866-5875.
- GodwinA.K., A. Meister, P.J. Odwyer, C.S. Huang, T.C. Hamilton, M.E. AndersonHigh resistance to cisplatin in human ovarian cancer cell lines is associated with marked increase of glutathione synthesis P. Natl. Acad. Sci. USA, 89 (7) (1992), pp. 3070-3074
- Gonzalez-Angulo, A. M., Timms, K. M., Liu, S., Chen, H., Litton, J. K., titter, J., *et al*. (2011). Incidence and outcome of *BRCA* mutations in unselected patients with triple receptor-negative breast cancer. Clin. Cancer Res. 17, 1082–1089. doi: 10.1158/1078-0432.CCR-10-2560
- Graham, K. and Unger, E., 2018. Overcoming tumor hypoxia as a barrier to radiotherapy, chemotherapy, and immunotherapy in cancer treatment. *International Journal of Nanomedicine*, Volume 13, pp.6049-6058.
- Great BRitian, Home Office statistics, (2022), Statistics of scientific procedures on living animals, Great Britain: 2022.
- Gross, M., Demo, S., Dennison, J., Chen, L., Chernov-Rogan, T., Goyal, B., Janes, J., Laidig, G., Lewis, E., Li, J., MacKinnon, A., Parlati, F., Rodriguez, M., Shwonek, P., Sjogren, E., Stanton, T., Wang, T., Yang, J., Zhao, F. and Bennett, M., 2014. Antitumor Activity of the Glutaminase Inhibitor CB-839 in Triple-Negative Breast Cancer. Molecular Cancer Therapeutics, 13(4), pp.890-901.
- Gupta N, Verma K, Nalla S, Kulshreshtha A, Lall R, Prasad S. Free Radicals as a Double-Edged Sword: The Cancer Preventive and Therapeutic Roles of Curcumin. Molecules. 2020 Nov 18;25(22):5390. doi: 10.3390/molecules25225390. PMID: 33217990; PMCID: PMC7698794.
- Hall, E. and Giaccia, A., n.d. *Radiobiology for the radiologist*. 7th ed. Philadelphia: LIPPINCOTT WILLIAMS & WILKINS, a WOLTERS KLUWER, pp.3-11.
- Hanahan D. and Weinberg R. A. (2011). Hallmarks of cancer: the next generation. Cell 144, 646-674. 10.1016/j.cell.2011.02.013
- Hargrave, S.D. *et al.* (2022) 'Cell fate following irradiation of MDA-MB-231 and MCF-7 breast cancer cells pre-exposed to the tetrahydroisoquinoline

sulfamate microtubule Disruptor STX3451', *Molecules*, 27(12), p. 3819. doi:10.3390/molecules27123819.

- Haycock, J.W., 2011. 3D cell culture: a review of current approaches and techniques. Methods Mol. Biol. Clifton NJ 695, 1–15. doi:10.1007/978-1-60761-984-0_1
- He MY, Rancoule C, Rehailia-Blanchard A, Espenel S, Trone JC, Bernichon E, Guillaume E, Vallard A, Magné N. Radiotherapy in triple-negative breast cancer: Current situation and upcoming strategies. Crit Rev Oncol Hematol. 2018 Nov; 131:96-101. doi: 10.1016/j.critrevonc.2018.09.004. Epub 2018 Sep 12. PMID: 30293712.
- He, J., Lee, HJ., Saha, S. *et al*. Inhibition of USP2 eliminates cancer stem cells and enhances TNBC responsiveness to chemotherapy. Cell Death Dis 10, 285 (2019). https://doi.org/10.1038/s41419-019-1512-6
- Hill, I.E., *et al.* (2023) 'Understanding radiation response and cell cycle variation in brain tumour cells using Raman spectroscopy', *The Analyst*, 148(11), pp. 2594–2608. doi:10.1039/d3an00121k.
- Hirschhaeuser, F., Menne, H., Dittfeld, C., West, J., Mueller-Klieser, W., Kunz-Schughart, L.A., 2010. Multicellular tumor spheroids: an underestimated tool is catching up again. J. Biotechnol. 148, 3–15. doi: 10.1016/j.jbiotec.2010.01.012
- Ho CJ, Gorski SM. Molecular Mechanisms Underlying Autophagy-Mediated Treatment Resistance in Cancer. Cancers (Basel). 2019 Nov 11;11(11):1775. doi: 10.3390/cancers11111775. PMID: 31717997; PMCID: PMC6896088.
- Hosey, A. M., Gorski, J. J., Murray, M. M., Quinn, J. E., Chung, W. Y., Stewart, G. E., *et al*. (2007). Molecular basis for estrogen receptor alpha deficiency in *BRCA*1-linked breast cancer. J. Natl. Cancer. Inst. 99, 683–694. doi: 10.1093/jnci/djm207
- Hou J, Zhou Z, Chen X, *et al*. HER2 reduces breast cancer radiosensitivity by activating focal adhesion kinase in vitro and in vivo. *Oncotarget*2016; 7:45186-98. 10.18632/oncotarget.9870
- https://doi.org/10.1016/j.crphar.2022.100110.
- Huang M, Haiderali A, Fox GE, Frederickson A, Cortes J, Fasching PA, O'Shaughnessy J. Economic and Humanistic Burden of Triple-Negative Breast Cancer: A Systematic Literature Review. Pharmacoeconomics. 2022

May;40(5):519-558. doi: 10.1007/s40273-021-01121-7. Epub 2022 Feb 3. PMID: 35112331; PMCID: PMC9095534.

- Huang Z, Yu P, Tang J. Characterization of Triple-Negative Breast Cancer MDA-MB-231 Cell Spheroid Model. Onco Targets Ther. 2020 Jun 11; 13:5395-5405. doi: 10.2147/OTT.S249756. PMID: 32606757; PMCID: PMC7295545.
- Huang, RX., Zhou, PK. DNA damage response signaling pathways and targets for radiotherapy sensitization in cancer. Sig Transduct Target Ther 5, 60 (2020). https://doi.org/10.1038/s41392-020-0150-x
- Hughes DA. Economics of Pharmacogenetic-Guided Treatments: Underwhelming or Overstated? Clin Pharmacol Ther. 2018 May;103(5):749-751. doi: 10.1002/cpt.1030. Epub 2018 Feb 13. PMID: 29435984.
- Indini A, Rijavec E, Ghidini M, Cortellini A, Grossi F. Targeting KRAS in Solid Tumors: Current Challenges and Future Opportunities of Novel KRAS Inhibitors. Pharmaceutics. 2021 May 4;13(5):653. doi: 10.3390/pharmaceutics13050653. PMID: 34064352; PMCID: PMC8147792.
- Isakoff, S., 2010. Triple-Negative Breast Cancer. The Cancer Journal, 16(1), pp.53-61.
- Ismail HM, Dorchies OM, Scapozza, L. The potential and benefits of repurposing existing drugs to treat rare muscular dystrophies. Expert Opin. Orphan Drugs, 6(4), 2018, 259-271.
- Jaramillo MC, Zhang DD the emerging role of the Nrf2-Keap1 signaling pathway in cancer. *Genes Dev*2013*;* **27:2179**–91*.*
- Jeddi, Farhad Narges Soozangar, Mohammad Reza Sadeghi, Mohammad Hossein Somi, Masoud Shirmohamadi, Amir-Taher Eftekhar-Sadat, Nasser Samadi,
- *Jia, T., Zhang, L., Duan, Y., Zhang, M., Wang, G., Zhang, J. and Zhao, Z., 2014. The differential susceptibilities of MCF-7 and MDA-MB-231 cells to the cytotoxic effects of curcumin are associated with the PI3K/Akt-SKP2-Cip/Kips pathway. Cancer Cell International, 14(1).*
- Johnson-Arbor K, Dubey R. Doxorubicin. [Updated 2020 Jul 26]. In: StatPearls [Internet]. Treasure Island (FL): StatPearls Publishing; 2021 Jan-. Available from: https://www.ncbi.nlm.nih.gov/books/NBK459232/
- Jögi A, Ehinger A, Hartman L, Alkner S. Expression of HIF-1α is related to a poor prognosis and tamoxifen resistance in contralateral breast cancer. PLoS

One. 2019 Dec 10;14(12):e0226150. doi: 10.1371/journal.pone.0226150. PMID: 31821370; PMCID: PMC6903737.

- Kennedy L, Sandhu JK, Harper ME, Cuperlovic-Culf M. Role of Glutathione in Cancer: From Mechanisms to Therapies. Biomolecules. 2020 Oct 9;10(10):1429. doi: 10.3390/biom10101429. PMID: 33050144; PMCID: PMC7600400.
- Kennedy L, Sandhu JK, Harper ME, Cuperlovic-Culf M. Role of Glutathione in Cancer: From Mechanisms to Therapies. Biomolecules. 2020 Oct 9;10(10):1429. doi: 10.3390/biom10101429. PMID: 33050144; PMCID: PMC7600400.
- *Kimbung, S., Biskup, E., Johansson, I., Aaltonen, K., Ottosson-Wadlund, A., Gruvberger-Saal, S., Cunliffe, H., Fadeel, B., Loman, N., Berglund, P. and Hedenfalk, I. (2012). Co-targeting of the PI3K pathway improves the response of BRCA1 deficient breast cancer cells to PARP1 inhibition. Cancer Letters, 319(2), pp.232-241.*
- Kirk, R. (2010). Surgical oncology: cancer risk reduction in *BRCA* mutation carriers. Nat. Rev. Clin. Oncol. 7:609. doi: 10.1038/nrclinonc.2010.157
- Koltai T, Reshkin SJ, Carvalho TMA, Di Molfetta D, Greco MR, Alfarouk KO, Cardone RA. Resistance to Gemcitabine in Pancreatic Ductal Adenocarcinoma: A Physiopathologic and Pharmacologic Review. Cancers (Basel). 2022 May 18;14(10):2486. doi: 10.3390/cancers14102486. PMID: 35626089; PMCID: PMC9139729.
- Kolyvas, E.A., Caldas, C., Kelly, K. *et al.* Androgen receptor function and targeted therapeutics across breast cancer subtypes. *Breast Cancer Res* **24**, 79 (2022). https://doi.org/10.1186/s13058-022-01574-4
- Krutzke L, Allmendinger E, Hirt K, Kochanek S. Chorioallantoic Membrane Tumor Model for Evaluating Oncolytic Viruses. Hum Gene Ther. 2020 Oct;31(19-20):1100-1113. doi: 10.1089/hum.2020.045. Epub 2020 Aug 17. PMID: 32552215; PMCID: PMC7585625.
- Kundeková B, Máčajová M, Meta M, Čavarga I, Bilčík B. Chorioallantoic Membrane Models of Various Avian Species: Differences and Applications. Biology (Basel). 2021 Apr 6;10(4):301. doi: 10.3390/biology10040301. PMID: 33917385; PMCID: PMC8067367.
- Kyndi M, Sørensen FB, Knudsen H, Overgaard M, Nielsen HM, Overgaard J; Danish Breast Cancer Cooperative Group. Estrogen receptor, progesterone

receptor, HER-2, and response to postmastectomy radiotherapy in high-risk breast cancer: the Danish Breast Cancer Cooperative Group. J Clin Oncol. 2008 Mar 20;26(9):1419-26. doi: 10.1200/JCO.2007.14.5565. Epub 2008 Feb 19. PMID: 18285604.

- L'Annunziata, M., 2008. *Radioactivity*. 1st ed. Amsterdam [etc.]: Elsevier, p.71.
- Lambin, P., Rios-Velazquez, E., Leijenaar, R., Carvalho, S., van Stiphout, R., Granton, P., Zegers, C., Gillies, R., Boellard, R., Dekker, A. and Aerts, H. (2012). Radiomics: Extracting more information from medical images using advanced feature analysis. *European Journal of Cancer*, 48(4), pp.441-446.
- Landeck L, Asadullah K, Amasuno A, Pau-Charles I, Mrowietz U. Dimethyl fumarate (DMF) vs. monoethyl fumarate (MEF) salts for the treatment of plaque psoriasis: a review of clinical data. Arch Dermatol Res. 2018 Aug;310(6):475-483. doi: 10.1007/s00403-018-1825-9. Epub 2018 Mar 24. PMID: 29574575; PMCID: PMC6060759.
- Lategan TW, Wang L, Sprague TN, Rousseau FS. Pharmacokinetics and Bioavailability of Monomethyl Fumarate Following a Single Oral Dose of Bafiertam™ (Monomethyl Fumarate) or Tecfidera® (Dimethyl Fumarate). CNS Drugs. 2021 May;35(5):567-574. doi: 10.1007/s40263-021-00799-9. Epub 2021 Mar 30. PMID: 33797063; PMCID: PMC8144082.
- Lee YS, Gupta DP, Park SH, Yang HJ, Song GJ. Anti-Inflammatory Effects of Dimethyl Fumarate in Microglia via an Autophagy Dependent Pathway. Front Pharmacol. 2021 May 7; 12:612981. doi: 10.3389/fphar.2021.612981. PMID: 34025399; PMCID: PMC8137969.
- Lee, G., Lee, H., Park, H., Schiebler, M., van Beek, E., Ohno, Y., Seo, J. and Leung, A. (2017). Radiomics and its emerging role in lung cancer research, imaging biomarkers and clinical management: State of the art. *European Journal of Radiology*, 86, pp.297-307.
- Li Y, Zhan Z, Yin X, Fu S, Deng X. Targeted Therapeutic Strategies for Triple-Negative Breast Cancer. Front Oncol. 2021 Oct 28; 11:731535. doi: 10.3389/fonc.2021.731535. PMID: 34778045; PMCID: PMC8581040.
- Li, Y. *et al.* (2021) “Targeted therapeutic strategies for triple-negative breast cancer,” *Frontiers in Oncology*, 11. Available at: https://doi.org/10.3389/fonc.2021.731535.

- Li, Y., Fan, J. and Ju, D. (2019) 'Neurotoxicity concern about the brain targeting delivery systems', *Brain Targeted Drug Delivery System*, pp. 377–408. doi:10.1016/b978-0-12-814001-7.00015-9.
- Lien, E., Lyssiotis, C., Juvekar, A., Hu, H., Asara, J., Cantley, L. and Toker, A., 2016. Glutathione biosynthesis is a metabolic vulnerability in PI (3)K/Akt-driven breast cancer. Nature Cell Biology, 18(5), pp.572-578.
- Lilley, J., and Murray, L.J. (2023) 'Radiotherapy: Technical aspects', *Medicine*, 51(1), pp. 11–16. doi: 10.1016/j.mpmed.2022.10.003.
- Litjens, N.H., van Strijen, E., van Gulpen, C. *et al. In vitro* pharmacokinetics of anti-psoriatic fumaric acid esters. *BMC Pharmacol* **4**, 22 (2004). https://doi.org/10.1186/1471-2210-4-22
- Liu, D. *et al.* (2022) 'Targeted disruption of mitochondria potently reverses Multidrug Resistance in Cancer therapy', *British Journal of Pharmacology*, 179(13), pp. 3346–3362. doi:10.1111/bph.15801.
- Logue, S., Elgendy, M. & Martin, S. Expression, purification, and use of recombinant annexin V for the detection of apoptotic cells. Nat Protoc 4, 1383–1395 (2009). https://doi.org/10.1038/nprot.2009.143
- Lovitt, C., Shelper, T. and Avery, V., 2018. Doxorubicin resistance in breast cancer cells is mediated by extracellular matrix proteins. BMC Cancer, 18(1).
- Lu, S.C. (2013) 'Glutathione synthesis', *Biochimica et Biophysica Acta (BBA) - General Subjects*, 1830(5), pp. 3143–3153. doi: 10.1016/j.bbagen.2012.09.008.
- Lushchak, V.I. (2012) 'Glutathione homeostasis and functions: Potential targets for medical interventions', *Journal of Amino Acids*, 2012, pp. 1–26. doi:10.1155/2012/736837.
- Luu, A., Chowdhury, B., Al-Omran, M., Teoh, H., Hess, D. and Verma, S., 2018. Role of Endothelium in Doxorubicin-Induced Cardiomyopathy. *JACC: Basic to Translational Science*, 3(6), pp.861-870.
- Malhotra V., Perry M.C. Classical chemotherapy: Mechanisms, toxicities, and the therapeutic window. Cancer Biol. Ther. 2003;2: S2–S4. doi: 10.4161/cbt.199.
- MANGIR, N. *et al.* (2018) 'An improved in vivo methodology to visualise tumour induced changes in vasculature using the chick chorionic allantoic membrane assay', *In Vivo*, 32(3). doi:10.21873/invivo.11262.

- Maugeri A, Lombardo GE, Navarra M, Cirmi S, Rapisarda A. The chorioallantoic membrane: A novel approach to extrapolate data from a well-established method. J Appl Toxicol. 2022 Jun;42(6):995-1003. doi: 10.1002/jat.4271. Epub 2021 Dec 7. PMID: 34874573; PMCID: PMC9300073.
- Mayo Clinic. (2019). *Managing the lingering side effects of cancer treatment*. [online] Available at: https://www.mayoclinic.org/diseases-conditions/cancer/in-depth/cancer-survivor/art-20045524 [Accessed 29 Jul. 2019].
- McCann, K. and Hurvitz, S., 2018. Advances in the use of PARP inhibitor therapy for breast cancer. Drugs in Context, 7, pp.1-30.
- McDermott, M. *et al*. (2014) 'In vitro development of chemotherapy and targeted therapy drug-resistant cancer cell lines: A practical guide with case studies', Frontiers in Oncology, 4. doi:10.3389/fonc.2014.00040.
- McGhan L.J., McCullough A.E., Protheroe C.A., Dueck A.C., Lee J.J., Nunez-Nateras R., Castle E.P., Gray R.J., Wasif N., Goetz M.P., *et al*. Androgen receptor-positive triple negative breast cancer: A unique breast cancer subtype. Ann. Surg. Oncol. 2014; 21:361–367. doi: 10.1245/s10434-013-3260-7.
- McNamara K.M., Yoda T., Miki Y., Chanplakorn N., Wongwaisayawan S., Incharoen P., Kongdan Y., Wang L., Takagi K., Mayu T., *et al*. Androgenic pathway in triple negative invasive ductal tumors: Its correlation with tumor cell proliferation. Cancer Sci. 2013; 104:639–646. doi: 10.1111/cas.12121.
- Mehta, G., Hsiao, A.Y., Ingram, M., Luker, G.D., Takayama, S., 2012. Opportunities and challenges for use of tumor spheroids as models to test drug delivery and efficacy. J. Controlled Release, Drug Delivery and Cancer: Today's Challenges, Tomorrow's Directions. 164, 192–204. doi: 10.1016/j.jconrel.2012.04.045
- Meyers, R., 2004. *Encyclopedia of physical science and technology*. 4th ed. Amsterdam: Elsevier, pp.603-650.
- Mills EA, Ogrodnik MA, Plave A, Mao-Draayer Y. Emerging Understanding of the Mechanism of Action for Dimethyl Fumarate in the Treatment of Multiple Sclerosis. Front Neurol. 2018 Jan 23; 9:5. doi: 10.3389/fneur.2018.00005. PMID: 29410647; PMCID: PMC5787128.
- Miran T, Vogg ATJ, Drude N, Mottaghy FM, Morgenroth A. Modulation of glutathione promotes apoptosis in triple-negative breast cancer cells. FASEB

J. 2018 May;32(5):2803-2813. doi: 10.1096/fj.201701157R. Epub 2018 Jan 8. PMID: 29301945.

- Mladenov, E., Magin, S., Soni, A. and Iliakis, G., 2013. DNA Double-Strand Break Repair as Determinant of Cellular Radiosensitivity to Killing and Target in Radiation Therapy. *Frontiers in Oncology*, 3.
- Moding EJ, Kastan MB, Kirsch DG. Strategies for optimizing the response of cancer and normal tissues to radiation. Nat Rev Drug Discov. 2013 Jul;12(7):526-42. doi: 10.1038/nrd4003. PMID: 23812271; PMCID: PMC3906736.
- Morrissey B., Blyth K., Carter P., Chelala C., Jones L., Holen I., and Speirs V. (2016). SEARCHBreast: a new online resource to make surplus material from in vivo models of breast cancer visible and accessible to researchers. *Breast Cancer Res.* 18, 59 10.1186/s13058-016-0716-2
- Moulder S., Dhillon N., Ng C., Hong D., Wheler J., Naing A., Tse S., La Paglia A., Dorr R., Hersh E. A phase I trial of imexon, a pro-oxidant, in combination with docetaxel for the treatment of patients with advanced breast, non-small cell lung and prostate cancer. *Investig. New Drugs.* 2010; 28:634–640. doi: 10.1007/s10637-009-9273-1.
- Murad H, Hawat M, Ekhtiar A, AlJapawe A, Abbas A, Darwish H, Sbenati O, Ghannam A. Induction of G1-phase cell cycle arrest and apoptosis pathway in MDA-MB-231 human breast cancer cells by sulfated polysaccharide extracted from Laurencia papillosa. Cancer Cell Int. 2016 May 26; 16:39. doi: 10.1186/s12935-016-0315-4. PMID: 27231438; PMCID: PMC4881178.
- Murai, J., Zhang, Y., Morris, J., Ji, J., Takeda, S., Doroshow, J. and Pommier, Y. (2014). Rationale for Poly (ADP-ribose) Polymerase (PARP) Inhibitors in Combination Therapy with Camptothecins or Temozolomide Based on PARP Trapping versus Catalytic Inhibition. Journal of Pharmacology and Experimental Therapeutics, 349(3), pp.408-416.
- Musaogullari A, Mandato A, Chai YC. Role of Glutathione Depletion and Reactive Oxygen Species Generation on Caspase-3 Activation: A Study with the Kinase Inhibitor Staurosporine. Front Physiol. 2020 Aug 28; 11:998. doi: 10.3389/fphys.2020.00998. PMID: 32982774; PMCID: PMC7485172.
- Musolino, A., Bella, M. A., Bortesi, B., Michiara, M., Naldi, N., Zanelli, P., *et al*. (2007). *BRCA* mutations, molecular markers, and clinical variables in early-

onset breast cancer: A population-based study. Breast 16, 280–292. doi: 10.1016/j.breast.2006.12.003

- Nakamura H, Takada K. Reactive oxygen species in cancer: Current findings and future directions. Cancer Sci. 2021 Oct;112(10):3945-3952. doi: 10.1111/cas.15068. Epub 2021 Aug 2. PMID: 34286881; PMCID: PMC8486193.
- Nath S, Devi GR. Three-dimensional culture systems in cancer research: Focus on tumor spheroid model. Pharmacol Ther. 2016 Jul; 163:94-108. doi: 10.1016/j.pharmthera.2016.03.013. Epub 2016 Apr 8. PMID: 27063403; PMCID: PMC4961208.
- Nedeljković M, Damjanović A. Mechanisms of Chemotherapy Resistance in Triple-Negative Breast Cancer-How We Can Rise to the Challenge. Cells. 2019 Aug 22;8(9):957. doi: 10.3390/cells8090957. PMID: 31443516; PMCID: PMC6770896.
- Nice.org.uk. 2020. [online] Available at: <https://www.nice.org.uk/guidance/csg1/resources/improving-outcomes-in-breast-cancer-update-773371117> [Accessed 17 June 2020].
- Nikolakopoulou A, Soni A, Habibi M, Karaiskos P, Pantelias G, Terzoudi GI, Iliakis G. G2/M Checkpoint Abrogation with Selective Inhibitors Results in Increased Chromatid Breaks and Radiosensitization of 82-6 hTERT and RPE Human Cells. Front Public Health. 2021 May 28; 9:675095. doi: 10.3389/fpubh.2021.675095. PMID: 34123995; PMCID: PMC8193504.
- Nitiss KC, Nitiss JL. Twisting and ironing: doxorubicin cardiotoxicity by mitochondrial DNA damage. Clin Cancer Res. 2014 Sep 15;20(18):4737-9. doi: 10.1158/1078-0432.CCR-14-0821. Epub 2014 Jun 10. PMID: 24916696; PMCID: PMC4204112.
- Noguchi, S., Kasugai, T., Miki, Y., Fukutomi, T., Emi, M., and Nomizu, T. (1999). Clinicopathologic analysis of *BRCA*1- or *BRCA*2-associated hereditary breast carcinoma in Japanese women. Cancer 85, 2200–2205. doi. 10.1002/(SICI)1097- 0142.
- Nowak-Sliwinska P, Segura T, Iruela-Arispe ML. The chicken chorioallantoic membrane model in biology, medicine, and bioengineering. Angiogenesis. 2014 Oct;17(4):779-804. doi: 10.1007/s10456-014-9440-7. Epub 2014 Aug 20. PMID: 25138280; PMCID: PMC4583126.

- O'Callaghan, Y.C., Woods, J.A. and O'Brien, N.M. (2001) 'Limitations of the single-cell gel electrophoresis assay to monitor apoptosis in U937 and Hepg2 cells exposed to 7β-hydroxycholesterol11abbreviations: Tunel, terminal Deoxynucleotidyl Transferase (TDT)-mediated dUTP Nick End-labelling of fragmented nuclear DNA in situ; 7BOHC, 7B-hydroxycholesterol; EtBr, ethidium bromide.', Biochemical Pharmacology, 61(10), pp. 1217–1226. doi:10.1016/s0006-2952(01)00587-1.
- Ochs K, Kaina B. Apoptosis induced by DNA damage O6-methylguanine is Bcl-2 and caspase-9/3 regulated and Fas/caspase-8 independent. Cancer Res. 2000 Oct 15;60(20):5815-24. PMID: 11059778.
- Ohno, R. *et al.* (2011) 'Cryptogein-induced cell cycle arrest at G2 phase is associated with inhibition of cyclin-dependent kinases, suppression of expression of cell cycle-related genes and protein degradation in synchronized tobacco by-2 cells', *Plant and Cell Physiology*, 52(5), pp. 922–932. doi:10.1093/pcp/pcr042.
- Oikonomou, E., Anastasiou, M., Siasos, G., Androulakis, E., Psyrri, A., Toutouzas, K. and Tousoulis, D., 2019. Cancer Therapeutics-Related Cardiovascular Complications. Mechanisms, Diagnosis and Treatment. *Current Pharmaceutical Design*, 24(37), pp.4424-4435.
- Okazaki, K., Papagiannakopoulos, T. & Motohashi, H. Metabolic features of cancer cells in NRF2 addiction status. Biophys Rev 12, 435–441 (2020). https://doi.org/10.1007/s12551-020-00659-8
- Ortiz-Ferron, W. by G. (2020) The proper way to use the sub-G1 assay, Bitesize Bio. Available at: https://bitesizebio.com/25876/the-proper-way-to-use-the-sub-g1-assay-tips-tricks-and-secrets/ (Accessed: 17 July 2023).
- Palte MJ, Wehr A, Tawa M, Perkin K, Leigh-Pemberton R, Hanna J, Miller C, Penner N: Improving the Gastrointestinal Tolerability of Fumaric Acid Esters: Early Findings on Gastrointestinal Events with Diroximel Fumarate in Patients with Relapsing-Remitting Multiple Sclerosis from the Phase 3, Open-Label EVOLVE-MS-1 Study. Adv Ther. 2019 Nov;36(11):3154-3165. doi: 10.1007/s12325-019-01085-3. Epub 2019 Sep 19.
- Paramanantham A, Jung EJ, Kim HJ, Jeong BK, Jung JM, Kim GS, Chan HS, Lee WS. Doxorubicin-Resistant TNBC Cells Exhibit Rapid Growth with Cancer Stem Cell-like Properties and EMT Phenotype, Which Can Be Transferred to Parental Cells through Autocrine Signaling. Int J Mol Sci. 2021 Nov

18;22(22):12438. doi: 10.3390/ijms222212438. PMID: 34830320; PMCID: PMC8623267.

- Paschall A. V. and Liu K. (2016). An orthotopic mouse model of spontaneous breast cancer metastasis. J. Vis. Exp. 14, 54040 10.3791/54040
- Pathania S., R. Bhatia, A. Baldi, R. Singh, R.K. Rawal Drug metabolizing enzymes and their inhibitors' role in cancer resistance, Biomed Pharmacother, 105 (2018)
- Pawlikowska, P., Tayoun, T., Oulhen, M. *et al*. Exploitation of the chick embryo chorioallantoic membrane (CAM) as a platform for anti-metastatic drug testing. Sci Rep 10, 16876 (2020). https://doi.org/10.1038/s41598-020-73632-w
- Peng, L., Xu, T., Long, L. T., and Zuo, H. (2016). Association between *BRCA* status and P53 status in breast cancer: a meta-analysis. Med. Sci. Monit. 8, 1939–1945. doi: 10.12659/MSM.896260
- Petroni G, Bagni G, Iorio J, Duranti C, Lottini T, Stefanini M, Kragol G, Becchetti A, Arcangeli A. Clarithromycin inhibits autophagy in colorectal cancer by regulating the hERG1 potassium channel interaction with PI3K. Cell Death Dis. 2020 Mar 2;11(3):161. doi: 10.1038/s41419-020-2349-8. Erratum in: Cell Death Dis. 2020 Mar 30;11(3):209. Erratum in: Cell Death Dis. 2020 Jul 17;11(7):541. PMID: 32123164; PMCID: PMC7052256.
- Petroni, G., Bagni, G., Iorio, J. *et al*. Clarithromycin inhibits autophagy in colorectal cancer by regulating the hERG1 potassium channel interaction with PI3K. Cell Death Dis 11, 161 (2020). https://doi.org/10.1038/s41419-020-2349-8
- Pizzorno J. Glutathione! Integr Med (Encinitas). 2014 Feb;13(1):8-12. PMID: 26770075; PMCID: PMC4684116.
- Pizzorno J. Glutathione! Integr Med (Encinitas). 2014 Feb;13(1):8-12. PMID: 26770075; PMCID: PMC4684116.
- Pizzorno J. The path ahead: persistent organic pollutants (POPs)—a serious clinical concern. *Integrative Med Clin J.* 2013;12(2):8–11.
- Plesca D, Mazumder S, Almasan A. DNA damage response and apoptosis. Methods Enzymol. 2008; 446:107-22. doi: 10.1016/S0076-6879(08)01606-6. PMID: 18603118; PMCID: PMC2911482.
- Plesca D, Mazumder S, Almasan A. DNA damage response and apoptosis. Methods Enzymol. 2008; 446:107-22. doi: 10.1016/S0076-6879(08)01606-6. PMID: 18603118; PMCID: PMC2911482.

- Potiron VA, *et al*. (2013). Radiosensitization of prostate cancer cells by the dual PI3K/mTOR inhibitor BEZ235 under normoxic and hypoxic conditions. Radiother Oncol 106:138-146.
- Promega.co.uk. 2021. *Introduction to 3D Cell Culture*. [online] Available at: <https://www.promega.co.uk/resources/guides/cell-biology/3d-cell-culture-guide/> [Accessed 27 July 2021].
- Pucci, B., Kasten, M. and Giordano, A. (2000) “Cell cycle and apoptosis,” Neoplasia, 2(4), pp. 291–299. Available at: https://doi.org/10.1038/sj.neo.7900101.
- Radiotherapy dose fractionation, third edition (11/5/23) Radiotherapy dose fractionation, third edition | The Royal College of Radiologists. Available at: https://www.rcr.ac.uk/publication/radiotherapy-dose-fractionation-third-edition (Accessed: 11 May 2023).
- Ramón Y Cajal S, Sesé M, Capdevila C, Aasen T, De Mattos-Arruda L, Diaz-Cano SJ, Hernández-Losa J, Castellví J. Clinical implications of intratumor heterogeneity: challenges and opportunities. J Mol Med (Berl). 2020 Feb;98(2):161-177. doi: 10.1007/s00109-020-01874-2. Epub 2020 Jan 22. PMID: 31970428; PMCID: PMC7007907.
- Ribatti D. Chicken chorioallantoic membrane angiogenesis model. Methods Mol Biol. 2012; 843:47-57. doi: 10.1007/978-1-61779-523-7_5. PMID: 22222520.
- Ribatti Domenico, the chick embryo chorioallantoic membrane as an experimental model to study in vivo angiogenesis in glioblastoma multiforme, Brain Research Bulletin, Volume 182,2022, Pages 26-29, ISSN 0361-9230,
- Rieger AM, Nelson KL, Konowalchuk JD, Barreda DR. Modified annexin V/propidium iodide apoptosis assay for accurate assessment of cell death. J Vis Exp. 2011 Apr 24;(50):2597. doi: 10.3791/2597. PMID: 21540825; PMCID: PMC3169266.
- Rose M, Burgess JT, O'Byrne K, Richard DJ, Bolderson E. PARP Inhibitors: Clinical Relevance, Mechanisms of Action, and Tumor Resistance. Front Cell Dev Biol. 2020 Sep 9; 8:564601. doi: 10.3389/fcell.2020.564601. PMID: 33015058; PMCID: PMC7509090.
- Rostami-Yazdi, M., Clement, B. and Mrowietz, U., 2010. Pharmacokinetics of anti-psoriatic fumaric acid esters in psoriasis patients. Archives of Dermatological Research, 302(7), pp.531-538.

- Rouzier R, Perou CM, Symmans WF, Ibrahim N, Cristofanilli M, Anderson K, Hess KR, Stec J, Ayers M, Wagner P, Morandi P, Fan C, Rabiul I, Ross JS, Hortobagyi GN, Pusztai L. Breast cancer molecular subtypes respond differently to preoperative chemotherapy. Clin Cancer Res. 2005 Aug 15;11(16):5678-85. doi: 10.1158/1078-0432.CCR-04-2421. PMID: 16115903.
- Saadettin Kilickap and others, Doxorubicin-induced second degree and complete atrioventricular block, *EP Europace*, Volume 7, Issue 3, 2005, Pages 227–230, https://doi.org/10.1016/j.eupc.2004.12.012
- Sabzichi, M. *et al.* (2019) 'The synergistic impact of quinacrine on cell cycle and anti-invasiveness behaviors of doxorubicin in MDA-MB-231 breast cancer cells', *Process Biochemistry*, 81, pp. 175–181. doi: 10.1016/j.procbio.2019.03.007.
- Saidu Bennett, N., Bretagne, M., Mansuet, A., Just, P., Leroy, K., Cerles, O., Chouzenoux, S., Nicco, C., Damotte, D., Alifano, M., Borghese, B., Goldwasser, F., Batteux, F. and Alexandre, J., 2018. Dimethyl fumarate is highly cytotoxic in KRAS mutated cancer cells but spares non-tumorigenic cells. Oncotarget, 9(10), pp.9088-9099.
- Saidu NE, Noé G, Cerles O, Cabel L, Kavian-Tessler N, Chouzenoux S, Bahuaud M, Chéreau C, Nicco C, Leroy K, Borghese B, Goldwasser F, Batteux F, Alexandre J. Dimethyl Fumarate Controls the NRF2/DJ-1 Axis in Cancer Cells: Therapeutic Applications. Mol Cancer Ther. 2017 Mar;16(3):529-539. doi: 10.1158/1535-7163.MCT-16-0405. Epub 2017 Jan 9. PMID: 28069874.
- Sajid MT, Ahmed M, Azhar M, Mustafa QU, Shukr I, Ahmed M, Kamal Z. Age-related frequency of triple negative breast cancer in women. J Coll Physicians Surg Pak. 2014 Jun;24(6):400-3. PMID: 24953912.
- Sala, E., Mema, E., Himoto, Y., Veeraraghavan, H., Brenton, J., Snyder, A., Weigelt, B. and Vargas, H. (2017). Unravelling tumour heterogeneity using next-generation imaging: radiomics, radiogenomics, and habitat imaging. *Clinical Radiology*, 72(1), pp.3-10.
- Scannevin R. H., S. Chollate, M. Y. Jung, M. Shackett, H. Patel, P. Bista, W. Zeng, S. Ryan, M. Yamamoto, M. Lukashev, K. J. Rhodes, *J. Pharmacol. Exp. Ther.* 2012, 341, 274.
- Schmid P., Adams S., Rugo H.S., Schneeweiss A., Barrios C.H., Iwata H., Diéras V., Hegg R., Im S.-A., Shaw Wright G., *et al*. Atezolizumab and Nab-

Paclitaxel in Advanced Triple-Negative Breast Cancer. N. Engl. J. Med. 2018; 379:2108–2121. doi: 10.1056/NEJMoa1809615.

- Schmitt, L.A. Loeb, J.J. Salk, The influence of subclonal resistance mutations on targeted cancer therapy, Nat. Rev. Clin. Oncol. 13 (2016) 335–347.
- Schutte, B. *et al.* (1998) 'Annexin V binding assay as a tool to measure apoptosis in differentiated neuronal cells', *Journal of Neuroscience Methods*, 86(1), pp. 63–69. doi: https://doi.org/10.1016/S0165-0270(98)00147-2.
- Semenza, G.L. (2016) 'Hypoxia-inducible factors: Coupling glucose metabolism and redox regulation with induction of the breast cancer stem cell phenotype', *The EMBO Journal*, 36(3), pp. 252–259. doi:10.15252/embj.201695204.
- Shafer, D., Tombes, M., Shrader, E., Ryan, A., Bandyopadhyay, D., Dent, P. and Malkin, M., 2020. Phase I trial of dimethyl fumarate, temozolomide, and radiation therapy in glioblastoma. Neuro-Oncology Advances, 2(1).
- Sharon E. Johnatty, Jonathan Beesley, Bo Gao, Xiaoqing Chen, Yi Lu, Matthew H. Law, Michelle J. Henderson, Amanda J. Russell, Ellen L. Hedditch, Catherine Emmanuel, Sian Fereday, Penelope M. Webb, Ellen L. Goode, Robert A. Vierkant, Brooke L. Fridley, Julie M Cunningham, Peter A. Fasching, Matthias W. Beckmann, Arif B. Ekici, Estrid Hogdall, Susanne K. Kjaer, Allan Jensen, Claus Hogdall, Robert Brown, Jim Paul, Sandrina Lambrechts, Evelyn Despierre, Ignace Vergote, Jenny Lester, Beth Y. Karlan, Florian Heitz, Andreas du Bois, Philipp Harter, Ira Schwaab, Yukie Bean, Tanja Pejovic, Douglas A. Levine, Marc T. Goodman, Michael E. Camey, Pamela J. Thompson, Galina Lurie, Joellen Shildkraut, Andrew Berchuck, Kathryn L. Terry, Daniel W. Cramer, Murray D. Norris, Michelle Haber, Stuart MacGregor, Anna deFazio, Georgia Chenevix-Trench,ABCB1 (MDR1) polymorphisms and ovarian cancer progression and survival: A comprehensive analysis from the Ovarian Cancer Association Consortium and The Cancer Genome Atlas, Gynecologic Oncology, Volume 131, Issue 1, 2013, Pages 8-14, ISSN 0090-8258, https://doi.org/10.1016/j.ygyno.2013.07.107.
- Sheveleva E.V., Landowski T.H., Samulitis B.K., Bartholomeusz G., Powis G., Dorr R.T. Imexon induces an oxidative endoplasmic reticulum stress response in pancreatic cancer cells. *Mol. Cancer Res.* 2012; 10:392–400. doi: 10.1158/1541-7786.MCR-11-0359.

- Sies, H. (1999). Glutathione and its role in cellular functions. Free Radic. Biol. Med. *27*, 916–921.
- Siles, E. *et al*. (1998) 'Apoptosis after gamma irradiation. is it an important cell death modality?', British Journal of Cancer, 78(12), pp. 1594–1599. doi:10.1038/bjc.1998.728.
- Simmons JK, Hildreth BE 3rd, Supsavhad W, Elshafae SM, Hassan BB, Dirksen WP, Toribio RE, Rosol TJ. Animal Models of Bone Metastasis. Vet Pathol. 2015 Sep;52(5):827-41. doi: 10.1177/0300985815586223. Epub 2015 May 28. PMID: 26021553; PMCID: PMC4545712.
- Stewart MD, Merino Vega D, Arend RC, Baden JF, Barbash O, Beaubier N, Collins G, French T, Ghahramani N, Hinson P, Jelinic P, Marton MJ, McGregor K, Parsons J, Ramamurthy L, Sausen M, Sokol ES, Stenzinger A, Stires H, Timms KM, Turco D, Wang I, Williams JA, Wong-Ho E, Allen J. Homologous Recombination Deficiency: Concepts, Definitions, and Assays. Oncologist. 2022 Mar 11;27(3):167-174. doi: 10.1093/oncolo/oyab053. PMID: 35274707; PMCID: PMC8914493.
- Sullivan LB, Martinez-Garcia E, Nguyen H, Mullen AR, Dufour E, Sudarshan S, Licht JD, Deberardinis RJ, Chandel NS. The proto-oncometabolite fumarate binds glutathione to amplify ROS-dependent signaling. Mol Cell. 2013 Jul 25;51(2):236-48. doi: 10.1016/j.molcel.2013.05.003. Epub 2013 Jun 6. Erratum in: Mol Cell. 2013 Jul 25;51(2):273. PMID: 23747014; PMCID: PMC3775267.
- Swadi, R., Mather, G., Pizer, B.L. *et al.* Optimising the chick chorioallantoic membrane xenograft model of neuroblastoma for drug delivery. *BMC Cancer* **18**, 28 (2018). https://doi.org/10.1186/s12885-017-3978-x
- Swadi, R.R., Sampat, K., Herrmann, A. *et al*. CDK inhibitors reduce cell proliferation and reverse hypoxia-induced metastasis of neuroblastoma tumours in a chick embryo model. Sci Rep 9, 9136 (2019). https://doi.org/10.1038/s41598-019-45571-8
- Synthetic lethality: Accelerating precision cancer treatments (no date) GSK. Available at: https://www.gsk.com/en-gb/behind-the-science-magazine/synthetic-lethality-accelerating-precision-cancer-treatments/#:~:text=Synthetic%20lethality%20can%20be%20applied,a%20synthetic%20lethal%20therapy%20can (Accessed: 27 June 2023).

- Syu JP, Chi JT, Kung HN. Nrf2 is the key to chemotherapy resistance in MCF7 breast cancer cells under hypoxia. Oncotarget. 2016 Mar 22;7(12):14659-72. doi: 10.18632/oncotarget.7406. PMID: 26894974; PMCID: PMC4924742.
- Tafreshi, N.K. *et al.* (2019) "Development of targeted alpha particle therapy for solid tumors," *Molecules*, 24(23), p. 4314. Available at: https://doi.org/10.3390/molecules24234314.
- Takebe, N. *et al.* (2006) 'IMP dehydrogenase inhibitor mycophenolate mofetil induces caspase-dependent apoptosis and cell cycle inhibition in multiple myeloma cells', *Molecular Cancer Therapeutics*, 5(2), pp. 457–466. doi: 10.1158/1535-7163.mct-05-0340.
- Taymaz-Nikerel, H., Karabekmez, M.E., Eraslan, S. *et al.* Doxorubicin induces an extensive transcriptional and metabolic rewiring in yeast cells. *Sci Rep* **8,** 13672 (2018). https://doi.org/10.1038/s41598-018-31939-9
- Tecfidera, inn-dimethyl fumarate - European medicines agency. Available at: https://www.ema.europa.eu/en/documents/smop-initial/chmp-summary-positive-opinion-tecfidera_en.pdf (Accessed: 28 June 2023).
- Thakkar A, Wang B, Picon-Ruiz M, Buchwald P, Ince TA. Vitamin D and androgen receptor-targeted therapy for triple-negative breast cancer. Breast Cancer Res Treat. 2016 May;157(1):77-90. doi: 10.1007/s10549-016-3807-y. Epub 2016 Apr 27. PMID: 27120467; PMCID: PMC4869778.
- Thakuri PS, Gupta M, Plaster M, Tavana H. Quantitative Size-Based Analysis of Tumor Spheroids and Responses to Therapeutics. Assay Drug Dev Technol. 2019 Apr;17(3):140-149. doi: 10.1089/adt.2018.895. PMID: 30958703; PMCID: PMC6599382.
- Theodossiou, T., Ali, M., Grigalavicius, M., Grallert, B., Dillard, P., Schink, K., Olsen, C., Wälchli, S., Inderberg, E., Kubin, A., Peng, Q. and Berg, K., 2019. Simultaneous defeat of MCF7 and MDA-MB-231 resistances by a hypericin PDT–tamoxifen hybrid therapy. npj Breast Cancer, 5(1).
- Thu KL, Soria-Bretones I, Mak TW, Cescon DW. Targeting the cell cycle in breast cancer: towards the next phase. Cell Cycle. 2018;17(15):1871-1885. doi: 10.1080/15384101.2018.1502567. Epub 2018 Sep 11. PMID: 30078354; PMCID: PMC6152498.
- Timmerman, L., Holton, T., Yuneva, M., Louie, R., Padró, M., Daemen, A., Hu, M., Chan, D., Ethier, S., van 't Veer, L., Polyak, K., McCormick, F. and Gray, J., 2013. Glutamine Sensitivity Analysis Identifies the xCT Antiporter as a

Common Triple-negative breast tumor therapeutic target. Cancer Cell. 2013 Oct 14;24(4):450-65. doi: 10.1016/j.ccr.2013.08.020. Epub 2013 Oct 3. PMID: 24094812; PMCID: PMC3931310.

- Tozbikian G.H., Zynger D.L. A combination of GATA3 and SOX10 is useful for the diagnosis of metastatic triple-negative breast cancer. Hum. Pathol. 2019; 85:221–227. doi: 10.1016/j.humpath.2018.11.005
- Traina TA, Miller K, Yardley DA, Eakle J, Schwartzberg LS, O'Shaughnessy J, Gradishar W, Schmid P, Winer E, Kelly C, Nanda R, Gucalp A, Awada A, Garcia-Estevez L, Trudeau ME, Steinberg J, Uppal H, Tudor IC, Peterson A, Cortes J. Enzalutamide for the Treatment of Androgen Receptor-Expressing Triple-Negative Breast Cancer. J Clin Oncol. 2018 Mar 20;36(9):884-890. doi: 10.1200/JCO.2016.71.3495. Epub 2018 Jan 26. PMID: 29373071; PMCID: PMC5858523.Negative Breast Tumor Therapeutic Target. Cancer Cell, 24(4), pp.450-465.
- Triple negative breast cancer (2023) Cancer Research UK. Available at: https://www.cancerresearchuk.org/about-cancer/breast-cancer/stages-types-grades/types/triple-negative-breast-cancer (Accessed: April 26, 2023).
- Vadivelu, MD, N., Maria, MBBS, M., Jolly, MD, S., Rosenbloom, MD, J., Prasad, MD, A. and Kaye, MD, PhD, A., 2013. Review article. Clinical applications of oxymorphone. *Journal of Opioid Management*, 9(6), pp.439-452.
- Van Nuffel AM, Sukhatme V, Pantziarka P, Meheus L, Sukhatme VP, Bouche G. Repurposing Drugs in Oncology (ReDO)-clarithromycin as an anti-cancer agent. Ecancermedicalscience. 2015 Feb 24; 9:513. doi: 10.3332/ecancer.2015.513. PMID: 25729426; PMCID: PMC4341996.
- Vondeling GT, Cao Q, Postma MJ, Rozenbaum MH. The Impact of Patent Expiry on Drug Prices: A Systematic Literature Review. Appl Health Econ Health Policy. 2018 Oct;16(5):653-660. doi: 10.1007/s40258-018-0406-6. PMID: 30019138; PMCID: PMC6132437.
- Wang YY, Chen J, Liu XM, Zhao R, Zhe H. Nrf2-Mediated Metabolic Reprogramming in Cancer. Oxid Med Cell Longev. 2018 Jan 29; 2018:9304091. doi: 10.1155/2018/9304091. PMID: 29670683; PMCID: PMC5833252.
- Wennstig A.K., Wadsten C., Garmo H., Fredriksson I., Blomqvist C., Holmberg L., Nilsson G., Sund M. Long-term risk of ischemic heart disease

after adjuvant radiotherapy in breast cancer: Results from a large population-based cohort. *Breast Cancer Res.* 2020; 22:10. doi: 10.1186/s13058-020-1249-2.

- Who.int. (2019). *Cancer*. [online] Available at: https://www.who.int/news-room/fact-sheets/detail/cancer [Accessed 18 Jun. 2019].
- Wiklund SJ, Agurell E. Aspects of design and statistical analysis in the Comet assay. Mutagenesis. 2003 Mar;18(2):167-75. doi: 10.1093/mutage/18.2.167. PMID: 12621073.
- Xupeng Bai, Jie Ni, Julia Beretov, Peter Graham, Yong Li, Y. Xu, X. Han, Y. Li, H. Min, X. Zhao, Y.
  Zhang, Y. Qi, J. Shi, S. Qi, Y. BaoYan, M., & Liu, Q. Q. (2013). Targeted therapy: tailoring cancer treatment. *Chinese journal of cancer*, *32*(7), 363–364. doi:10.5732/cjc.013.10114
- Xinyu Li, Yong Zhou, Yongshuang Li, Liang Yang, Yingbo Ma, Xueqiang Peng, Shuo Yang, Jingang Liu, Hangyu Li, Autophagy: A novel mechanism of chemoresistance in cancers, Biomedicine & Pharmacotherapy, Volume 119, 2019, 109415, ISSN 0753-3322, https://doi.org/10.1016/j.biopha.2019.109415.
- Yin, L., Duan, JJ., Bian, XW. et al. Triple-negative breast cancer molecular subtyping and treatment progress. Breast Cancer Res 22, 61 (2020). https://doi.org/10.1186/s13058-020-01296-5
- Yolanda Lorenzo and others, the comet assay, DNA damage, DNA repair and cytotoxicity: hedgehogs are not always dead, *Mutagenesis*, Volume 28, Issue 4, July 2013, Pages 427–432,
- Zhang M, Cao G, Guo X, Gao Y, Li W, Lu D. A Comet Assay for DNA Damage and Repair After Exposure to Carbon-Ion Beams or X-rays in *Saccharomyces Cerevisiae*. Dose Response. 2018 Aug 9;16(3):1559325818792467. doi: 10.1177/1559325818792467. PMID: 30116170; PMCID: PMC6088507.
- Zhang Z, Liu X, Chen D, Yu J. Radiotherapy combined with immunotherapy: the dawn of cancer treatment. Signal Transduct Target Ther. 2022 Jul 29;7(1):258. doi: 10.1038/s41392-022-01102-y. PMID: 35906199; PMCID: PMC9338328.
- Zhang, D. and Zhang, J. (2018). Diagnosis and Treatment of Triple Negative Breast Cancer. Cancer Genetics and Epigenetics.

- Zhang, Z., Liu, X., Chen, D. *et al*. Radiotherapy combined with immunotherapy: the dawn of cancer treatment. Sig Transduct Target Ther 7, 258 (2022). https://doi.org/10.1038/s41392-022-01102-y
- Zorov DB, Juhaszova M, Sollott SJ. Mitochondrial reactive oxygen species (ROS) and ROS-induced ROS release. Physiol Rev. 2014 Jul;94(3):909-50. doi: 10.1152/physrev.00026.2013. PMID: 24987008; PMCID: PMC4101632.
- Zumsteg ZS, Morrow M, Arnold B, Zheng J, Zhang Z, Robson M, Traina T, McCormick B, Powell S, Ho AY. Breast-conserving therapy achieves locoregional outcomes comparable to mastectomy in women with T1-2N0 triple-negative breast cancer. Ann Surg Oncol. 2013 Oct;20(11):3469-76. doi: 10.1245/s10434-013-3011-9. Epub 2013 May 19. PMID: 23686101; PMCID: PMC5730455